The effects of growth conditions on the elemental and biochemical composition of the diatom *Thalassiosira weissflogii* and the haptophyte *Emiliania huxleyi*

Narin Chansawang

A thesis submitted for the degree of
Ph.D. Biological Sciences

School of Biological Sciences

University of Essex

December 2015

Acknowledgements

First, I would like to express my deepest gratitude to my supervisor, Prof. Richard Geider for taking me as his Ph.D. student. I also would like to thank him for his invaluable knowledge, support and guidance throughout the course of this research. He is a very kind advisor and one of the smartest person I have ever known.

My thanks also go to Tracy Lawson and Michael Steinke for their teaching and advice in the research methodologies. I would not have succeeded without everyone in the algal, microbial ecology, and bioimaging lab, in particular Dawn Rose, Boyd McKew, Sue Corbett, John Green, Tania Cresswell-Maynard, Farid Benyahia, Philippe Laissue, and fellow Ph.D. friends.
I would like to give special thanks to Phil Davey for his tireless help with my laboratory work. It would be impossible to complete this research without him.

I would like to thank The Royal Thai Government and Thailand Institute of Scientific and Technological Research (TISTR) who have provided a full scholarship.

Last but not least, I would like to thank my family for their unconditionally love and support throughout my Ph.D. study.

Abstract

A change in environmental conditions often leads to changes of physiology and biochemical composition of microalgae. Temperature and light intensity are important environmental factors regulating the growth of microalgae. In this study, the elemental and biochemical composition were measured in 2 marine microalgae under different temperatures and light intensities in nutrient replete and deplete conditions. The effect of temperature was observed in the marine haptophyte *Emiliania huxleyi* (CCMP 1516) at nutrient replete semi-continuous cultures. Triplicate cultures were incubated different temperature from 14 to 22^{o}C and under photon flux densities (PFD) 600 µmol photons m^{-2} s^{-1}. The growth rate (GR) of *E. huxleyi* increased with temperature. Cell volume varied with temperature, being about 40% smaller at higher temperature (22^{o}C). Cellular chlorophyll *a* (chl *a*), nitrogen, phosphorus, and carbon contents were also lower at 22^{o}C than other temperatures. Protein, total amino acids from free and combined amino acid, and total pigments [mol accessory pigment (mol chl *a*)$^{-1}$] were decreased with increasing temperature; however, the opposite response was observed in fatty acids. In addition to the effect of combined temperature and light intensity was investigated in the marine diatom *Thalassiosira weissflogii* (CCMP 1056) under nutrient-limited semi-continuous cultures. The cultures were incubated at 16 and 26°C and PFD of 50 ± 10 (low light; LL) and 500 ± 10 (high light; HL) µmol photons m^{-2} s^{-1}. HL incubated-cultures were diluted at 50% day^{-1} and LL incubated-cultures were diluted at 25% day^{-1}. The GR were largely set by dilution rate (nitrogen limitation), but not by temperature and irradiance. The GR were around 0.72 d^{-1} in HL placed-cultures and 0.32 d^{-1} in the LL placed-cultures. Temperature did not affect mean cell size, whereas mean cell size decreased with increased irradiance by 20 to 29 %. Both temperature and irradiance influenced cellular chl *a,* carbon and chl *a* specific light absorption. Cellular nitrogen and phosphorus varied with temperature and irradiance. Protein, total amino acid (free and combined amino acid) and total fatty acid increased with increased temperature and irradiance; however, the opposite response was found in carbohydrate. Overall, temperature and light affected elemental and biochemical composition in 2 marine microalgae. Both relationship of the chlorophyll (chl):carbon (C) and RNA:protein ratio and growth rate in *E. huxleyi* under variable temperature positively supported a bio-optical and growth rate hypothesis respectively. However, the opposite response was found in *T. weissflogii.* Instead the C:chl and RNA:protein ratio and growth rate in *T. weissflogii* under variable irradiance positively supported a bio-optical and growth rate hypothesis.

Abbreviations

AA	Amino acid
a^{Chl}	Chlorophyll *a* specific absorption coefficient
AQC	6-aminoquinolyl-N-hydroxysuccinimidyl carbamate
Beta C	Beta carotene
BSA	Bovine serum albumin
Chl *a*	Chlorophyll *a*
Chl *c*	Chlorophyll *c*
CHO	Carbohydrate
CLSM	Confocal laser scanning microscope
CTAB	Cetyl-trimethyl-ammonium-bromide
DAD	Diode array detector
DD	Diadinoxanthin
DHA	Docosahexaenoic acid
DMSO	Dimethyl sulfoxide
DNA	Deoxyribonucleic acid
DT	Diatoxanthin
E	The molar extinction coefficient
E_k	Light saturation index (µmol photons m^{-2} s^{-1})
EPA	Eicosapentaenoic acid
EXPO	Exponential phase
FA	Fatty acid
FAME	Fatty acid methyl ester
Fuco	Fucoxanthin
GC/MS	Gas chromatography/mass spectrometer
GR	Growth rate
GRH	Growth rate hypothesis
Hex-fuco	19'-hexanoyloxyfucoxanthin
Hex-kfuco	4-keto-19'-hexanoyloxyfucoxanthin
HL	High light
LL	Low light
MUFA	Monounsaturated fatty acid
NR	Nile red
P_m^{Cell}	Cell-specific light-saturated photosynthetic rate (pg C $cell^{-1}$ h^{-1})
P_m^{Chl}	Chlorophyll *a*-specific light-saturated photosynthetic rate (g C [g Chl]$^{-1}$ h^{-1})

Abbreviations (cont.)

PE	Photosynthesis-irradiance curve
PFD	Photon flux densities
PN	Particulate nitrogen
PP	Particulate phosphorus
PUFA	Polyunsaturated fatty acid
RNA	Ribonucleic acid
RuBisCO	Ribulose-1,5-bisphosphate carboxylase/oxygenase
SFA	Saturated fatty acid
STAT	Stationary phase
UPLC	Ultra performance liquid chromatography
α (P^{Chl})	The initial slope of the photosynthesis versus irradiance curve normalized to cell (pg C $cell^{-1}$ h^{-1} [µmol photons m^{-2} $s^{-1}]^{-1}$)
α (P^{Cell})	The initial slope of the photosynthesis versus irradiance curve normalized to chlorophyll (g C [g Chl]$^{-1}$ h^{-1} [µmol photons m^{-2} $s^{-1}]^{-1}$)

Contents

List of tables

List of tables (cont.)

List of tables (cont.)

List of figures

List of figures (cont.)

List of figures (cont.)

List of figures (cont.)

List of figures (cont.)

List of figures (cont.)

List of figures (cont.)

Chapter 1: General introduction

1.1. Introduction

Microalgae are photosynthetic organisms can be found in aquatic and terrestrial environments such as oceans, water, lakes as well as soil. Most aquatic microalgae are free-living and are buoyant and float in the upper part of the ocean and are called plankton; however, some microalgae live in symbiotic association with a variety of other organisms (Muller-Parker & D'Elia 1997). For example, microalgae genus *Symbiodinium* have a mutually beneficial symbiotic relationship with many coral reef animals. Microalgae are primary producers that are able to synthesize organic molecules from water and carbon dioxide via photosynthesis using sunlight as a source of energy. Algae account for approximately half of photosynthetic production of organic material by the global biosphere and are the main primary producers in many freshwater and marine environments. Marine microalgae can influence ecological systems because oceans are Earth's largest ecosystem. In particular, marine microalgae can influence climate by affecting the carbon dioxide level in atmosphere since higher carbon dioxide levels leads to an increase in air temperatures as more of the outgoing radiation is intercepted and radiated back to our planet.

Marine microalgae are a diverse group. One major group of algae are the diatoms of which there are approximately 8,400 species (Guiry 2012). Diatoms belong to the taxonomic phylum Bacillariophyta. Diatoms are unicellular with a silica-based cell wall called a frustule. Many diatom species are planktonic, suspended in the water column moving at the mercy of water currents. Planktonic diatoms may account for as much as 20% of global photosynthetic carbon dioxide fixation (Nelson *et al.* 1995).

Another interesting group of the algae is coccolithophores are extremely widespread, with some species (e.g. *Emiliania huxleyi*, *Gephyrocapsa oceanic*) occasionally forming extensive algae

blooms (Ferńandez *et al*. 1993). Coccolithophores can form a layer of $CaCO_3$ around their cells called a coccolith (Paasche 2001). Calcification affects CO_2 partitioning between atmosphere and ocean (Rost & Riebesell 2004). Moreover, when coccolithophores die, $CaCO_3$ is accumulated as inorganic mineral matter into the deep sea approximately 0.1 Pg C/year or 6-14% of annual production (Buitenhuis *et al*. 1999; Berelson *et al*. 2007).

Both coccolithophorids and diatoms are valuable indicators of environmental conditions because they respond directly and sensitively to many physical, chemical and biological changes in ecosystem such as temperature, light and nutrient concentrations. The species-specific sensitivity of their physiology to many environmental conditions is manifested in the great variability in biomass and biochemical composition (Thompson *et al*. 1992). Such a change results in a metabolic imbalance that requires biochemical and metabolic adjustments before a new steady state of growth can be established (Rost & Riebesell 2004).

Microalgae produce organic matter (proteins, lipids, and carbohydrates) that can be used in both commercial and industrial applications such as health food, pharmaceuticals, biomolecules, agriculture and material in nanotechnology (Spolaore *et al.* 2006). At present, different species from numerous algal classes can be grown in laboratory and outdoor cultures; among the best known algae are the diatoms (Bacillariophyta), the green algae (Chlorophyta), the blue-green algae (Cyanophyta) and dinoflagellates (Dinophyta).

Microalgae can grow under unfavorable conditions often represent significant variations in their biochemical composition (Table 1-1). Diatoms can be used in animal feed because of high protein and lipid contents, particularly polyunsaturated fatty acids (PUFAs) when they grow under stressful environmental condition. The importance of these PUFAs is nutritional value for aquatic organisms which animals cannot synthesize by themselves (Volkman *et al*. 1989; Goulden & Place 1990). For example, *T. weissflogii* is a potential candidate for larviculture such as fish, shrimp and copepod because it contains high value chemicals such as proteins and PUFAs especially eicosopentaenoic acid (EPA, C20:5n-3) and decosahexaenoic acid (DHA,

C22:6n-3) (Kiatmetha *et al*. 2011). Several studies have revealed that *T. weissflogii* enhanced survival and metamorphosis in the black tiger shrimp *Penaeus monodon* larvae (Kiatmetha *et al*. 2011). *T. weissflogii* also influences development and growth (total length) in the Indian white prawn *Penaeus indicus* larvae (Emmerson 1980). Moreover, *T. weissflogii* supported development of the copepod *Acartia tonsa* through the entire life cycle from larval development and survival up to adulthood *(*Ismar *et al.* 2008) and egg production rate and hatching in the calanoid copepod *Temora longicornis* (Arendt *et al*. 2005).

Table 1-1. Summary of general effect of environmental factors on biochemical composition of microalgae (modified from Juneja *et al*. 2013).

Factor	Organism	Conditions	Biochemical changes observed	Reference
Temperature	*Chlorella vulgaris*	Increased from 20 to 38°C Increased from 10 to 38°C	Decrease in starch resulting in increase in sucrose Transformation of L-starch (high molecular weight) to S- starch (low molecular weight), reversible with temperature	Nakamura *et al.* 1982 Nakamura *et al.* 1983
	Haematococcus pluvialis	Increased from 20 to 30°C	3-fold increase in astaxanthin formation	Tjahjono *et al*. 1994
	Chlorococcum sp.	Increased from 20 to 35°C under nitrogen deprivation	Two fold increase in total carotenoid content	Liu & Lee 2000
	Botryccoccus braunii	Increased from 25 to 32°C	Decrease in intracellular lipid content from 22% to 5% wt., accumulation of polysaccharides	Kalacheva *et al*. 2002
	Nitzschia laevis	Increased from 15 to 27°C	Decrease in triacylglycerol content	Chen *et al.* 2008
Light	*Chlorella vulgaris*	Red light Blue light	Increase in sucrose and starch formation Increase in lipid fraction and alcohol-water insoluble non carbohydrate fraction	Miyachi & Kamiya 1978
	Dunaliella virdis	Darkness (No light)	Increase in total lipid content, decrease in free fatty acids, alcohol, sterol	Gordillo *et al.* 1998
	Nannochloropsis sp.	Light limited conditions	Increase in lipid content; Increase in EPA proportions	Sukenik *et al.* 1989
	Chlorella sp. and *Monoraphidium* sp.	Increased from 40-400 µmol photons m^{-2} s^{-1}	Three fold increase in neutral lipid productivity, decrease in protein and carbohydrate content	He *et al.* 2015
Nitrogen	*Phaeodactylum tricornutum*	Nitrogen limitation	Increase in lipid synthesis; decrease in protein content	Morris *et al*. 1974
	Haematococcus pluvialis	Nitrogen limitation	Increase in carotenoid formation (13% w/w)	Borowitzka *et al*. 1991
	Chlorella vulgaris	75% decrease in nitrogen	Increase in lipid synthesis from 5.90% to 16.41%	Converti *et al*. 2009
	Nannochloropsis oculata	75% decrease in nitrogen	Increase in lipid synthesis from 7.90% to 15.31%	Converti *et al.* 2009
	Isochrysis sp. (clone T-iso)	Nitrogen starvation	Increase in neutral lipid and carbohydrate	Lacour *et al.* 2012
		Nitrogen limitation	Increase in carbohydrate, decrease in neutral lipid	
	Scenedesmus quadricauda	Nitrogen depletion	2.27-fold increase in lipid yield	Anand & Arumugam 2015

1.2 Organisms

Marine phytoplankton have evolved over many millions of years, modulating with carbon flux by the relative abundance of cocolithophores and diatoms, resulting in biological feedback on atmospheric CO_2 between the atmosphere and ocean (Cermeño *et al*. 2008). Cocolithophores and diatoms are derived from a common Rhodophyte ancestor and found throughout in World's ocean (Cermeño *et al.* 2008). Coccolithophorids, through the formation of calcium carbonate ($CaCO_3$) shells, alter the inorganic carbon system and alkalinity of seawater and release CO_2, which may escape to the atmosphere (Frankignoulle *et al.* 1994). In contrast, diatoms dominate the export flux of carbon, providing significantly to the long-term sequestration of atmospheric CO_2 in the ocean interior (Smetacek 1999). Therefore the balance between coccolithophorids and diatoms potentially affects the $CaCO_3$ to organic carbon export ratio, a major factor determining the partitioning of CO_2 between the atmosphere and ocean (Cermeño *et al.* 2008). The dominance of diatoms in the oceans is reflected by their contributions to massive deposits of the mineral diatomite which has industrial applications as well as their contribution to petroleum reserves (Smetacek 1999). Moreover, coccolithophorids and diatoms are the main providers of the oceans' ecological and biogeochemical services because they generate the basis of the marine food web. *E. huxleyi* is the highest abundant cocolithophore in the world's ocean (Lefebvre *et al.* 2012). *T. weissflogii* is one of the diatoms that has been widely used in many research such as live feed in aquaculture (García *et al.* 2012) and indicators of environment changes (Stevenson & Pan 1999). Therefore *E. huxleyi*, the representative of cocolithophore, and *T. weissflogii,* the representative of diatoms, will be the focus of the research described in this thesis.

1.2.1 Characteristics of *Emiliania huxleyi*

Emiliania huxleyi is a coccolithophorid marine phytoplankton which can produce calcium carbonate ($CaCO_3$) scales (or plates) called coccoliths (Fig. 1-1). *E. huxleyi* is classified in systematic categories from the highest to the lowest as follows:

Kingdom: Chromista

Phylum: Haptophyta

Class: Prymnesiophyceae

Order: Isochrysidales

Family: Noelaerhabdaceae

Genus: *Emiliania*

Speicies: *E. huxleyi*

(Source: http://www.algaebase.org/search/species/detail/?species_id=51619)

E. huxleyi has a spherical shape, with a diameter that is approximately 4-5 μm and is often covered by 10-15 coccoliths in a single layer. Calcite-forming cells are nonmotile: lacking flagella and haptonema (Paasche 2001).

Coccolithophorids play an important role in the oceanic carbon cycle (Brown & Yoder 1994) through their production of $CaCO_3$ coccoliths and uptake of CO_2 for photosynthesis. Coccolithophorids also contribute to the sulfur cycle via production of dimethyl sulfide (DMS). DMS is a precursor for cloud condensation nuclei that are small particles size of a cloud droplet and may influence regional albedo (the proportion of Sun's radiation reflected from a surface) via increased cloud formation (Bates *et al*., 1987).

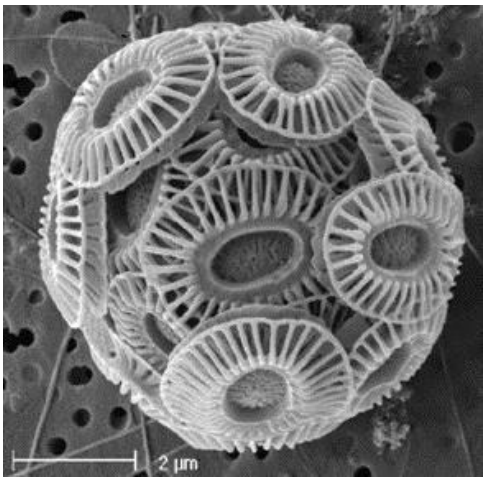

Figure 1-1. Scanning electron micrograph of a coccosphere of *Emiliania huxleyi*.
(Source: http://www.noc.soton.ac.uk/soes/staff/tt/eh/)

Biological oceanographers and phycologists have been investigating the physiology and ecology of different groups of marine phytoplankton with the objective of understanding and ultimately predicting how marine primary productivity responds to climate change. In particular, *E. huxleyi* has been the subject of extensive investigations because it is found ubiquitously in most parts of the marine environment except the Arctic and Antarctic (Brand 1994; Winter *et al* 1994). For example, *E. huxleyi* has generated blooms extending over 250,000 square kilometres (km^2) in the North Atlantic (Holligan *et al.* 1993) and over 200,000 km^2 in the Eastern Bering Sea (North Pacific) and Bering Straits in 1997 (Sukhanova & Flint 1998). $CaCO_3$ account for most of the inorganic carbons deposited in the deep sea. (Armstrong *et al.* 2002; Francois *et al.* 2002). $CaCO_3$ levels have been estimated to be approximately 83 percent of the organic carbon contents to the seafloor (Zondervan *et al*. 2001; Klaas & Archer 2002).

1.2.2 Characteristic of *Thalassiosira weissflogii*

Thalassiosira weissflogii is a centric diatom that found widely in marine habitats. *T. weissflogii* is identified in systematic categories from the highest to the lowest as follows:

Kingdom: Chromista

Phylum: Bacillariophyta

Class: Mediophyceae

Sub-class: Thalassiosirophycidae

Order: Thalassiosirales

Family: Thalassiosiraceae

Genus: *Thalassiosira*

Species: *T. weissflogii*

(Source: http://www.algaebase.org/search/species/detail/?species_id=32240)

The predominant feature of a diatom is a highly ornamented external cell wall made of amorphous silica, called a frustule (Hoagland *et al*. 1993). The frustule is composed of two plates called valves; the epitheca valve (top plate) fits onto the hypotheca valve (low plate) like a petri dish. A number of smaller plates called girdle bands link the two valves. The frustules have developed as mechanical protections for the cells from predators in pelagic food webs and biogeochemical cycles (Hamm *et al*. 2003).

1.3 Effect of environment factors on algal growth and physiology

1.3.2 Temperature

Temperature is an important environmental factor that affects algal growth rate, biochemical composition, nutrient requirements, and cell size (Juneja *et al.* 2013). Microalgae can grow under a broad range of temperatures, for example the Bacillariophyceae have optimal temperatures (T_{opt}) that range from 5 to 25°C, the Dinophyceae range from 15 to 25°C, and the Chlorophyceae range from 20 to 36°C (Ras *et al.* 2013; Bernard & Rémond 2012). A high

growth rate at optimal growth temperature is likely to reflect a good energy balance in the cell. Microalgae attempt to maintain a balance between energy consumption within the Calvin cycle and the photosynthetic energy supply by the thylakoid membranes. Environmental changes cause imbalance of energy supply and consumption often lead to a modification of photosynthetic apparatus such as amounts of Calvin cycle enzymes or photosynthetic unit size. Modifications due to temperature changes is named temperature acclimation (Öquist 1983). Below optimal growth temperature, growth rate (GR) increases with increasing temperature; however, GR declines remarkably above optimal temperature (Renaud *et al.* 2002).

Temperature affects cell size and the efficiency of carbon and nitrogen utilization decreases under non-optimal temperature. This suggests that changes in cytoplasmic viscosity below optimal temperature result in a reduction of efficient carbon and nitrogen utilization (Raven & Geider 1988). Several cellular mechanisms are associated with low temperature. There are 1) low temperature causes reduction of electron transport because CO_2 fixation rate is slow, 2) low temperature often reduces carboxylase activity, 3) low temperature inhibits the active of oxygen species resulting in a decrease of photoinhibition by protecting photosystem II (PSII), and 4) low temperature also inhibits degradation of D1 protein during photoinhibition consequently leading to a block in the PSII repair cycle. Moreover, low temperature influences the levels of fatty acids in lipid membranes. Psychrotrophic organisms change the fatty acid composition of membranes to regulate the fluidity of membranes at low temperature such as a buildup polyunsaturated, branched, short- chain or cyclic fatty acids (White *et al*. 2000). Unsaturated fatty acids were found in higher amounts in membrane lipids that play a key role in avoiding membrane rigidification at sub-optimal temperature (Morgan-Kiss *et al.* 2006). For example, saturated fatty acid (C16:0) increased from 18.8 % at 10^{o}C to 25.8 % total fatty acid at 25°C in *Phaeodactylum tricornutum,* whereas, polyunsaturated fatty acids (PUFAs) increased gradually from high to low temperature (Jiang & Gao 2004). Therefore, lower temperature decreases the fluidity in the cell membrane and cells compensate by increasing levels of PUFA to increase fluidity. This also

makes the membranes more susceptible to damage by free radicals from photoinhibition (Raven & Geider 1988; Nishida & Murata 1996).

On the other hand, above optimal temperature leads to reduction of protein synthesis and results in slower growth rates (Rhee & Gotham 1981). For example, protein content at high temperature (30°C) was below that of low temperature (15°C) at the exponential growth phase in the haptophyte *Isochrysis galbana*. Similarly, protein in the chlorophyte *Scenedesmus* sp. decreased at higher temperature (Rhee & Gotham 1981). Moreover, the rate of protein synthesis per unit RNA decreased with increased temperature from 20 to 30°C in macroalgae *Ulva pertusa* cultures and consequently resulting in lower protein content and greater free amino acid content in cells (Kakinuma *et al*. 2006).

1.3.2. Light

Light intensity affects growth of microalgae as it influences photosynthesis. Light is the energy source in photosynthesis. Microalgae use light to convert carbon dioxide to organic compounds as primary product. The maximal growth rate is found at the saturation intensity, and the growth rate decelerates if the light intensity is below or above saturation (Sorokin & Krauss 1958). Falkowski & La Roche (1991) refer to processes that lead to changes in cell properties according to the availability of light as photoacclimation. Photoacclimation can affect growth rate, quantities and types of pigments, dark respiration or fatty acid content (Fábregas *et al.* 2004), the number and density of thylakoid membranes and cell size (Berner *et al.* 1989). For example, Anning *et al*. (2000) found that cell division rates in the marine diatom *Skeletonema costatum* were three times higher in cultures acclimated to 1,200 µmol photons m^{-2} s^{-1} than in cultures acclimated to 50 µmol photons m^{-2} s^{-1}. Cellular chlorophyll *a* and fucoxanthin contents were also higher but diadinoxanthin and diatoxanthin contents lower in cells grown at low light than in cells shifted to high light.

Light intensity also affects the biochemical composition of microalgae. High light intensities tend to enhance polysaccharide production in microalgal cells. Friedman *et al.* (1991) reported that

Porphyridium sp. and *Porphyridium aerugineum* grown under increased light intensity from 75 to 300 µmol photons m^{-2} s^{-1} had 0.6- and 3-fold increases in polysaccharide content respectively. Low light intensity has been observed to result in higher protein content. For instance, protein content was greater when *Scenedesmus* spp. grown at low light (50 µmol photons m^{-2} s^{-1}) than high light conditions (400 µmol photons m^{-2} s^{-1}) while lipid content and neutral lipid content was higher at high light than at low light (Liu *et al*. 2012). Many studies with microalgae of various groups suggest that the cellular content of lipids and total PUFAs including EPA, are negatively related to growth light intensity (Cohen 1999). Sukenik *et al.* (1989) reported that 40% of the total lipids of *Nannochloropsis* sp., grown under low light conditions (35 µmol photons m^{-2} s^{-1}) were found to be galactolipids and 26 % were found to be triacylglycerols. However, high light (550 µmol photons m^{-2} s^{-1}) led to an increased synthesis of triacylglycerol with a reduction in galactolipid synthesis. Sukenik *et al.* (1989) showed that *Nannochloropsis* sp. cultures were characterized by a high lipid content and high proportion of EPA under light-limiting conditions, whereas palmitic acid (C16:0) and palmitoleic acid (C16:1) increased gradually until to a saturated light level. Since PUFAs are the major constituents of the thylakoid membranes, low light-accumulated production of PUFA is commonly coupled with a concomitant increase in total thylakoid membranes in the cells (Berner *et al*. 1989). There are, however, some exceptions. PUFA decrease with increase in light intensity, possibly resulting from an increase in oxygen-mediated lipid in *E. huxleyi* (Rontani *et al.* 2006).

1.3.3. Nutrients

Nitrogen and phosphate are two main macronutrients for growth and metabolism of algal cells. Nitrogen is a fundamental element for the formation of amino acids which make up proteins. Nitrogen is also required for synthesis of chlorophylls and nucleic acids. In addition, nitrogen is also an integral part of energy transfer molecules such as adenosine triphosphate (ATP) and adenosine diphosphate (ADP). Phosphate is a part of the backbone of DNA and RNA, which

are essential macromolecules for all living cells. Phosphorus is also an important component of phospholipids (Juneja *et al*. 2013).

Nitrogen generally accounts for about 7-10% of cell dry weight (Hu 2004). It is not unusual to take advantage of nitrogen limitation to obtain high value-compounds. For example, nitrogen depletion shifts the lipid metabolism from membrane lipid synthesis to neutral lipid storage. The depletion of intracellular nitrogen generates a decline in chlorophyll content and an onset of lipid and carotenoid accumulation in *Isochrysis galbana* (Roopnarain *et al.* 2014). Although nitrogen limitation leads to lipid accumulation, reduction in protein content also occurs and consequently growth rate declines (Morris *et al.* 1974; Lynn *et al*. 2000). Microalgae grown in nitrogen-deplete condition are likely to divert their photosynthetically fixed carbon to carbohydrate and neutral lipid synthesis; however, the physical significance of this is not clear (Hu 2004; Juneja *et al.* 2013).

1.4 The growth rate hypothesis (GRH)

Both N and P have major roles in protein synthesis and growth. N is required for amino acid synthesis and nucleotide synthesis. P is major component in ribosome and thus has a role in potential for limiting ribonucleic acid (RNA) since P-rich ribosomes are needed for protein synthesis. This is implicit that P-deficiency could limit protein synthesis and growth. The growth rate hypothesis states that ribosomes and rRNA contribute to rapid protein synthesis related to fast growth. GRH can links growth rate, RNA content and P content, especially when P is the factor that constrains growth. It implies that for many P-rich and fast- growing invertebrates, RNA constitutes a major faction of P content and that there is a close association between the specific P-content and growth rate (Hessen 1990; Andersen & Hessen 1991; Sterner & Hessen 1994; Elser *et al*. 1996). There are many studies that apply GRH in various organisms. For example, studies by Karpinets *et al*. (2006) found that *Escherichia coli* (bacteria), *Neurospora crassa* (fungi) *Saccharomyces cerevisiae* (budding yeast), *Streptomyces coelicolor* (bacteria)

have correlation between the relative growth rate and P:N ratio which were calculated as a coefficient of determination (R^2) from 0.67 to 0.99. In addition, they also found that this ratio in *Prototheca zopfii* (algae) and *Selenomonas ruminantium* (bacteria) is not correlated with the relative growth rate. . Thus, limiting nutrient and stoichiometric constraint influences food web dynamic (Anderson 1997; Elser *et al.* 1998).

1.5 Testing of growth rate hypothesis

To test the GRH, reliable measurements of the concentrations of protein and ribosome are needed. In general, the total concentrations of protein and RNA are measured and it is assumed that ribosomes densities are associated with RNA concentration. Flynn *et al.* (2010) discussed the limitations of the methods that are used to test the growth rate hypothesis. These include 1) errors in measurements of RNA and protein content, and 2) errors in measurement of growth rate.

1) Measurements of RNA and protein

GRH requires accurate measurements of RNA and protein in the cellular material of the organisms. Unfortunately, there are no methods that can measure the exact quantity RNA and protein (Ågren 2004, 2008; Flynn *et al*. 2010). Flynn *et al.* (2010) state that there are two common methods for measuring RNA: 1) orcinol determination of ribose and 2) binding of fluorescent compounds to RNA (Fara *et al*. 1996). A major problem of the orcinal method is interference with sugars, whereas a problem with the fluorescence methods is correcting for the amount of dye binding to DNA. Thus, the second measurement tends to overestimate the amount of RNA. The two most commonly used spectrophotometric assays for measuring protein are the Lowry and Bradford assays which measure different properties of proteins. When using BSA as the standard, the Lowry assay gives higher protein values for phytoplankton samples than the Bradford assay (Clayton *et al*. 1988; Berges *et al.* 1993; Crossman *et al.* 2000; Barbarino & Lourenco 2005). Thus, the accuracy of the RNA:protein ratio rely on the methods and standards used to measure RNA and protein. The quantities of

proteins in phytoplankton are likely to overestimate the RNA:protein and underestimate the rate of protein synthesis per ribosome.

2) Growth rate

Growth rate (GR) is a measurement of change in metabolism in organisms via biomass or cell number in the exponential phase. Flow cytometry, fluorescent staining and high pressure liquid chromatography are methods for measuring growth rate. However, these methods still rely on the same basic mathematical formulations for calculating exponential growth rate. Moreover, techniques for measuring growth rates of natural populations using measurement of rRNA content by using rRNA-targeted nucleic acid probes is not usually used because the principal method used to demonstrate the growth-rate dependence of rRNA content by investigators who are developing the targeted rRNA approach (Binder & Liu 1998, Worden & Binder 2003).

1.6 Evidence for support and against the application of the GRH to microalgae

Karpinets *et al*. (2006) found that P:N ratios calculated from RNA and protein contents in bacteria, budding yeast, fungi and algae had similar positive relationships with growth rate and matched with the growth-rate hypothesis.

Flynn *et al.* (2010) summarized the relationships between RNA:protein and growth rate (GR) for cyanobacteria and eukaryote microalgae (Table 1-2). The relationship between RNA and GR were exponential or sigmoidal; the relationship was not linear, as would be predicted by the GRH if protein concentrations were constant. Similarly, Worden & Binder (2003) reported that there were triphasic relationships between RNA and GR in different strains of marine prokaryotic photo-autotrophs (*Prochlorococcus* and *Synechococcus*), which were qualified by: (i) little change at low GR, (ii) linear increase in the ranged of medium GR, and (ii) a plateau and/or decrease at the highest GR. In *Synechococcus* WH 8103 there was a positive relationship between RNA and GR but not in strain WH 7803 and WH 8101 which expressed

the highest growth rate at intermediate RNA concentration. Thus, these two strains were not consistent with GRH. *Selenastrum minutum* and *Scenedesmus* spp. (3 species) were cultured in freshwater where light was limited. Both RNA and GR were increased. Thus, this study was consistent with GRH. However, when this two strains were cultured under temperature limition GR decreased and RNA was increased, opposite to the GRH (Schlesinger & Shuter 1981). In *Amphidinium carterae* and *Thalasssiosira nordenskioeldii* cultured in sea water under ammonium and nitrate depletion and ammonium constraint condition, both RNA and GR decreased inparallel supporting the GRH (Dortch *et al.* 1983; Thomas & Carr 1985).

Lourenco *et al*. (1998, 2002, 2004) studied protein and RNA content at different growth rates of 10 phytoplankton and found that *Prorocentrum minimum* had the highest cell volume approximately 1395.0 μm^3, RNA content 33 fg RNA per cell and protein content 1423.4 fg protein per cell (Table 1-3). Whereas *Dunaliella tertiorecta* gave the highest RNA content per gram protein of about 0.139 (g RNA (g protein)$^{-1}$). At the same time, *Chlorell minutissima*, phytoplankton from Trebouxiophyceae, had RNA and protein content roughly 0.16 fg RNA μm^{-3} cell and 5.28 fg protein μm^{-3} cell respectively. However, RNA content per cell volume varied 12-fold and the RNA-specific rate of protein synthesis varied 10-fold. Therefore, there is a much greater range of RNA-specific protein synthesis rates than of growth rate.

Table 1-2. Summary of studies relevant to the growth rate hypothesis (GRH) in prokaryote and eukaryote microalgae (Flynn *et al.* 2010).

Group	Organism	Environment	Limiting resource	Observation	GRH support	Reference
Cy	*Synechococcus* sp. PCC 6301[a]	fw	Light	Exponential increase in RNA with GR	Yes?	Mann and Carr (1974)
Cy	*Synechococcus* sp. PCC 6301[a]	fw	Light or CO_2	Sigmoidal increase in RNA with GR	Yes?	Parrott and Slater (1980)
Cy	*Synechococcus* sp. PCC 6301[a]	fw	Mg	Sigmoidal increase in RNA with GR	Yes?	Binder and Liu (1998) using data from Utkilen (1982)
Cy	*Synechococcus* sp. PCC6301	sea	Light	Exponential increase in RNA with GR	Yes?	Lepp and Schmidt (1998)
Cy	*Synechococcus* sp. WH8103	sea	Light	Increases	Yes	Lepp and Schmidt (1998)
Cy	*Synechococcus* sp. WH7803	sea	Light	RNA constant at low GR; linear up to 0.7 d^{-1}; decline at higher GR	No	Kramer and Morris (1990)
Cy	*Synechococcus* sp. WH7803	sea	?	RNA constant at low GR; linear at intermediate GRs; decline at higher GR (?)	No?	Worden and Binder (2003)
Cy	*Synechococcus* sp. WH8101	sea	Light	RNA constant at low GR; linear at intermediate GRs; decline at higher GR (?)	No	Binder and Liu (1998)
Cy	*Prochlorococcus* sp.	sea	?	RNA constant at low GR; linear at intermediate GRs; decline at higher GR (?)	No	Worden and Binder (2003)
Ch	*Polytomella caeca*	fw	Organic nutrients	RNA increase with GR	Yes	Jeener (1953)
Tre	*Prototheca zopfii*	fw	Organic nutrients	rRNA decreases with increasing GR	No	Poynton (1973); nonphotosynthetic
Eu	*Euglena gracilis*	fw	Light	RNA increase with GR	Yes	Cook (1963)
Ch	*Scenedesmus* sp.	fw	P and N	GR saturating function of RNA	No?	Rhee (1973, 1978)
Ch	*Selenastrum minutum*	fw	Light	Increase in RNA with increase in GR	Yes	Schlesinger and Shuter (1981)
Ch	*Scenedesmus* spp. (3 species)	fw	Light	Increase in RNA with increase in GR	Yes	Schlesinger and Shuter (1981)
Ch	*Selenastrum minutum*	fw	Temperature	Temperature down, decreases GR, increases RNA	No	Schlesinger and Shuter (1981)
Chl	*Scenedesmus* spp. (3 species)	fw	Temperature	Temperature down, decreases GR, increases RNA	No	Schlesinger and Shuter (1981)
Di	*Amphidinium carterae*	sea	Ammonium and nitrate	Decrease in RNA with decreasing growth	Yes	Dortch *et al.* (1983)
Bac	*Thalassiosira nordenskioldii*	sea	Ammonium	Decrease in RNA with decreasing growth	Yes	Dortch *et al.* (1983)
Di	*Amphidinium carterae*	sea	Light	No change in RNA with growth rate	No	Thomas and Carr (1985)

Bac, Bacillariophyceae; Cy, Cyanobacteria; Ch, Chlorophyceae; Di, Dinophyceae; Eu, Euglenophyceae; Tre, Trebouxiophyceae; fw, freshwater.

[a] Synonym *Anacystis nidulans*

Table 1-3. Organism's growth rate versus RNA and protein per cell (Flynn *et al.* 2010).

Organism	Cell volume (μm^3)[a]	Growth rate (d^{-1})[a]	fg RNA $cell^{-1}$ (late log)[b]	fg protein $cell^{-1}$ (late log)[b,c]	g RNA g^{-1} protein (late log)[d]	fg RNA $\mu m^{-3} cell$[d]	fg protein $\mu m^{-3} cell$[d]	Net protein synthesis
Synechococcus subsalsus (Cy)	2.3	1	0.2	11.9	0.016	0.08	5.25	62.5
Chlorella minutissima (Tre)	1.3	0.5	0.2	6.7	0.03	0.16	5.28	16.7
Dunaliella tertiolecta (Ch)	178	0.87	16.3	117.2	0.139	0.09	0.66	6.25
Tetraselmis gracilis (Pra)	640	0.78	8	574.8	0.014	0.01	0.9	55.7
Hilsea sp. (Cry)	190	0.64	22.6	246.3	0.092	0.12	1.3	6.96
Isochrysis galbana (Pry)	60.8	0.87	1.9	38.8	0.049	0.03	0.64	17.8
Nannochloropsis oculata (Eus)	13.3	0.64	0.3	19.3	0.016	0.02	1.45	40
Phaeodactylum tricornutum (Bac)	124	1.12	2.5	59.3	0.042	0.02	0.48	26.7
Skeletonema costatum (Bac)	110	1.2	12.1	144.2	0.084	0.11	1.31	14.3
Prorocentrum minimum (Dino)	1,395	0.65	33	1,423.40	0.023	0.02	1.02	28.3

Bac, Bacillariophyceae; Ch, Chlorophyceae; Cry, Cryptophyceae; Cy, Cyanobacteria; Dino, Dinophyceae; Eus, Eustigmatophyceae; Pra, Prasinophyceae; Pry, Prymnesiophyceae; Tre, Trebouxiophyceae.
[a,b,c]Lourenco *et al.* (1998, 2002, 2004); [d]calculated from columns 2-5.

1.7 Bio-optical hypothesis

Chlorophyll *a* (chl *a*) is commonly used as an index to quantify algal abundance (Bidigare *et al*. 1987), even though chl *a* is a small component and variable part of phytoplankton biomass (Geider *et al*. 1997). Chl *a* and other photosynthetic pigments capture the sun's energy and turn it into organic matter by photosynthesis. Chl *a* accounts for approximately 0.1-5 percent of organic matter (Geider *et al*. 1997).

Light plays a major role in photosynthesis in marine phytoplankton which synthesize biochemical compounds from CO_2 and water using light energy. The light reactions of photosynthesis separate electrons and protons from water and reduce $NADP^+$ (Nicotinamide adenine dinucleotide phosphate) to NADPH and drive ATP (Adenosine triphosphate) production (Fallowski & Raven 2007). The NADPH and ATP are in turn used in the Calvin cycle to fix CO_2 into triose phosphates (Fallowski & Raven 2007).

The relationship between growth rate and the chl *a* to C ratio is central to bio-optical models of algal growth (Kiefer & Mitchell 1983). The bio-optical model states that photosynthetic rate depends upon rate of photon capture. The effectiveness of utilizing photons relies on two coefficients: the absorption coefficient and the quantum yield of photosynthesis. The former represents the ability of the pigments to absorb photons and the latter represents the efficiency of absorbed radiation which is used to fix carbon (Bidigare *et al*. 1987). Kiefer & Mitchell (1983) hypothesized that growth rate should be proportional to the rate of light absorption times the quantum efficiency of photosynthesis. The chl *a* to C ratio varies from <0.01 to >0.1 g:g in phytoplankton cultures (Geider *et al.* 1987, 1993, 1997). Typically, the chl *a* to C ratio is higher under conditions of high temperature (25-30^{o}C), low light (<20 µmol photons m^{-2} s^{-1}) and replete nutrients (Geider *et al.* 1997).

The relationship between chlorophyll concentration and phytoplankton carbon biomass in the ocean is non-linear not only because of the complicated influences of environmental conditions (light, nutrients and temperature) on the chl *a* to C ratio within particular species, but also the different responses of variable phytoplankton groups and the structure size of the phytoplankton community (Armstrong 2006; Behrenfeld *et al.* 2002, 2005; Brown *et al.* 2003; Cullen 1990; Geider *et al.* 1996, 1997, 1998; Le Bouteiller *et al*. 2003; Wang *et al*. 2009). For instance, the chl *a* to C ratio is lower in large phytoplankton cells than in the small ones (Le Bouteiller *et al*. 2003).

1.8 Microalgae for biotechnological and industrial implications

At the present, the high value compounds from microalgae play important role in many industries. The high protein contents of various microalgae are used widely as nutritional supplements for humans and as animal feed additives. In addition, microalgae can produce essential amino acid for humans and animals. The pigment content in microalgae is a specific feature of each species. For example, beta carotene is often found in the green algal *Dunaliela*

salina, whereas astraxanthin is usually found in *Heamatococus pluvialis*. Microalgal lipid can be esterified to saturated or unsaturated fatty acids and be used in commercial and industry applications (Table 1-4). The lipid content varies between 5 to 63 % but can reach 90 % of dry weight (Spolaore *et al.* 2006).

Table1-4. The properties of fatty acid for biotechnological applications (modified form Mohan & Devi 2012).

Fatty acid	Lipid number	Properties
Caprylic acid	C8:0	Commercial production of esters perfumes and dyes. As an antimicrobial pesticide
Capric acid	C10:0	Making of perfumes, greases food additives and medicines
Lauric acid	C12:0	Antibacterial, antioxidant and antiviral inhibitor
Tridecanoic acid	C13:0	Ingredient in methyl ester formation
Myristic acid	C14:0	Manufacturing of Biofuels, cosmetics and tropical medicines
Myristoleic acid	C14:1n9c	Anti-inflammatory agent, pain reliever and an immune system modulator
Pentadecanoic acid	C15:0	Combustion, marker in butter fat composition
Palmitic acid	C16:0	Biofuels and cosmetics preparation
Palmitoleic acid	C16:1n7	Combustion and skin care products
Heptadecanoic acid	C17:0	Combustion of diesel engines
Stearic acid	C18:0	Biofuels and dietary supplements preparation
Elaidic acid	C18:1n9t	Used in food industry
Oleic acid	C18:1n9c	Excipient in medicines, emulsifier and solubiliser in aerosols and combustion
Linoleic acid	C18:2n6c	Making of soaps, emulsifiers, beauty products, anti-inflammatory agent
Arachidonic acid	C20:0	Production of detergents, photographic materials and lubricants
Cis-11-eicosenoic acid	C20:1	Used as a lubricant
Linolenic acid	C18:3n3	Main component in drying of oils
Behenic acid	C22:0	Lubricating oils, making of detergents and hair conditioners. Also as a paint remover and floor polisher
Erucic acid	C22:1n9c	Good lubricant properties, component in biodiesel, binder in paints
Eicosapentaenoic acid (EPA)	C20:5n3	Enhancing human health and treating a variety of diseases such as atherosclerosis, rheumatoid, arrhythmia, psoriasis, diabetes and cancers.
Docosahexaenoic acid (DHA)	C22:6n3	Infant diets, prevention and treatment of chronic diseases (such as coronary heart disease, hypertension, type II diabetes, ocular diseases, arthritis and cystic fibrosis)

Many studies have mentioned that beta carotene and fucoxanthin are high value products because they possess properties that protect against cell damage and cancer by scavenging free radicals. Beta carotene is a precursor that can be converted into vitamin A (Chidambara-Murthy *et al*. 2005), El Baz *et al.* 2002), Plaza *et al*. 2009). The antioxidant properties from

carotenoid were claimed in nutraceutical applications resulting in the market value of carotenoids reached over US$ 1,000 million or approximately £ 630 million (Del Campo *et al*. 2007). In addition, carotenoids are used in cosmetics and food products as feed additives for poultry, livestock, fish/ ornamental fish and crustaceans (Del Campo *et al*. 2007). Recently, the growing market of carotenoid has increased due to the interest of bio-produced resources instead of synthesis. Thus, it is good opportunities for microalgae to be one of the possible candidates for carotene production to reserve in many applications.

Many microalgae have been found to grow rapidly and produce massive amount of triacylglycerols (TAGs) which are the primary lipid storage used as energy reserves. There has been widespread interest in the possibility of growing microalgae for use as a feedstock for producing biodiesel. Furthermore, the need to reduce consumption of fossil fuels to meet targets for reducing emission of CO_2 is the main motivation for seeking alternative energy sources including plant and algae biomass. The commercialization of biomass as feedstock for the production of bio-energy depends on social, environment, economic system, industry as well as cost. Biodiesel production from plants such as grain legume, palms, coconuts, jatropha, rapeseed etc. requires the use of large tracts of arable land and fresh water for cultivation. In addition, there is the possible competition with food production of direct use to man or animal that influences productivity. Moreover, the use of herbicides to get rid of agricultural pests leads to environmental pollution (Aktar *et al*., 2009).

Marine microalgae are also important organisms in the production of polyunsaturated fatty acids (PUFAs) (Guschina & Harwood 2006) particularly eicosapentaenoic acid (EPA) and docosahexaenoic acid (DHA) (Table 1-5). Fatty acids can account for from 5 to 63 % dry weight of biomass and lipid productivity can account for from 0.2 to 3701.1 mg L^{-1} day^{-1} depending on cultivation conditions (Chen *et al.* 2011).

Table 1-5. Eicosapentaenoic acid (EPA) and docosahexaenoic acid (DHA) content (percentage of total fatty acid) of microalgae.

Microalgae	Condition			EPA	DHA	Reference
Pavlova viridis	Batch mode, 0% CO_2		Temp. 22°C and light intensity 50 µmol photons m^{-2} s^{-1}	16.97±1.13	10.79±0.08	Carvalho & Malcata 2005
	1% CO_2			15.55±0.07	7.44±0.70	
	2% CO_2			14.68±1.14	7.18±0.27	
	Continuous mode, 0.5% CO_2			13.99±0.04	5.78±0.28	
	1% CO_2			11.70±0.16	4.54±0.06	
Nannochloropsis sp.	Photoautrophic	350 µL CO_2 L^{-1}	Temp. 22°C and light intensity 50 µmol photons m^{-2} s^{-1}	21.9±1.5	1.4±0.6	Hu & Gai 2006
		2800 µL CO_2 L^{-1}		25.3±1.0	1.4±0.2	
	Mixotrophic	350 µL CO_2 L^{-1}		18.0±1.5	1.3±0.3	
		2800 µL CO_2 L^{-1}		21.2±1.0	1.3±0.3	
Pheodactylum tricornutum	Nitrate	final conc. 0.88 mM	Temp. 18±1°C and light intensity 60 µmol photons m^{-2} s^{-1}	20.26±0.12	1.78±0.05	Liang *et al*. 2006
	Ammonium			21.01±0.22	1.61±0.02	
	Urea			23.43±0.56	2.52±0.07	
Cheatoceros muelleri	Nitrate	final conc. 0.88 mM		13.12±0.60	1.13±0.12	
	Ammonium			11.74±0.72	1.23±0.11	
	Urea			13.39±0.04	1.42±0.06	
Pavlova viridis	Indoor	f/2 medium	Latitude 31° 57' N, longitude 118° 51' E (Nanjing, China)	25.23±2.17	10.71±1.16	Hu *et al.* 2008
	Outdoor			21.20±2.16	8.70±0.72	

Polyunsaturated fatty acids (PUFAs) have important roles in cellular and tissue metabolism, the regulation of membrane fluidity, electron and oxygen transport, as well as thermal adaptation (Funk 2001). Many studies have shown that dietary supplementation with EPA and DHA for enhancing human health and treating a variety of diseases such as asthma, rheumatoid arthritis, psoriasis, inflammatory bowel disease, cardiovascular diseases, allergies, cancer, among others (Radwan 1991; Simopoulos 2002; Burdge *et al*. 2002; Field & Schley 2004; Doshi *et al*. 2004; Calder 2010; Mozaffarian & Wu 2011). There is increasing interest in a PUFA family particularly EPA and DHA. Higher plants and some animals cannot synthesize PUFA because of lacking of enzyme. Thus, they have to receive them from their food. Although fish and fish oil are common sources of PUFAs as food additive; however, smell is unpleasant and poor

oxidative stability. Therefore microalgae is an alternative sources for serving biotechnological and industrial implications.

1.9 Aims and objectives

The aims of the research presented in this thesis were to expand the understanding of how environmental factors affect the physiological and biochemical composition of the marine haptophyte *Emiliania huxleyi* and the marine diatom *Thalassiosira weissflogii*. An improved understanding of *E. huxleyi* and *T. weissflogii* physiological and biochemical composition will allow better prediction to be made regarding the impending acclimation and adaptation requirements of microalgae to future climate scenarios. Moreover, high value-chemicals (such as, neutral lipid, polyunsaturated fatty acids, pigments etc.) can be obtained from microalgae grown under unfavorable environmental conditions resulting in the benefits for humans to apply in biotechnological industries.

Accurate information on the concentrations of lipids, proteins and other compounds in microalgae is essential for understanding how cells adjust their physiology to changes in their environment and for optimizing production of desired products in algal biotechnology. However, many publish studies contain underestimates or overestimates of the concentrations of biochemical compounds, particularly neutral lipid (Doan & Obbard 2011) and protein (Flynn *et al*. 2010). Therefore, one of the goals of my research was to implement accurate, reliable methods for determining the neutral lipid and protein contents of microalgae (chapters 3 and 4).

Neutral lipids are an important energy storage compound in microalgae and are a crucial aspect of research in the biotechnological application such as biofuels. Therefore the main objectives of chapter 3 were as follows:

(1) To develop the optimal assay for accurate quantification of intracellular neutral lipids in the diatom *T. weissfogii* using a fluorescence dye.

(2) To evaluate the effect of the concentration of inorganic nitrogen in the growth medium on intracellular neutral lipid content *T. weissflogii* using a developed method.

In microalgae and in other microorganisms a high growth rate requires a high rate of protein synthesis. Since proteins are synthesized by ribosomes, a high growth rate requires a high cellular content of ribosomes. These ideas lead to the growth rate hypothesis (GRH) which implies that growth rate should increase in parallel with increases of the ratio RNA:protein. Flynn *et al.* 2010 reported that the uncertainty of the RNA:protein ratio due to the accuracy of the methods for measuring RNA and protein can result in the misinterpretation of data for testing the growth rate hypothesis, and concluded that the RNA:protein ratio has a tendency to be overestimated in many published studies. Therefore the objectives of chapter 4 were:

(1) To develop the protocol for determining the amino acid composition of proteins (combined amino acids) extracted from microalgae.

(2) To evaluate recovery using BSA as a standard to developed a protocol was used for quantifying the combined amino acid contents in the marine haptophyte *E. huxleyi* (chapter 5) and the marine diatom *T. weissflogii* (chapter 6).

The remainder of my research investigated how temperature, light and nitrogen availability affects the elemental and biochemical composition in two microalgae, *E. huxleyi* (chapter 5) and *T. weissflogii* (chapters 6 and 7). In the algal physiology lab at University of Essex, McKew *et al.* (2013 a,b) studied an effect of light intensities and nutrient limitation on the growth rate of *E. huxleyi* CCMP 1516. However, the effect of temperature on *E. huxleyi* CCMP 1516 grown under replete nutrient has not been studied. Furthermore, the application of the bio-optical model (Kiefer & Mitchell 1981) and growth rate hypothesis (GRH) to temperature-limited growth of *E. huxleyi* had not been investigated. The bio-optical model predicts that higher growth requires higher Chl *a*:C because faster growing cells require more energy which requires more

light-harvesting pigments to absorb more light energy, whereas the GRH predicted that growth rate should be correlated with RNA:protein. Therefore the objectives of chapter 5 were:

1) To determine the effect of temperature on growth rate and biochemical composition of *E. huxleyi* using the developed methods from chapters 3 and 4.
2) To examine the correlations between growth rate and RNA:protein to test whether the growth rate hypothesis can be applied to temperature.
3) To examine the correlations between growth rate and chl *a*:C to test whether the bio-optical hypothesis can be applied to temperature.

For the diatom *T. weissflogii*, the interaction between nutrient-limitation with temperature and irradiance has not been investigated previously. Therefore the effect of temperature and light on the diatom *T. weissflogii* was investigated (chapter 6) and focuses on the following objectives:

1) To determine the effect of temperature and irradiance on biochemical composition of *T. weissflogii* in nutrient-limited cultures using the developed methods from chapters 3 and 4.
2) To examine correlations between growth rate and RNA:protein ratio to test whether the growth rate hypothesis can be applied to temperature and irradiance.
3) To examine the correlations between growth rate and C:chl *a* ratio to test whether the bio-optical hypothesis can be applied to temperature and irradiance.
4) To evaluate the imaging proportion of ultrastructure cell using the developed method based on the Nile red stain for neutral lipid droplets.

Dilution rate is one of the key variables in the operation of microalgal cultures. Microalgae grown under the high load of nutrient lead to fast growth rate. In contrast, microalgae have slow growth rate when cells grown under low nutrient. *T. weissflogii* can typically flow with the currents which might contain low or high nutrients. To understanding the elemental and biochemical composition of *T. weissflogii* under different nutrient concentration, the examination of effect of

dilution rate in the cultures was set in a laboratory. Therefore the objective of chapter 7 was to determine the effect of dilution rate on growth rate and biochemical composition of *T. weissflogii.*

Chapter 2: Materials and methods

2.1 Microalgae and culture systems

Organisms: Two species of eukaryotic marine microalgae, *Emiliania huxleyi* (CCMP 1516) and *Thalassiosira weissflogii* (CCMP 1051), were used in this research. The stains were maintained in batch system before they were used in research. They were incubated in 125 mL Erlenmayer flasks containing 50 mL of f/2 medium (Guillard & Ryther 1962) plus silicate for *T. weissflogii* and without silicate for *E. huxleyi.* The flasks were incubated in a culture room at 16^{o}C under a 14:10-h light: dark cycle using photon flux density around 500 µmol photons m^{-2} s^{-1} and without aeration.

Culture media: Cultures were grown in artificial seawater (Berges *et al*. 2001) with added selenium (1 nM Na_2SeO_3), typically enriched to f/2 medium (Guillard & Ryther 1962) for *E. huxleyi* or f/2 plus silicate for *T. weissflogii*. Variations in the concentrations of $NaHCO_3$, NaH_2PO_4, $NaNO_3$, trace metals, and vitamins from the standard artificial seawater and f/2 formulations were employed in most experiments as described in the methods section of Chapters 3 to 7.

Culture systems: Techniques for culturing microalgae in this research are batch and semi-continuous culture. Batch culture is widely used in laboratory and commercial industry because it is easy to operate (Lee & Shen 2004). A batch culture is a closed system. The sterilised culture media is inoculated with microalgae and there is no refill of media in this system. In the beginning, microalgae do not increase the number of cell due to adaptation with the new environment and then they grow rapidly owing to availability of replete nutrients in the media. As time passes, they increase in number with rapid use nutrients and excrete toxic metabolites resulting in a slowdown of growth during the later stages of the process. However, the number

of cells increases gradually or may remain constant. Growth last stage, cells die because nutrients exhausted.

Semi-continuous culture techniques have often been used to investigate cell growth, rate of nutrient consumption, and metabolite production (Quinlan 1986). The semi-continuous culture, culture volume is removed and an equal volume of fresh medium is immediately replaced at regular time intervals in accordance to the desired dilution rate. Hence, this technique is associated with instantaneously enhancing nutrient concentration and diluting cell concentration. This culture method can obtain stable and continuous production and also avoid re-starting microalgae cultures constantly (Fuentes-Grünewald *et al*. 2015).

2.2 Determination of growth rate

Algal cell number was determined using a haemocytometer (chapter 5 and 7) under light microscopy (x 400 magnification) or a Coulter counter (chapter 3 and 6) (Z2 Series COULTER COUNTER®, Beckman Coulter Inc., USA). Specific growth rate (μ) was calculated from cell counts.

$$\mu = \frac{\ln [N (T_2) / N (T_1)]}{T_2 - T_1}$$

Where N (T_1) is the cell concentration (cell mL^{-1}) at time T_1, N (T_2) is the cell concentration at time T_2, and T_2-T_1 is the time difference.

2.3 Determination of chlorophyll *a*

Samples (100 mL of algal suspension) collected on glass fibre filters (MF 200, Fisher Scientific UK Ltd., UK) were put in centrifuge tubes (15 mL). Methanol (100%, 5.0 mL) was immediately added and the samples were ground using a plastic rod until the filters were completely macerated. Then, the sample tubes were kept in the refrigerator at -20°C for 24 hr and centrifuged at 3000 x g for 10 min (Mistral 2000, DJB Labcare Ltd, UK) at room temperature

(RT). The supernatant was removed and an absorbance spectrum measured from 350 to 800 nm using a spectrophotometer (U-3000, Hitachi; Japan). Chlorophyll *a* (chl *a*) was determined using the following equation (Ritchie 2006):

$$\text{Chl } a \ (\text{mg L}^{-1}) = -8.0962\ (A_{652} - A_{750}) + 16.5169\ (A_{665} - A_{750})$$

2.4 Determination of particulate elemental and biochemical composition

Samples of algal suspensions (typically 50 or 100 mL) for determination of particulate elemental composition (C, N, P) and biochemical composition (protein, carbohydrate, neutral lipid) were collected on a pre-combusted glass fiber filters by gentle filtration or centrifugation (for nucleotide).

2.4.1 Particulate nitrogen (PN)

Samples (50 mL of algal suspension) collected on glass fibre filters (MF 200, Fisher Scientific UK Ltd., UK). Filtered samples were dried in an oven at 35°C and stored in a vacuum desiccator until analysis. For determination of particulate nitrogen (Bronk *et al*. 2000), the sample was placed in glass vial (diameter x length: 2.5 x 4 cm) and then 7.5 mL MiliQ water was added and 1.0 mL oxidizing reagent (5.0 g potassium persulfate and 3.0 g boric acid in 35 mL of 1 N NaOH) added. The glass vial was capped with polytetrafluoroethylene (PTFE) lined cap and then placed in a boiling water bath for 1 h. After the bottle was cooled to room temperature, the sample solution was centrifuged at 1,700 x g for 5 min and supernatant was removed to measure the optical density at 220 nm (Collos *et al.* 1999) using the spectrophotometer (U-3000, Hitachi, Japan). A standard curve was prepared using 0, 12.5, 25, 50, 100, 150 and 300 µM $NaNO_3$, with deionised water (Mili Q pore, Mili-Q® Gradient, France) used as a blank.

2.4.2 Particulate phosphorus (PP)

To determine particulate phosphorus (Solórzano & Sharp 1980), the filter containing the sample (50 mL) was soaked in a glass bottle (diameter x length: 2.5 x 4 cm) with 2 mL of 0.017 M $MgSO_4$ and then dried in an oven at 80^oC. The bottle was baked in a muffle furnace (AAF 1100, Cabolite Limited, UK) at 500^oC for 2 h. After that, the bottle was cooled at room temperature (RT), 5 mL 0.2 M HCl was added and covered tightly and then incubated in an oven at 80^oC for 30 min. The bottle was allowed to cool and the supernatant was poured into a centrifuge tube and the bottle was rinsed with 5 mL of Milli Q water. The centrifuge tube was centrifuged at 1,700 x g for 5 min, and the supernatant removed to determine phosphate concentration. For measuring phosphate level (Strickland & Parsons 1972), 0.1 mL oxidizing agent (mixed reagent: 0.024 M ammonium molybdate solution, 0.23 M sulfuric acid, 0.31 M ascorbic acid solution and 1.1 mM potassium antimonyl-tartrate solution following ratios 1:2.5:1:0.5 respectively) was added to 1 mL of sample. After allowing the solution to stand at room temperature for 30-60 min, the absorbance was read at 885 nm using a spectrophotometer (Genway 6300, USA). A standard curve was prepared using 0, 2.5, 5 and 10 µM $NaH_2PO_4 \cdot H_2O$, with deionised water used as a blank.

2.4.3 Particulate organic carbon (POC)

Samples (100 mL of algal suspension) collected on combusted-glass fibre filters (MF 200, Fisher Scientific UK Ltd., UK). Filtered samples were dried in an oven at 35^oC. Calcium carbonate was removed from the dried sample by adding 150 µl 2.0 M HCl and incubated at 35^oC for 3 hours. POC was measured using a solid sample module for total organic carbon analyser (SSM-5000A, Shimadzu, Japan). The acidified dried sample was placed in a ceramic boat that had been baked previously in a muffle furnace at 500^oC for 5 h. The conditions for

analysis were as follows; air flow rate 0.5 L/min, pressure 200 KPa and temperature of 900ºC. The TOC analyzer was calibrated using glucose as a standard (300, 750, 1500, 2250 and 3000 µg C).

2.4.4 Protein content

Filtered samples were obtained by filtering 100 mL of algal suspensions on glass fibre filters (MF 200, Fisher Scientific UK Ltd., UK) and washing using 100 mL 0.5 M ammonium formate to remove salts. The filtered samples were placed in a centrifuge tube (15 mL) and 4.0 mL 0.5 N NaOH was added. The samples were incubated for 10 min at 100ºC and were shaken occasionally. Afterward the samples were cooled quickly by running them with cold water, and samples were centrifuged at 6000 xg (Harrier 15/80, Sanyo, Japan) for 5 min at room temperature. The supernatant was collected for protein assay and the pellet was re-extracted with 2.0 mL 0.5 N NaOH (Modified from Rausch 1981). The supernatants were pooled together and the final volume of the extract was 6.0 mL. Protein content in the sample was measured using the bicinchoninic acid (BCA) assay as modified by Walker (2002). Bovine serum albumin (BSA) and bovine gamma globulin (BGG) were used as protein standards. The standard curves were prepared using concentrates of 0, 25, 50, 100 and 200 µg mL^{-1} and deionised water used as a blank.

Samples or standards 25 µL were put in a 96 well microplate and 200 µL of BCA working reagent was gently added. The working reagent was prepared by mixing a 100:2 ratio reagents A and B. Reagent A consisted of 1.0 g sodium bicinchoninate, 2.0 g $Na_2CO_3 \cdot H_2O$, 0.16 g sodium tartrate dihydrate, 0.4 g NaOH, and 0.95 g $NaHCO_3$ made up to 100 mL with deionised water, pH 11.25. Reagent B consisted of 0.4 g $CuSO_4 \cdot 5H_2O$ in 10 mL of deionised water. After adding the working reagent, the microplate was shaken for 30 seconds using a minishaker (IKA, USA). Microplates were incubated at 37ºC for 30 min and allowed to cool at room temperature. The optical density at 562 nm was measured using a microplate reader (VersaMax, USA) and the protein contents were calculated by comparing with protein standard curve.

2.4.5 Carbohydrate content

Filtered samples were dried in an oven (35ºC) overnight. Total carbohydrate (CHO) content was determined following Aslam *et al*. (2012). Briefly, total CHO consists of 4 fractions; these are colloidal CHO (fraction 1), intracellular-stored CHO (fraction 2), water-insoluble CHO (fraction 3) and residual CHO (fraction 4).

Fraction 1 consists of the CHO in the cultured medium that was secreted by cell. This colloidal CHO was collected by filtering through the glass fibre filters (MF 200, Fisher Scientific UK Ltd., UK). Fraction 2 was obtained by extracting the filter in 3.0 mL 33% (v/v) NaCl (the same as NaCl concentration in media) at 100ºC in a boiling bath for 1 h (Clifton, Nickel-Elctro Ltd, UK). The samples were centrifuged at 3500 x g for 15 min (Mistral 2000, DJB Labcare Ltd, UK) and the supernatant was collected. Although this fraction consists primarily of intracellular-stored carbohydrates (mainly glucan), there could also be a contribution from some external carbohydrate coating the cell.

Fraction 3 consists of the water-insoluble CHO (mainly mucilage from surface of the frustule) that was extracted using hot bicarbonate. 3.0 mL 0.5 M $NaHCO_3$ was added into the pellet from the fraction 2 and incubated for 1 hour at 100ºC. The samples were centrifuged as described above and the supernatant was collected as CHO fraction 3. Fraction 4 consists of the bicarbonate-insoluble CHO that was attached and linked with the silica cell wall. It was extracted by adding 2.0 mL 1 M NaOH and 0.2 M $NaBH_4$ to the pellet, followed by incubating and centrifuging as described above. The supernatant was collected and CHO was liberated from the cell wall as CHO fraction 4.

The CHO concentration in each of the extracts was determined using the phenol sulfuric assay (modified from Dubois *et al*. 1956). Briefly, 0.5 mL each extracted CHO fraction was added to a glass test tube (1.5 x 10 cm) and 0.5 mL 5% phenol solution was added. The samples were mixed using a vortex (MS2 Minishaker, UK). Then 2.5 mL concentrated H_2SO_4 was added and

the sample mixed immediately and allowed to stand in a fume hood cabinet for 30 min before measuring the carbohydrate content using a spectrophotometer (GENESYS 10S UV-Vis, Thermo Fisher Scientific Inc., USA) at 490 nm. Glucose was used as a standard at concentrations of 0, 10, 20, 40, 60, 80, and 100 µg mL^{-1}. The detection limits of glucose for phenolic sulfuric assay was 5 µg mL^{-1} (Aslam *et al*. 2012). Total carbohydrate contents were calculated from the collecting CHO part 1 to part 4 following equation:

$$\text{Total carbohydrate } (\mu g\ mL^{-1}) = \sum (CHO_{\text{fraction 1}} + CHO_{\text{fraction 2}} + CHO_{\text{fraction 3}} + CHO_{\text{fraction 4}})$$

2.4.6 Neutral lipid content

2.4.6.1 Nile red (NR) preparation

A stock solution of 500 µg mL^{-1} Nile Red (Nile red 99%, ACROS Organics™, UK) was prepared by dissolving 5 mg NR in 1.0 mL acetone (HPLC grade). Aliquots (100 µL) of the NR solution were transferred into a brown-coloured bottles, each containing 900 µL of acetone. The aliquoted NR stock solution bottles were wrapped on top using parafilm and stored in a freezer (-20°C). The NR solution was thawed at room temperature (RT) before using.

2.4.6.2 Triolein preparation

Triolein (1,2,3-Tri(cis-9-octadecenoyl)glycerol) was used as a lipid standard in the neutral lipid assay. Triolein (≥99%, Sigma-Aldrich, USA) 500 mg mL^{-1} (in chloroform) was diluted with isopropanol to make an intermediate stock of 1 mg mL^{-1}. Isopropanol has relatively low background fluorescence (Priscu *et al*. 1990). A working standard (100 µg mL^{-1}) was prepared by bringing 500 µL of the intermediate stock to 5.0 mL with deionized water in a volumetric flask. The working stock was vortexed forcefully for about 1 min to form micelles before preparing a standard curve.

The development of the neutral lipid assay is fully described in chapter 3. Briefly, 3 mL cell samples (9 samples from triplicate cultures) were collected in clear plastic cuvettes (length x width x high: 1 x 1 x 4.5 cm) and then kept in a freezer (-20°C) until analysis. The samples were

thawed at RT and then 150 µL dimethyl sulfoxide (DMSO) was added to reach 5% (v/v) for enhancing the efficiency of NR penetration into the algal cells. 6.3 µL of 500 µg mL^{-1} NR stock solution was added to obtain 1 µg mL^{-1} final concentration. The top of cuvette was covered with parafilm to prevent the loss of acetone vapors, and the sample was mixed using a vortex mixer (MS2 Minishaker, UK) at speed 1800 rpm min^{-1} for 10 seconds. The samples were kept in a dark room for 5 min before measuring lipid using a fluorescence spectrometer (LS 50B, Perkin Elmer; UK) using a fixed excitation wavelength of 529 nm and emission wavelength of 589 nm. The excitation and emission slit widths were set 5.0 nm and scanned at speed 200 nm min^{-1}. To allow quantification, standard curves of triolein suspensions were prepared to give concentrations of 0, 2.5, 5, 10, and 20 µg mL^{-1} and deionised water used as a blank.

2.5 Determination of nucleotide

2.5.1 Determination of RNA

To obtain samples for RNA, algal suspensions (100 mL) were centrifuged at 6000 x g for 10 min. The supernatant was discarded and the pellet was washed three times using 20 mL of 0.5 M ammonium sulfate to remove salts. The pellet was kept at -80^{o}C if the sample was not extracted immediately. RNA from pellet was extracted using TRI reagent® (Sigma-Aldrich, USA). Then, RNA was measured content at 260 nm using a Nanodrop spectrophotometer (Labtech, UK).

2.5.2 Determination of DNA

Samples for DNA were collected in the same way as those for RNA. DNA was extracted from the pellet using a modification of Griffiths *et al*. (2009). The pellet was transferred to a silica (0.1 mm diameter) beating tube and put on ice bath. Then, 600 µL of Cetyl-trimethyl-ammonium-bromide (CTAB) and 500 µL of phenol:chloroform:isoamyl alcohol mixture; 25:24:1 (sigma, USA) were added, and the tube was put in a beating machine to break cells for 48 seconds (2 times). After beating, the tube was put on ice and centrifuged at 15000 x g for 15 min. 700 µL of

supernatant was transferred into a sterile microcentrifuge tube and 1 mL of 30% PEG 6000 in 1.6 M NaCl solution was added and left at room temperature overnight. The sample tube was centrifuged at 15000 x g for 5 min and supernatant was decanted. 500 µL of 70% ethanol was added to wash the pellet and centrifuged at 15000 x g for 5 min. The supernatant was decanted and a tube was allowed to dry for 15 min before the DNA was resuspended with 40 µL deionised water and measured DNA content at 280 nm using a Nanodrop spectrophotometer (Labtech, UK).

2.6 Photosynthesis parameters

A 30 mL sample was taken for measuring the photosynthesis versus irradiance (PE) curve. The sample was enriched to an activity of 1 µCi mL^{-1} of $Na^{14}CO_3$ and 24 x 1 mL aliquots dispensed into glass 8 mL (diameter 1.5 cm) scintillation vials. The aliquots were incubated over a gradient of irradiances in a temperature-controlled "photosynthetron" (Lewis & Smith, 1983). The temperature during the incubations was kept constant at 14, 18 and 22°C with a circulating water bath. Incubations were terminated after 30 min. Dissolved inorganic carbon was driven off by adding 250 µl of 3 N HCl and then the vials were left overnight without caps in a fume hood before adding 4.5 mL of scintillation cocktail (ULTIMA GOLD™ LLT, Perkin Elmer) and counting with liquid scintillation analyzer (Tricarb 2910 TR; Perkin Elmer, USA). Total activity of $NaH^{14}CO_3$ in the incubation was determined on 20 µl aliquots of sample taken directly into 4.5 mL of scintillation cocktail with 200 µl of phenylethyamine.

The CO_2 fixation rate was calculated from:

$$\frac{mmol\ \ C\ \ fixed}{L\ \ h} = \frac{DPM(sample) - DPM(T_0)}{DPM(TA)} \cdot \frac{Volume(TA)}{Volume(Sample)} \cdot \frac{[TCO_2]}{Incubation\ \ time}$$

Where: DPM (sample) = disintegrations per minute in the sample

DPM (T_0) = disintegrations per minute in the time zero

DPM (TA) = disintegrations per minute in the total activity vial

Volume (TA) = volume of sample in the TA vial (e.g., 20 µL = 0.02 mL)

Volume (Sample) = sample volume (e.g., 1.0 mL)

TCO_2 = total inorganic carbon concentration (mmol L^{-1})

The total inorganic carbon concentration (TCO_2) was measured on filtered (0.2 µm pore filter) medium using a liquid sample module for total organic carbon analyzer (SSM-5000A, Shimadzu, Japan).

The CO_2 fixation rate was converted from mmol L^{-1} to mg L^{-1} by multiplying by 12 (the atomic weight of C) and then dividing by the chlorophyll *a* concentration to obtain chlorophyll *a*-specific rates, and the results were fitted using least-squares non-linear regression (Solver, Excel 2007) to the model of Platt *et al*. (1980).

$$\mathrm{P}^{Chl} = P_m^{Chl}\left[1 - exp\left(\frac{-\propto^{Chl} E}{\mathrm{P}_m^{Chl}}\right)\right]$$

Where: P^{Chl} is the rate of photosynthesis, normalized to Chl *a* (gC $gChl^{-1}$ h^{-1}) at irradiance *E* (µmol photons m^{-2} s^{-1}), P_m^{Chl} is the light-saturated photosynthesis rate and $\propto^{Chl}$ (gC $gChl^{-1}$ h^{-1}) (µmol photons $m^{-2}s^{-1})^{-1}$ is the initial slope of the PE curve.

2.7 Light absorption

Culture samples of 30 mL were collected and centrifuged at 3000 x g for 10 min (Mistral 2000, DJB Labcare Ltd, UK) at room temperature. The supernatant was removed and 3 mL of fresh medium was added. The samples were mixed gently and an absorbance spectrum measured from 380 to 800 nm using a spectrophotometer fitted with an integrating sphere to collect

forward scattered light (U-3000, Hitachi, Japan). Fresh medium was used as blank. The chlorophyll specific light absorption coefficient of light capture in the cultures was determined by following the equation:

$$a^{Chl} = 2.303 \frac{O.D.}{(0.01\ [Chl\ a])}$$

Where: a^{Chl} is the chlorophyll specific light absorption coefficient [with units of m^2 (g Chl *a*)$^{-1}$]

O.D. is the optical density in a 1 centimetre of path length cuvette

[Chl *a*] is the chlorophyll *a* concentration in mg chl *a* L^{-1} in the sample (which is the same value as g m^{-3})

0.01 is the conversion from centimetre to metre

2.8 Pigment analysis

2.8.1 Sample preparation and extraction

Ultra performance liquid chromatography (UPLC) was used to quantify chlorophylls and carotenoids. Culture samples of 100 mL were filtered through glass fibre filters and stored in the freezer (-80ºC) for *E. huxleyi* (chapter 5) and in liquid N_2 for *T. weissflogii* (chapters 6 and 7) until analysis. Whilst still frozen, the filtered samples were placed in Teflon lined screw-capped tube and extracted using 2.0 mL 98 % buffered methanol (buffered with 2% 0.5 M ammonium acetate pH 7.1) under dim light. The samples were incubated in a beaker containing ice to reduce the conversion of chlorophyll *a* into chlorophyllide *a* by chlorophyllase. The samples were then ultrasonicated for 8 min for *E. huxleyi* and for 12 min for *T. weissflogii*. The extracts were filtered through a 0.2 µm pore polypropylene filter using a glass syringe to remove cell debris.

2.8.2 Pigment assay

Pigment separation was performed using a method modified from Zapata *et al*. (2000, 2004). Briefly, the filtered MeOH extracts were automatically injected into the ultra performance liquid chromatography (UPLC) of *ACQUITY^{TM} Waters* System (MS, USA). A C_8 column (50 mm x 2.1 mm, 1.7 µM particle size, 100 Å pore size: Waters; MS, USA) was used to separate pigments. The column was thermostatted at 25^{o}C and the sample chamber was held at 5^{o}C. The mobile phases were HPLC glade. Eluent A was a mixture of methanol: acetonitrile: aqueous pyridine (0.25 M, pH adjusted to 5.0 with pure acetic acid) (50:25:25 v/v/v) while eluent B was comprised of acetonitrile: acetone (80:20 v/v). The programed flow rates and gradient is given in Table 2-1. Peak detection was determined using a diode array absorption detector (PDA Eλ Detector, Waters, USA). Pigments were identified by comparison of relative retention times given by Zapata *et al*. (2000, 2004) and reference absorbance spectra from Jeffrey *et al*. (2005). The detector was calibrated with a chlorophyll *a* standard (Sigma Aldrich, USA) run at concentrations of 0, 0.5, 1, 2, 4, 6, 8, and 10 µg mL^{-1}.

Table 2-1. The gradient elution of pigment analysis using UPLC.

Time (min)	Flow (mL min^{-1})	% A	% B	Curve*
0.00	0.2	100	0	-
1.00	0.2	100	0	1
2.57	0.2	80	20	2
6.50	0.2	0	100	8
9.00	0.2	100	0	6

* Eleven gradient curves for the gradient segment. For example, No. 1: immediately specified condition, No. 2-5: convex, No. 6: linear, No. 7-10: concave, and No. 11: maintain start condition.

2.8.3 Pigment quantification

Chl *a* was used as reference pigment because it is a common pigment in all marine algae, and the accessory pigments were quantified as pigment-to-Chl *a* (molar : molar) ratios. Light

absorption was measured at a wavelength of 440 nm and reported as integrated area unit (AU). The molar extinction coefficients (*E*) at 440 nm acquired from Jeffrey *et al*. (2005) were used for pigment quantification. For 4-keto-19'-hexanoyloxyfucoxanthin (Hex-kfuco) whose molar extinction coefficients is not available, the molar extinction coefficient of 19'-hexanoyloxyfucoxanthin (Hex-fuco) was used.

2.9 Fatty acid profile

2.9.1 Preparation of glassware

Glassware, glass vials and PTFE lids were immersed in the dishwasher detergent for 2 hours and rinsed with water and then immersed in 5% hydrochloric acid bath at least for 2 hours. All glass and plastic ware was then rinsed with deionised water and methanol respectively.

2.9.2 Lipid extraction

Samples of algal suspensions (100 mL) were filtered onto glass fibre filters and stored in liquid N_2 until analysis. The filtered samples were placed into a glass screw-cap vial (20x80 mm). Lipids were extracted in 9.5 mL of a solution of methanol: chloroform: water (10:5:4 v/v/v) following Bligh & Dyer (1956). The glass vials were covered with PTFE lid and then sonicated for 30 min at room temperature. Then 2.5 mL chloroform and 2.5 mL deionised water were added to the samples, which were then placed in the freezer (-20^{o}C) overnight to separate the two phases. The upper aqueous layer was removed using glass Pasteur pipette. The lipids were contained in the lower chloroform layer. The solvent combined in lipid extraction was evaporated under a stream of nitrogen gas at 37^{o}C using a heating block.

2.9.3 Preparation of methyl esterification

The dried lipids were resuspended using 1.0 mL of the mixed reagent (toluene: methanol 1:1 v/v). Then, 1.0 mL of 0.2 M methanolic potassium hydroxide was added to the sample to hydrolyse the lipids. The organic aqueous phase was swirled to mix and incubated at 37^{o}C for

30 min, then 0.25 mL of 1 M acetic acid was added into the solution phase to stop the reaction and to neutralize the pH of the sample. Next, 5 mL of the mixed reagent (hexane: chloroform 4:1 v/v) and 3.0 mL deionised water were added to the sample. The extract was sonicated for 30 min and then kept in a refrigerator overnight to separate the two phases. The aqueous lower layer was removed using a glass Pasteur pipette and 3.0 mL of 0.3 M sodium hydroxide was then added to the sample. The upper aqueous phase (the nonpolar organic solvent phase) was filtered using a glass syringe (10 mL) which contained the glass wool fibre with 300 mg of sodium hydroxide on top in order to absorb and remove water from aqueous phase. The sample was evaporated under a stream of nitrogen at 20-25^{o}C until dry. The dried fatty acids were resuspended with 0.5 mL of hexane before injection on GC/MS.

2.9.4 GC/MS condition

Fatty acids methyl ester (FAME) standards and samples were analysed using gas chromatography/mass spectrometer (GC/MS) (7890A, Agilent Technologies, USA) at an ionization energy of 70 eV for m/z range of 50-500, and using helium as carrier gas at a flow rate of 1.0 mL min^{-1}. A HP-5 capillary column (30 m x 0.25 mm x 0.25 µm; Agilent J&W, USA) consisted of 5%-phenyl methylpolysiloxane was used to separate the fatty acids. The injector (splitless mode) and detector temperatures were 310^{o}C and 320^{o}C, respectively. The initial column temperature was held for 5 min at 40^{o}C, then increased at 25^{o}C min^{-1} (ramp 1) to 160^{o}C, and then at 2^{o}C min^{-1} (ramp 2) to 240^{o}C, then finally increased at 25^{o}C min^{-1} (ramp 3) to 310^{o}C and held for 5 min. A standard fatty acids methyl ester (37 component FAME, Supelco, USA) solution was prepared 50-800 µg mL^{-1} and 20 µg mL^{-1} of nonadecanoic acid methyl ester (C19:0) (Sigma-Aldrich, USA) was used as internal standard. A calibration curve between the peak abundance of each standard FAME and the peak abundance of the internal standard was established to calculate the concentration of each of the FAMEs in the samples. Fatty acid identities were determined by comparison with the FAME standard retention time and mass spectra of the National Institute of Standards and Technology (NIST) spectral database version 11.

Using the GC protocol outlined above, 33 peaks from 37 components of FAME standard were identified. This protocol was used to collect the data reported in chapters 5 and 6. A new GC protocol was therefore developed to obtain more FAME standard peaks. With the new protocol, 35 of the 37 components of FAME standard could be identified. The new condition was held for 1 min at 50^{o}C, then increased at 4^{o}C min^{-1} (ramp 1) to 160^{o}C, and then at 3^{o}C min^{-1} (ramp 2) to 200^{o}C, then finally increased at 10^{o}C min^{-1} (ramp 3) to 230^{o}C and held for 5 min. The flow rate was 1.2 mL min^{-1}. This protocol was used to collect the data reported in chapter 7.

2.10 Amino acids assay

2.10.1 Samples preparation

Algal samples (50 mL) was centrifuged at 10000 x g for 5 min (Centrifuge 5403, Eppendorf, Germany) at the same temperature following the cultured cells. The supernatant was discarded and a pellet was washed three times using 20 mL of 0.5 M ammonium sulfate to remove salts. The pellet was transferred to a sterile microcentrifuge tube (2 mL) and stored at -80^{o}C.

2.10.2 Extraction of free amino acids

Free amino acids were extracted from *E. huxleyi* (chapter 5) and *T. weissflogii* (chapter 6) using a modification of Salazar *et al*. (2012). Briefly, a clean, sterile glass bead (diameter = 2 mm) was placed into a pellet sample tube. Then, 125 µL of ice cold 50% (v/v) methanol:deionised water was added to the sample tube, and the sample tubes were mixed using a minishaker (MS2 Minishaker, UK) at 1800 rpm/min for 3 min. The samples were incubated on a dry ice bath for 5 min and sonicated in an ultrasonic cleaner (Decon Ultrasonic, England) for 1 min. Then the samples were centrifuged at 15000 x g (Centrifuge 5403, Eppendorf, Germany) at 4^{o}C for 5 min. The supernatant was collected and a pellet was reextracted with 125 µL of an ice cold 50% (v/v) solution as described above. The supernatants were combined and stored at -80^{o}C if the sample was not derivatised immediately.

2.10.3 Extraction of combined amino acids

The pellets from 2.10.2 were extracted to obtain bound amino acids in cell using a modification of Kaiser & Benner (2005). Each pellet was transferred into an unused glass vial (1.5 x 10 cm). 5 µL of 12 mM ascorbic acid (final concentration at 10 µL mL^{-1}) was added to prevent oxidation of amino acids by nitrate (Kaiser & Benner claimed from Robertson *et al*. 1987). 500 µL of 6 M hydrochloric acid (HCl) was added and mixed gently using a vortex mixer (MS2 Minishaker, UK). Then, 5 µL of 100 mM phenol (final concentration at 1 mM) was pipetted in to the hydrolysis sample vials to protect tryptophan from hydrolysis and then mixed gently again. The hydrolysis glass vials were capped with polytetrafluoroethylene (PTFE) lined caps and purged with nitrogen gas for 5 min. Then the glass vials were placed on a heating block (BT3, Grant Instruments Ltd, England) at 110^{o}C for 20 h. The hydrolysed samples were allowed to cool at room temperature. 1500 µL of deionised water was added and mixed. The sample solution was transferred to a microcentrifuge tube and centrifuged (5415D, Eppendorf, Germany) at 10000 x g for 10 min to remove cells debris. Next, 50 µL of the supernatant was transferred to an unused small HPLC vial (1 x 3 cm) and dried under a stream of nitrogen. 50 µL of water was added twice after drying the amino acid samples to ensure that all the HCl was removed.

2.10.4 AccQ·Tag ultra amino acid derivatisation

Prior to LC-MS/MS analysis, amino acids were derivertised with a 6-aminoquinolyl-N-hydroxysuccinimidyl carbamate (AQC) based kit (Waters, Massachusetts, USA). For free amino acids, 10 µL of extracted sample was mixed with 70 µL of AccQ·Tag Ultra borate buffer. After that, 20 µL of AccQ·Tag reagent (1 mL of 2B reagent was added in 2A reagent bottle and mixed using vortex for 10 seconds and then the mixing solution reagent was incubated at 55^{o}C for 10 min). The sample solution was kept for 1 min at RT before incubating in an oven (Shake 'n' Stack, Themo Scientific Ltd., USA) for 10 min at 55^{o}C. For bound amino acid, 80 µL with AccQ·Tag Ultra borate buffer was added to the vials containing the dried amino acid samples. Then 20 µL of AccQ·Tag reagent was added in each sample and as described above. A

standard curve was prepared from an amino acid standard solution containing 17 amino acids (Waters Massachusetts, USA) at concentrations of 0, 1, 2, 4, 6, 8, and 10 pM μL^{-1} and deionised water used as a blank.

2.10.5 Amino acid quantification using LC-MS/MS

Amino acids were analysed using a LC-MS/MS system (Acquity, Quatro Premier XE, Waters, Massachusetts, USA). Amino acids were separated using a 1.7 µm column (AccQ·Tag Ultra column, Waters, Massachusetts, USA) set to 55ºC. A flow rate of mobile phase in column was 0.7 mL min^{-1}. Mobile phase was made using manufacturer's solvents which consisted of 10% AccQ·Tag Ultra concentrate solvent A (eluent A, Massachusetts, USA), and 100% AccQ·Tag Ultra solvent B (eluent B, Massachusetts, USA). The amino acids were separated using a gradient method: 0-0.54 min (99.9% A), 5.74 min (90.0% A), 7.74 min (78.8% A), 8.04-8.64 min (40.4 %A), 8.73-10 min (99.9% A). The mixtures of amino acids were determined using multiple reaction monitoring (MRM) under ESi+ mode with the conditions and transitions as stated in Salazar *et al*. (2012).

2.11 Microscopic image

2.11.1 DAPI preparation

A stock solution of DAPI (4′,6-diamidino-2-phenylindole, Invitrogen™, USA) was prepared by dissolving 5 mg mL^{-1} in distilled water under dim light and aliquots stored at -20°C.

2.11.2 Sample preparation

Cells grown under exponential phase were harvested at the cell density of approximately 1.5 - 2.0 × 10^5 cells mL^{-1}, placed in a sterile microcentrifuge (1.5 mL) and then centrifuged at 4,000 x g for 5 min. The pellet was resuspended using fresh media. DAPI was added to a final concentration of 10 µg mL^{-1}. The sample was mixed gently and kept in the dark at room temperature (RT) for 2 min. Nile red solution (from 2.4.6.1) was added to a yield a final concentration of 10 µg mL^{-1} and kept at RT for 1 min.

2.11.3 Microscopy

For image acquisition, a Nikon A1si confocal laser scanning microscope (CLSM) was used with a planapochromatic VC 1.4 NA 60x magnifying oil-immersion objective (Nikon Corp., Tokyo, Japan). Images were acquired in four channels, using one-way sequential line scans. Nile red was excited at 488 nm, and its emission collected from 500 to 550 nm. Chlorophyll *a* autofluorescence in chloroplasts was excited at 637 nm, and its emission collected from 662 to 737 nm. DAPI labelling dsDNA was excited at 405 nm, and its emission collected from 425 to 475 nm. Differential interference contrast images for cellular outlines were acquired using the transmitted light detector. In all cases, no offset was used, and the scan speed was ¼ frame s^{-1} (galvano scanner). The pinhole size was 34.5 µm approximating 1.2 times the Airy disk size of the 1.4 NA objective at 525 nm. Scanner zoom was centred on the optical axis and set to a lateral magnification of 55 nm $pixel^{-1}$. Axial step size was 140 nm, with 30-50 image planes per z-stack. At least 50 cells with average to fair signal strength in all channels were examined.

2.11.4 Image processing and analysis

2.11.4.1 Pruning

Datasets should be checked for cellular integrity and signal strength. Cells that appear damage, with poor contrast, or that moved during image acquisition were excluded from the analysis.

2.11.4.2 Cellular volume determination

The cellular volume can be approximated by measuring a cylindrical shape of *T. weissflogii* calculated using geometric equation (Hillebrand *et al.* 1999).

$$V = \P \cdot r^2 \cdot h$$

Where: V = cell volume (μm^3)

¶ = 3.14

r = radius (µm) or half the diameter of the cylindrical shape

h = high (µm) or length of cylindrical shape

2.11.4.3 Volume quantification

The MATLAB software (version R2012b with Image Processing Toolbox; Math Works Inc., Natick, Massachusetts, USA) was used to analysis the images in which objects are white and background is black. The images were used to determine the volume of the objects of interest in each channel (Fig 2-1).

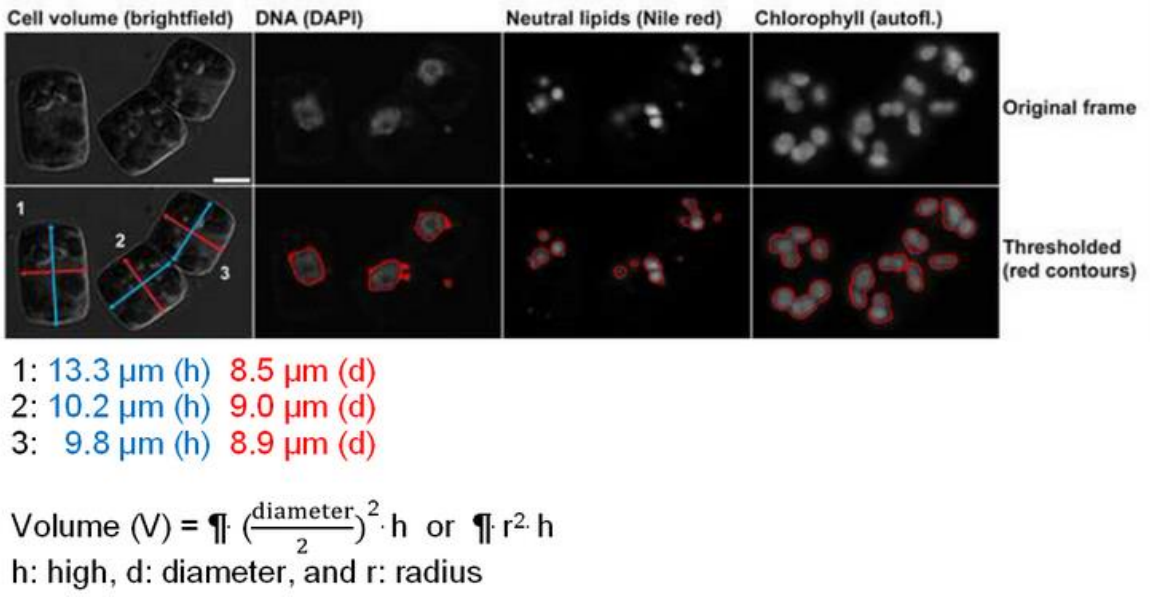

Figure 2-1. The four acquired channels (top row) of differential interference contrast (DIC) for cell volume, DAPI for DNA, Nile red for neutral lipids, and autofluorescence of chlorophyll for chloroplasts. Radius (r), a half of diameter, and high (h) are determined in DIC images (first column), and cell volume (V) approximated using a cylindrical model. The volume of the subcellular, fluorescent components is determined by global thresholding (bottom row). Scalebar 5 µm.

Chapter 3: Development and application of Nile red (NR) fluorescence based method for quantification of neutral lipid content in a marine diatom

3.1 Introduction

Increased fuel demand and dramatic changes in the climate including global warming have turned worldwide attention to the identification of alternative energy sources to replace fossil fuels. Microalgae are among possible candidates for biofuel production and may replace fossil fuel because they yield high quantities neutral lipid content (Singh & Gu 2010; Amaro *et al*. 2011). The method for neutral lipids quantification needs to be an accurate determination.

Chemical lipid extraction is a traditional technique used to quantify lipid content in microalgae; however, the method can be complex, time consuming and labor intensive. It requires a large sample size and causes decomposition or oxidation of the lipids. Fluorescence measurement is an alternative technique that employs fluorescent lipophilic dyes for quantification of neutral lipids in microalgae. Nile red (NR) has been suggested for use in screening and quantifying intracellular neutral lipid (Cirulis *et al*. 2012) because NR does not cause dye precipitation when determining lipid quantification (count) with cytometry (Cirulis *et al*. 2012). Additionally, NR is a quick and inexpensive method (Lee *et al*. 1998; Huang *et al*. 2009; Orr & Rehmann 2014). The fluorescence intensity of the stained samples is correlated to the neutral lipid content using a calibration curve (Bertozzini *et al*. 2012).

Nile red (9-diethylamino-5H-benzo[alpha]phenoxazine-5-one), or Nile blue oxazone, is a benzophenoxazone dye synthesized from Nile Blue (Fig. 3-1). The excitation and emission spectra of Nile red shift further toward the blue end of the spectrum as the polarity of the solvent decreases (Dutta *et al*. 1996). Nile red fluoresces poorly in water, but in other solvents its

maximum fluorescence intensity is a good indicator of the dye's hydrophobic environment (Jose & Burgess 2006; Stuart *et al*. 2005).

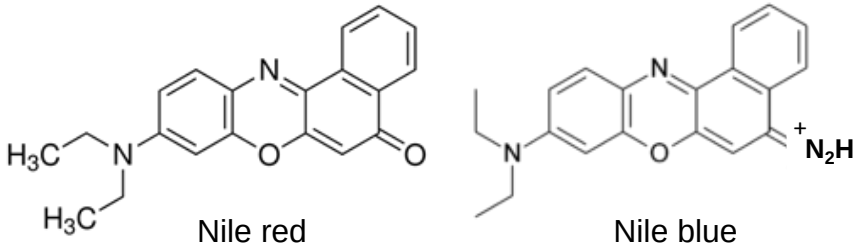

Nile red Nile blue

Figure 3-1. Structure of Nile red and Nile blue

Recently, there have been several NR studies that have developed or improved techniques to achieve accurately quantification intracellular lipid (Pick & Rachutin-Zalogin 2012; Abdo *et al*. 2014). The factors, affecting the success of reading for lipid quantification staining approach, are presented as follow:

1) the dyes

NR (2 µg mL^{-1}) was found to be an optimal lipophilic dye for staining *Scenedesmus dimorphus* and *Chlorella vulgaris* to develop correlation between fluorescence intensity and cellular lipid content, compared with BODIPY 505/515 (4,4-difluro-1,3,5,7-tetramethyl-4-bora-3a,4a-diaza-s-indacene) and Vybrant DiO-C18 (3,3'-dioctadecyloxacarbocyanine perchlorate). Using NR reduced the noncellular events and fluorescence variability in a flow cytometer (Cirulis *et al*. 2012). Furthermore, Wu *et al*. (2014) found that both NR and BODIPY 505/515 can be used as staining dyes for the detection of intracellular neutral lipid content using a fluorescence spectrophotometer in the dinoflagellate *Prorocentrum micans* and the diatom *Phaeodactylum tricornutum*.

2) Nitrogen in cell

NR fluorescence emission in the N-deficient cells in the green microalgae *Dunaliala salina* showed a predominant emission peak of the maximal emission at around 580 nm that had a high lipid content. While N-saturated control cells with low lipid contents presented a much smaller peak at around 625 nm (Pick & Rachutin-Zalogin 2012).

3) NaCl concentration

The maximum-emission wavelength of NR in *D. salina* incubated in 3 M NaCl was blue-shifted by about 20 nm, as compared to 0.5 M NaCl (Pick & Rachutin-Zalogin 2012).

4) Solvents

Polar substituents on the aromatic rings of many fluorescent compounds are known to be sensitive to the chemical and physical properties of solvents which leads to different emission spectra (Table 3-1).

Table 3-1. Solvent dependence of wavelength absorption and emission in Nile Red (Greenspan & Fowler 1985).

Solvent	λmax absorption (nm)	λmax emission (nm)
Water	591	657
Ethanol	559	629
Acetone	536	608
Chloroform	543	595
iso-Amyl acetate	517	584
Xylene	523	565
n-Dodecane	492	531
n-Heptane	484	529

The robust cell walls of many microalgae can prevent NR from crossing cell membrane and entering the cell (Chen *et al*. 2009). To overcome this problem, it has been suggested that using a permeabilisation treatment and extending incubation time may allow NR screening to be used on cells that possess robust cell walls (Krishnamoorthy & Ira 2001; Elsey *et al*. 2007; Doan & Obbard 2011). Dimethyl sulfoxide (DMSO), glycerol, and ethylene glycol are widely used to promote NR permeability into the cell (Doan & Obbard 2011; Natunen *et al*. 2014).

Accurate information on the concentrations of lipids and other compounds in microalgae is essential for understanding how cells adjust their physiology to changes in their environment and for optimizing production of desired products in algal biotechnology. However, many publish studies contain underestimates or overestimates of the concentrations of biochemical compounds, particularly neutral lipid (Doan & Obbard 2011). Therefore, one of the goals of my

research was to implement accurate, reliable methods for determining the neutral lipid contents of microalgae (chapters 3 and 4). The objectives of this study were: (i) to find out the optimal assay for accurate quantification of intracellular neutral lipids in *Thalassiosira weissfogii*, and (ii) to evaluate the effect of the concentration of inorganic nitrogen in the growth medium on intracellular neutral lipid content and cellular chlorophyll content of *T. weissflogii*.

3.2 Operating conditions and sampling

3.2.1 Development of protocol to measure neutral lipid content

Thalassiosira weissflogii CCMP 1051 was grown in 1,000 mL in pyrex flask with 400 litre working volume of artificial seawater (Berges *et al*. 2001) enriched to f/2 plus silicate (Guillard & Ryther 1962) medium, with 3 mM $NaHCO_3$ and 1 nM Na_2SeO_3. Duplicate batch cultures were incubated at 16°C and photosynthetic photon flux densities (PFD) of 500 ± 10 µmol photons $m^{-2}s^{-1}$ on a 14:10 h light:dark cycle. Cells in the late exponential phase were used to provide material for optimizing the neutral lipid assay.

The relative neutral lipid content of cells was determined by fluorometric assay using the dye Nile red (NR). The assay was optimized by assessing the effects of NR concentration (0.5 to 2.0 µg mL^{-1}), incubation time (1-20 minutes), and incubation with DMSO as a carrier (0-20%), on the peak wavelengths of fluorescence excitation and emission and the intensity of the measured fluorescence. Nile red (Nile red 99%, ACROS Organics™) was dissolved in 100 % acetone (HPLC grade) and aliquots stored at -20°C. 3-12 µL of NR solution were added to 3 mL of sample to obtain final concentration of NR in the sample ranging from 0.5 to 2.0 µg mL^{-1}. Excitation and emission spectra were measured using a fluorescence spectrometer (LS 50B, Perkin Elmer; UK) and fixed wavelength excitation at 529 nm, emission at 589 nm, and both slit of excitation and emission at 5 nm. Triolein (1,2,3-Tri(cis-9-octadecenoyl)glycerol) (≥99%, Sigma, USA) was used as lipid standard for calibrating the process.

3.2.2 Application of developed protocol: the effect of nitrogen on growth and elemental composition

T. weissflogii CCMP 1051 was maintained in f/2 plus silicate medium, with 3 mM $NaHCO_3$. Cells in the exponential phase were used to inoculate batch cultures, containing 20 µM $NaH_2PO_4 \cdot H_2O$, f/8 metals, 1 nM Na_2SeO_3, f/4 vitamins, and different concentrations of $NaNO_3$ (50, 100, 200 and 882 µM). The initial cell density was approximately $1x10^4$ cells mL^{-1}. Cultures were incubated in duplicate in 1-litre glass bottles at 16ºC on a 14:10 h light:dark cycle under fluorescent light of 500 µmol photons m^{-2} s^{-1}. The cultures were gently stirred with a magnetic stir bar and continuously aerated with filtered air through a 0.22 µm membrane filter.

Cultures were sampled daily to obtain material for chemical and physiological assays. Cell abundance was determined using a Coulter particle counter (Z2 Series COULTER COUNTER®, Beckman Coulter Inc., USA). Samples were collected for chlorophyll *a* content (see chapter 2), particulate nitrogen (PN), particulate phosphorus (PP) and lipid content. Lipid content was assessed using the optimized NR method developed for *T. weissflogii* CCMP 1051.

3.3 Statistical analysis

Statistical analysis was performed using Statistical Package for the Social Sciences (SPSS version 19). A paired sample student t-test was performed for pair-wise comparison, while an analysis of variance (ANOVA) with the post hoc test (Tukey HSD) used for multiple comparisons.

3.4 Results

3.4.1 Development of fluorometric quantification of neutral lipid content

The relative neutral lipid in *T. weissflogii* CCMP 1051 was determined by fluorometric assay using the dye Nile Red (NR). Initially, the excitation wavelength was set at 530 nm to obtain an emission spectrum from 500 to 800 nm for NR stained *T. weissflogii* because this wavelength was used previously on *T. pseudonana* CCMP 1335 (Yu *et al*. 2009). When the excitation wavelength was fixed at 530 nm, the emission was scanned under conditions: an excitation slit width of 5.0 nm and emission slit width of 5.0 nm at a scan speed of 200 nm min^{-1}. Unstained *T. weissflogii* cells gave the highest peak at 684-686 nm (Fig. 3-2), which is the chlorophyll peak (Eltgroth *et al*. 2005; De la Hoz Siegler *et al*. 2012). Cells stained with NR (1 $\mu g \cdot mL^{-1}$) gave peak emission at a wavelength of 589 nm (Fig. 3-2). Therefore, emission wavelength at 589 nm was fixed to optimize the excitation wavelength.

Having shown in figure 3-2 that the maximum fluorescence emission was at a wavelength of 589 nm, *T. weissflogii* cells yielded maximum excitation at 529 nm when cells were stained with different NR concentrations (0.5, 1.0, 1.5 and 2.0 $\mu g\ mL^{-1}$). In addition, concentration of NR at 1.0 $\mu g\ mL^{-1}$ gave the highest fluorescence intensity (Fig. 3-3). Therefore, 1.0 $\mu g\ mL^{-1}$ of NR was be used to dye the samples.

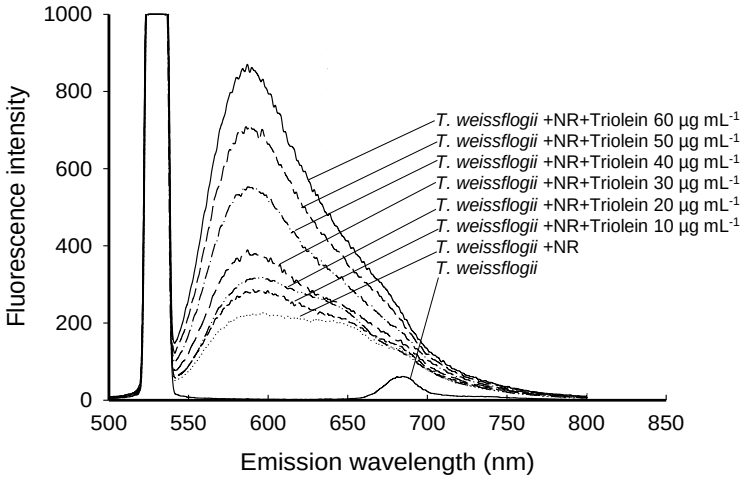

Figure 3-2. Emission spectra of *T. weissflogii* CCMP 1051. The excitation wavelength was fixed at 530 nm. Unstained cells (the lowest black line) show the chlorophyll peak at 684-686 nm. Emission spectra of *T. weissflogii* stained with NR 1 µg mL^{-1} in samples containing different amounts of Triolein at final concentrations: 0, 10, 20, 30, 40, 50 and 60 µg mL^{-1}.

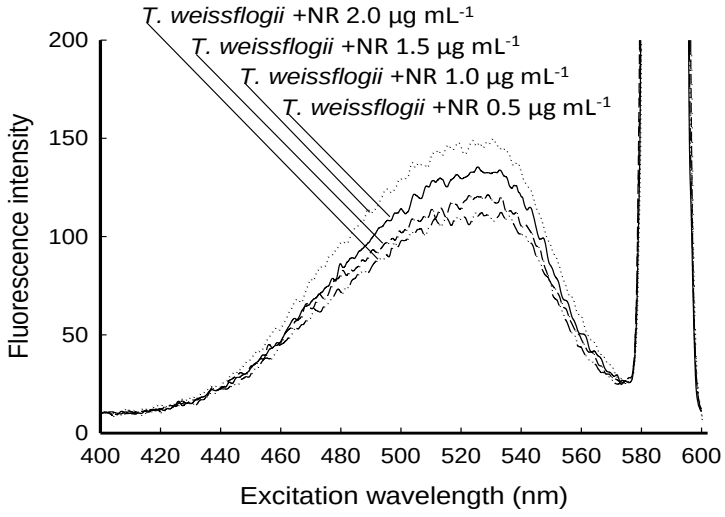

Figure 3-3. Excitation spectra of *T. weissflogii* CCMP 1051 stained with four different amounts of Nile red (0.5, 1.0, 1.5, and 2.0 µg mL^{-1}). The emission wavelength was fixed at 589 nm.

To improve NR staining of microalgae, extended incubation time of lipid accumulating algae with NR was recommended (Krishnamoorthy, 2001; Elsey *et al*. 2007). The optimal incubation duration for measuring lipid accumulation in *T. weissflogii* with NR 1.0 µg mL^{-1} was after 5 minutes (Fig. 3-4A).

To determine the optimal cell biomass concentration for assessing cellular lipid contents, *T. weissflogii* was diluted serially in f/2 medium before staining with NR. Although fluorescence intensity increased linearly with cell abundance (Fig. 3-4B), cell abundance was selected between 200,000 and 400,000 cells mL^{-1} because this gave fluorescence intensity within the range of the Triolein standard curve (< 20 µg mL^{-1}). This concentration range is similar to the study by Yu *et al*. (2009) which used 600,000 cells mL^{-1} of *T. pseudonana* for determining neutral lipid content.

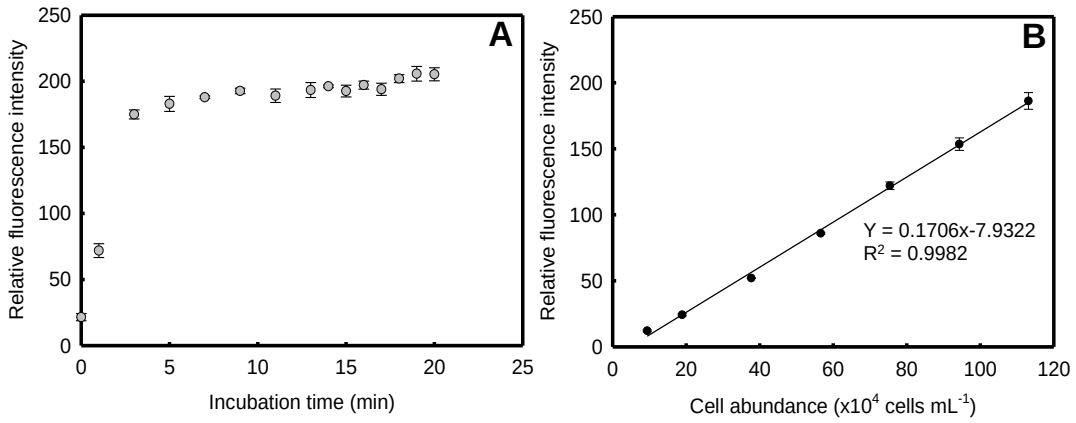

Figure 3-4. The relationship between NR fluorescence intensity and incubation time for *T. weissflogii*. NR is shown in the relative fluorescence intensity at different times after adding 1.0 µg mL^{-1} (A). The relationship between relative fluorescence intensity and cell abundance for a culture of *T. weissflogii* stained with NR 1.0 µg mL^{-1} (B). Values are mean ± standard deviation, n= 3.

DMSO as a carrier is also important for enhancing the lipid staining efficiency. 5% or 10% DMSO increased fluorescence intensity by approximately 10 % when compared with *T. weissflogii* (200,000 cells mL^{-1}) incubated without DMSO (Fig. 3-5).

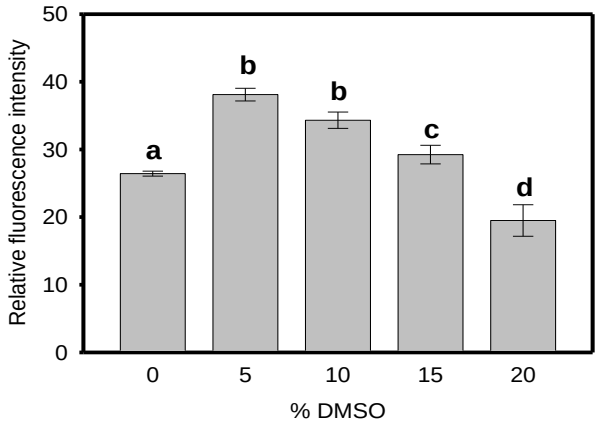

Figure 3-5. Fluorescence intensity of *T. weissflogii* using NR with and without adding different amounts of DMSO. The bars labelled with the same letter were not significant different (one way ANOVA Turkey's test; $p < 0.05$). Samples were incubated with NR 1.0 µg mL^{-1} for 5 minutes. Values are mean ± standard deviation, n= 3.

In this study, the optimal method for quantifying neutral lipid in *T. weissflogii* CCMP 1051 using Nile red was fixed excitation at 529 nm, slit excitation 5 nm, emission at 589 nm slit excitation 5 nm. Nile red concentration was 1.0 µg mL^{-1} for staining cell abundance 2-4 x 10^4 cells mL^{-1}. The time for reaching a maximum of fluorescence intensity was 5 minutes and 5 % DMSO enhanced lipid staining efficiency of stained cells. Therefore, these conditions will be used in future experiments.

3.4.2 Application of fluorometric quantification of neutral lipid content in a marine diatom

3.4.2.1 Growth rate

The triplicate cultures of *T. weissflogii* were grown under different nitrogen concentrations (50, 100, 200 and 882 µM $NaNO_3$) in batch mode. The maximum cell abundance of *T. weissflogii* in stationary phase increased from 1.65 x 10^5 cells mL^{-1} in the lowest N concentration to 2.32 x 10^5 cells mL^{-1} in the highest N concentration (Fig. 3-6A). The growth rate during exponential phase (days 0-2) ranged from 0.88 to 1.19 d^{-1}, and did not differ between treatments (Fig. 3-6B). The growth rate dropped in all treatments at day 3.

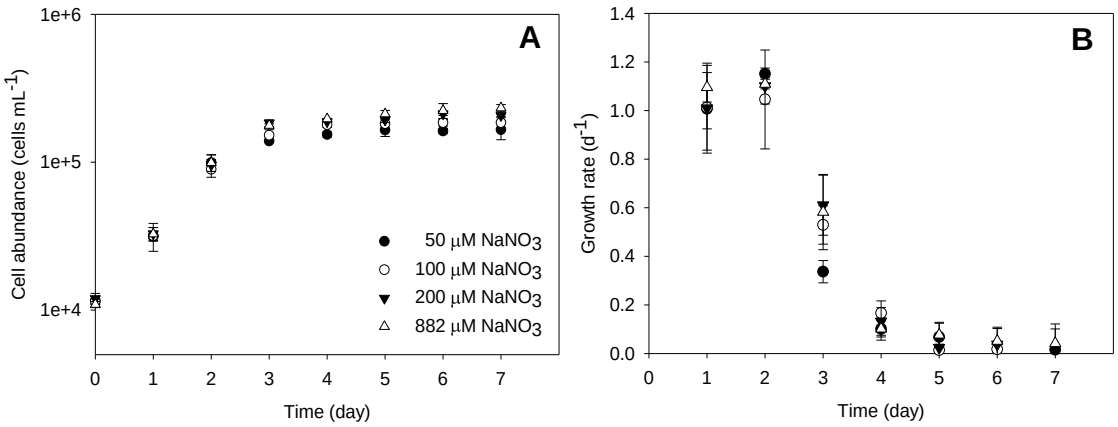

Figure 3-6. Time dependence of cell abundance (A) and growth rate (B) of *T. weissflogii* in batch cultures with different initial $NaNO_3$ concentrations. Mean values ± standard deviation, n=3 at 50 (black circle), 100 (open circle), 200 (black triangle) and 882 µM (open triangle) $NaNO_3$ are shown.

3.4.2.2 Intracellular chlorophyll *a*

T. weissflogii grown under 50 µM NO_3 gave the lowest cellular chl *a* content, which dropped continuously from day 1, whereas chl *a* content from 100 to 200 µM declined after day 2 (Fig. 3-7). At 882 µM $NaNO_3$, the highest cellular chl *a* content was observed on day 4 when it was around 5 times greater than the 50 µM $NaNO_3$ treatment on the same day.

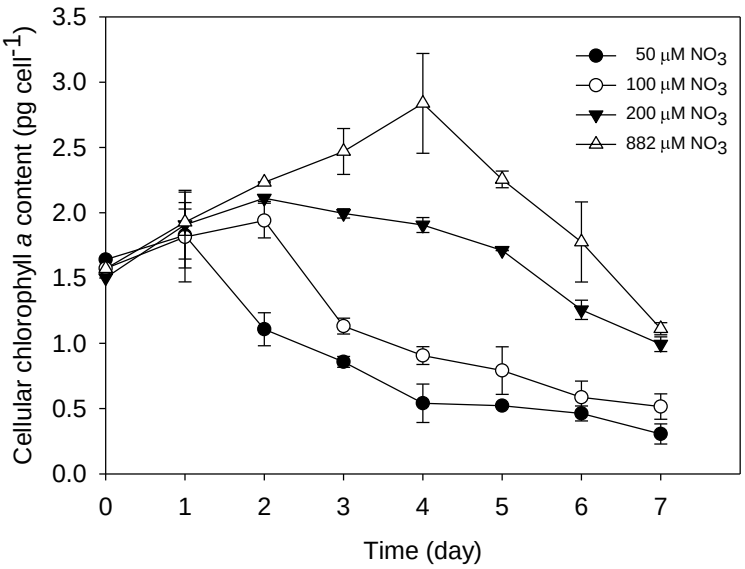

Figure 3-7. Intracellular chlorophyll *a* content of *T. weissflogii* grown under different nitrate (50, 100, 200, and 882 µM $NaNO_3$) concentrations. Values are mean ± standard deviation, n= 3.

3.4.2.3 Particulate nitrogen (PN) and phosphorus (PP) levels

Cellular N and P contents gradually dropped with increasing time in all treatments. Cells grown under 50 µM $NaNO_3$, the lowest $NaNO_3$ concentration, gave the lowest cellular N and P content (Figs. 3-8A,B). The concentration of particulate N (µmol L^{-1}) in the culture increased until day 3 except in the 50 µM $NaNO_3$ treatment which increased on day 2 and then dropped when cells entered the stationary phase (Figs. 3-8C,D). Although particulate P concentration increased until day 3, it was steady thereafter.

The ratio N:P (mol:mol) of all treatments in exponential phase ranged between 16.95-18.55 and then dropped as time increased. Cells grown at replete condition of 882 µM $NaNO_3$ had the highest N:P, whereas cells grown at 50 µM $NaNO_3$ showed the lowest N:P (Fig. 3-8E).

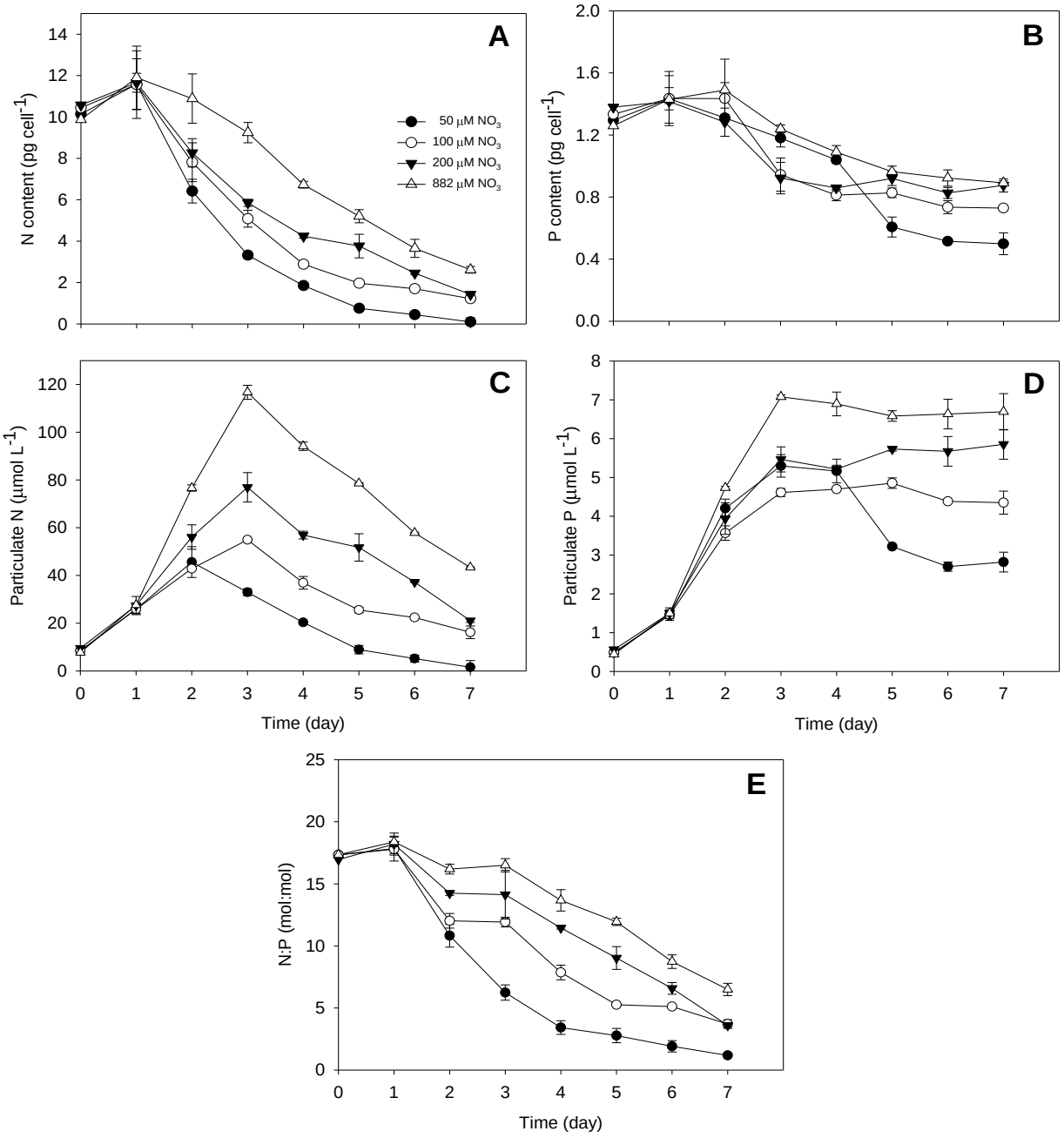

Figure 3-8. Intracellular concentrations of nitrogen (A) and phosphorus (B) in unit pg cell^{-1}, particulate nitrogen (C) and particulate phosphorus (D) in unit µmol L^{-1}, and N:P ratio (E) of *T. weissflogii*. Concentrations are expressed in units of mass per cell (pg cell^{-1}) under nutrient limited batch cultures at 50, 100, 200 µM $NaNO_3$ and replete batch culture at 882 µM $NaNO_3$ concentration. Values are mean ± standard deviation, n= 3.

3.4.2.4 Lipid content

Cellular neutral lipid content was similar in all cultures during exponential phase; however, differences were observed at stationary phase. *T. weissflogii*, which was grown in 200 µM $NaNO_3$, showed the highest cellular lipid content which was approximately 3.5 fold higher than in the nitrate replete (882 µM NO_3) at stationary phase (Fig. 3-9A,B).

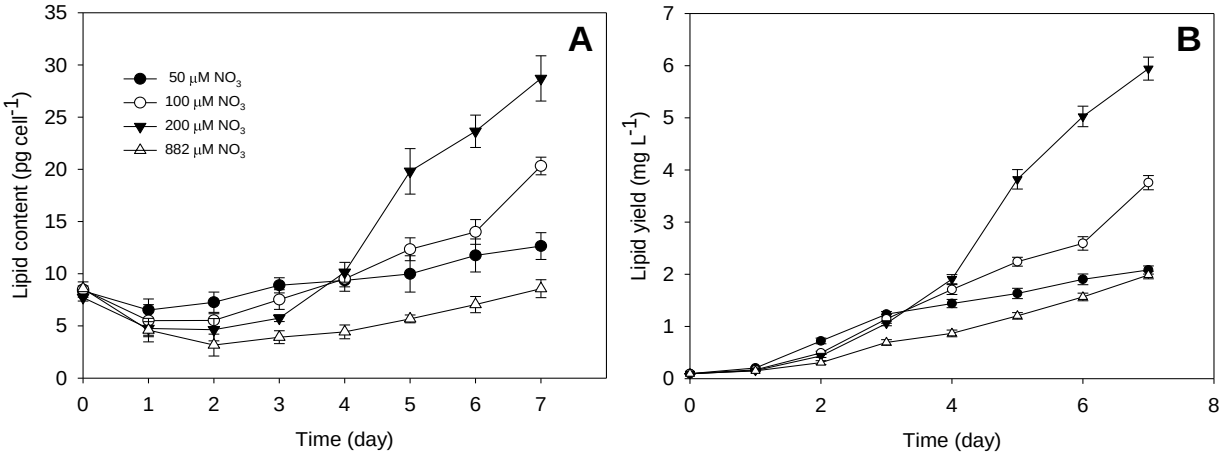

Figure 3-9. Lipid content in unit pg $cell^{-1}$ (A) and lipid yield in unit mg L^{-1} (B) of *T. weissflogii* as a function of time (day) at different $NaNO_3$ concentrations (50, 100, 200, and 882 µM) in batch culture. Values are mean ± standard deviation, n= 9.

The lipid yield (mg L^{-1}) and productivity (mg L^{-1} d^{-1}) of *T. weissflogii* incubated in different nitrate concentrations are shown in Table 3-2. The highest lipid yield and productivity was observed at 200 µM nitrate concentration, which was 3-time higher than that under nitrogen-replete condition (882 µM).

Table 3-2 Lipid yield (mg L^{-1}) and productivity (mg L^{-1} d^{-1}) of *T. weissflogii* under different nitrate concentrations at day 7 of stationary phase. Values are mean ± standard error, n= 9. Means with a column followed by the same letter are not significantly different (one way ANOVA Tukey's test; $p< 0.05$).

Nitrate concentration (µM)	Lipid yield (mg L^{-1})	Lipid productivity (mg L^{-1} d^{-1})
50	2.1 ± 0.1^{a}	0.26 ± 0.01^{A}
100	3.6 ± 0.1^{b}	0.47 ± 0.02^{B}
200	5.9 ± 0.2^{c}	0.74 ± 0.03^{C}
882	2.0 ± 0.1^{a}	0.25 ± 0.01^{A}

3.5 Discussion

3.5.1 Application of fluorometric quantification of neutral lipid content in a marine diatom

In this study, the optimal excitation and emission wavelengths for lipid quantification were 529 nm and 580 nm respectively. However, the wavelengths used depend upon the sample conditions (Elsey *et al*. 2007). For example, Yu *et al*. (2009) determined lipid in *Thalassiosira pseudonana* and *Phaeodactylum tricornutum* (class Baccilariophyceae) using excitation and emission at 530 and 550-570 nm respectively under N-limited culture. In contrast, excitation at 480 and emission at 570 nm were used for the dinoflagellate *Prorocentrum micans* and the diatom *Phaeodactylum tricornutum* maintained under N-deprived conditions (Wu *et al*. 2014). Therefore, the ability to effectively and successfully quantify lipid production from diversity of microalgae species requires the optimal excitation and emission wavelengths.

NR dissolved in acetone was used for staining neutral lipid in *T. weissflogii* CCMP 1051 at a final concentration 1 µg mL^{-1}. Cirulis *et al*. (2012) found that NR (2 µg mL^{-1}) was a suitable dye and <1 % acetone in the sample for staining *Scenedesmus dimorphus* and *Chlorella vulgaris.* This suggests that the fluorescence of Nile red interacted with extreamely hydrophobic substances (i.e., neutral lipid droplets) leading to high relative fluorescence unit.

DMSO is miscible in a range of organic solvents allowing it to be used broadly as a stain carrier (Chen *et al*. 2009). Using DMSO enhanced lipid staining efficiency and elevated the fluorescence unit of stained cells because DMSO promoted NR permeability and decreased hydrophobicity. This finding is consistent with the study by Doan *et al*. (2011) who found that DMSO stimulated the fluorescence intensity of stained cells more than glycerol in the green alga *Nannochloropsis* sp. Moreover, DMSO has been widely used as a carrier in other microalgae such as *Chrysochromulina* sp. in class Prymnesiophyceae, *Mallomonas splendens* in class Synurophyceae (Cooper *et al*. 2010), *Chaetoceros muelleri* in class Bacillariophyceae, *Chlorella*

vulgaris in class Trebouxiophyceae, *Chlorococcum littorale* in class Chlorophyceae, *Botryococcus braunii* in class Trebouxiophyceae, *Nannochloris* sp. in class Chlorophyceae, (Chen *et al*. 2011), *Pseudochlorococcum* sp. in class Chlorophyceae (Li *et al*. 2011).

3.5.2 The effect of nitrate concentration on growth rate and chemical composition of marine microalgae

There were no significant differences in growth rate during exponential phase in *T. weissflogii* grown under different NO_3 concentrations. Similarly, in green algae *Nannochloropsis oculata* and *Chlorella vulgaris* constant growth rate were observed at different nitrate concentrations (0.9, 1.8 and 3.5 mM $NaNO_3$) grown in batch culture for 14 days (Converti *et al*. 2009). This could be inoculum cells maintained in replete medium before transferring to a batch culture remained in nutrient-replete exponential growth immediately following transfer to the experimental medium.

Cellular N and P contents decreased gradually with incubation time but concentrations of particulate N and particulate P (µmol L^{-1}) increased sharply until day 3 (late exponential phase). The N:P ratio also decreased gradually with incubation time owing to the reduction of nutrients in medium. This suggests that cells grew faster due to enrich nutrients and cells accumulated inorganics substance when serving in stressful environmental condition. The reduction of nitrate concentration led to a decrease in maximum biomass. Nitrogen limited conditions decrease growth; however, significantly increase the lipid content of many microalgae. Additionally, the reduction of nitrate may limit protein biosynthesis that lead to an increase the lipid or carbohydrate as energy source (Converti *et al*. 2009).

T. weissflogii at 200 µM $NaNO_3$ gave the highest lipid yield (approximately 6 mg L^{-1}) and productivity (approximately 0.7 mg L^{-1} day^{-1}) in term of fresh weight. The lipid yield of cells under the nitrogen-limited condition (200 µM $NaNO_3$) was more than double that under nitrogen-

replete (882 µM $NaNO_3$) conditions at day 7 of stationary phase. In another study, d'Ippolito *et al.* (2015) who studied *T. weissflogii* P09 and *Cyclotella cryptica* CCMP 331 grown in nitrogen limitation (~180 µM $NaNO_3$) gave approximately 3.4-3.8 fold increase in lipid productivity (mg L^{-1} day^{-1}) compared with nitrogen-sufficient condition (882 µM $NaNO_3$). This suggests that under nitrogen limitation, the cultures positively affect oil production in these photoautotrophic organisms.

3.6 Conclusions

- The developed method for quantifying neutral lipid in *T. weissflogii* using NR used an excitation wavelength at 529 nm, slit width 5 nm, with emission wavelength at 589 nm, slit width 5 nm. A Nile red concentration of 1.0 µg mL^{-1} was used for staining 400,000 cells mL^{-1}. The incubation time for reaching the maximum fluorescence intensity was found to be 5 min. Using 5 % DMSO enhanced lipid staining efficiency by approximately 10 percent.
- This method was used to assess the effect of nitrate concentrations on lipid content of *T. weissflogii*. Of particular interest was the influence of nitrogen concentrations on chlorophyll *a*, elemental composition as well as lipid content in stationary phase batch cultures of *T. weissflogii*. Although cellular contents of chlorophyll *a*, particulate nitrogen and particulate phosphorus levels decreased with time in stationary phase, the absolute values depended on the initial nitrate concentration in the culture medium. In contrast, cellular lipid content increased with time in stationary phase cultures.
- The effect of nitrate concentration on *T. weissflogii* showed the lipid content and lipid yield increased with increasing concentrations of nitrate when cells were grown under nitrogen-limited medium (50, 100, and 200 µM $NaNO_3$). However, the lowest lipid content and yield was observed in nitrogen-enriched medium (882 µM $NaNO_3$).
- The highest lipid yield and productivity was observed at 200 µM nitrate concentration, which was three times higher than that observed under nitrogen-replete condition (882 µM). Since cells gave the greatest lipid content at 200 µM $NaNO_3$. Based on these results, this concentration was used the experiments described in the remainder of this thesis.

Chapter 4: Development of a method for determining the combined amino acid composition of microalgae using ultra performance liquid chromatography (UPLC)

4.1 Introduction

Proteins are macromolecules consisting of many amino acids linked together through peptide bonds and cross-linked between chains such as sulfhydryl bonds, hydrogen bonds and van der Waals forces. There are about 300 amino acids present in various animal, plant and microbial systems, but only 20 amino acids serves as building blocks of proteins (Gromiha 2010). Amino acid analysis can be used to quantify protein content and to identify proteins based on their amino acid composition. For example, tyrosine is the source of a group of excitatory neurotransmitters and hormones called catecholamines including adrenaline**,** noradrenaline and dopamine (Hardie 1991). Glutamate is the source of gamma-aminobutyric acid (GABA), a major inhibitory brain neurotransmitter (Shelp *et al*. 1999).

The protein content of microalgae varies greatly and depends on both the species and environmental growth conditions. For example, the protein content of green algal species, e.g., *Dunaliella tertiolecta*, *Nannochloropsis atomus* is around 21.4- 99.9 pg cell^{-1} dry weight; of diatoms, e.g., *Chaetoceros calcitrans*, *C. garacillis. P. triconutum, S. costatum, T. pseudonana* is about 28.4-76.4 pg cell^{-1} dry weight; of haptophytes e.g. *Isochrysis galbana*, *I*. aff. *galbanna* (T-iso), *Pavlova lutheri, P. salina* is approximately 29.7-102.3 pg cell^{-1} dry weight (Brown 1991).

Microalgae are capable of synthesizing amino acids and they can provide the essential amino acids to humans and animals which must come from diet. Such essential amino acids are histidine, isoleucine, leucine, lysine, methionine, phenylalanine, threonine, tryptophan, and valine. There are variations in the amino acid profiles in microalgae. For instance, aspartate and glutamate were generally found in highest contents approximately 7.6-12.4 % total amino acid,

whereas cystine, histidine, hydroxy-proline, methionine, *γ*-amino-butyric acid, ornithine, and tryptophan were found in the lowest concentrations around 0.04-3.23 % total amino acid at the end of exponential growth phase of 16 microalgal species (Brown 1991).

The traditional method for determination of amino acid content is ion-exchange chromatography combined with post-column ninhydrin derivatisation (Boogers *et al*. 2008 cited Horwitz 2002). However, high-performance liquid chromatography (HPLC) in combination with pre-column derivertisation is more sensitive and faster. The reagents frequently used for pre-column derivitization include O-phthalaldehyde (OPA) (Gardner & Miller 1980; Blankenship *et al.* 1989), 9-fluorenylmethylchloroformate (FMOC) (Brown 1991; Bank *et al.* 1996; Ou *et al*. 1996), phenylisothiocyanate (PITC) (Sarwar & Botting 1989; Shang & Wang 1996), and 6-aminoquinolyl-N-hydroxysuccinimidyl carbamate (AQC) (Hong 1994; Diaz *et al*. 1996; Boogers *et al*. 2008; da Silva Gorgônio *et al.* 2013).

The AccQ · Tag method is widely used for the chemical derivitisation in analysis of amino acids (Boogers *et al*. 2008; Hou *et al*. 2009; Salazar *et al*. 2012). In this method, 6-aminoquinolyl-N-hydroxysuccinimidyl carbamate (AQC) reacts with primary and secondary amines or amino acids to generate the first product which is a stable unsymmetrical amine derivative. The derivative is highly fluorescent (Fig. 4-1). The second product is the excess reagent reacts with H_2O that is generated 6-aminoquinoline (AMQ), N-hydroxysuccinimide (NHS) and carbon dioxide. This process is a slower reaction. The derivertised amino acid and AMQ have the same excitation at 248 nm; however, amino acid products have an emission maxima approximately 395 nm and the emission of maxima AMQ is around 520 nm. The different emissions do not interfere with the measurements of amino acid content (Cohen 2003).

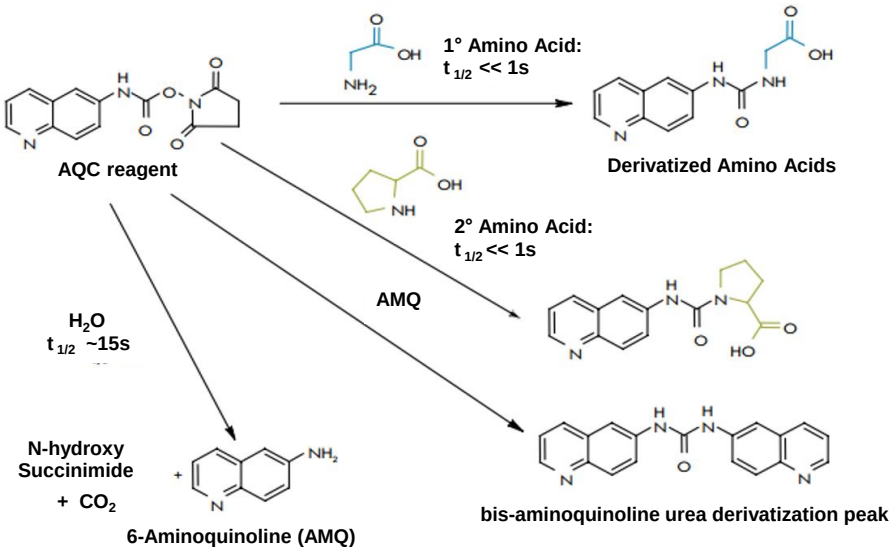

Figure 4-1. 6-aminoquinolyl-N-hydroxy-succinimidyl carbamate (AQC) reacts with amine or amino acid to produce highly stable fluorescent products. The excess reagent reacts with water to generate a product with different fluorescence spectra.
(Source: http://www.waters.com/waters/en_GB/AccQ%E2%80%A2Tag-and-Pico%E2%80%A2Tag-Methods/nav.htm?cid=1000897&locale=en_GB)

Ultra performance liquid chromatography (UPLC) has been widely used in the analysis of small molecules in pharmaceutical (Wren & Tchelitcheff 2006), food (Dadáková *et al.* 2009), and environmental areas (Mezcua *et al*. 2006) because UPLC is faster and provides improved resolution and sensitivity compared to high performance liquid chromatography (HPLC) (Swartz 2005). Although UPLC offers many advantages over conventional HPLC, few applications in marine microalgae have been reported.

The aims of this research were to (i) develop the protocol for determining the amino acid composition of proteins (combined amino acids) extracted from microalgae, and (ii) evaluate recovery using BSA as a standard to developed a protocol was used for quantifying the combined amino acid contents in the marine haptophyte *Emiliania huxleyi* (chapter 5) and the marine diatom *Thalassiosira weissflogii* (chapter 6).

4.2 Materials and methods

4.2.1 Preparation of amino acids standard

A stock solution of 100 pmol μL^{-1} amino acid hydrolysate standard containing 17 amino acids (WAT088122, Waters, Massachusetts, USA) was prepared by transferring 40 µL amino acid standard into a plastic vial and mixing with 960 µL of deionized water (Mili Q pore, MiliQ® Gradient, France). The standard stock solution vials were mixed and stored in a freezer (-20°C).

4.2.2 Preparation of bovine serum albumin (BSA)

A stock solution of 500 µg mL^{-1} BSA (A7906-10G, 98% BSA, Sigma Aldrich, USA) was prepared in 2 steps. First, 10.0 mg of BSA were placed into a dried volumetric flask and deionized water was then added until a total volume of 5.00 mL was reached (final concentration 2,000 µg mL^{-1}). Second, 250 µL of 2,000 µg mL^{-1} BSA were mixed with 750 µL deionized water. Aliquots of the BSA stock were kept in a freezer (-20°C).

4.2.3 Preparation of glycine ^{13}C

A stock solution of 100 µg mL^{-1} glycine ^{13}C (279439-250MG, glycine ^{13}C, Sigma Aldrich, USA) was prepared in 2 steps. First, 10.0 mg of glycine ^{13}C were placed into a dried volumetric flask and deionized water was then added until a total volume of 5.00 mL was reached (final concentration 2.0 mg mL^{-1}). Second, 50 µL of 2.0 mg mL^{-1} glycine ^{13}C were mixed with 950 µL deionized water. The glycine ^{13}C stock vials were stored in a freezer (-20°C).

4.2.4 Extraction of amino acids in BSA

50 µL of 500 µg mL^{-1} BSA (from 4.2.2) were pipetted into an unused glass vial (1.5 x 10 cm.) in triplicate and placed in an oven at approximately 40°C until dried. The BSA extraction was modified from Kaiser & Benner (2005). Briefly, 5 µL of 12 mM ascorbic acid (final concentration at 10 µL mL^{-1}) were added into the dried BSA vial to prevent oxidation of amino acids by nitrate (Kaiser & Benner cited from Robertson *et al*. 1987). 500 µL of 6 M hydrochloric acid (HCl) were added and mixed gently using a vortex mixer (MS2 Minishaker, UK). Then, 5 µL of 100 mM

phenol (final concentration at 1 mM) were pipetted into the hydrolysis sample vials to protect tryptophan from hydrolysis and then mixed gently again. The hydrolysis glass vials were capped with polytetrafluoroethylene (PTFE) lined cap tightly and purged with nitrogen gas for 5 min. Then the glass vials were placed on a heating block (BT3, Grant Instruments Ltd, England) at 110^{o}C for 20 h. The hydrolysed samples were allowed to cool at room temperature. 1,500 µL of deionized water were added and mixed. The sample solution was transferred to a microcentrifuge tube and centrifuged (5415D, Eppendorf, Germany) at 10000 x g for 10 min to remove debris. Next, 50 µL of the supernatant were transferred to an unused small HPLC vial (diameter x length: 1 x 3 cm) and dried under a stream of nitrogen (Fig. 4-2) at room temperature (RT). 50 µL of deioised water were added twice after drying the amino acid samples to ensure that HCl was removed.

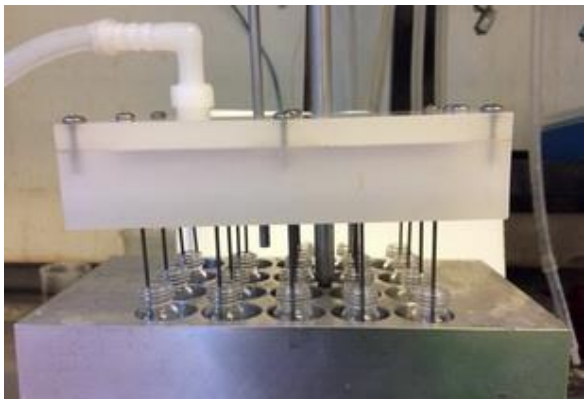

Figure 4-2. The supernatant containing amino acids was dried under a stream of nitrogen before derivatisation of AccQ·Tag ultra reagent.

4.2.5 Preparation of reconstitute AccQ·Tag ultra reagent powder

1.0 ml of 2B reagent (WAT052887, Waters, Massachusetts, USA) was added in 2A reagent (WAT052887, Waters, Massachusetts, USA) powder bottle and mixed using vortex for 10 seconds and solution reagent was then incubated at 55^{o}C for 10-15 min and shaken occasionally until the powder dissolved.

4.2.6 AccQ·Tag ultra amino acid derivatisation

Prior to UPLC-MS analysis, amino acids were derivertised with a 6-aminoquinolyl-N-hydroxysuccinimidyl carbamate (AQC) based kit (Waters, Massachusetts, USA). A standard curve was prepared from an amino acid standard solution (from 4.2.1) at concentrations of 0, 1, 2, 4, 6, 8, and 10 pM μL^{-1} and deionized water used as a blank.

The dried supernatant containing the amino acid (from 4.2.4.) was mixed with 80 µL of AccQ·Tag ultra borate buffer (WAT052887 Waters, Massachusetts, USA). After that, 20 µL of AccQ·Tag reagent (from 4.2.5) were added and mixed gently. The sample solution was kept for 1 min at RT before incubating in an oven (Shake 'n' Stack, Themo Scientific Ltd., USA) for 10 min at 55^{o}C.

4.2.7 Amino acid quantification using UPLC-MS

Amino acids were analysed using a UPLC-MS system (Acquity, Quatro Premier XE, Waters, Massachusetts, USA). Amino acids were separated using C18 column (50 mm x 2.1 mm x 1.7 µm, Waters, Massachusetts, USA) set to 55^{o}C. The flow rate of mobile phase in the column was 0.7 mL min^{-1}. The mobile phase was made using the manufacturer's solvents which consisted of 10% AccQ·Tag Ultra concentrate solvent A (186003838 eluent A, Massachusetts, USA), and 100% AccQ·Tag Ultra solvent B (186003839 eluent B, Massachusetts, USA). The amino acids were separated using a gradient method: 0-0.54 min (99.9% A), 5.74 min (90.0% A), 7.74 min (78.8% A), 8.04-8.64 min (40.4 % A), 8.73-10 min (99.9% A). To achieve a good separation efficiency by ions according to their mass to charge ratio (m/z) of amino acids, time setup was set in 4 types. Taurine, serine, arginine and glycine were group 1 separated at 0-4.2 min; aspartic acid, asparagine, glutamic acid, threonine, and proline were group 2 separated at 3.5-6.6 min; cysteine, tyrosine, methionine, valine, and lysine were group 3 separated at 6.0-7.4 min, and isoleucine and phenylalanine were group 4 separated at 7.4-10.0 min. The mixture of

amino acids was determined using multiple reaction monitoring (MRM) under ESi+ (electrospray) mode with the conditions and transitions as stated in Salazar *et al*. (2012).

4.2.8 Recovery of Glycine ^{13}C

50 µL of 100 µg mL^{-1} glycine ^{13}C were placed into an unused glass vials (1.5 x 10 cm.) and dried in an oven at 40^{o}C. The dried glycine ^{13}C was hydrolysed using hydrochloric acid following 4.2.4. To test the recovery of substances, both hydrolysed glycine ^{13}C and non-hydrolysed glycine ^{13}C were derivatised with AccQ·Tag ultra reagent following 4.2.6 and samples were injected by following 4.2.7. The percentage of glycine recovery was calculated as follows:

$$\% \text{ Recovery} = \frac{\text{Area unit (AU.) of recovered substance after hydrolysis}}{\text{Area unit (AU.) of substance before hydrolysis}} \text{ X } 100$$

4.3 Results

4.3.2 Amino acid standard curve

Using the protocol described above, 17 peaks were detected in the amino acids standards within 10 min (Table 4-1). Individual amino acids were identified using mass spectroscopy as shown in figure 4-3.

The limit of detection of AccQ·Tag–derivertised amino acids was 62.5 fmol μL^{-1} and the coefficient of determination (R^2) value was more than 0.96 when mixed amino acids were prepared concentration from 62.5 fmole to 1 pmole amino acids.

Table 4-1. The retention time (min), R^2, and mass to charge ratio (m/z) of amino acid standards.

No.	Amino acid	RT. (min)	R^2 (from 62.5 fmol to 1 pmol μL^{-1})	Parent ion (m/z)
1	Taurine	2.53	1	296.11
2	Serine	3.39	1	276.21
3	Arginine	3.59	0.99	345.21
4	Glycine	3.66	0.99	246.08
5	Aspartic acid	3.96	0.96	304.11
6	Asparagine	3.96	1	303.13
7	Glutamic acid	4.40	1	318.11
8	Threonine	4.75	1	290.11
9	Sacrosine	5.25	0.98	260.17
10	Proline	5.96	1	286.17
11	Cysteine	6.58	0.98	581.64
12	Tyrosine	6.67	0.99	352.21
13	Methionine	6.78	1	320.21
14	Valine	6.92	0.99	288.21
15	Lysine	7.03	0.99	487.21
16	Isoleucine	7.76	1	302.21
17	Phenylalanine	7.96	1	336.21

*p: pico (10^{-12}); f: femto (10^{-15})

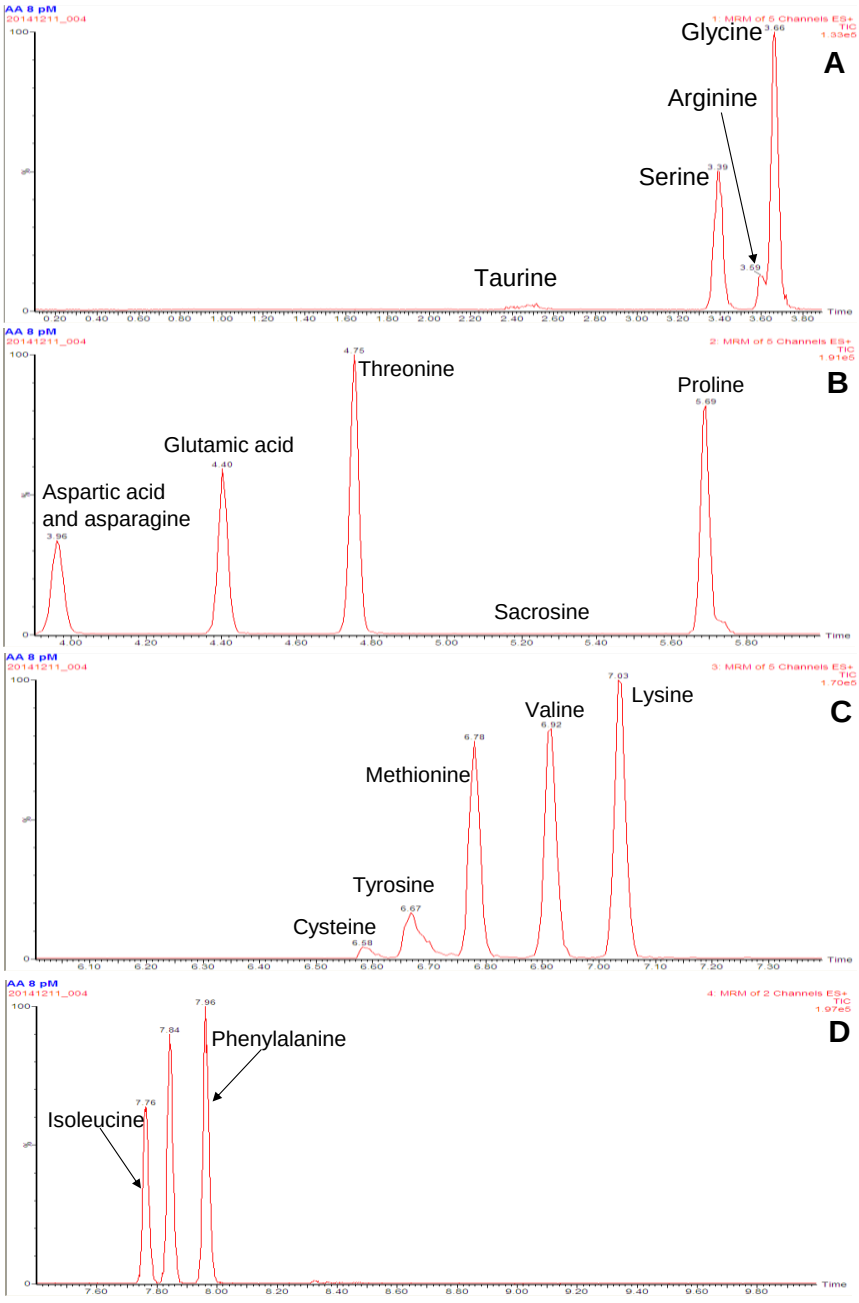

Figure 4-3. UPLC chromatograms of AccQ Tag-derivatised amino acids standard with time (min). The time setup for separation of taurine, serine, arginine and glycine at 0-4.2 min (A), of aspartic acid, asparagine, glutamic acid, threonine, and proline at 3.5-6.6 min (B), of cysteine, tyrosine, methionine, valine, and lysine at 6.0-7.4 min (C), and of isoleucine and phenylalanine at 7.4-10.0 min (D).

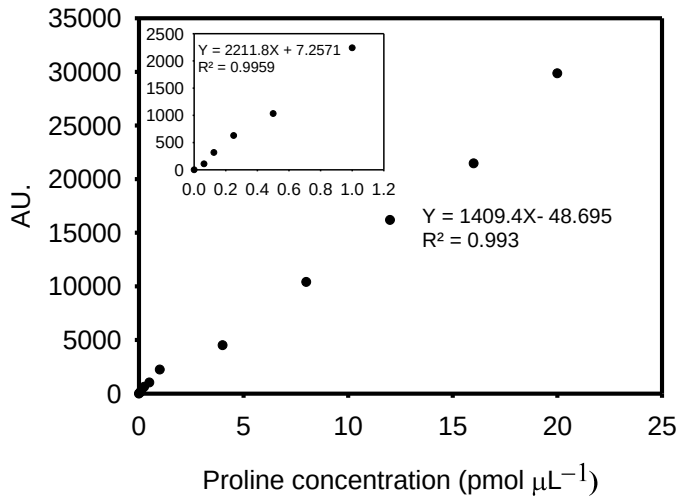

Figure 4-4. The relationship between concentration of proline at concentrations of 0.0625 - 20 pmol μL^{-1} and AU detected by UPLC.

4.3.3 Recovery of amino acid in BSA

Seventeen types of amino acids were detected in the hydrolysed BSA using the protocol described above. We did not detect leucine or tryptophan, and could not differentiate between aspartic acid and asparagine, which co-eluted. In addition, taurine and sacrosine, which were included in our amino acid standards, are not found in BSA published in the Universal Protein Resource (www.uniprot.org/). We can infer that taurine is actually histidine because the parent ion mass/charge ratio (m/z) of histidine was 326.21 in the chromatogram (Fig. 4-5A) while m/z of taurine is 296.11 (Salazar *et al*. 2012). We can also infer that sacrosine could be alanine because they also have the same parent ion at 260.17 (Fig. 4-5B). Therefore, in this experiment, we concluded that we detected both histidine and alanine in the hydrolysed BSA samples.

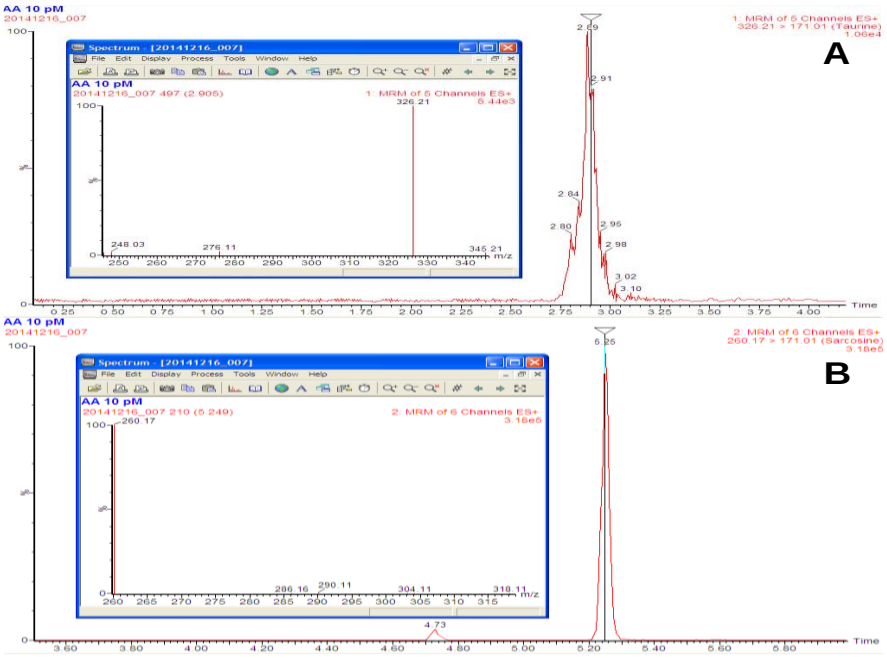

Figure 4-5. UPLC spectrum of parent ions (m/z) at 326.1 (histidine) and 260.17 (sacrosine/alanine).

The amount of each amino acid in the hydrolysed BSA was estimated using amino acid standard curves. Aspartic acid and asparagine were combined together in this work because asparagine can be degraded easily into aspartic acid. Good agreement was found between the amounts of amino acid that we detected in BSA and the expected values from the protein sequence obtained from Uniprot (http://www.uniprot.org/uniprot/P02769) as shown in Fig. 4-6.

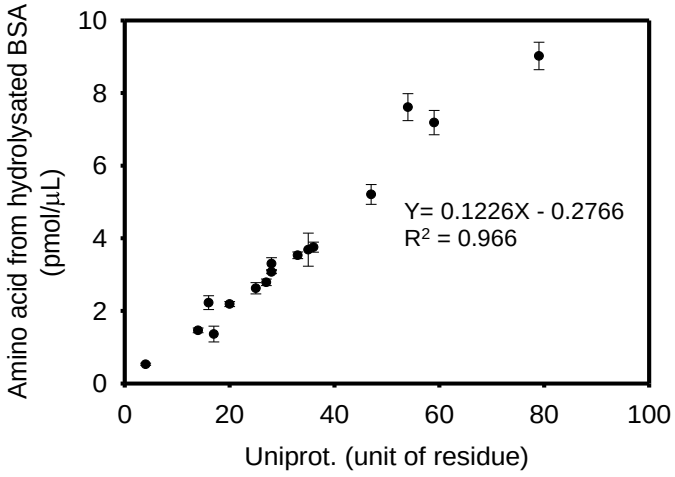

Figure 4-6. The relationship between amino acid concentrations from the hydrolysed BSA sample (pmol μL^{-1}) and number of residues of each amino acids reported for BSA from the universal protein resource (www.uniprot.org/). Each point in the graph refers to means and standard errors obtained from triplicates.

To evaluate the recovery of individual amino acids from protein hydrolysates using the protocol described above, the mass of each amino acid residue from hydrolysed BSA that was detected was compared with the mass expected based on the amount of BSA used in the standard (Table 4-2). An example of how this calculation was performed follows:

Example, 1). Calculation of mass residue of amino acid from hydrolysed BSA in an experiment.

The concentration (pmol μL^{-1}) of the amino acid in the derivatized sample was calculated from the peak area using a standard curve (example; valine standard curve (Fig. 4-7)):

Y= aX + b from linear curve of amino acid, where Y is the amino acid concentration (pmol μL^{-1}) and X is the peak area (Area Units = AU).

$$\text{Amino acid (AA) concentration in unit pmol } \mu L^{-1} \text{ (column 2)} = \frac{\text{Area unit (AU.)} - b}{\text{Slope (a)}}$$

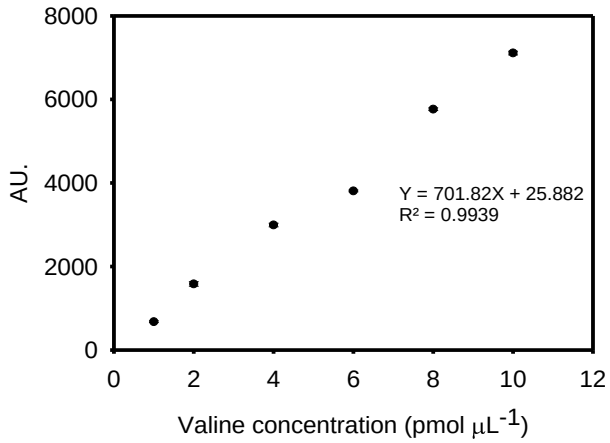

Figure 4-7. The relationship between concentration of valine at concentrations of 1, 2, 4, 6, 8, and 10 pmol μL^{-1} and AU detected by UPLC.

The mass concentration (pg μL^{-1}) of the amino acid was then calculated from the concentration (pmol μL^{-1}) and the molecular weight.

AA content in unit pg μL^{-1} (column 4) = AA content in unit pmol μL^{-1} (column 2) X Molecular weight (column 1)

It is necessary to correct for the proportion of the derivatized sample that was injected (2 µL of 100 µL derivertised sample solution) and the conversion from pg μL^{-1} to pg mL^{-1} (1000 pg μL^{-1} = 1 pg mL^{-1}) to obtain mass detected.

$$\text{Mass detected (column 5)} = \text{AA content in unit pg } \mu L^{-1} \text{ on column (column 4)} \times \frac{50}{1000}$$

2). Calculation of mass residue of amino acid from Uniprot. (source: http://www.uniprot.org/uniprot/P02769)

The mass of a particular amino acid in one mole of BSA was calculated from the number (No.) of amino acid (AA) residues reported in Uniprot as follows:

Mass of AA residue (column 8) = No. of AA residues (column 7) X Molecular weight (column 1)

The proportion of mass AA of each amino acid to the total was then calculated as:

$$\text{Proportion of mass AA (column 9)} = \frac{\text{Mass of each AA residue (column 8)}}{\text{Total mass of AA residue (column 8)}}$$

The expected mass of the detected amino acids in the 500 $\mu g\ mL^{-1}$ BSA standard solution was then calculated from the sum of the masses of the individual amino acids in BSA, taking into account that we did not detect leucine or tryptophan.

Mass expected-amino acid (column 10) = Proportion of mass AA (column 9) x BSA content

The recovery was then calculated as:

$$\%\ \text{recovery} = \frac{\text{Mass detected-amino acid (column 5)}}{\text{Mass expected-amino acid (column 10)}} \times 100$$

$$\%\ \text{recovery} = \frac{337.23}{445.46} \times 100 = 75.70$$

Table 4-2. The mass recovered-amino acid received from hydrolysed BSA and from the universal protein resource (www.uniprot.org/).

Amino acid	Hydrolysed BSA						Uniprot.			
	1	2	3	4	5	6	7	8	9	10
	MW	Mean (pmol µL^{-1})	SE	AA (pg µL^{-1})	Mass Detected	SE	No. of residues	Mass of residues	Proportion of mass	Mass Expected
Alanine	71.09	5.21	0.27	370.23	18.51	0.97	47	3341.23	0.05	25.05
Arginine	156.19	2.62	0.16	409.60	20.48	1.21	25	3904.75	0.06	29.27
Asparagine*	114.60	7.61*	0.37	872.32	43.62	3.00	54*	6188.40	0.09	46.39
Cysteine	103.15	3.69	0.46	380.20	19.01	2.35	35	3610.25	0.05	27.07
Glutamic acid**	128.60	9.02**	0.38	1160.25	58.01	2.43	79**	10159.40	0.15	76.16
Glycine	57.05	2.23	0.19	127.04	6.35	0.55	16	912.80	0.01	6.84
Histidine	137.14	1.36	0.22	186.86	9.34	1.49	17	2331.38	0.03	17.48
Isoleucine	113.16	1.46	0.07	165.58	8.28	0.37	14	1584.24	0.02	11.88
Leucine	113.16	NT					61	6902.76	0.10	
Lysine	128.17	7.19	0.34	921.09	46.05	2.15	59	7562.03	0.11	56.69
Methionine	131.19	0.53	0.03	69.49	3.47	0.19	4	524.76	0.01	3.93
Phenylalanine	147.18	2.79	0.09	410.02	20.50	0.66	27	3973.86	0.06	29.79
Proline	97.12	3.07	0.05	298.36	14.92	0.22	28	2719.36	0.04	20.39
Serine	87.08	3.30	0.17	287.41	14.37	0.72	28	2438.24	0.04	18.28
Threonine	101.11	3.53	0.09	357.03	17.85	0.46	33	3336.63	0.05	25.01
Tryptophan	186.21	NT					2	372.42	0.01	
Tyrosine	163.18	2.19	0.12	356.96	17.85	0.57	20	3263.60	0.05	24.47
Valine	99.14	3.76	0.24	372.26	18.61	0.69	36	3569.04	0.05	26.76
Total				**6015.46**	**337.23**	**18.03**	**585**	**66695.15**	**1.00**	**445.46*** **

NT: not determined, MW: molecular weight, SE: standard error

*: Sum of asparagine and aspartic acid as these co-elute

**: Sum of glutamic acid and glutamine as these co-elute

***: Sum of mass recovered without including leucine and tryptophan

Amino acid content was positively correlated with the unit of residue and the coefficient of determination was 0.97 (Fig. 4-6). Moreover, 76 % of recovery was estimated from mass detected-amino acid by hydrolysed BSA compared with mass expected-amino acid from universal protein resource. This suggests that amino acids from hydrolysed BSA and subsequent derivatisation with AccQ Tag ultra reagent provided an efficient protocol to quantify amino acids in marine microalgae samples.

4.3.4 Recovery of glycine ^{13}C

The hydrolysed glycine ^{13}C and non-hydrolysed glycine ^{13}C were derivatised with AccQ·Tag ultra reagent to estimate the percentage of recovery substance. The parent ion of non-hydrolysed glycine ^{13}C is 248.03 (Fig. 4-8A) and area unit was integrated as shown in chromatogram (Fig. 4-8B). Percentage recovery was calculated as:

$$\% \text{ Recovery} = \frac{\text{Area unit (AU.) of recovered substance after hydrolysis}}{\text{Area unit (AU.) of substance before hydrolysis}} \text{ X } 100$$

The recovery of glycine ^{13}C was 70.9 ± 2.8 % (mean ± SE). This is similar to the recovery of 75.7 ± 2.6 % calculated for total amino acids in BSA.

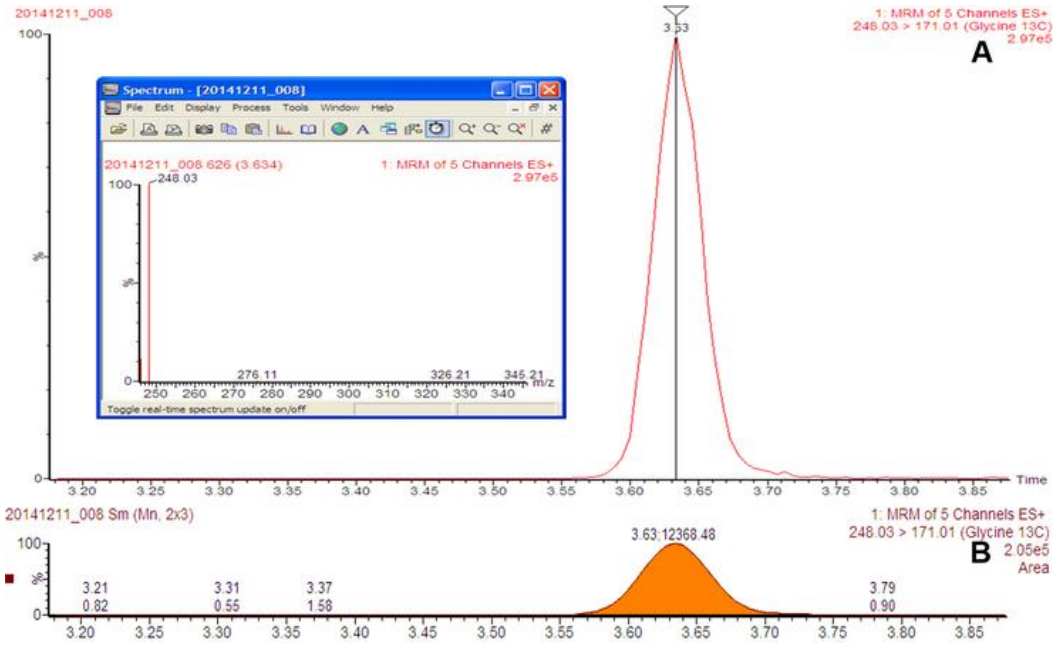

Figure 4-8. UPLC spectrum of parent ion glycine ^{13}C (A) and integrated area of glycine ^{13}C chromatogram (B).

4.4 Conclusions

• A UPLC amino acid analysis was developed for identifying and quantifying amino acids in microalgae. The method combining sensitive 6-aminoquinolyl-N-hydroxy-succinimidyl carbamate (AQC) amino acid derivatization with UPLC offered significant advantages such as a shorter runtime and enhanced chromatographic resolution relative to HPLC methods.

• Bovine serum albumin (BSA) was used as a standard to assess the efficiency of hydrolysis by hydrochloric acid and amino acid composition was quantified using the derivatised AQC reagent. This showed a high coefficient of variation (R^2 = 0.97) with recovery approximately 76 %.

• The efficiency of the protocol was also tested using hydrolysed and non-hydrolysed glycine ^{13}C. Recovery was calculated to be 71% which was similar to that obtained for BSA.

• Thus, this protocol was found to be reliable and appropriate for quantifying free and combined amino acids in the marine haptophyte *Emiliania huxleyi* (chapter 5) and the marine diatom *Thalassiosira weissflogii* (chapter 6).

• The developed UPLC amino acid analysis was found to be a valuable tool for measuring amino acids following the hydrolysis of proteins in samples of microalgae.

Chapter 5: The effect of temperature on growth rate of *Emiliania huxleyi* CCMP 1516

5.1 Introduction

Marine phytoplankton account for about 50% of global primary productivity (Field *et al*. 1998) and play important roles in marine ecology by providing the energy that sustains open ocean food webs, and in marine biogeochemistry by fixing CO_2 into organic matter and consuming inorganic nutrients particularly calcium carbonate precipitation by coccolithophores.

Phytoplankton productivity is affected by a wide range of environmental factors including light, nutrients and temperature. Temperature affects phytoplankton growth as temperature activates enzymes that catalyse many metabolic processes. Below the optimum temperature, reactions proceed faster with increasing temperature; however, different phytoplankton species respond differently to temperature changes. Above the optimum temperature, growth rate declines due to high-temperature inactivation of key enzymes.

5.1.1 Effect of temperature on algal growth and physiology

Increasing atmospheric CO_2 concentration caused from man-made and fossil fuels-combusted emission is leading to climate change and global warming (the greenhouse effect). Houghton *et al.* (2001) hypothesized that global warming will elevate the temperature of surface ocean water by 1-7^{o}C. Microalgae and phytoplankton are able to acclimate or adapt to growth at different temperatures (Li 1980; Smith *et al.* 1994; Suzuki & Takahashi 1995). Temperature has a strong regulation on algal growth and photosynthesis (Raven & Geider 1988; Davison 1991). Temperature also plays a key role in influencing the outcome of competition between phytoplankton species in both the laboratory and outdoor cultures (Goldman & Ryther 1976; Goldman, 1977). For example, *Skeletonema costatum* predominated at temperature below 10°C, *Phaeodactylum tricornutum* between 10-23°C, and other species (e.g., *Amphora* sp.,

Nannochloris sp., *Nitzschia closterium*, *Stichococcus* sp.,) above 23°C when these species were maintained in outdoor culture. (Goldman & Mann 1980; Goldman & Ryther 1975, 1976; D'Elia *et al.* 1977).

Many studies showed that temperature affects growth rate in phytoplankton (Thomas 1966; Rajadurai *et al*. 2005; Lassen *et al.* 2010). For instance, in the marine diatom *Chaetoceros calcitrans*, growth rates increased from 0.3 d^{-1} at 6^{o}C to 1.0 d^{-1} at 15^{o}C, and to 1.4 d^{-1} at 25^{o}C (Anning *et al*. 2001). In addition, *Cryptomonas* sp., *Rhodomonas* sp. and Prymnesiophyte NT19 growth rate increased with temperature between 25 to 30^{o}C; however, growth rated declined at temperatures above 30^{o}C (Renaud *et al.* 2002).

Temperature influences not only growth rate, but also cellular carbon (C), nitrogen (N) and chlorophyll a (chl *a*) concentrations (Goldman, 1979; Yoder, 1979; Goldman and Mann, 1980; Montagnes & Franklin 2001). Cellular C, Chl *a*, and C:N increased with increasing temperatures in the diatom *Thalassiosira pseudonana* (Berges *et al*. 2002). Growth temperature also has a strong influence on the biochemical composition of algae. Protein content increased markedly in the chlorophyte *Dunaliella tertiolecta* and the haptophyte *Isochrysis galbana* grown at temperatures higher than 15^{o}C (Thompson *et al*. 1992). Zhu *et al.* (1997) found that *Isochrysis galbana* TK1 gave the highest protein and carbohydrate contents at 15^{o}C in exponential and stationary growth phase respectively, whereas lipid content was higher at 30^{o}C than at 15^{o}C at stationary growth phase.

Phenotypic or genotypic changes algae species in response to temperature affects the photosynthetic rate (Davison 1991). For example, maximum photosynthetic rate (P_{max}) increased progressively when benthic microalgae were maintained at increasing temperature up to 25^{o}C (optimal temperature) and it declined at 30^{o}C (Blanchard *et al.* 1997; Defew *et al*. 2004).

5.1.2 Aims and Objectives

In the laboratory, the growth rate of *E. huxleyi* CCMP 1516 is correlated with RNA:protein under limited nutrient (N and P) and low and high light conditions (McKew *et al.* 2013a,b). However, the effect of temperature has not been studied. Temperature affects how fast ribosomes can synthesize proteins; typically the rate of protein synthesis per ribosome should increase by about two times if temperature is increased by 10ºC. If growth rate also doubles when temperature is increased by 10 ºC, then we should expect that the ratio of RNA-to-protein will not be affected by temperature. In contrast to enzymatic reactions and protein synthesis, temperature does not affect the rate at which chlorophyll *a* and other pigments absorb photons. Therefore, we can also predict that the ratio of chl *a*-to-RNA should increase when temperature increases

Therefore, to test the hypotheses that

1. RNA:protein will not be affect by temperature and
2. that chl *a*:RNA will be higher at high temperature than at low temperature,

a study was conducted to evaluate the response of *E. huxleyi* CCMP 1516 to various temperatures with the following objectives:

1) To determine the effect of temperature on growth rate and biochemical composition of microalgae.
2) To examine the correlations between growth rate and RNA:protein to test whether the growth rate hypothesis can be applied to temperature.
3) To examine the correlations between growth rate and chl *a*:C to test whether the bio-optical hypothesis can be applied to temperature.

5.2 Operating conditions and sampling

Emiliania huxleyi CCMP 1516 was grown in 3 litre volume semi-continuous cultures in artificial seawater (Berges *et al*. 2001), enriched to f/2 medium (Guillard & Ryther 1962) with 3 mM $NaHCO_3$ and 1 nM Na_2SeO_3. Cells in exponential phase were used to inoculate continuous cultures containing 20 µM NaH_2PO_4, 300 µM $NaNO_3$, f/8 metals, and f/4 vitamins. Triplicate cultures were illuminated under photosynthetic photon flux densities of 600 ± 10 µmol photons m^{-2} s^{-1} on a 14:10 h light:dark cycle. Initially, *E. huxleyi* was grown in a batch culture mode at 16ºC. After which, cells in exponential growth were moved to continuous culture mode and incubated at 18 ± 0.1ºC using a temperature controlled water bath. The cultures were gently stirred with a magnetic stir bar and continuously aerated with filtered air through a 0.22 µm membrane filter. Cell abundance was determined daily using a hemocytometer and kept in the range of approximately 50-100 $x10^4$ cells mL^{-1} by adjusting the dilution rate in order to prevent nutrient limitation and minimize light attenuation due to self-shading .

Cultures were harvested at intervals of 4 to 5 days to obtain material for chemical and physiological assays. Samples were typically collected in triplicate from each of the 3 replicate cultures on three occasions. Specifically, 15x100 mL volumes of suspension were collected on glass microfiber filters for measuring chlorophyll *a*, particulate organic carbon (POC), protein, fatty acid profile and pigments. In addition, 6x25 mL of suspension was collected for measuring particulate nitrogen (PN), particulate phosphorus (PP) and 9x100 mL of culture suspension was centrifuged at 3000 x g for 7 min for measuring total amino acids, RNA and DNA. Moreover, at selected times when the radiotracer lab was available, 30 mL of culture suspension was collected for determining photosynthesis-light response curves. Cell size (equivalent spherical diameter and volume) was determined using a Coulter particle counter and size analyzer (Z2, Beckman coulter Inc., USA). Samples for POC were collected on pre-combusted filters, which

were baked at 500^{o}C for 5 h in a muffle furnace (Carbolite, AAF 1100, UK). All elemental and biochemical composition were measured using the methods described in chapter 2.

After samples were collected at 18^{o}C (I, first treatment), the temperature was reduced from 18^{o}C (I) to 14^{o}C and additional samples were collected in the same way as described above. Following this, the temperature was increased from 14^{o}C to 18^{o}C (II, second treatment) and then to 22^{o}C respectively and sampling was repeated.

5.3 Statistical analysis

Statistical analysis was performed using Statistical Package for the Social Sciences (SPSS version 19). A paired sample student t-test was performed for pair-wise comparison, while an analysis of variance (ANOVA) with the post hoc test (Tukey HSD) used for multiple comparisons.

5.4 Results

5.4.1 Growth rate, Chl *a*, PN, PP, and POC

The abundance of *E. huxleyi* was maintained at between 5 and 10 x 10^5 cells mL^{-1} in all vessels (Fig 5-1A). Cell abundances at 18 (II) and 22ºC were higher than at 14ºC. There were differences in growth rate (Fig 5-1B) and biovolume (Fig 5-1C) with elevated temperature.

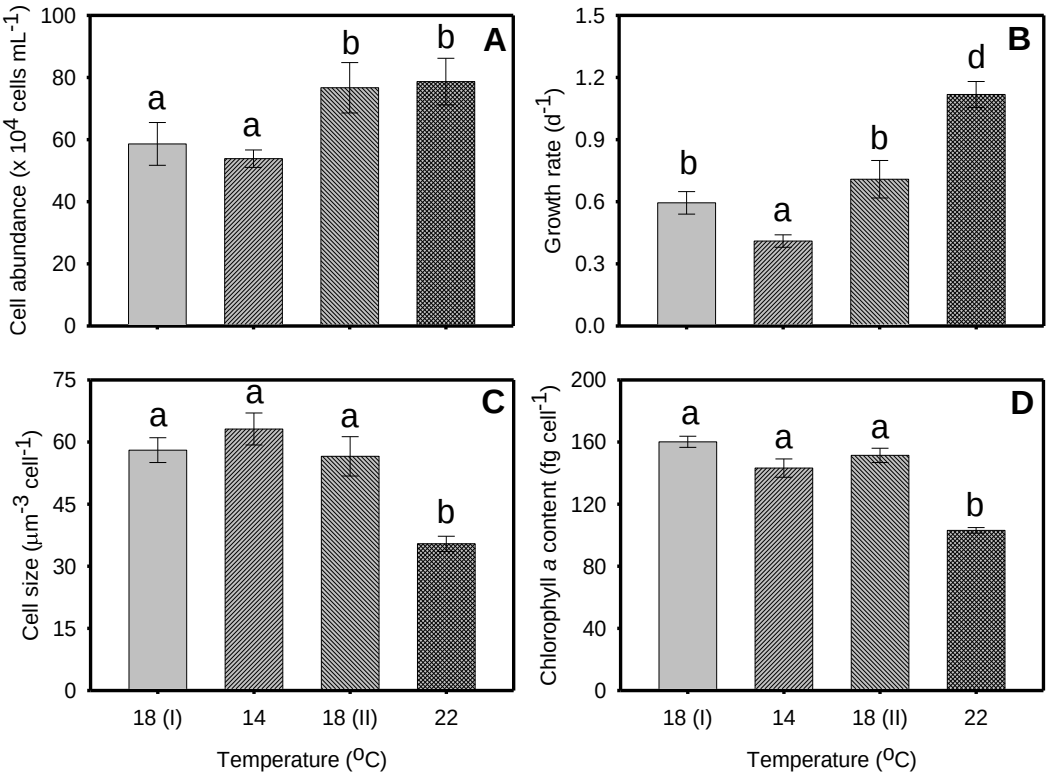

Figure 5-1. Temperature dependence of cell abundance (A), growth rate (B), cellular volume (C), and chlorophyll *a* content (D) of *E. huxleyi* CCMP 1516. Values are mean ± standard errors for three replicate vessels (n = 9) at temperatures of 18(I), 14, 18(II), and 22ºC. Bars labelled with the same letter were not significantly different (one way ANOVA Tukey's test; $p < 0.05$).

The growth rate of *E. huxleyi* increased significantly with elevated temperature (Fig 5-1B; ANOVA, $p<0.05$). The growth rate of *E. huxleyi* was about 2.7 times higher at 22ºC (1.12 d^{-1}) than at 14ºC (0.41 d^{-1}) with an intermediate growth rate observed at 18ºC. Temperature significantly affected biovolume (ANOVA; $p< 0.05$), with the lowest value observed at 22ºC (Fig

5-1C). Cellular chlorophyll *a* content decreased with increased temperature of 22ºC while at temperatures of 18 (I), 14 and 18 (II)ºC no significance was observed (Fig 5-1D).

The intracellular nitrogen (N) and phosphorus (P) contents of *E. huxleyi* at temperature of 18 (I)ºC and 14ºC were not significantly different. Lower N and P were observed at 18 (II) and 22ºC (Figs 5-2A,B). Whereas, intracellular carbon (C) content decreased with increased temperature (Fig 5-2C). When *E. huxleyi* was cultured at 22ºC N:P ratio was approximately 23.8, the highest N:P ratio observed. However, the averages of N:P ratios were 15.7, 16.3, and 18.1 at temperatures of 18(I), 14, and 18(II)ºC respectively (Fig 5-2D).

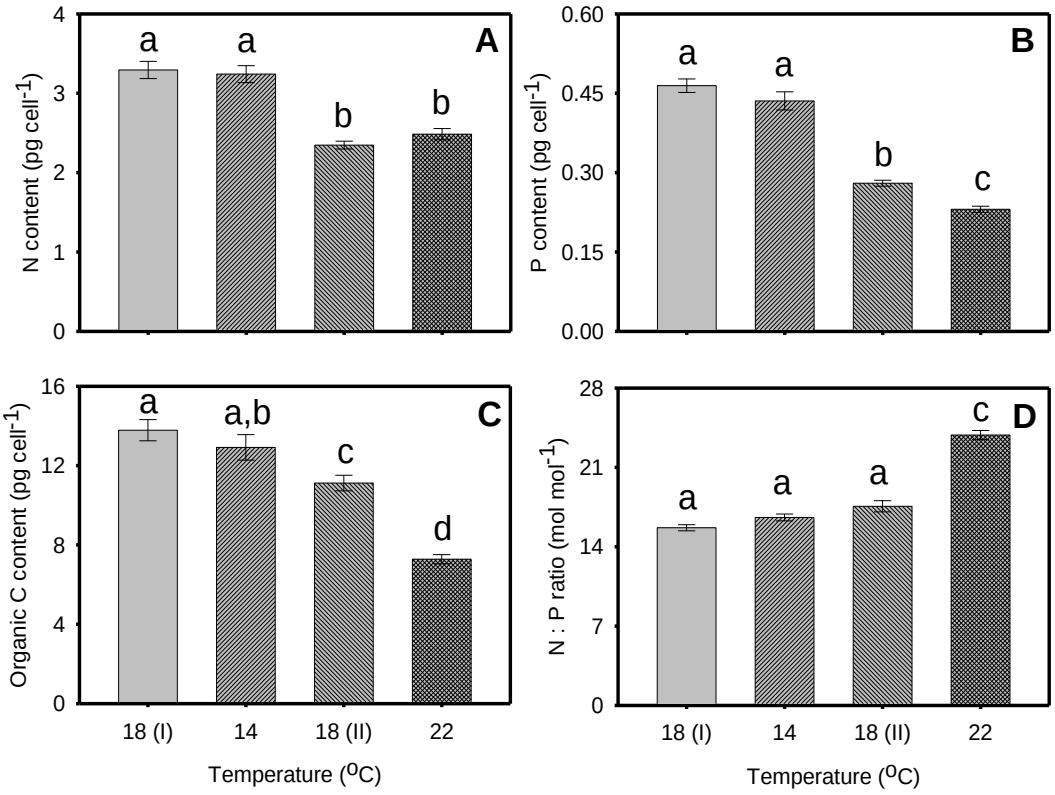

Figure 5-2. Intracellular content of nitrogen (A), phosphorus (B), organic carbon (C), and N:P ratios (D) of *E. huxleyi* CCMP 1516. Mean values ± standard errors are shown for three replicate vessels, n = 9 at temperatures of 18(I), 14, 18(II), and 22ºC. Bars labelled with the same letter were not significantly different (one way ANOVA Tukey's test; $p < 0.05$).

The chl *a* to C ratio increased with temperature (Fig 5-3A) and the chl *a* : C was positively correlated with growth rate (Fig 5-3B). However, the increase in growth rate was approximately 3.3 fold, whereas the increase in chl *a* : C was only about 1.4 fold.

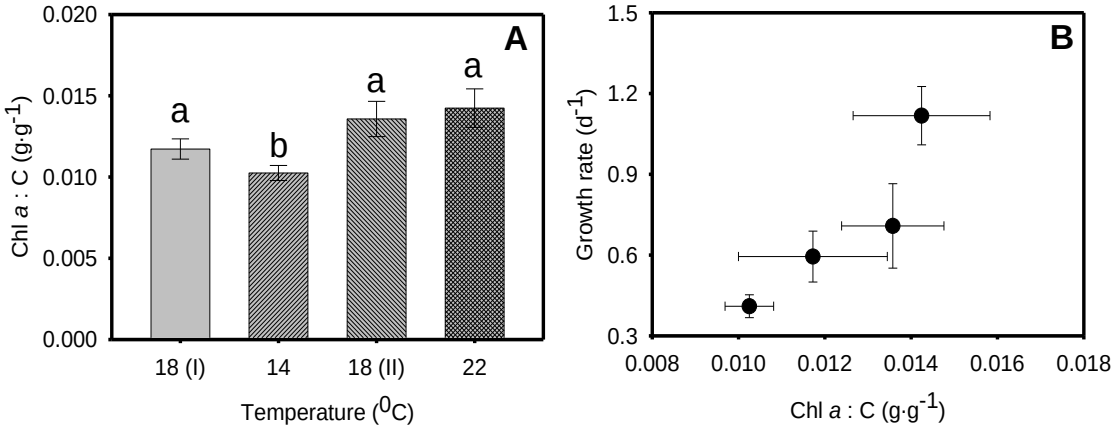

Figure 5-3. The chl *a* to C ratio in unit g g^{-1} (A) of *E. huxleyi* CCMP 1516 under different temperatures of 18(I), 14, 18(II) and 22°C and the relationship between chl *a* : C and growth rate (d^{-1}) (B). Values are mean ± standard errors for three replicate vessels. Bars labelled with the same letter were not significantly different (one way ANOVA Tukey's test; $p < 0.05$).

5.4.2 Chlorophyll *a* (chl *a*) and elemental contents per volume

Chl *a* content at 14°C was approximately 2.14 fg cell μm^{-3} (Fig 5-4A), about 25% lower than at higher temperatures. There were no significant changes in chl *a* contents per cell volume (μm^{-3}) with temperature at 18 (I), 18(II) and 22°C ($p<0.05$). The PN, PP, and organic C contents had a tendency to decline with increasing temperature (Fig 5-2) following the same trend as cell size so biovolume may affect the contents of these. N per unit biovolume (fg cell μm^{-3}) was highest at 22°C (Fig 5-4B). There was no significant differences in carbon contents per biovolume at 14, 18(II) and 22°C (Fig 5-4C). P content per unit biovolume was lowest at 18°C (II) (Fig 5-4D).

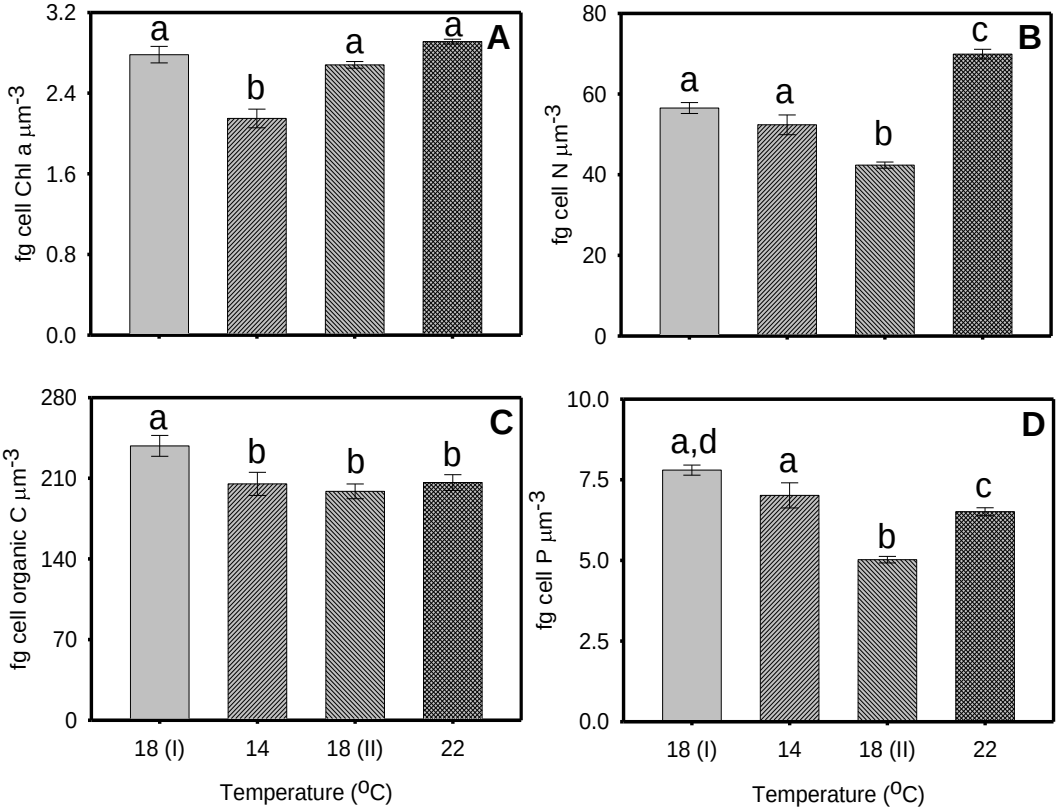

Figure 5-4. Intracellular concentrations of chlorophyll *a* (A), nitrogen (B), organic carbon (C) and phosphorus (D) of *E. huxleyi* CCMP 1516. Concentrations are expressed in units of mass per unit cell volume (fg μm^{-3}) of cell. Values are mean ± standard errors for three replicate vessels (n = 9) at temperatures of 18(I), 14, 18(II), and 22°C. Bars labelled with the same letter were not significantly different (one way ANOVA Turkey's test; $p < 0.05$).

5.4.3 Protein contents and protein per volume

Protein content was measured using two different standards for calibrating the assay. Using BSA as a standard provided the same protein contents as using BGG (Fig 5-5A). Protein content decreased with elevated temperature. *E. huxleyi* grown at 14 and 18°C had protein contents of approximately 8.4-9.1 pg $cell^{-1}$. The lowest protein levels of about 3.5 pg $cell^{-1}$ were observed at 22°C. In the same way, using BSA as a standard gave the same protein contents per biovolume ($cell^{-1}$ volume μm^{-3}) as using BGG (Fig 5-5B). Both BSA and BGG as a standard

no significant differences in protein concentration were observed at growth temperatures of 18 (I), 14, and 18 (II) (ANOVA, $p<0.05$) exception 22°C.

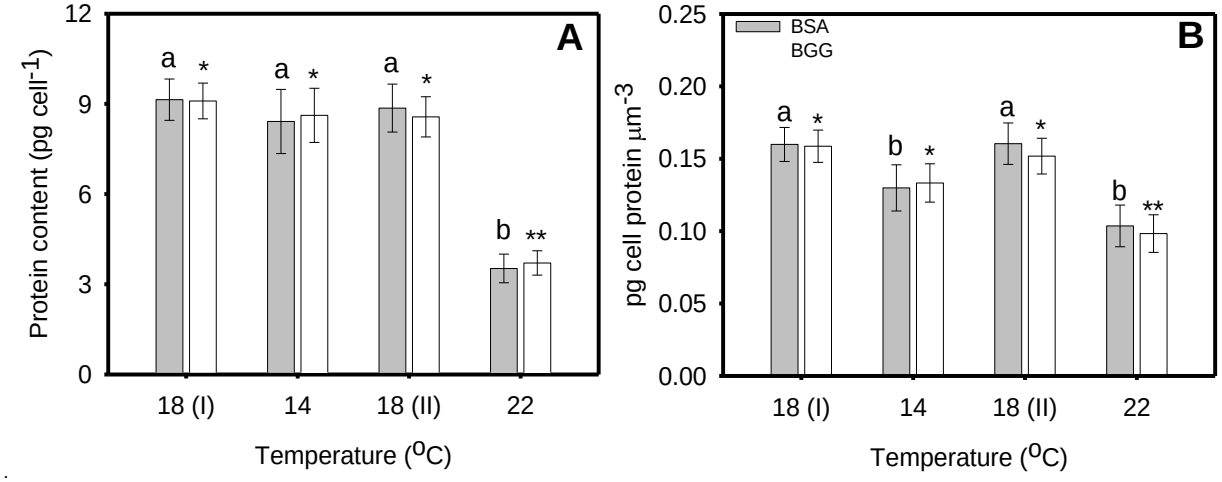

Figure 5-5. Temperature dependence of cellular protein contents of *E. huxleyi* CCMP 1516. Values are mean ± standard errors for three replicate vessels (n = 9) of the two different standards (BSA; grey bar and BGG; white bar) used to calibrate the protein assays. Bars labelled with the same letter were not significantly different (one way ANOVA Turkey's test; $p< 0.05$).

5.4.4 DNA and RNA contents

E. huxleyi grown at 18(I), 14 and 18(II)°C had similar DNA contents, but the lowest DNA content was found at 22°C (Fig. 5-6A). The lowest RNA content was observed at 22°C (Fig. 5-6B). When DNA and RNA content were compared with biovolume (μm^3), both DNA:biovolume and RNA:biovolume gave the highest levels at 22°C (Figs. 5-6C,D). In the present study, RNA:DNA ratios were >1, and the RNA:DNA ratio was not affected by temperature (Fig 5-7A). The growth rate was positively correlated with RNA:protein (Fig. 5-7B). However, the growth rate increased by about 3 fold from 14 to 22°C, whereas RNA:protein increased by only about 1.5 times over the same temperature range.

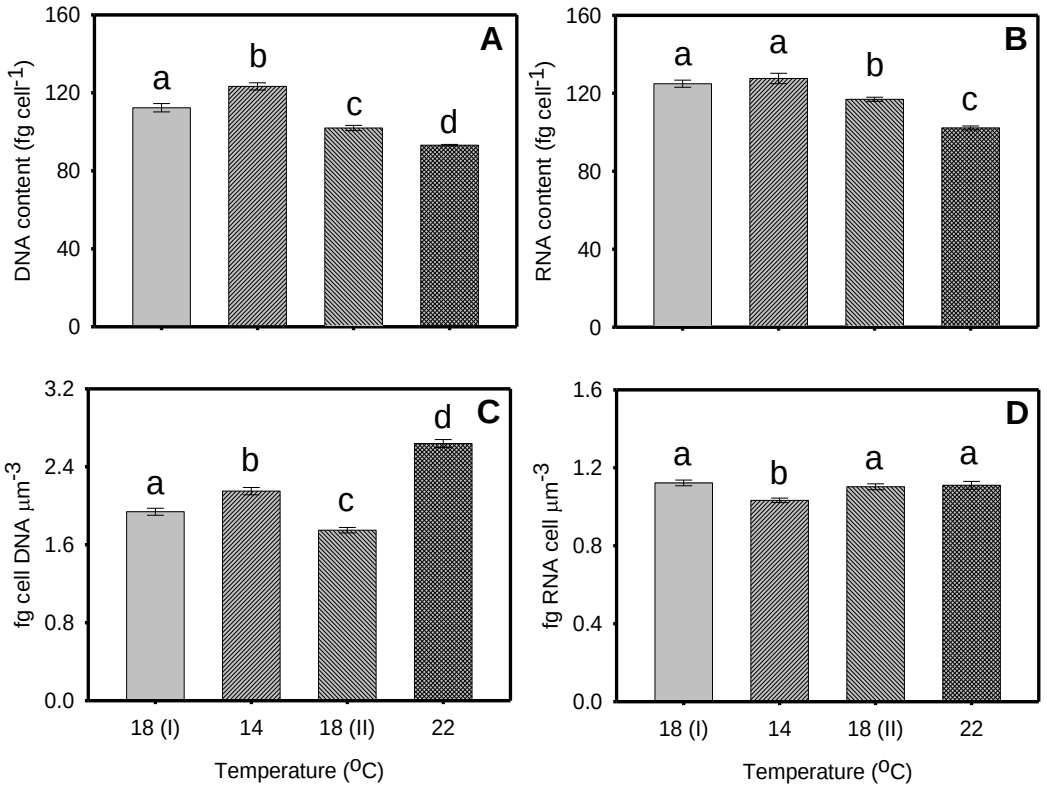

Figure 5-6. Temperature dependence of DNA content (A), RNA content (B), DNA:biovolume (C), and RNA:biovolume (D) of *E. huxleyi* CCMP 1516. Values are mean ± standard errors for three replicate vessels (n = 9) at temperatures of 18(I), 14, 18(II), and 22°C. Bars labelled with the same letter were not significantly different (one way ANOVA Turkey's test; $p < 0.05$).

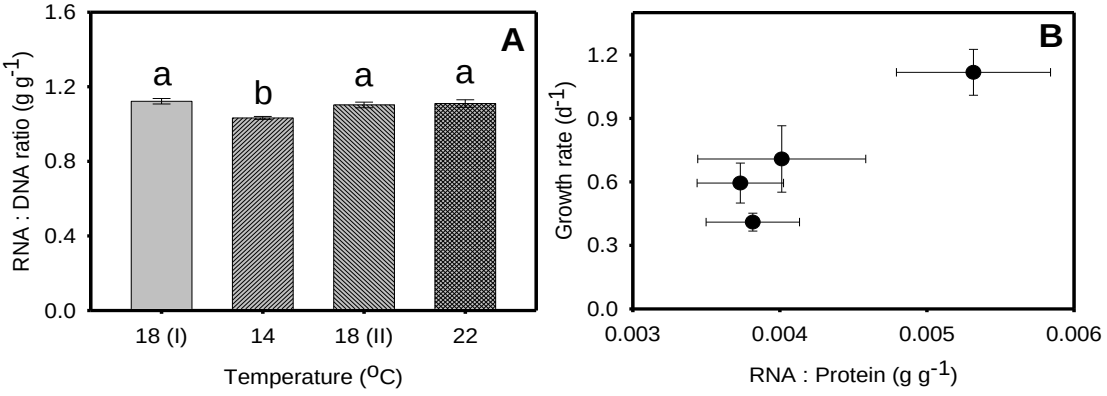

Figure 5-7. RNA : DNA ratio (A) are expressed in unit of $g \cdot g^{-1}$ of *E. huxleyi* CCMP 1516 and the relationship between RNA : protein ($g\ g^{-1}$) ratio and growth rate (d^{-1}) (B). Values are mean ± standard errors for three replicate vessels (n = 9) at temperatures of 18(I), 14, 18(II), and 22°C.

Bars labelled with the same letter were not significantly different (one way ANOVA Turkey's test; $p< 0.05$).

5.4.5 Amino acids

Seventeen free and combined amino acids were identified. The total amino acid content in cells is shown in Fig. 5-8 consisted of both free amino acids and combined amino acids. Total amino acid content decreased with increased temperature. Total amino acid at 14°C had the highest value of roughly 2.65 ± 0.30 pg cell^{-1}, while at 22°C the lowest value was about 1.77 ± 0.23 pg cell^{-1}.

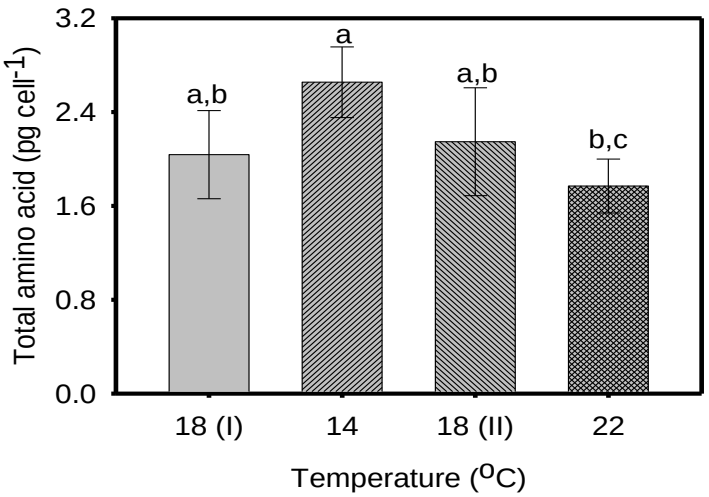

Figure 5-8. Temperature dependence of total amino acid content of *E. huxleyi* CCMP 1516 in different vessels at temperatures 18(I), 14, 18(II) and 22°C. Values are mean ± standard errors for three replicate vessels (n = 3-6). Bars labelled with the same letter were not significantly different (one way ANOVA Tukey's test; $p< 0.05$).

The highest free amino acid content of the cells was approximately 0.062-0.064 pg cell^{-1} at 18°C, whilst the lowest was at 22°C approximately 0.015 pg cell^{-1} (Table 5-1). Glutamic acid was the most abundant free amino acid at temperature $\leqslant$ 18°C following alanine.

The amount of combined amino acids in all temperatures was greater than the amount of free amino acids (Table 5-2). Glutamic acid and arginine was the most abundant amino acid content in cells, accounting for approximately 11-16 % of total amino acids. Serine, glycine, asparagine, threonine, proline, lysine, tyrosine, alanine, and valine were all present at contents > 5 % of total amino acids. Six amino acids (histidine, cysteine, methionine, phenylalanine, tyrosine and isoleucine) were < 5 % of the total amino acids (Fig. 5-9 and Table 5-3). Most of both free and combined amino acid composition at high temperature (22^{o}C) was less than at low temperature.

Table 5-1. Free amino acid (pg cell^{-1}) of *Emiliania huxleyi* in response to different growth temperatures. Values are mean and standard errors for three replicate vessels, n = 3-6. Means with a row followed by the same letter are not significantly different (one way ANOVA Tukey's test; $p < 0.05$).

	Amount of free amino acid (pg cell^{-1}) in *Emiliania huxleyi*							
Amino acid	18 (I)^{o}C		14^{o}C		18 (II)^{o}C		22^{o}C	
	Mean	SE	Mean	SE	Mean	SE	Mean	SE
Essential amino acid								
Histidine	0.0001^{A}	0.0000	0.0004^{A}	0.0003	0.0001^{A}	0.0001	0.0000^{A}	0.0000
Lysine	0.0046^{C}	0.0003	0.0008^{A}	0.0001	0.0021^{B}	0.0006	0.0009^{A}	0.0003
Methionine	0.0015^{C}	0.0000	0.0010^{B}	0.0002	0.0017^{C}	0.0002	0.0005^{A}	0.0000
Valine	0.0025^{B}	0.0002	0.0014^{A}	0.0002	0.0025^{B}	0.0004	0.0011^{A}	0.0001
Phenylalanine	0.0025^{B}	0.0002	0.0013^{A}	0.0004	0.0026^{B}	0.0005	0.0008^{A}	0.0002
Isoleucine	0.0005^{B}	0.0002	0.0001^{A}	0.0001	0.0005^{B}	0.0001	0.0001^{A}	0.0000
Non-essential amino acid								
Arginine	0.0057^{B}	0.0023	0.0010^{A}	0.0003	0.0059^{B}	0.0028	0.0006^{A}	0.0003
Serine	0.0052^{C}	0.0000	0.0032^{B}	0.0006	0.0057^{C}	0.0007	0.0012^{A}	0.0003
Glycine	0.0017^{B}	0.0000	0.0011^{A}	0.0003	0.0018^{B}	0.0002	0.0008^{A}	0.0001
Glutamic acid	0.0155^{B}	0.0003	0.0117^{A}	0.0010	0.0176^{C}	0.0027	0.0013^{A}	0.0006
Asparagine*	0.0070^{D}	0.0008	0.0031^{B}	0.0005	0.0044^{C}	0.0008	0.0022^{A}	0.0006
Proline	0.0017^{C}	0.0001	0.0011^{B}	0.0002	0.0019^{C}	0.0002	0.0007^{A}	0.0001
Cysteine	0.0006^{A}	0.0000	0.0008^{A}	0.0001	0.0009^{A}	0.0002	0.0009^{A}	0.0002
Tyrosine	0.0013^{A}	0.0001	0.0012^{A}	0.0000	0.0014^{A}	0.0001	0.0012^{A}	0.0000
Threonine	0.0020^{C}	0.0001	0.0013^{B}	0.0003	0.0023^{C}	0.0002	0.0006^{A}	0.0000
Alanine	0.0115^{D}	0.0017	0.0056^{B}	0.0012	0.0107^{C}	0.0018	0.0017^{A}	0.0005
Total	0.0638	0.0065	0.0352	0.0060	0.0623	0.0116	0.0151	0.0033

* Average of asparagine and aspartic acid due to co-eluting

Table 5-2. The combined amino acid (pg cell^{-1}) of *Emiliania huxleyi* in response to different growth temperatures. Values are mean and standard errors for three replicate vessels, n = 3-6. Means with a row followed by the same letter were not significantly different (one way ANOVA Tukey's test; $p < 0.05$).

	Combined amino acid of *Emiliania huxleyi*							
Amino acid	18 (I)^{o}C		14^{o}C		18 (II)^{o}C		22^{o}C	
	Mean	SE	Mean	SE	Mean	SE	Mean	SE
Essential amino acid								
Histidine	0.02^{A}	0.00	0.03^{A}	0.00	0.01^{A}	0.00	0.01^{A}	0.00
Lysine	0.15^{A}	0.04	0.23^{B}	0.02	0.14^{A}	0.03	0.14^{A}	0.02
Methionine	0.06^{A}	0.02	0.09^{A}	0.00	0.07^{A}	0.01	0.06^{A}	0.00
Valine	0.15^{A}	0.03	0.18^{A}	0.03	0.16^{A}	0.03	0.14^{A}	0.01
Phenylalanine	0.08^{A}	0.02	0.12^{B}	0.02	0.06^{A}	0.02	0.11^{B}	0.03
Isoleucine	0.08^{A}	0.03	0.12^{A}	0.01	0.11^{A}	0.03	0.08^{A}	0.00
Non-essential amino acid								
Arginine	0.24^{A}	0.01	0.30^{B}	0.04	0.22^{A}	0.06	0.21^{A}	0.03
Serine	0.10^{A}	0.02	0.13^{A}	0.00	0.13^{A}	0.04	0.10^{A}	0.01
Glycine	0.10^{A}	0.02	0.14^{A}	0.01	0.11^{A}	0.03	0.11^{A}	0.00
Glutamic acid	0.31^{B}	0.05	0.38^{C}	0.05	0.26^{A}	0.05	0.26^{A}	0.04
Asparagine*	0.22^{B}	0.02	0.26^{B}	0.03	0.24^{B}	0.05	0.11^{A}	0.03
Proline	0.11^{A}	0.04	0.12^{A}	0.02	0.11^{A}	0.03	0.12^{A}	0.01
Cysteine	0.02^{A}	0.01	0.02^{A}	0.00	0.02^{A}	0.00	0.01^{A}	0.01
Tyrosine	0.08^{A}	0.02	0.14^{A}	0.00	0.14^{A}	0.04	0.10^{A}	0.01
Threonine	0.11^{A}	0.03	0.17^{B}	0.01	0.12^{A}	0.02	0.11^{A}	0.01
Alanine	0.14^{A}	0.03	0.16^{A}	0.03	0.15^{A}	0.02	0.17^{A}	0.00
Total	1.95	0.36	2.59	0.28	2.07	0.90	1.74	0.22

* Average of asparagine and aspartic acid due to co-eluting

Table 5-3. Total amino acid content (percentage of total amino acids) of *Emiliania huxleyi* in response to different growth temperatures. Values are mean and standard errors for three replicate vessels, n = 3-6. Means with a row followed by the same letter were not significantly different (one way ANOVA Tukey's test; $p < 0.05$).

Amino acid	Percentage of total amino acid*							
	18 (I)°C		14°C		18 (II)°C		22°C	
	Mean	SE	Mean	SE	Mean	SE	Mean	SE
Essential amino acid								
Histidine	1.50^{D}	0.19	1.17^{C}	0.01	0.83^{B}	0.04	0.71^{A}	0.08
Lysine	7.27^{B}	0.58	8.85^{C}	1.26	6.63^{A}	0.03	7.62^{B}	0.24
Methionine	2.81^{A}	0.40	3.39^{A}	0.31	3.52^{A}	0.39	3.10^{A}	0.08
Valine	7.42^{A}	0.06	6.66^{A}	0.84	7.62^{A}	0.45	7.48^{A}	0.13
Phenylalanine	4.09^{B}	0.19	4.47^{B}	0.77	3.02^{A}	0.15	5.93^{C}	2.30
Isoleucine	3.84^{A}	0.63	4.48^{A}	0.44	5.06^{B}	0.29	4.20^{A}	0.44
Non-essential amino acid								
Arginine	11.96^{A}	2.00	11.39^{A}	1.05	10.52^{A}	0.41	11.37^{A}	0.92
Serine	5.81^{A}	0.18	5.50^{A}	0.09	7.20^{B}	0.50	5.57^{A}	0.29
Glycine	5.14^{A}	0.03	5.58^{A}	0.25	5.38^{A}	0.09	6.01^{B}	0.42
Glutamic acid	15.54^{B}	0.51	14.58^{B}	1.30	12.47^{A}	0.31	10.57^{A}	1.04
Asparagine**	10.94^{B}	0.99	9.65^{B}	0.66	11.24^{C}	0.17	5.79^{A}	1.16
Proline	5.46^{A}	0.88	5.16^{A}	0.84	5.10^{A}	0.22	6.94^{B}	0.10
Cysteine	1.04^{A}	0.29	0.96^{A}	0.05	1.22^{A}	0.05	0.61^{B}	0.44
Tyrosine	4.70^{A}	0.07	5.62^{B}	0.42	7.00^{C}	0.70	5.35^{B}	0.13
Threonine	5.44^{A}	0.30	6.46^{A}	0.84	5.94^{A}	0.32	5.84^{A}	0.16
Alanine	7.03^{A}	0.07	6.09^{A}	0.92	7.26^{A}	0.68	9.02^{B}	0.59

* Sum of free and combined amino acids

** Sum of asparagine and aspartic acid due to co-eluting

5.4.6 Photosynthesis rate

The photosynthetic rate of *E. huxleyi* at 18(I), 14, and 18 (II)°C increased linearly with photon flux density until the maximum level was reached at approximately 250-300 µmol photons m^{-2} s^{-1} (Figs. 5-9 A-G) after which the photosynthetic rates remained constant at higher irradiances (or saturated light). In contrast, at 22°C the photosynthesis rate increased hyperbolically (Figs. 5-9 D,H).

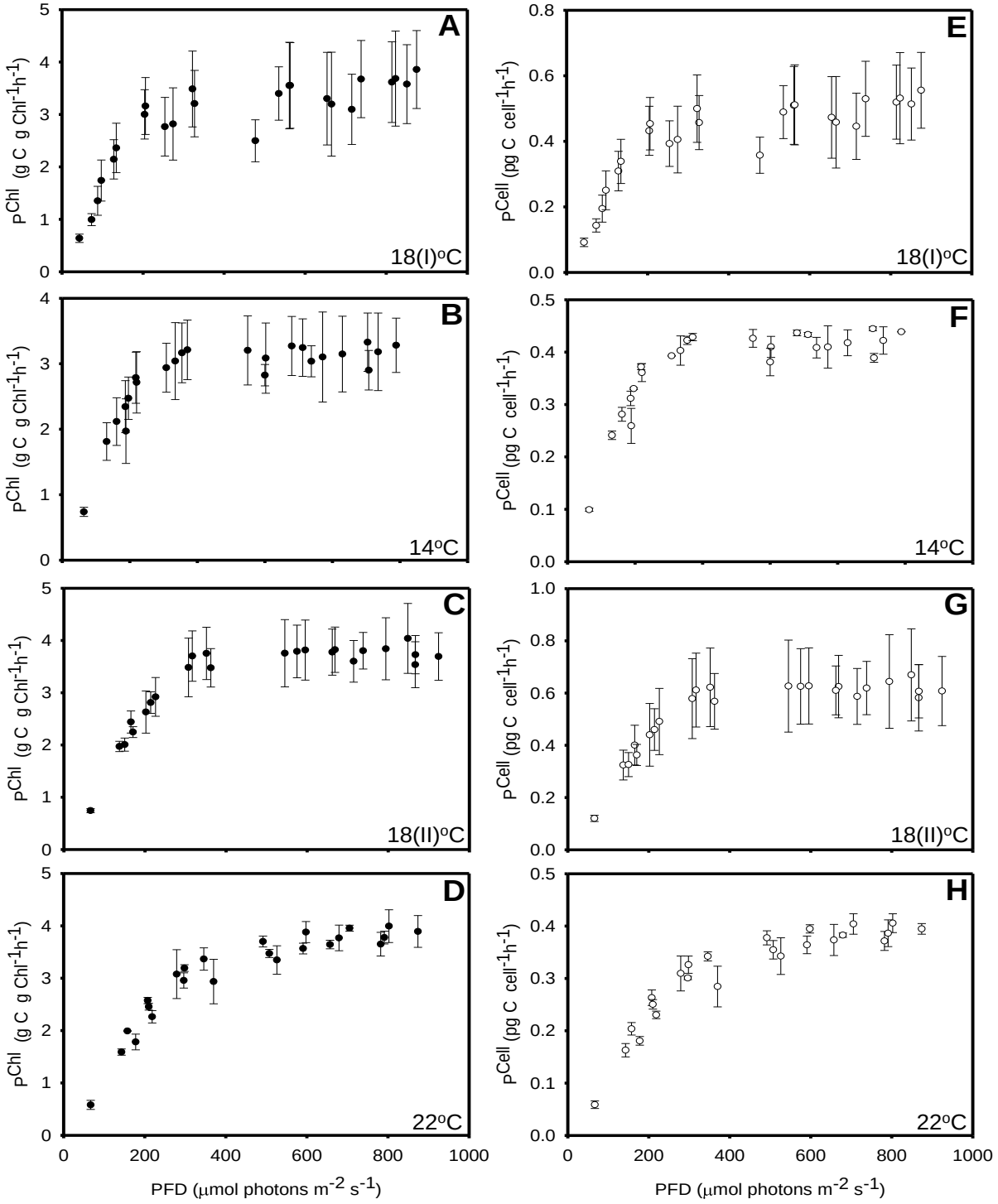

Figure 5-9. Temperature dependence of the chlorophyll *a*-specific rate of photosynthesis (P^{Chl} in unit g C g Chl^{-1} h^{-1}) at temperatures: 18(I)ºC (A), 14ºC (B), 18(II)ºC (C), and 22ºC (D). Temperature dependence of the cell-specific rate of photosynthesis (P^{Cell} in unit pg C $cell^{-1}$ h^{-1}): 18 (I)ºC (E), 14ºC (F), 18 (II)ºC (G), and 22ºC (H). Values are mean ± standard errors for three replicate vessels, n = 3.

The light saturated rate of photosynthesis rate is called P_{max}. Both P_{max} per unit chlorophyll (P^{Chl}_{max}) and per cell (P^{Cell}_{max}) did not change significantly with increasing temperature (Table 5-4). The slope of the linear part of the PE curve is given the symbol α. Both α from P^{Chl} and P^{Cell} did not increase progressively with increasing temperature. E_k is the saturation irradiance, which was significantly greater at 22°C than at 14 and 18°C (Table 5-4).

Table 5-4. Photosynthetic rate parameters of *E. huxleyi* at different temperatures.

Parameter	Temperature (°C)	Photosynthetic rate derived from	
		Chlorophyll	Cell
P_{max}	18 (I)	3.50 (0.09)^{a}	0.50 (0.01)^{A}
	14	3.20 (0.06)^{a}	0.43 (0.08)^{A}
	18 (II)	3.88 (0.07)^{a}	0.64 (0.01)^{C}
	22	4.00 (0.02)^{a}	0.41 (0.01)^{A}
α	18 (I)	0.021 (0.003)^{b,c}	0.0033 (0.001)^{A}
	14	0.019 (0.003)^{a,b}	0.0034 (0.000)^{A}
	18 (II)	0.019 (0.004)^{a,b}	0.0034 (0.000)^{A}
	22	0.015 (0.002)^{a}	0.0026 (0.000)^{A}
E_k	18 (I)	170 (20.00)^{a}	168 (24.13)^{A}
	14	161 (10.06)^{a}	155 (8.21)^{A}
	18 (II)	158 (11.43)^{a}	146 (12.67)^{A}
	22	250 (13.64)^{b}	238 (15.52)^{B}

* Unit: P^{Chl}_{max}: gC gchl^{-1} h^{-1}; P^{Cell}_{max}: pgC cell^{-1} h^{-1}; α (P^{Chl}): gC gchl^{-1} h^{-1} (µmol photons m^{-2} s^{-1})$^{-1}$; α (P^{Cell}): pgC cell^{-1} h^{-1} (µmol photons m^{-2} s^{-1})$^{-1}$; E_k: µmol photons m^{-2} s^{-1}. Values given are the means and values in parentheses are the standard error of the estimates (n = 3). Entries labelled with the same letter were not significantly different (one way ANOVA Tukey's test; $p < 0.05$).

5.4.7 Pigments

Eight accessory pigments (beta carotene, chlorophyll *c*, chlorophyll c_2, fucoxanthin, 4-keto-19'-hexanoyloxyfucoxanthin, 19'-hexanoyloxyfucoxanthin, diatoxanthin, and diadinoxanthin), in addition to chlorophyll *a*, were found 19'-hexanoyloxyfucoxanthin gave the highest pigment ratio [mol (mol chl *a*)$^{-1}$] while beta carotene gave the lowest content (Table 5-5). 4-keto-19'-

hexanoyloxyfucoxanthin, 19'-hexanoyloxyfucoxanthin, and chlorophyll c_2 ratios did not vary significantly with temperatures at confidence level 95 %. Total pigment to chl *a* ratios at 18(I), 18(II) and 14°C were not significantly different, while at higher temperature (22°C) there was a slight decrease. Similarly, beta carotene, diatoxanthin, and diadinoxanthin ratios decreased with increasing temperature; however, fucoxanthin ratio increased with elevated temperature, from 0.13 at 14°C to 0.24 at 22°C. Chlorophyll *c* to chl *a* ratios at 18(I), 14 and 18(II) were not significantly different, whereas at 22°C the highest ratio was observed. The ratio of the photoprotective pigments diatoxanthin and diadinoxanthin (DT+DD) per chl *a* and per total fucoxanthin decreased at higher temperatures.

Table 5-5. Pigment composition [mol accessory pigment (mol chl *a*)$^{-1}$] of *E. huxleyi* grown under different temperatures. Values are mean and standard errors (SE) for three replicate vessels, n=3. Means with a row followed by the same letter are not significantly different (one way ANOVA Tukey's test; $p < 0.05$).

Pigment	Pigment composition [mol accessory pigment (mol chl *a*)$^{-1}$] of *E. huxleyi*							
	18 (I) °C		14 °C		18 (II) °C		22 °C	
	Mean	SE	Mean	SE	Mean	SE	Mean	SE
Beta C (mmol)	9.19^{A}	0.29	8.52^{A}	0.62	9.10^{A}	0.55	4.01^{B}	0.22
Hex-kfuco	0.09^{A}	0.00	0.08^{A}	0.00	0.07^{A}	0.00	0.09^{A}	0.01
DT	0.11^{A}	0.01	0.15^{A}	0.01	0.10^{A}	0.01	0.05^{B}	0.00
Chl *c*	0.17^{A}	0.01	0.18^{A}	0.01	0.19^{A}	0.00	0.24^{B}	0.01
Fuco	0.21^{A}	0.01	0.13^{B}	0.01	0.22^{A}	0.01	0.24^{A}	0.02
Chl c_2	0.30^{A}	0.01	0.30^{A}	0.01	0.30^{A}	0.01	0.33^{A}	0.01
DD	0.55^{B}	0.02	0.64^{A}	0.02	0.56^{B}	0.02	0.19^{C}	0.01
Hex-fuco	1.33^{A}	0.04	1.23^{A}	0.05	1.24^{A}	0.02	1.20^{A}	0.02
Total fuco	1.64^{A}	0.05	1.44^{B}	0.05	1.54^{A}	0.03	1.53^{A}	0.05
Total pigment/ Chl *a*	2.78^{A}	0.44	2.73^{A}	0.77	2.70^{A}	0.65	2.34^{B}	0.34
Total Chls *c*/ Chl *a*	0.46^{A}	0.01	0.48^{A}	0.02	0.49^{A}	0.01	0.57^{B}	0.01
(DD+DT)/ Chl *a*	0.66^{A}	0.03	0.80^{B}	0.03	0.66^{A}	0.03	0.24^{C}	0.01
Total Chls *c*/ T fuco	0.28^{A}	0.01	0.33^{B}	0.01	0.32^{B}	0.01	0.37^{C}	0.01
(DD+DT)/ T fuco	0.40^{A}	0.02	0.55^{B}	0.02	0.43^{A}	0.02	0.16^{C}	0.01
DT/ (DD+DT)	0.16^{A}	0.00	0.19^{B}	0.00	0.15^{A}	0.00	0.22^{B}	0.00

Beta C: Beta carotene, Hex-kfuco: 4-keto-19'-hexanoyloxyfucoxanthin, DT: Diatoxanthin, Chl *c*: Chlorophyll *c*, DD: Diadinoxanthin, Chl c_2 : Chlorophyll c_2, Fuco: Fucoxanthin, Hex-fuco: 19'-hexanoyloxyfucoxanthin, Total pigment = Σ(Beta C+ Hex-kfuco+ DT + Chl *c* + DD + Chl c_2 + Fuco + Hex-fuco), Total fuco = Σ (Fuco+Hex-kfuco+Hex-fuco), and Total chls *c* = Σ (Chl *c* + Chl c_2).

5.4.8 Fatty acid profile

The fatty acid composition of *E. huxleyi* at the different temperatures is shown in Tables 5-6 and 5-7. Total fatty acid content (fg cell^{-1}) increased with decreasing temperature. Cells grown at 14ºC gave the highest fatty acid content approximately 982 fg cell^{-1}. Even though 21 fatty acids were detected, most of these contributed to < 3% of the total. The two fatty acids present in the largest amounts (>15 %) were myristic acid (C14:0; 20-23 % of total) and Oleic acid (C18:1; 18-25 % of total). There were five components with lower amounts; palmitic acid (16:0; 8-10 % of the total), linolenic acid (C18:2; 3-7 % of the total), eicosapentaenoic acid (C20:5; 3-4 % of the total), docosahexaenoic acid (22:6; 5-9 % of the total) and behenic acid (C22:0; 4-6 % of the total). Of these seven fatty acids, significant treatment effects were only found for linolenic acid, elaidic acid, eicosapentaenoic acid (EPA), and docosahexaenoic acid (DHA). Oleic acid at 14ºC was the highest percentage of fatty acid roughly 25 % of the total while at 22ºC, this dropped to approximately 18 % of the total fatty acid. Cells had the greatest percentage of EPA at highest growth temperature (4 % total of fatty acid at 22ºC). There were no significant differences in DHA between 14 and 18ºC; however, cells had higher percentage of DHA approximately 7-8 % of total fatty acid at these lower temperatures than at 22ºC (6 % of total fatty acid).

Saturated fatty acid and polyunsaturated fatty acid at 14ºC had lower percentage (23 %) of total fatty acid than at higher temperatures; however, monounsaturated fatty acid was the highest percentage (37 %) of total fatty acid.

Table 5-6. Fatty acid composition (fg cell^{-1}) in exponential growth phase in *E. huxleyi* grown at different temperatures. Values are mean and standard errors (SE) for three replicate vessels, n = 3. Means with a row followed by the same letter are not significantly different (one way ANOVA Tukey's test; p< 0.05). Values shown in bold face are the most abundant fatty acids.

Fatty acid (fg cell^{-1})	Fatty acid content (pg cell^{-1})							
	18 (I)^{o}C		14^{o}C		18 (II)^{o}C		22^{o}C	
	Mean	SE	Mean	SE	Mean	SE	Mean	SE
Lauric acid	6.9	0.8	7.4	0.6	7.6	1.2	5.6	0.6
Myristic acid	**155.8^{A}**	**14.6**	**200.7^{B}**	**10.7**	**122.3^{C}**	**8.9**	**108.6^{D}**	**9.0**
Pentadecanoic acid	18.2	4.6	16.6	5.5	12.5	0.8	11.5	1.1
Palmitoleic acid	19.3	2.9	15.9	1.3	14.0	3.7	9.9	0.9
Palmitic acid	**74.1^{A}**	**7.2**	**94.2^{B}**	**7.1**	**52.3^{C}**	**6.8**	**38.7^{D}**	**2.9**
cis-10-Heptadecenoic acid	7.4	0.6	8.7	0.7	6.0	0.7	6.0	0.6
γ-Linolenic acid	12.1	1.0	13.6	1.0	9.9	1.0	9.7	0.6
Linoleic acid	**38.6^{B}**	**6.4**	**27.2^{A}**	**6.3**	**37.0^{B}**	**1.9**	**30.6^{A}**	**1.8**
Elaidic acid	16.9	5.2	65.1	9.7	33.3	7.5	10.1	1.6
Oleic acid	**154.2^{B}**	**15.1**	**250.7^{A}**	**26.0**	**123.7^{C}**	**14.2**	**84.5^{D}**	**5.8**
Stearic acid	15.1	1.8	20.0	2.4	16.7	2.8	9.6	0.9
Arachidonic acid	18.7	1.5	22.6	1.4	16.1	1.7	14.0	1.0
cis-5,8,11,14,17-Eicosapentaenoic acid	**25.2^{A}**	**2.3**	**28.3^{A}**	**1.4**	**24.0^{A}**	**2.5**	**18.3^{B}**	**0.9**
cis-8,11,14-Eicosatrienoic acid	16.4	2.0	22.2	1.6	15.1	1.6	12.8	0.9
cis-11,14-Eicosadienoic acid	12.8	1.5	18.2	1.5	14.6	1.7	9.2	0.9
cis-11-Eicosenoic acid	8.5	0.7	9.7	0.7	8.0	1.0	6.2	0.4
cis-11,14,17-Eicosatrienoic acid	7.8	0.7	8.9	0.7	9.0	1.1	5.7	0.4
Arachidic acid	11.9	3.0	10.8	1.0	8.0	1.1	7.0	0.4
4,7,10,13,16,19-Docosahexaenoic acid	**59.7^{B}**	**5.8**	**80.1^{A}**	**11.5**	**44.1^{C}**	**6.2**	**29.2^{D}**	**2.0**
Erucic acid	9.9	0.7	19.6	6.7	9.2	1.2	16.8	5.2
Behenic acid	**35.2^{A}**	**4.2**	**41.5^{A}**	**6.1**	**35.1^{A}**	**7.1**	**26.8^{B}**	**4.9**
Total fatty acid	724.4	82.4	981.9	103.6	618.6	74.4	470.7	42.5

Statistical analyses were not conducted using ANOVA on fatty acids less than 20 fg cell^{-1}.

Table 5-7. Fatty acid composition (% fatty acid) of *E. huxleyi* grown in exponential growth phase at different temperatures. Values are mean and standard errors (SE) for three replicate vessels, n = 3. Means with a row followed by the same letter are not significantly different (one way ANOVA Tukey's test; $p < 0.05$). Values shown in bold face are the most abundant fatty acids.

	% total fatty acid							
Fatty acid	18 (I)ºC		14ºC		18 (II)ºC		22ºC	
	Mean	SE	Mean	SE	Mean	SE	Mean	SE
Lauric acid	0.9	0.1	0.8	0.0	1.3	0.2	1.2	0.1
Myristic acid	**21.5^{A}**	**1.4**	**20.5^{A}**	**0.2**	**20.0^{A}**	**0.5**	**22.9^{A}**	**0.7**
Pentadecanoic acid	2.5	0.6	1.8	0.6	2.1	0.2	2.4	0.2
Palmitoleic acid	2.7	0.3	1.6	0.1	2.1	0.3	2.1	0.1
Palmitic acid	**10.3^{A}**	**0.9**	**9.6^{A}**	**0.3**	**8.4^{A}**	**0.3**	**8.2^{A}**	**0.2**
cis-10-Heptadecenoic acid	1.0	0.0	0.9	0.0	1.0	0.0	1.3	0.1
γ-Linolenic acid	1.7	0.1	1.4	0.0	1.6	0.0	2.1	0.0
Linoleic acid	**5.3^{B}**	**0.7**	**2.8^{A}**	**0.7**	**6.1^{B}**	**0.3**	**6.6^{B}**	**0.3**
Elaidic acid	2.5	0.8	6.6	0.7	5.2	0.6	2.1	0.2
Oleic acid	**21.2^{B}**	**1.0**	**25.4^{A}**	**1.5**	**19.9^{B}**	**0.5**	**18.1^{BC}**	**1.1**
Stearic acid	2.1	0.2	2.0	0.2	2.7	0.2	2.0	0.1
Arachidonic acid	2.6	0.1	2.3	0.0	2.6	0.1	3.0	0.1
cis-5,8,11,14,17-Eicosapentaenoic acid	**3.5^{A}**	**0.2**	**2.9^{A}**	**0.1**	**3.9^{A}**	**0.1**	**3.9^{A}**	**0.1**
cis-8,11,14-Eicosatrienoic acid	2.3	0.2	2.3	0.1	2.4	0.1	2.7	0.1
cis-11,14-Eicosadienoic Acid	1.8	0.1	1.9	0.1	2.4	0.3	1.9	0.1
cis-11-Eicosenoic acid	1.2	0.1	1.0	0.0	1.3	0.2	1.3	0.0
cis-11,14,17-Eicosatrienoic acid	1.1	0.0	0.9	0.0	1.5	0.2	1.2	0.0
Arachidic acid	1.6	0.3	1.1	0.1	1.3	0.1	1.5	0.0
4,7,10,13,16,19-Docosahexaenoic acid	**8.2^{A}**	**0.7**	**8.3^{A}**	**1.3**	**7.0^{A}**	**0.3**	**6.2^{B}**	**0.2**
Erucic acid	1.4	0.1	2.0	0.7	1.5	0.1	3.5	0.8
Behenic acid	**4.8^{A}**	**0.4**	**4.3^{A}**	**0.6**	**5.7^{A}**	**0.9**	**5.7^{A}**	**0.9**
% SFA	43.7	3.8	39.9	2.0	41.4	2.3	44.0	2.1
% MUFA	29.9	2.3	37.4	3.1	31.0	1.6	28.4	2.3
% PUFA	26.4	2.1	22.7	2.3	27.6	1.3	27.6	0.8
∑ n-3	12.8		12.1		12.4		11.4	
∑ n-6	11.8		8.7		12.7		14.3	
∑ n-3/ ∑ n-6	1.4		1.8		1.3		0.8	

Statistical analyses were not conducted using ANOVA on fatty acids less than 3 % fatty acid.
SFA: Saturated fatty acid, MUFA: Monounsaturated fatty acid, PUFA: Polyunsaturated fatty acid
∑ n-3: Sum of cis-5,8,11,14-eicosatetraenoic acid (C20:5n3),cis-11,14,17-eicosatrienoic acid (C20:3n3), and 4,7,10,13,16,19-docosahexaenoic acid (C22:6n3)
∑ n-6: Sum of linoleic acid (C18:3n6), γ-linolenic acid (C18:2n6c), arachidonic acid (C20:4n6), and cis-8, 11, 14-eicosatrienoic acid (C20:3n6)

5.5 Discussion

5.5.1 Growth rate, chl *a*, PN, PP, POC and protein content

In this study, the growth of *E. huxleyi* was measured at different temperatures (from 14 to 22ºC) under nutrient-replete semi-continuous culture. The results showed that algal growth increased with raised temperature. Moreover, increased temperature stimulated the cell division rate of *E. huxleyi*. This is consistent with the linear dependence of growth rate with temperature that is typically observed in other microalgae when temperature is at or below the optimum for growth (Claquin *et al*. 2008). The optimal temperature for maximal growth has previously been reported to be 24.4ºC (0.94 d^{-1}) for *E. huxleyi* AC474 (Claquin *et al.* 2008) and optimal temperatures ranging from about 18 to 24ºC have been found for other strains of *E. huxleyi* (Thomas *et al*. 2012, Supplementary Table S5). Thus, the growth rate of *E. huxleyi* is linearly related to elevated temperature and the highest temperature (22ºC) in this study is likely to be close to the optimum temperature which would lead to the selection of the best growth.

E. huxleyi had the highest growth rate at high temperature (22ºC); however, cells were the lowest cell size. The decreased cell size are associated with increase in cell division rate. This indicates that smaller cell tended to have higher growth rate. Similarly, Olson *et al*. (1986) found that the mean volume cell of *Hymenomonas carterae* Braarud and Fagerl (clone Cocco II) grown in laboratory decreased as temperature increased from 13 to 23ºC. Moreover, the haptophyte cell sizes in the East China Sea were smaller in summer (average temperature 26.6 ± 1.5ºC) than in spring (average temperature 19.4 ± 2.3ºC) (Lin *et al*. 2014). The decrease of cell size may keep the balance between anabolic and catabolic processes in cell (von Bertalanffy 1960; Raven & Geider 1988; Geider *et al*. 1998). In addition to the decrease the average cell size of primary producers tends to affect the transfer of energy to higher temperature levels (Svensson *et al*. 2014). This implies that microalgae community size structure may vary across aquatic ecosystems under ongoing climate change.

The lowest cellular chl *a* content was found at the high temperature (22ºC) which related to the deactivation of enzymes in the mechanism of chlorophyll biosynthesis and the maintenance of a constant carbon assimilation rate in photosysthetic carbon fixation (Dutta *et al*. 2009). This suggests that *E. huxleyi* appears to possess the ability to acclimate to high temperature. A similar behaviour was demonstrated for *Phaeodactylum tricornutum*, which exhibited maximum chlorophyll concentrations at the extremes of the temperature growth range (Goldman & Mann 1980). Moreover, a similar result was found in the cold water diatom *Skeletonema costatum* which had higher variability in the chlorophyll *a* content per cell at low temperatures (Yoder 1979).

Given the wide variation in how cell biovolume depends on temperature described above, one can expect that the cellular contents of C, N, P and chlorophyll may either increase, decrease, or be unaffected by temperature. It is thus more informative to examine how temperature affects the ratios C:biovolume etc. Microalgal biovolume is widely estimated to assess the relative abundance of co-occuring algae varying in shape and/or size under different environmental conditions (Hillebrand *et al.* 1999).

Temperature affected nitrogen, phosphorus and carbon contents. The N:P ratio of *E. huxleyi* at low temperature was approximately 16-18, close to the Redfield ratio (16:1); however, N:P ratio shifted at a high temperature (22ºC) to approximately 23.8. This result was similar for *I. galbana* grown in f/2 medium with the N:P ratio increasing from 15:1 to 26:1 between 10ºC and 20ºC (Roleda *et al.* 2013). Geider & La Roche (2002) reported that N:P ratio under optimal nutrient-replete growth conditions was ranged from about 5-19 mol N:mol P in a wide variety of microalgae. While Klausmeier *et al*. (2004) reported that N:P ratio of 29 algal species was flexible and depended on environmental conditions. This results suggest that the excess and nitrogen can be maintained as protein (free and combined amino acid) or stored into photosynthesis pigments (Rhee 1978; Spilling *et al*. 2015).

The C:N ratio (mol:mol) at low temperature (14ºC) was higher than at high temperature (22ºC). Uptake and storage of available NO_3^- of *E. huxleyi* may lead to a lower C:N ratio. Whereas the C:N ratio of *I. galbana* was 9:1 and 10:1 at 10ºC and 20ºC respectively (Roleda *et al.* 2013). Generally, the range of C:N ratio in marine algae was around 4-17 (Geider & La Roche 2002). This implies that the higher C:N ratio at low temperature has the excess carbon which can be stored as an energy reserve such as lipid (Guschina & Harwood 2006).

The ratio of chl *a*:C in *E. huxleyi* progressively increased with elevated temperature. Cells responded to change in temperature by adjusting cellular chlorophyll levels to match in the demands for photosynthesis and this response is quantified by changes in the ratio of chlorophylls to carbon. The changes in chl *a*:C resulted form changes in growth conditions (Behrenfeld et al. 2005). In this study, chl *a*: C ratio also was positively correlated with growth rate (Fig 5-3A). This phenomenon is referred to as the bio-optical hypothesis. Similarly, the chl *a*:C ratio of the diatom *Thalassiosira allenii* was positively correlated with temperature (>25ºC) under both saturating and non-saturating light (Redalje & Laws 1983). The light saturation index (E_k) also showed a positive relationship with increasing temperature. Thus, the correlation of chl *a*:C with growth rate supports the bio-optical model.

The protein content of *E. huxleyi* decreased significantly with increased temperature, and the lowest protein content (approximately 3.53-3.71 pg $cell^{-1}$) was observed at 22ºC. The nitrogen content was low at high temperature which had the lowest protein fraction. Additionally, the carbon content was at the lowest level which was probably a result of the low protein content fraction. Furthermore, the model protein also presented in carbon structure. Similarly, Raghavan *et al*. (2008) reported that *C. calcitrans* grown under increasing temperature (20, 25, and 30ºC) had low protein at higher temperature but lipid content increased. Rhee & Gotham (1981) mentioned that there was an increase in protein concentration with decreased temperature in *Scenedesmus* sp. It is known that temperature affects growth of microalgae via control of enzyme kinetics. Thus, the decrease in the proportion of carbon incorporated in

proteins observed when temperature increase reflects the insufficiency of enzymes (Thompson & Guo 1992).

5.5.2 DNA, RNA and RNA:protein

DNA and RNA content of *E. huxleyi* decreased at high temperature with the lowest values at 22^{o}C. Phosphorus (P) influences by the concentration of P-rich ribosomes with their associated rRNA. Thus, decreasing rRNA in *E. huxleyi* has been presented to increase the N:P ratio. Olson *et al.* (1986) reported that cell size, cell protein content, and cell RNA content in marine phytoplankton may be possible controllers of the cell cycle. N is a component of both protein and nucleic acids, and P is an essential element of the nucleic acid skeleton. Therefore, the depletion of one or other nutrient should affect differentially to the internal concentration of both classes of macromolecules (Berdalet *et al.* 1994).

The RNA: protein content of *E. huxleyi* was highly correlated with growth rate. This suggests that the increasing RNA: protein ratio reflects the control of the rate protein synthesis by the number of ribosome. When the growth rate increased, the rate of ribosome function approached a maximum value, corresponding to 21 amino acids polymerization (Bremer and Dennis 1996). This phenomenon is referred to as the growth-rate hypothesis (GRH).Therefore, this result supported GRH. This seems likely that some of the ratios involving DNA, RNA, and protein could characterise N or P content.

5.5.3 Free and combined amino acids

Glutamic acid, arginine, and asparagine (or aspartic acid) were the highest contents approximately 9.7-15.5 % of total amino acid in *E. huxleyi* grown at low temperature. These are the charged amino acid residues which cover the surface of the molecule and favour to contact with solvent because of their ability to form hydrogen bonds. Thus, the charged amino acid

residues were mainly found. This finding is similar to that reported for 16 species (six diatoms, four prymnesiophytes, two prasinophytes, two chlorophytes, one eustigmatophyte, and one cryptophyte) of microalgae in mariculture (Brown 1991). In this work, the essential amino acids for humans and animals were not significantly affected by temperature. Villanueva *et al.* 2004 reported that protein and amino acid contents increased in *Octopus vulgaris* paralarvae which were fed by amino acids such as lysine, leucine, arginine, glutamate, and aspartate. Moreover, the octopuses had the high survivals rate when they compaired with control group. This implies that amino acids were produced by microalgae and were fed to aquatic animals, resulted in better health. Thus, *E. huxleyi*, which has these amino acids, could be a good food for mariculture application.

5.5.4 Photosynthesis rate

Temperature affects growth of phytoplankton through its control of enzyme kinetics (Davison 1991). The capacity for photosynthesis (P^{Chl}_{max} and P^{Cell}_{max}) remained approximately constant, even though higher value of the saturation irradiance (E_K) was observed at 22°C. This result suggests that this may be the optimal temperature range for photosynthesis. The Calvin Cycle enzymes of the dark reaction system might operate at a higher rate and thus consume $NADPH_2$ and ATP at a faster rate at higher temperatures (Kirk 1994). However, Clanquin *et al.* (2008) reported that *E. huxleyi, I. galbana* and *I.* aff. *galbana* had maximal photosynthetic capacity at the optimal temperature for electron transport rate approximately at 24.4, 21.9 and 30.7°C respectively.

The photosynthetic efficiency (α) for the rate of photosynthesis per unit chlorophyll (α^{Chl}) and per unit cell (α^{Cellll}) did not change significantly with temperature. However, *E. huxleyi* CCMP 1516 had a higher value of α^{Chl} at 18°C than at 14 and 22°C. This was because cell size and chl *a* concentration may be factors influencing α due to self-shading (Taguchi 1976).

The light saturation index (E_k) is an indication of the optimum light intensity for cells to maintain a balance between capacity of the photosynthesis and photosynthetic energy capture (Falkowski & Raven 2007). The E_k value in *E. huxleyi* had a positive relationship with elevated temperature. This was likley due to incresed RUBISCO activity and various Calvin cycle enzymes that directly influence photosynthetic efficiency of PSII in the light-adapted state (Raven & Geider 1988, Davison 1991, Kuebler *et al*. 1991).

5.5.5 Accessory pigment

Cellular chl *a* content in this experiment decreased with increased temperature; however, cell biovolume decreased even more, As a consequence, cellular chl *a* per unit of biovolume increased with increased temperature. The ratios of chl *a*:C and chl *a*:protein also increased with increasing temperature. Thomson *et al*. (1992) reported that chl *a* content increased at higher temperatures (10, 15, 20, and 25^{o}C) in eight marine phytoplankton that could result from rate of declining enzymatic reaction rate at low temperatures. Additionally, in haptophyte *Pavlova lutheri* grown in batch mode, chl *a* and carotenoid contents increased with temperature (10, 14, 18, 22, and 26°C) regardless of the irradiance (Carvalho *et al.* 2009). This probably associated with adaptation of light-harvesting complex (LHC) of photosystem I (PS I) and II (PS II) to a stress environment and related to electron transport activities in both photosystems. Similarly, chl *a* content increased with an increase temperature and phosphorus concentrations increased in blue green alga *Microcystis aeruginosa* and green alga *Scenedesmus obliquus* (Chen *et al.* 2011). Moreover, temperature directly affected phytoplankton community size structure. This led to a decrease in cells of the community with increased temperature irrespective of ambient nutrient availability (Mousing *et al*. 2014).

Plants-like microalgae, accessory pigments have difference function. Beta carotene as a singlet oxygen quencher is mainly localised in the reaction centre in core complex of PS II and PS I

and plays an key role in protecting the pigment-protein complexes (Young & Britton 1990), whereas xanthrophyll (DD and DT) cycle components are associated with LHC within PS I at lipid shield around the fucoxanthin chlorophyll protein (FCP) complexes (Lepetit *et al*. 2010).

The highest pigment content was the ratio of Hex-fuco to chl *a* in this study. Moreover, this pigment was found in haptophytes *Chrysochromulina acanthi, C. pringsheimii*, *C. throndsenii*, and *Emiliania huxleyi* collected from Nervion River estuary (Spain) and cultured in f/2 medium, 18 ± 1ºC, a light intensity of 60-180 µmol photons m^{-2} s^{-1} under a 12 h Light: 12 h dark cycle (Seoane *et al.* 2009). Additionally, Stolte *et al.* (2000) reported that the Hex-fuxo was the major pigment content in different strains of *E. huxleyi* from the Atlantic Ocean; however, fucoxanthin was the main content in the Indian and Pacific Ocean strains. This implies that Hex-fuxo as accessory photosynthetic pigment was exclusively found in chloroplasts of haptophyte origin. This can be investigated in phytoplankton taxonomy.

DD and DT as photoprotectors are de-epoxidation/epoxidation and are turned over by the enzyme diadinoxanthin deepoxilase or diatoxanthin epoxilase under light-regulated cycle called xanthrophyll cycle (Arsalane *et al*. 1994). DD, DT, and (DD+DT) to Chl *a* ratio decreased with increased temperature accompanied by an increase in total fucoxanthin to chl *a* ratio at high temperature. These changes are similar to observations in diatom *Chlorella calcitrans* (Anning *et al.* 2001). Those may result from high temperature i) affected enzymatic reaction, ii) led to low turnover rate in xanthrophyll cycle (Fujiki *et al.* 2003) and iii) associated with the redox state of the plastoquinone pool (Escoubas *et al.* 1996).

5.5.6 Fatty acid profile

The fatty acid composition in the cells of *E. huxleyi* was influenced by temperature. The oleic acid and myristic acid were the main fatty acids in *E. huxleyi*. Additionally, the oleic acid (C18:1) was dominant in neutral lipids of the haptophyte *Isochrysis galbana*, while the saturated fatty acids myristic acid (C14:0) and palmitic acid (C16:0) were mainly found in phospholipids of this

alga (Lin *et al*. 2007). The fatty acid profile of *E. huxleyi* included myristic acid, palmitic acid, linoleic acid, oleic acid, behenic acid, EPA and DHA as a major fatty acid, which were also found by Pond & Harris (1996) in eight species of *E. huxleyi.* However, Pond & Harris (1996) also found stearidonic acid (18:4n-3) and octadecapentaenoic acid (18:5n-3) in *E. huxleyi*. *Isochrysis galbana* CCMP 1332 (Prynesiophyceae) also contained stearidonic acid (18:4n-3) as the dominant fatty acids at all growth phases (Lin *et al*. 2007). In this study, stearidonic acid (18:4n-3) and octadecapentaenoic acid (18:5n-3) were not identified because these two components were not available in commercial FAME standards. However, unknown peaks were found in chromatographic analysis. Similarly, *I. galbana* CCMP 1324 (Prymnesiophyceae) contained some of the same components as *E huxleyi* except behenic acid and EPA.

The proportion of MUFA was larger at 14^{o}C (37 % of total fatty acid) compared to 22^{o}C (28 % of total fatty acid). The most abundant MUFA was oleic acid (C18:1). This result was similar to that reported for the chlorophyte *Derbesia tenuissima* (Gosch *et al.* 2015). This is suggested that physiological membrane responses to water fluidity at lower temperature because unsaturated fatty acid has the melting point lower than saturated fatty acid (Thompson *et al*. 1992; Los *et al.* 2013). Even though the increase of unsaturated fatty acid was found with the decreased temperature by increasing the biosynthesis of shorter-chain fatty acids in many algae, this is not the case in all species of algae (Renaud *et al.* 2002).

Among n-3 PUFA, the EPA (20:5n-3) and DHA (22:6n-3) are the major essential for the growth and maintenance of aquacultures. DHA was found in a small amount in *E. huxleyi* (3-4 % of total fatty acid). Commonly, there was small amount EPA content in *E. huxleyi*; however, EPA was not found in some *E. huxleyi* species (Pond & Harris 1996). The n-3 to n-6 ratio is used to estimate the nutritional value of microalgal cells. The n-3 to n-6 ratio >2 was optimal for feeding larvae and juvenile oysters (Enright *et al.* 1986). Although stearidonic acid was not measured, the highest level of n-3 to n-6 ratio of the remaining fatty acids (~ 2) was achieved at 14^{o}C of *E. huxleyi* which would make *E. huxleyi* suitable as a feed stock for aquaculture.

5.6 Conclusions

- The haptophyte *E. huxleyi* cultures were under a range of temperatures from 14 to 22^{o}C and examined for variation in elemental and biochemical composition as well as cell size.
- Cell size and carbon content were non-linear relationship with temperature. Protein (both free and combined amino acid) and total pigments [mol accessory pigment (mol chl *a*)$^{-1}$] decreased with increasing temperature; however, the opposite response was observed in fatty acids. This could lead to efficiency of the cell's absorption and waste expulsion processes for survival in unfavorable condition.
- When growth rate varied due to variable temperature conditions in nutrient replete conditions at constant light intensity, the growth rate was found to be positively correlated with RNA:protein, which is consistent with the growth rate hypothesis. In the same way, the relationship of chl:C and growth rate was used to test the applicability of a bio-optical hypothesis. Growth rate covaried with chl:C, which is consistent with the bio-optical hypothesis.
- These changes of cell properties with temperature may have an impact on sinking rate of inorganic carbon, CO_2 budgets, and potential changes of predators in ecological system.

Chapter 6: The effects of temperature and irradiance on *Thalassiosira weissflogii* CCMP 1056 in nutrient-limited semi-continuous cultures

6.1 Introductions

Increasing ocean temperature can have an impact on aquatic communities and lead to shifts in population size (Boyce *et al.* 2010; Finkel *et al*. 2009), phenology (Edwards & Richardson 2004), food web structure and productivity of phytoplankton. (Huertas *et al.* 2011; Thomas *et al*. 2012). The effect of temperature on growth rate, elemental and biochemical composition may be both indirect and direct. Physical changes in ocean stratification due to temperature can indirectly influence biogeochemical cycles by the affecting inputs of essential elements into surface waters (Huertas *et al.* 2011). Temperature directly affects the individual plankton species present in a waterbody. Phytoplankton can grow under wide temperature ranges. Thomas *et al.* (2012) reported that the optimal temperature for phytoplankton varied across a gradient of ocean temperature. This suggests that phytoplankton are adapted to the temperatures in the environments where they are found. A difference in the optimal growth temperature in different species leads to differences in production of biomass.

Temperature, together with light and nutrients, can directly influence phytoplankton physiology, biochemical composition and primary production (Rhee 1982; Kana *et al*. 1997; Geider *et al*. 1998). The direct effect of temperature on physiology and growth is generally associated with the effect on enzymatic activity (Eppley 1972; Raven & Geider 1988; Davison 1991). The rates of enzymatic reactions typically increase by about a factor of two for each 10^{o}C increase of temperature. However, the rate of light absorption by pigment molecules is unaffected by temperature.

Light is one of the essential factors influencing diatom growth. Many marine phytoplanktons are suspended in the water column and exposed to dramatic changes in the light field. Therefore,

phytoplanktons have adapted to be able to survive the variable ecological conditions. Growth, biochemical composition and photosynthetic production of marine phytoplankton are also influenced by changes in light quality (Aidar *et al.* 1994). Blue light is predominant at greater depths in oceanic waters.

Adaptation to light and temperature can occur through many mechanisms such as changes in growth rate, quantities of pigments, elemental and biochemical composition (Stramski *et al.* 2002; Wang *et al.* 2009; Goiris *et al*. 2015). Additionally, adaptation can involve the change of cell morphology, cell volume, subcellular structure and density of thylakoid membranes (Bayraktaroğlu *et al*. 2003).

Many studies have used *T. weissflogii* to investigate the biochemical and physiology of cells grown under different temperatures and irradiances. For examples, i) the effect of temperature on cell volume, growth rate, and carbon and nitrogen content in dinoflagellates and diatoms including *T. weissflogii* grown in f/2 media, 16±1^{o}C, PFD 50 µmol photons $m^{-2}s^{-1}$ on a 14:10 LD cycle (Montagnes & Franklin 2001), ii) the combined effect of temperature (18 and 23^{o}C) and UVR on the photosynthesis performance of two diatoms *T. weissflogii* (Grunow) and *Chaetoceros gracilis* Schütt. (Halac *et al*. 2010), iii) the effects of temperature (15 and 20^{o}C) and increased pCO_2 (400 and 1000 ppm) on carbon uptake by two marine diatom species *T. weissflogii* and *Dactyliosolen fragilissimus* grown under PFD 100 µmol photons $m^{-2}s^{-1}$ on a 14/10 h in all treatments (Taucher *et al*. 2015), iv) Influence of irradiances from 6 to 108 µmol photons $m^{-2}s^{-1}$ and temperatures from 10 to 29°C on the elemental and biochemical composition of *T. weissflogii* (Grun.) grown in both NO_3^- and NH_4^+ modified seawater medium containing high Fe (8.4 µM) contents (Strzepek & Price 2000), v) the interaction between photoacclimation and excessive photosynthetically active (PAR; 400–700 nm) and ultraviolet radiation (UVR; 280–400 nm) on *T. weissflogii* (Grunow) under exposure to high and low irradiance (van de Poll *et al*. 2006), vi) the influence of low (50) and high (150 µmol photons m^{-2} s^{-1}) light intensities on pigment composition of *T. weissflogii* and *Heterocapsa* sp. (Latasa 1995), vii) the effect of changes in growth irradiance from high to low irradiance (593 to 72 µmol

photons m^{-2} s^{-1}) and vice versa on physiological responses in *T. weissflogii* clone T-VIC (Post *et al*. 1985), viii) the effects of temperature (13 - 23°C), light (10-70 µmol photons m^{-2} s^{-1}) and nutrient (200 µM ammonium) limitation on the cell cycle of two marine phytoplankton species including *T. weissflogii* (Olson 1986).

Aims and objectives

Previous studies mentioned above have investigated the influences of temperature and irradiance on *T. weissflogii*; however, the interaction between nutrient-limitation with temperature and irradiance has not been investigated in the publication. In addition, the previous research cited above did not address directly either the bio-optical or the growth rate hypothesises described in chapter 1. Therefore, this study was conducted to evaluate the response of *T. weissflogii* CCMP 1056 to different temperatures (16 and 26°C) and irradiances (50 and 500 µmol photons m^{-2} s^{-1}) with the following objectives:

1) To determine the effect of temperature and irradiance on biochemical composition of this microalga in nutrient-limited cultures.
2) To examine correlations between growth rate and RNA:protein to test whether the growth rate hypothesis can be applied to temperature and irradiance.
3) To examine the correlations between growth rate and C:chl *a* to test whether the bio-optical hypothesis can be applied to temperature and irradiance.

6.2 Operating conditions and sampling

Thalassiosira weissflogii CCMP 1051 was grown in 2 litre pyrex vessels with 1.8 litre working volume in artificial seawater (Berges *et al*. 2001). Cells in exponential phase were used to inoculate semi-continuous cultures that were grown into nutrient limitation in medium containing 20 µM NaH_2PO_4, 200 µM $NaNO_3$, f/2 silicate, f/8 metals, and f/4 vitamins (Guillard & Ryther 1962) with 3 mM $NaHCO_3$ and 1 nM Na_2SeO_3. Triplicate cultures were incubated at two different temperatures 16 and 26°C and two different photosynthetic photon flux densities of 50 ± 10 (low light; LL) and 500 ± 10 (high light; HL) µmol photons m^{-2} s^{-1} on a 14:10 h light:dark cycle.

The semi-continuous process was started after cultures reached late exponential phase of growth. At this time, medium (900 mL) was removed as a dilution rate of 50% day^{-1} and the same volume of fresh sterile medium was fed into the culture every day at 16^{o}C; high light (16 HL) and 26^{o}C; high light (26 HL) treatments to maintain steady state. Similarly, at 16^{o}C, low light (16 LL) and 26^{o}C, low light (26 LL) the medium was removed and fed into the culture every other day. The cultures were gently stirred with a magnetic stir bar and continuously aerated with filtered air through a 0.22 µm membrane filter.

Samples were typically collected in triplicate from each of the 3 replicate cultures on two occasions during the exponential phase and then the cultures were allowed to grow until stationary growth phase (day 7). Cell abundance was determined daily using a haemocytometer. Samples during the exponential phase were collected to measure particulate phosphorus (PP), nitrogen (PN), organic carbon (POC), cellular chlorophyll *a*, light absorption, amino acid, protein, pigments, DNA and RNA. While carbohydrate, neutral lipid, and fatty acid profiles were determined in both the exponential and stationary growth phases. All elemental and biochemical composition were measured using the methods described in chapter 2.

Moreover, 30 ml of culture suspension was collected for determining photosynthesis-light response curves as described in chapter 2. In addition, cell size, nucleus (DNA), lipid droplet and chloroplast volumes were determined from microscopic images obtained using a confocal laser scanning microscope (Nikon A1si, Nikon Corp., Tokyo, Japan) as described in chapter 2.

6.3 Statistical analysis

Datasets of all measured parameters were analysed for significant differences between culturing conditions and tested parameters using an analysis of variance (ANOVA) with the post hoc test (Tukey HSD) used for multiple comparisons. For the volume size data, they were tested for normal distribution using Shapiro-Wilk test. Since the distributions were not normal, they were tested for significant differences using Kruskal-Wallis test with the post hoc test (Dunn's multiple comparison test).

6.4 Results

6.4.1 Cell density and growth rate

The effect of temperature and irradiance on the biomass of *T. weissflogii* grown in exponential growth phase is shown in Fig. 6-1. In the triplicate cultures at both 16 HL and 26 HL, cells increased for the first 3 days during the exponential phase and became constant until the stationary phase. A different growth pattern was observed in the cultures at 16 LL and 26 LL; that showed a lower cell density than high light regardless of temperature.

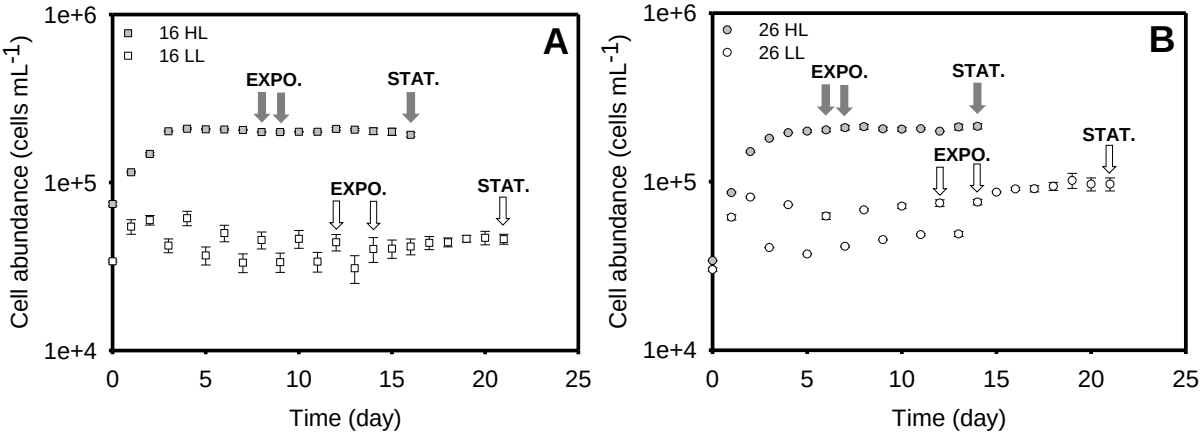

Figure 6-1. Temperature and irradiance dependencies of cell abundance of *T. weissflogii* cultures harvested during the exponential (EXPO.; n=6) and stationary (STAT.; n=3) phases. Mean values ± standard errors are shown for the three replicate vessels at 16 HL (grey squares) and 16 LL (white squares) (A) and at 26 HL (grey dots) and 26 LL (white dots) (B).

Temperature affected cell abundance of *T. weissflogii* under low light (from 16 LL to 26 LL); however, there were not significant differences under high irradiance (from 16 HL to 26 HL). Cell abundance increased with increased irradiance at both temperatures (Fig. 6-2A). HL placed-cultures had the highest cell abundance (16 HL and 26 HL) with a density of 2.0-2.1 $x10^5$ ± 1.9-4.6 x 10^3 (mean ± SE) cells mL^{-1}, whereas the lowest cell density of 0.5 $x10^5$ ± 6.4 x 10^3

cells mL^{-1} was observed at 16 LL with an intermediate value of 0.8 $x10^5 \pm 5.0 \times 10^3$ cells mL^{-1} at 26 LL.

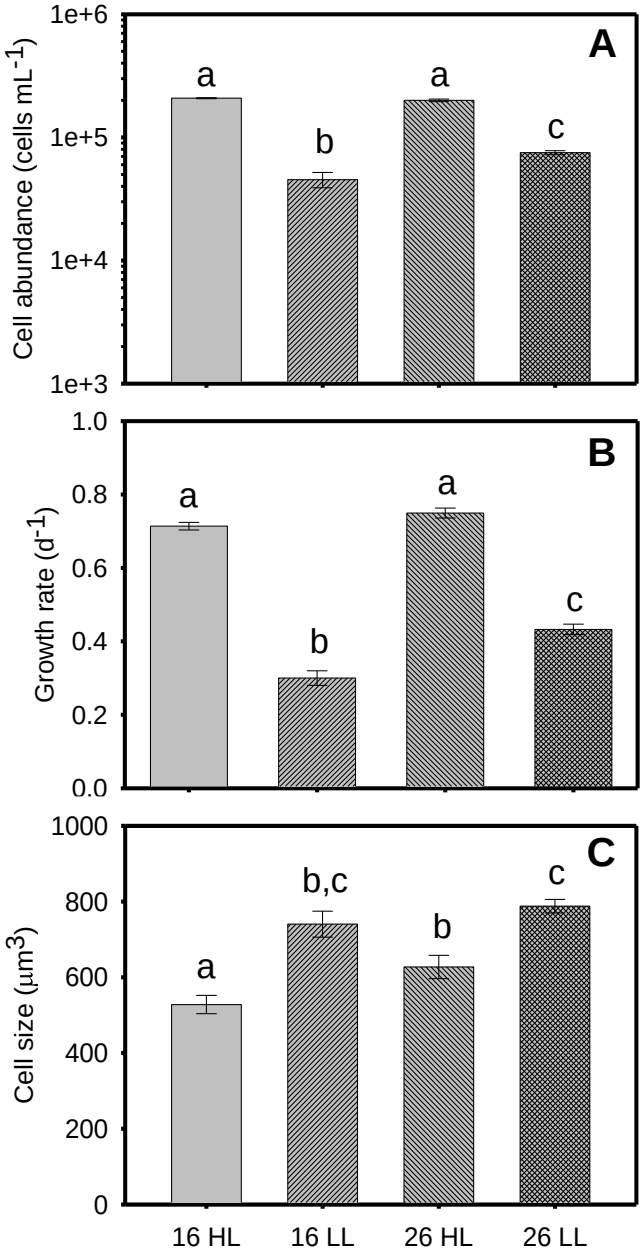

Figure 6-2. Temperature and irradiance dependencies of cell abundance (A), growth rate (B), and mean cell volume (C) in *T. weissflogii.* Mean values ± standard errors are shown for three replicate vessels at exponential phase (n = 6) of 16 HL, 16 LL, 26 HL, and 26 LL. Bars labelled with the same letter were not significantly different (one way ANOVA Tukey's test; $p < 0.05$).

In these semi-continuous cultures, which were operated until cell abundances prior to each dilution reached stable values, the growth rate is expected to be determined by the dilution rate. Thus, the expected growth rate (GR) of the high light cultures should be GR = ln(1800/900)/(1 day) = 0.69 d^{-1}, whereas that of the low-light cultures should be GR = ln(1800/900)/(2 days) = 0.34 d^{-1}. The observed growth rates were close to these calculated values. The GR of *T. weissflogii* (mean ± SE) was about 2.4 times higher at 16 HL (0.75 ± 0.02 d^{-1}) than at 16 LL (0.30 ± 0.03 d^{-1}), whereas at 26^{o}C presented a greater 1.7 fold GR from LL to HL (Fig. 6-1B). GR at 16 HL and 26 HL were not significantly different. Given the relatively small sample size (n = 52-87) and the high variance, the median is a better measure of the central tendency than the mean since the mean can be affected more by a small number of extremely high values (Fig. 6-2).

Mean cell size was not significantly affected by temperature under low light (16 LL and 26 LL) at 95% confidence level (Fig. 6-2C). However, mean cell size decreased with increasing irradiance from 16 LL; 740.4 ± 34.3 μm^3 to 16 HL; 528.1 ± 24.2 μm^3 (constant 16^{o}C) by -28.7% and from 26 LL; 787.8 ± 18.0 μm^3 to 26 HL; 627.2 ± 30.8 μm^3 (constant 26^{o}C) by -20.4%. Median cell size decreased with decreased temperature and with increased irradiance (Fig. 6-2D).

6.4.2 Cellular chlorophyll *a* (chl *a*)

T. weissflogii had the highest cellular chl *a* content at 26 LL (7.4 ± 0.9 pg $cell^{-1}$). There were significant differences at cellular chl *a* with irradiance at low light cultures and temperatures (Fig. 6-3A). The cellular chl *a* contents of the low light cultures were not significantly different at 16 and 26ºC. Cellular chl *a* per cell volume (chl *a* μm^{-3}) increased significantly with increasing temperature at high light, but decreased with increasing temperature under low light (Fig. 6-3B).

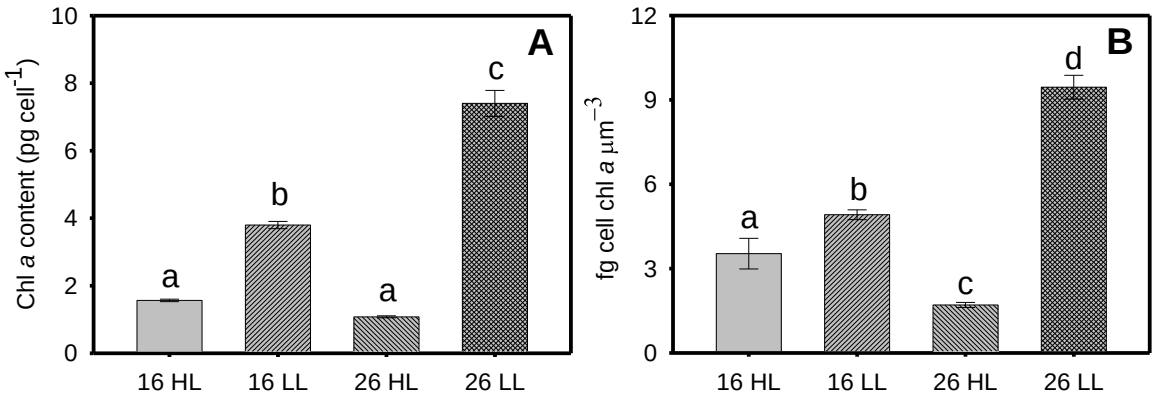

Figure 6-3. Temperature and irradiance dependencies of cellular chl *a* (A) and cellular chl *a* per cell volume (B) of *T. weissflogii.* Mean values ± standard errors are shown for three replicate vessels (n = 6) at 16 HL, 16 LL, 26 HL, and 26 LL. Bars labelled with the same letter were not significantly different (one way ANOVA Tukey's test; $p < 0.05$).

6.4.3 Elemental contents

The cellular N and P contents varied with temperature and irradiance (Figs. 6-4 A,B and Table 6-1). The cellular N contents significantly decreased with increased temperature from 16 LL to 26 LL (one way ANOVA, $p<0.05$). The N content decreased with increased irradiance at 16°C by around -37.0 % while that the opposite response was observed at 26°C. The P content also decreased by about -57.9 % at increased irradiance from 16 LL to 16 HL. The POC content had a tendency to rise with increased temperature (Fig. 6-4C); however, the opposite response was observed with increased irradiance.

In terms of the elemental ratio, the N:P ratios decreased with increased temperature, whereas the opposite response was observed under increased irradiance (Table 6-1). The C:N and the C:P ratios increased with temperature at both irradiances (Table 6-1). C:N and C:P were not affect by irradiances at 16°C and showed opposite patterns of response to irradiance at 26°C (Table 6-1) irradiance.

The N and P contents per unit biovolume varied with temperature and irradiance. N contents per unit biovolume increased significantly with increasing irradiance from 26 LL to 26 HL by about 34.0 % (Fig. 6-5A). While P contents per unit biovolume decreased significantly with increasing irradiance from 16 LL to 16 HL by about -37.3 % (Fig. 6-5B). There was no significant differences of carbon contents per biovolume at different temperature and irradiance (Fig. 6-5C).

Table 6-1. Summary of trends in particulate nitrogen (PN), phosphorus (PP), organic carbon (POC), N:P, C:N, and C:P to increased temperature and irradiance in *T. weissflogii*.

Parameters	Increased temperature at constant irradiance		Increased irradiance at constant temperature	
	16 HL to 26 HL	16 LL to 26 LL	16 LL to 16 HL	26 LL to 26 HL
PN	=	↓	↓	↑
PP	=	↓	↓	↓
POC	↑	↑	↓	↓
N:P	↓	↓	↑	↑
C:N	↑	↑	=	↓
C:P	↑	↑	↑	=

↑ : increase, ↓: decrease, = : equal level in statistic

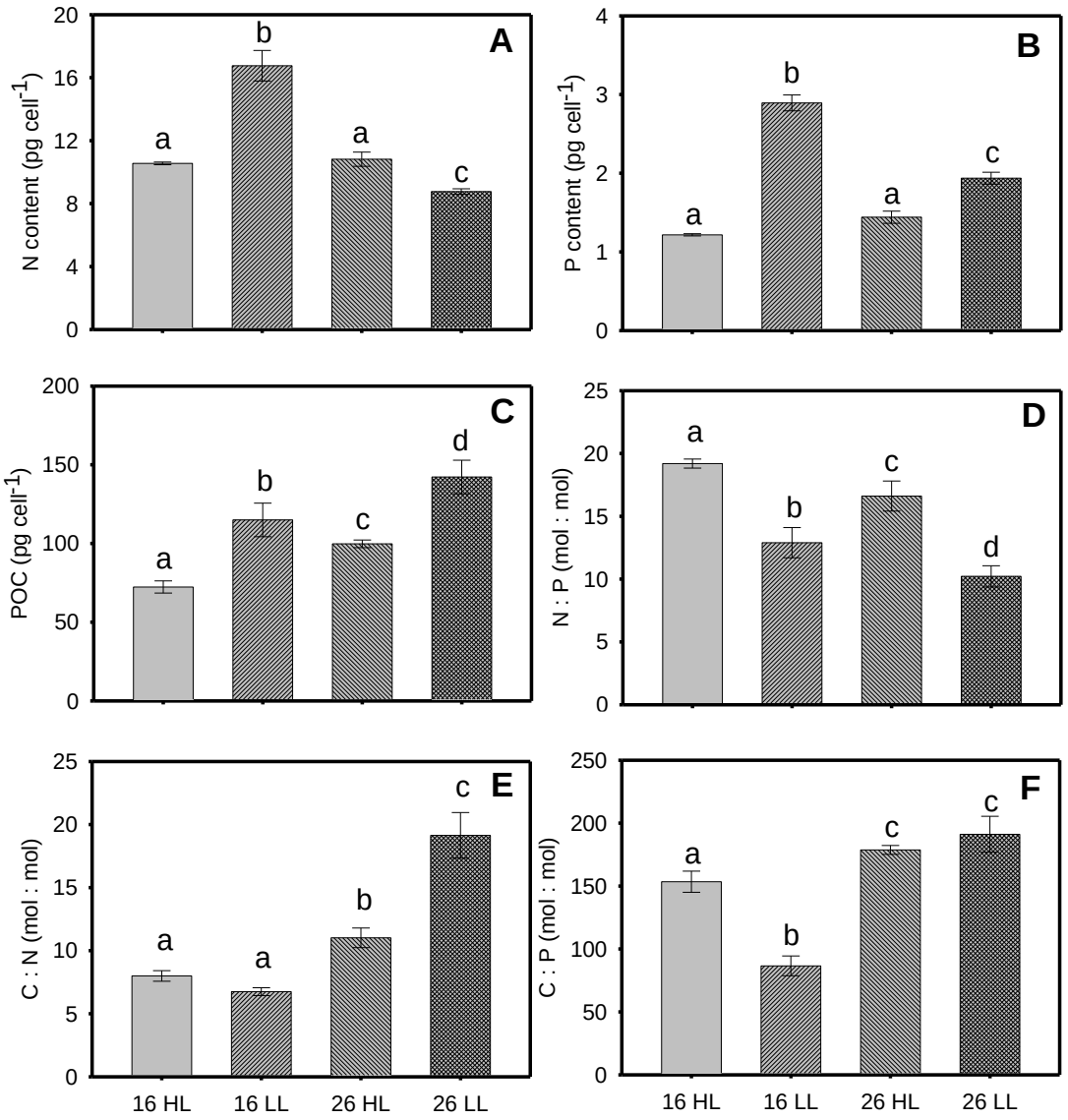

Figure 6-4. Temperature and irradiance dependencies of cellular N (A), cellular P (B), organic C (C), N:P (mol:mol) ratio (D), C:N ratio, and C:P ratio (F) of *T. weissflogii.* Mean values ± standard errors are shown for three replicate vessels (n=6) at 16 HL, 16 LL, 26 HL, and 26 LL. Bars labelled with the same letter were not significantly different (one way ANOVA Tukey's test; $p < 0.05$).

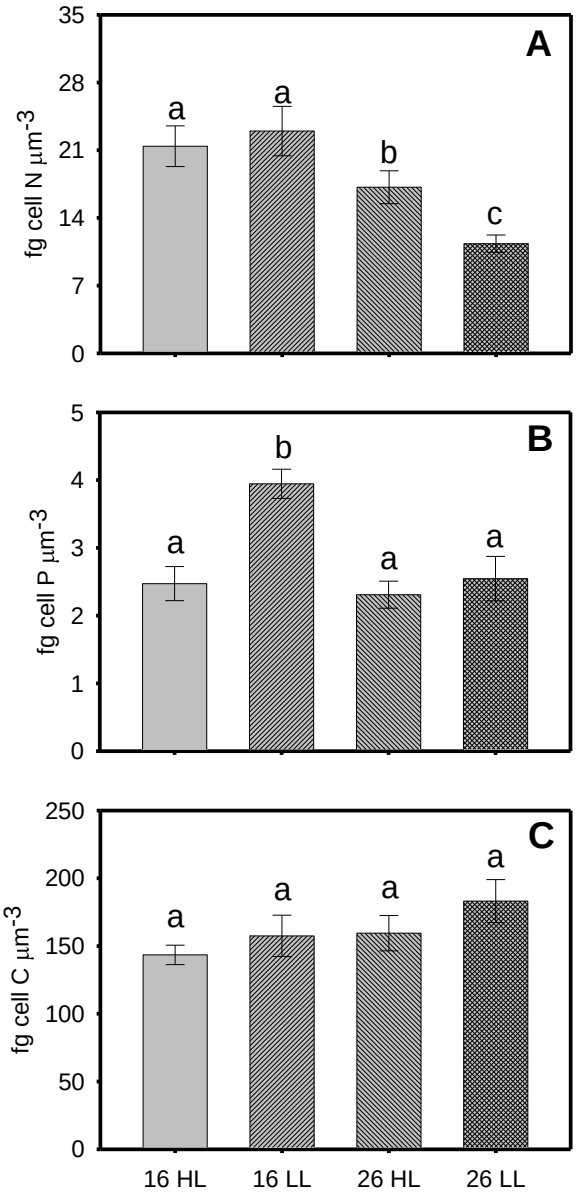

Figure 6-5. Temperature and irradiance dependencies of cellular N per biovolume (A), cellular P per biovolume (B), organic C per biovolume (C), of *T. weissflogii.* Mean values ± standard errors are shown for three replicate vessels (n=6) at 16 HL, 16 LL, 26 HL, and 26 LL. Bars labelled with the same letter were not significantly different (one way ANOVA Tukey's test; $p < 0.05$).

The C:chl *a* ratio varied with temperature and irradiance (Fig. 6-6A) and the C:chl *a* ratio was also positively associated with growth rate (Fig. 6-6B).

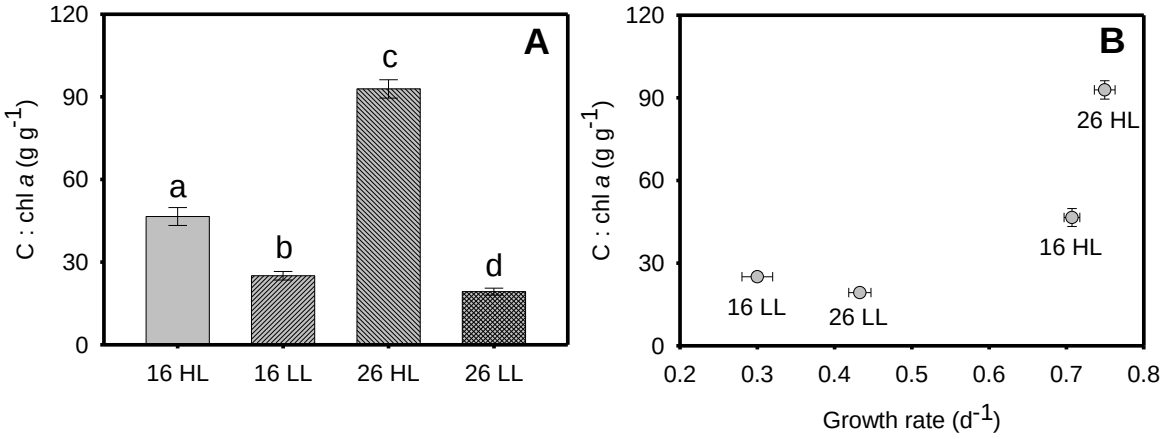

Figure 6-6. C:chl *a* ratio in unit g per g (A) of *T. weissflogii* in different treatments 16 HL, 16 LL, 26 HL, and 26 LL and the relationship between C:chl *a* ratio and growth rate (d^{-1}) (B). Mean values ± standard errors are shown for three replicate vessels (n=6) at 16 HL, 16 LL, 26 HL, and 26 LL. Bars labelled with the same letter were not significantly different (one way ANOVA Tukey's test; $p < 0.05$).

6.4.4 Protein, carbohydrate, and neutral lipid content

Temperature and irradiance affected cellular protein content and protein content per unit biovolume of *T. weissflogii* all treatments (Figs. 6-7A,B). Cellular protein content decreased about two fold with increased irradiance from low to high light intensity regardless temperature. Carbohydrate content decreased with increasing irradiance at constant 16°C, whereas there was no significant difference in carbohydrate content per cell volume with irradiance under constant 16°C. Carbohydrate content and carbohydrate content per cell volume decreased significantly with increasing temperature from 16 LL to 26 LL (Figs. 6-7C, D).

Cellular neutral lipid content assessed using the Nile red staining method was not significantly different during the semi-continuous phase of culturing (Fig. 6-7D). However, neutral lipid

contents gradually increased with time in the stationary phase and became constant after day 6 except 16 HL. The neutral lipid content per volume was not affected temperature but an increase was observed under increased irradiance at both temperatures (Fig. 6-7F).

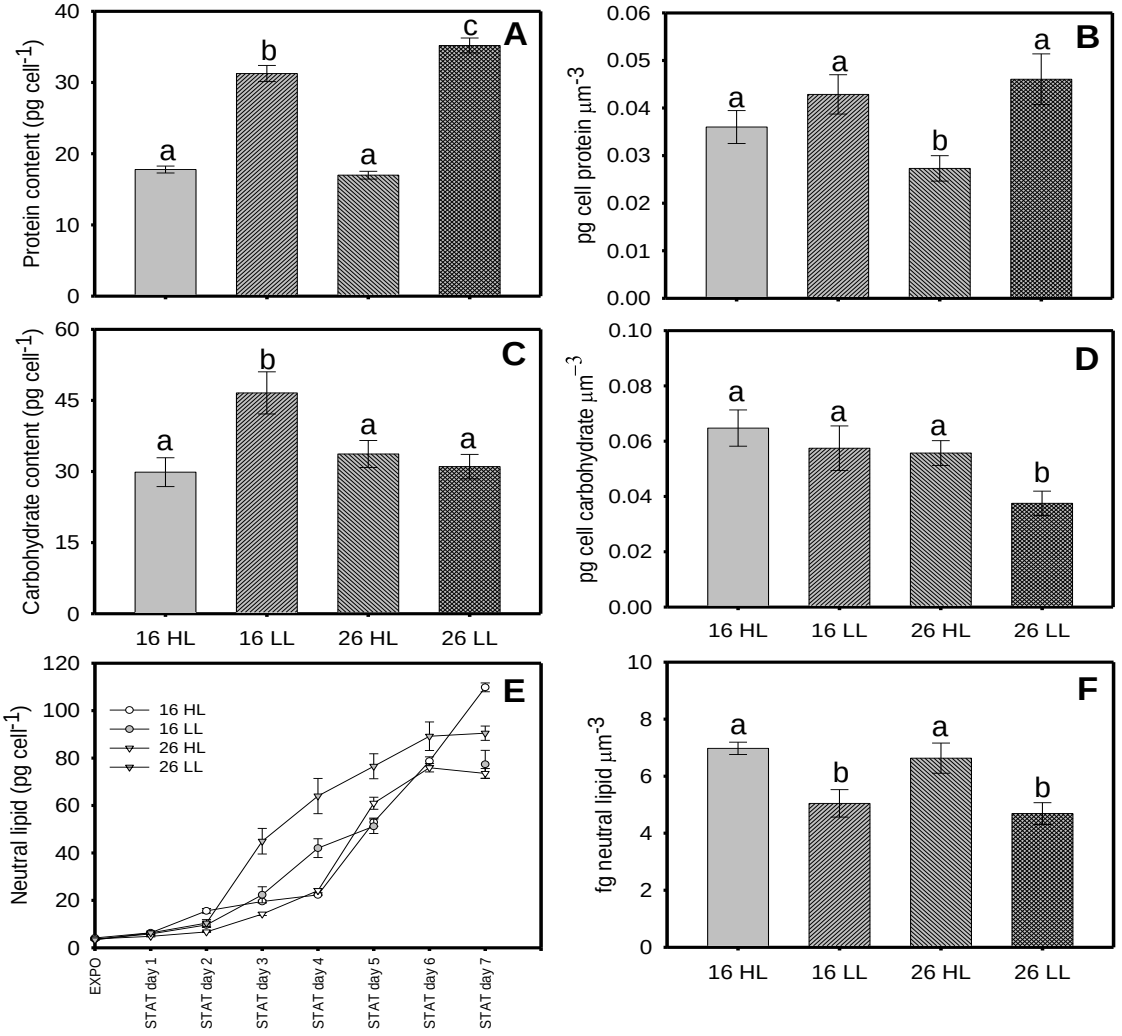

Figure 6-7. Temperature and irradiance dependencies of protein (A), protein per biovolume (B), carbohydrate (C), and carbohydrate per biovolume (D). The neutral lipid content (E) at exponential (EXPO) and stationary (STAT) phases and neutral lipid per biovolume (F) at exponential phase of *T. weissflogii*. Mean values ± standard errors are shown for three replicate vessels (EXPO, n=6 and STAT, n=3) at 16 HL, 16 LL, 26 HL, and 26 LL. Bars labelled with the same letter were not significantly different (one way ANOVA Tukey's test; $p < 0.05$).

The lipid yield (mg L^{-1}) and productivity (mg $L^{-1}d^{-1}$) of *T. weissflogii* incubated at different temperatures and irradiances were shown in Table 6-2. The highest lipid yield and lipid productivity were found at low temperature and high light (16 HL). The lipid yield and productivity at 16 HL were approximately 2.4-times higher than at 26 LL.

Table 6-2. Lipid yield (mg L^{-1}) and productivity (mg $L^{-1}d^{-1}$) of *T. weissflogii* under different temperatures and irradiances at day 7 of stationary phase. Values are mean and standard errors (SE) for three replicate vessels, n = 3. Means with a column followed by the same letter are not significantly different (one way ANOVA Tukey's test; $p < 0.05$).

Treatment	Lipid yield (mg L^{-1})		Lipid productivity (mg L^{-1} day^{-1})	
	Mean	SE	Mean	SE
16 HL	20.08^{a}	0.44	2.85^{A}	0.06
16 LL	13.01^{b}	0.38	1.83^{B}	0.05
26 HL	15.45^{b}	0.36	2.18^{B}	0.04
26 LL	8.36^{c}	0.29	1.19^{C}	0.04

6.4.5 DNA and RNA contents

Relatively small differences were observed in DNA per cell (Fig. 6-8A) and RNA per cell (Fig 6-8B). The greatest DNA and RNA contents were observed at 26 HL, whereas the lowest DNA and RNA contents were found at 16 LL (Figs. 6-8A, B). There was no significant difference in cellular DNA content with temperature in the high light treatments or with irradiance in the low temperature treatments, although a slightly higher value was observed in the 26HL treatment.

RNA per cell was more variable than DNA per cell (Fig. 6-8B), and significant differences due to irradiance were observed in both the low and high temperature treatments. At constant irradiance, RNA per cell was significantly higher at the higher temperature.

In the present study, RNA:DNA ratios were >1; however, the RNA:DNA ratio did not show significant differences amongst the treatments (Fig. 6-8D).

Growth rate was positively correlated with RNA:protein (Fig. 6-9A). Growth rate increased by about 2.4 fold from 16 LL to 16 HL, whereas RNA:protein increased nearly by about 1.9 times over this irradiance range. In contrast, the growth rate increased by about 1.7 fold from 26 LL to 26 HL, whereas RNA:protein increased nearly by about 2.6 times (Fig. 6-9B).

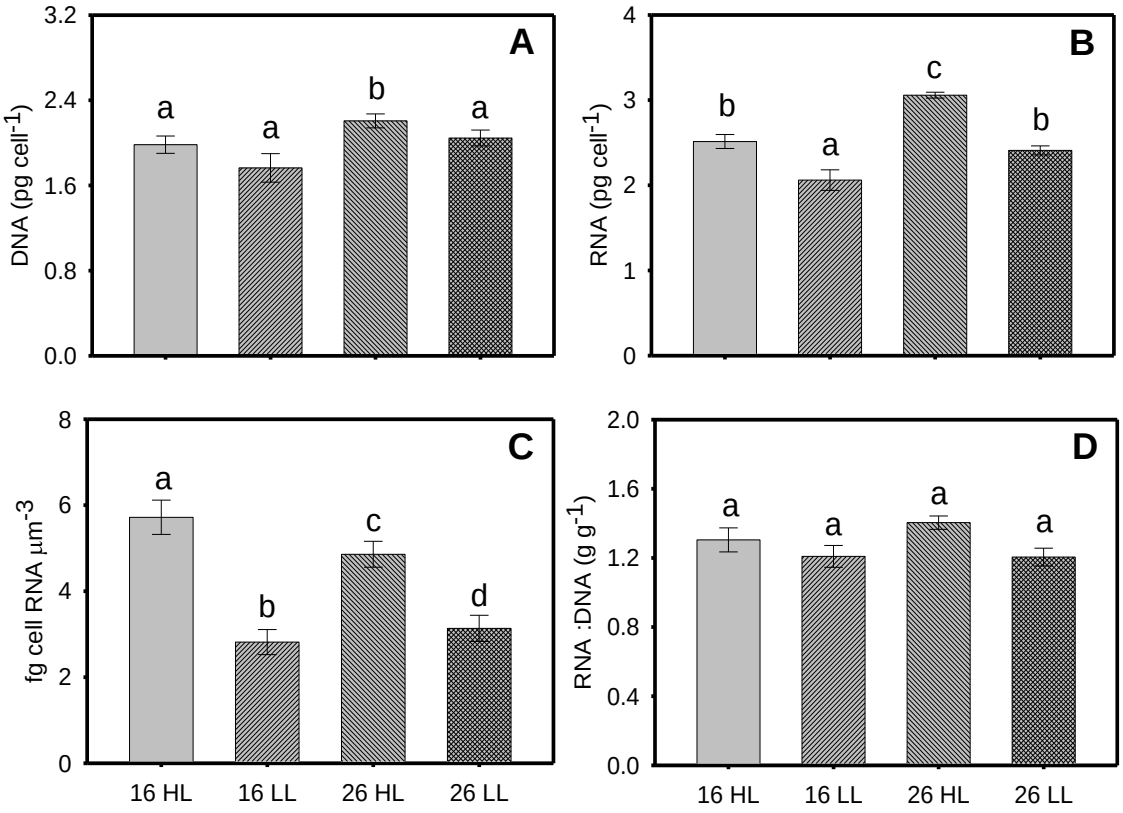

Figure 6-8. Temperature and irradiance dependencies of DNA content (A), RNA content (B), RNA per biovolume (C) and RNA : DNA ratio (D) of *T. weissflogii* in different vessels at 16 HL, 16 LL, 26 HL and 26 LL. Mean values ± standard errors are shown for three replicate vessels. Bars labelled with the same letter were not significantly different (one way ANOVA Tukey's test; $p < 0.05$).

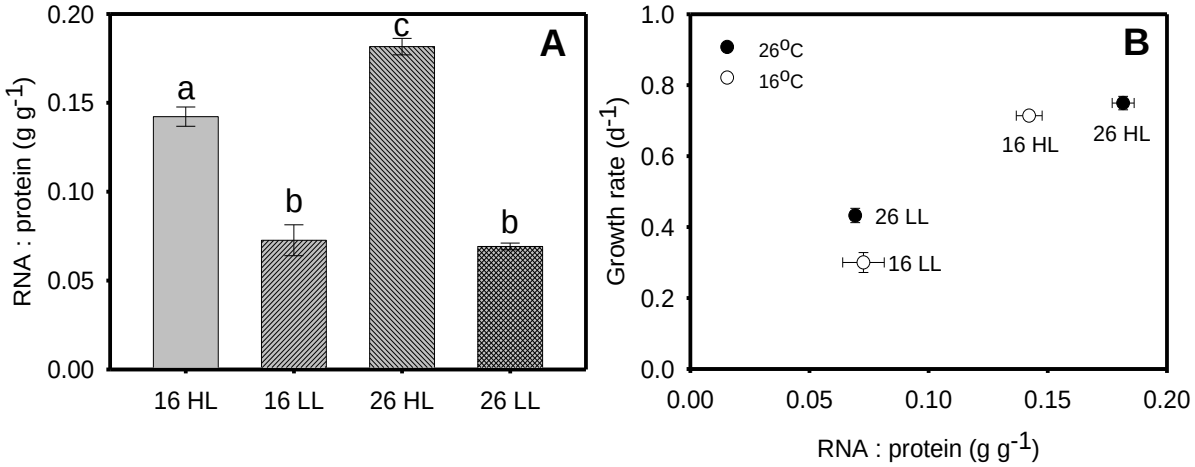

Figure 6-9. RNA : protein ratio (A) which are expressed in unit of g g^{-1} of *T. weissflogii*; the relationship between RNA : protein (g g^{-1}) and growth rate (d^{-1}) (B). Bars labelled with the same letter were not significantly different (one way ANOVA; $p < 0.05$).

6.4.6 Bioimaging of *T. weissflogii*

Subcellular components were visualised with high contrast using fluorescent staining and autofluorescence approaches (Figs. 6-10,11). Lipid droplets were labelled with Nile red (green in Fig 6-10), the DNA was stained with DAPI (blue in Fig 6-10) and chloroplasts identified from chlorophyll autofluorescence (red in Fig 6-10). Temperature and irradiance affected the volumes of the subcellular components. Mean cell size and chloroplast volume decreased with increased temperature and irradiance while lipid volume increased with increased temperature and irradiance (Fig. 6-12). There were no significant differences in the mean nucleus (DNA-labelled volumes) amongst the temperature and irradiance conditions (Fig. 6-13 and Table 6-3).

Given the relatively small sample size (n = 52-87) and the high variance, the median is a better measure of the central tendency than the mean since the mean can be affected more by a small number of extremely high values. Data is not normally distributed then they were compared statistically using a non-parametric statistical test.

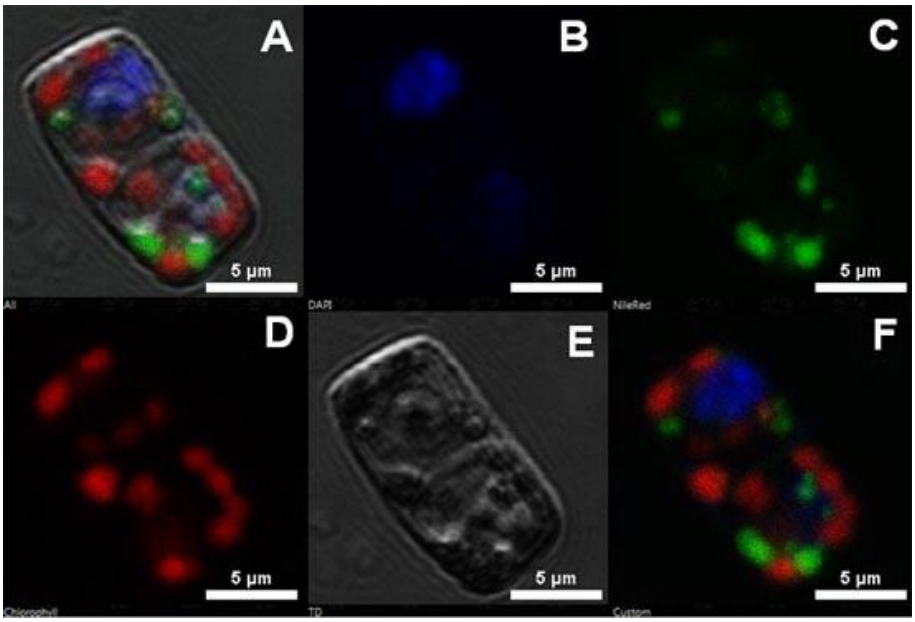

Figure 6-10. Confocal images of subcellular components of *T. weissflogii* grown under 16^{o}C and high light condition (A). DNA image is labelled from DAPI as blue (B), lipid droplets are stained from Nile red as green (C), chloroplast is autofluorescence of chlorophyll *a* as red (D), transmission image is collected from transmission detector (TD) as grey (E), and single image is produced from merging channels (F).

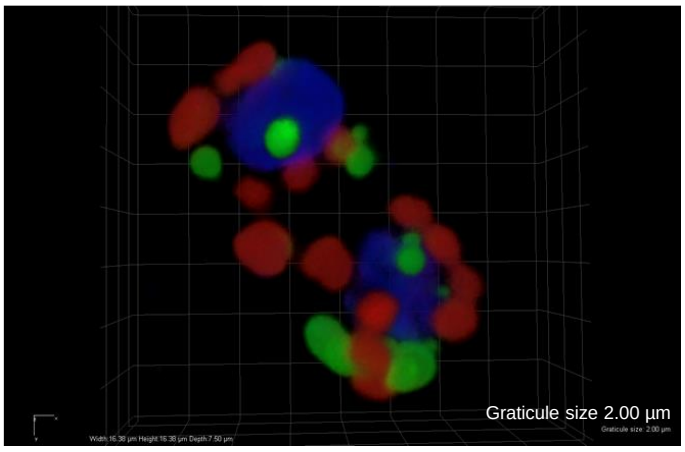

Figure 6-11. Visualisation of *T. weissflogii,* under 16^{o}C and high light condition, in 3-dimensional reconstruction from merging channels.

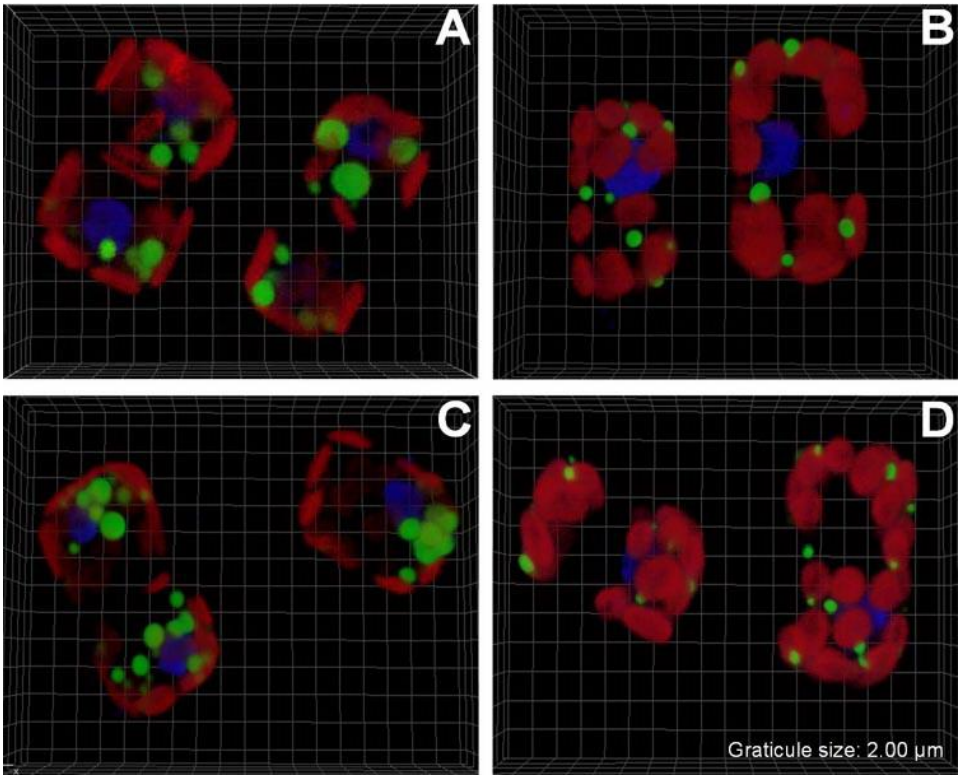

Figure 6-12. Three-dimensional reconstructions of *Thalassiosira weissflogii*, in semi-continuous culture phase, grown under different treatments: (A) 16°C and high light; (B) 16°C and low light; (C) 26°C and high light; (D) 26°C and low light. Red is chlorophyll fluorescence, blue is DNA and green is lipid droplets.

Table 6-3. Statistical comparison, using Kruskal-Wallis test with Dunn's multiple comparison test, of cell size, DNA, lipid, and chloroplast volume (μm^3) in *Thalassiosira weissflogii* grown at different temperature and irradiance levels. Mean values ± standard errors (SE) are shown for three replicate vessels (n=6). Entries labelled with the same letter were not significantly different ($p<0.05$).

Volume (μm^3)	Treatment	Median	Mean	SE
Cell size	16 HL	492.6	528.1[a]	24.2
	16 LL	676.7	740.1[bc]	34.3
	26 HL	594.1	627.2[b]	30.8
	26 LL	758.4	787.8[c]	18.0
DNA	16 HL	65.2	79.5[a]	5.5
	16 LL	71.9	90.1[a]	10.9
	26 HL	68.0	72.1[a]	3.8
	26 LL	66.4	71.3[b]	1.7
Lipid	16 HL	39.3	46.2[a]	3.0
	16 LL	18.5	20.8[b]	1.7
	26 HL	55.5	60.7[c]	3.5
	26 LL	28.5	31.4[d]	1.2
Chloroplast	16 HL	359.7	374.0[a]	17.4
	16 LL	565.9	585.0[b]	21.9
	26 HL	433.0	496.1[c]	28.7
	26 LL	645.0	679.8[d]	16.4

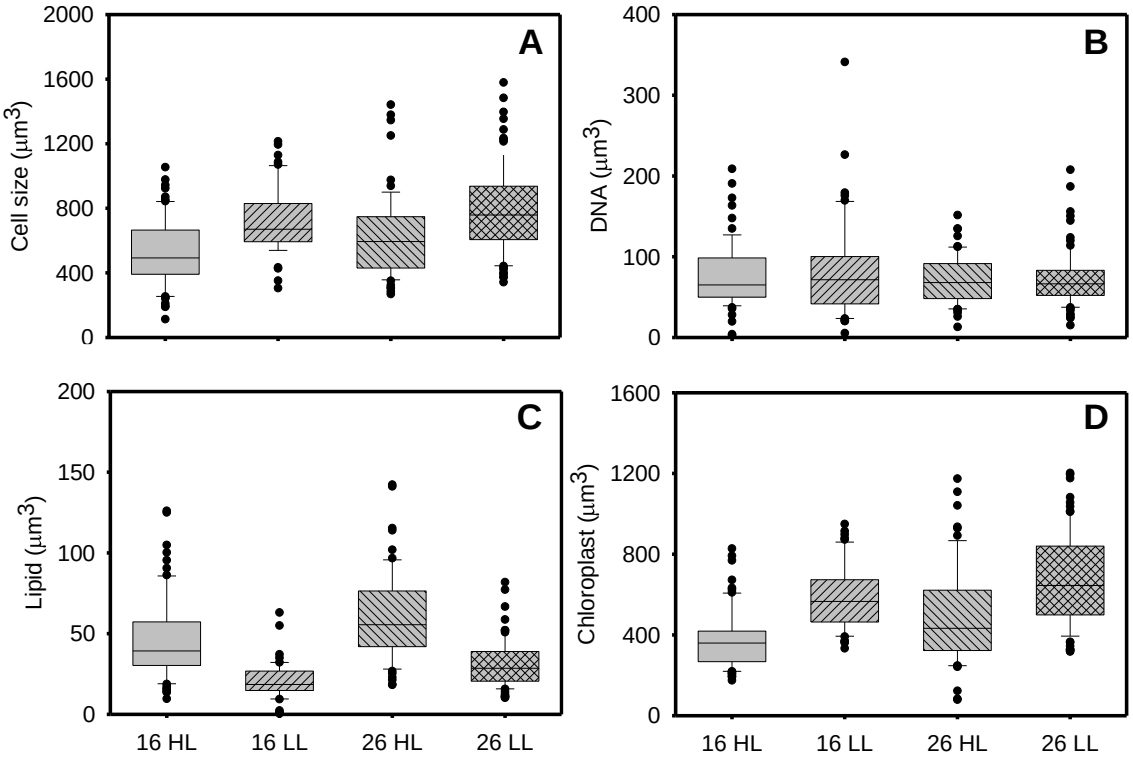

Figure 6-13. Temperature and irradiance dependencies of cell volume (A), nucleus (DNA) volume (B), lipid droplet volume (C), and chloroplast volume (D) in *T. weissflogii* grown at 16 HL (n=71), 16 LL (n=52), 26 HL (n=68), and 26 LL (n=87). The horizontal line is the median and the box-whisker plots presents the upper and lower quartiles (Q3 and Q1) and the range of cell size. The data can be found in Table 6-3.

6.4.7 Amino acids

Seventeen free and bound amino acids were identified. The total free amino acid content of the cells was approximately 1.9-5.7 pg cell^{-1} (Table 6-4) which in all cases was around 16-22 % of the total amino acids.

Table 6-4. Essential and non-essential free amino acids (pg cell^{-1}) of *T. weissflogii* grown under different temperature and irradiances. Values are mean and standard errors (SE) for three replicate vessels, n = 3. Means with a row followed by the same letter were not significantly different (one way ANOVA Tukey's test; $p < 0.05$).

	Amount of free amino acid (pg cell^{-1})							
Amino acid	16 HL		16 LL		26 HL		26 LL	
	Mean	SE	Mean	SE	Mean	SE	Mean	SE
Essential amino acid								
Histidine	0.25^{A}	0.00	0.21^{A}	0.17	0.26^{A}	0.10	0.23^{A}	0.08
Lysine	0.07^{A}	0.01	0.41^{C}	0.04	0.07^{A}	0.01	0.18^{B}	0.03
Methionine	0.25^{A}	0.00	0.39^{B}	0.11	0.25^{A}	0.01	0.60^{C}	0.02
Valine	0.11^{A}	0.01	0.59^{C}	0.09	0.13^{A}	0.01	0.33^{B}	0.02
Phenylalanine	0.08^{A}	0.03	0.25^{B}	0.00	0.06^{A}	0.02	0.51^{C}	0.08
Isoleucine	0.07^{A}	0.01	0.25^{B}	0.04	0.12^{A}	0.01	0.10^{A}	0.02
Non-essential amino acid								
Arginine	0.14^{A}	0.00	0.75^{C}	0.15	0.15^{A}	0.00	0.38^{B}	0.01
Serine	0.22^{A}	0.01	0.60^{C}	0.05	0.20^{A}	0.00	0.46^{B}	0.04
Glycine	0.20^{B}	0.04	0.07^{A}	0.04	0.04^{A}	0.00	0.22^{B}	0.05
Glutamic acid	0.10^{A}	0.03	0.45^{C}	0.03	0.15^{A}	0.01	0.26^{B}	0.05
Asparagine*	0.04^{A}	0.02	0.19^{B}	0.06	0.21^{B}	0.10	0.09^{A}	0.04
Proline	0.08^{A}	0.01	0.41^{B}	0.02	0.50^{B}	0.25	0.45^{B}	0.09
Cysteine	0.01^{A}	0.00	0.02^{A}	0.04	0.02^{A}	0.00	0.03^{A}	0.01
Tyrosine	0.02^{A}	0.00	0.13^{B}	0.09	0.03^{A}	0.01	0.14^{B}	0.08
Threonine	0.24^{A}	0.01	0.44^{B}	0.08	0.21^{A}	0.01	0.59^{B}	0.04
Alanine	0.05^{A}	0.00	0.46^{C}	0.10	0.07^{A}	0.01	0.28^{B}	0.00
Sum	1.93	0.24	5.71	1.14	2.46	0.55	4.82	0.72

* Average of aspartic acid and asparagine.

Glutamic acid was the most abundant amino acid in cells at 26 LL while cysteine was the lowest in all treatments (Tables 6-5 and 6-6). Glutamic acid accounted for approximately 13.7 % of total amino acids. Arginine, serine, glycine, aspartic acid, asparagine, threonine, proline, lysine,

valine and phenylalanine, isoleucine, alanine were all present at contents between 5-10 % of total amino acids. Four amino acids (cysteine, tyrosine, methionine and histidine) were < 5 % of total amino acids (Table 6-6).

Table 6-5. Amino acid content (pg cell^{-1}) from hydrolysed *T. weissflogii* grown at different temperatures and irradiances. Values are mean and standard errors (SE) for three replicate vessels, n = 3. Means with a row followed by the same letter were not significantly different (one way ANOVA Tukey's test; p< 0.05).

	Amount of combined amino acid (pg cell^{-1})							
Amino acid	16 HL		16 LL		26 HL		26 LL	
	Mean	SE	Mean	SE	Mean	SE	Mean	SE
Essential amino acid								
Histidine	0.13^{A}	0.02	0.32^{B}	0.09	0.18^{A}	0.09	0.33^{B}	0.16
Lysine	0.67^{A}	0.11	1.45^{B}	0.05	0.89^{A}	0.15	2.78^{C}	0.06
Methionine	0.23^{A}	0.02	0.62^{C}	0.02	0.36^{B}	0.01	0.62^{C}	0.05
Valine	0.56^{A}	0.02	1.29^{C}	0.03	0.77^{B}	0.10	1.35^{C}	0.11
Phenylalanine	0.64^{A}	0.04	1.42^{B}	0.07	0.90^{C}	0.11	2.12^{D}	0.03
Isoleucine	0.54^{A}	0.03	1.15^{B}	0.07	0.71^{C}	0.08	1.28^{B}	0.08
Non-essential amino acid								
Arginine	0.76^{A}	0.03	1.61^{B}	0.13	0.95^{A}	0.17	1.85^{B}	0.06
Serine	0.47^{A}	0.01	1.14^{C}	0.04	0.66^{B}	0.06	1.22^{C}	0.01
Glycine	0.38^{A}	0.02	1.06^{D}	0.02	0.53^{B}	0.03	0.74^{C}	0.04
Glutamic acid	1.03^{A}	0.15	2.68^{C}	0.10	1.49^{B}	0.09	3.89^{D}	0.09
Asparagine*	0.99^{A}	0.16	2.33^{C}	0.24	0.91^{A}	0.34	1.74^{B}	0.07
Proline	0.49^{A}	0.02	1.08^{B}	0.09	0.66^{A}	0.09	1.98^{C}	0.05
Cysteine	0.11^{A}	0.01	0.25^{B}	0.03	0.12^{A}	0.05	0.39^{C}	0.06
Tyrosine	0.45^{A}	0.01	1.05^{C}	0.03	0.61^{B}	0.05	1.62^{D}	0.05
Threonine	0.46^{A}	0.02	1.06^{C}	0.05	0.65^{B}	0.05	1.71^{D}	0.04
Alanine	0.46^{A}	0.04	1.29^{C}	0.04	0.67^{B}	0.03	1.79^{D}	0.05
Sum	8.38	0.70	19.80	1.09	11.06	1.49	25.41	1.00

* Average of aspartic acid and asparagine.

Table 6-6. Percentage of total amino acids in *T. weissflogii* grown at different temperatures and irradiances. Values are mean and standard errors (SE) for three replicate vessels, n = 3. Means with a row followed by the same letter were not significantly different (one way ANOVA Tukey's test; $p < 0.05$).

	Percentage of total amino acid							
Amino acid	16 HL		16 LL		26 HL		26 LL	
	Mean	SE	Mean	SE	Mean	SE	Mean	SE
Essential amino acid								
Histidine	3.75^{B}	0.28	2.08^{A}	0.34	3.29^{B}	0.64	1.87^{A}	0.48
Lysine	7.16^{A}	0.82	7.29^{A}	0.40	7.10^{A}	0.66	9.77^{B}	0.23
Methionine	4.65^{B}	0.03	3.95^{A}	0.08	4.49^{B}	0.27	4.05^{A}	0.20
Valine	6.45^{B}	0.23	7.38^{C}	0.16	6.67^{B}	0.40	5.57^{A}	0.43
Phenylalanine	6.99^{A}	0.96	6.54^{A}	0.04	7.06^{A}	0.56	8.68^{B}	0.13
Isoleucine	5.92^{B}	0.05	5.52^{B}	0.10	6.12^{B}	0.17	4.55^{A}	0.29
Non-essential amino acid								
Arginine	8.70^{A}	0.39	9.26^{B}	0.26	8.13^{A}	0.74	7.35^{A}	0.20
Serine	6.75^{C}	0.27	6.81^{C}	0.13	6.37^{B}	0.29	5.55^{A}	0.07
Glycine	5.66^{C}	0.14	4.43^{B}	0.26	4.23^{B}	0.32	3.16^{A}	0.19
Glutamic acid	10.97^{A}	1.09	12.24^{A}	0.11	12.14^{A}	0.95	13.71^{B}	0.31
Asparagine*	10.08^{C}	1.12	9.85^{C}	0.51	8.29^{B}	2.22	6.06^{A}	0.40
Proline	5.54^{A}	0.19	5.83^{A}	0.20	8.56^{B}	0.48	8.02^{B}	0.23
Cysteine	1.10^{A}	0.16	1.42^{A}	0.15	0.98^{A}	0.30	1.40^{A}	0.23
Tyrosine	4.54^{A}	0.39	4.64^{A}	0.08	4.69^{A}	0.29	5.81^{B}	0.19
Threonine	6.86^{B}	0.16	5.91^{A}	0.11	6.38^{A}	0.22	7.61^{C}	0.18
Alanine	4.88^{A}	0.09	6.87^{B}	0.14	5.49^{A}	0.41	6.85^{B}	0.21

* Average of aspartic acid and asparagine.

6.4.8 Photosynthesis rate

The photosynthesis rate of *T. weissflogii* grown increased with photon flux density until the maximum level was reached at approximately 200 and 300 µmol photons $m^{-2}s^{-1}$ respectively. The chl *a*-specific light saturated rate of photosynthesis rate (P^{Chl}_{max}) increased with increased temperature and irradiance (Figs 6-14 A,B,C,D). P^{Chl}_{max} increased approximately 1.4-1.9 fold after cells were exposed with high temperature and irradiance. The slope (α) of the linear part

of the PE curve decreased with increased temperature, whereas α was not affected by irradiance (Table 6-7). E_k is the saturation irradiance, which increased with temperature and irradiance.

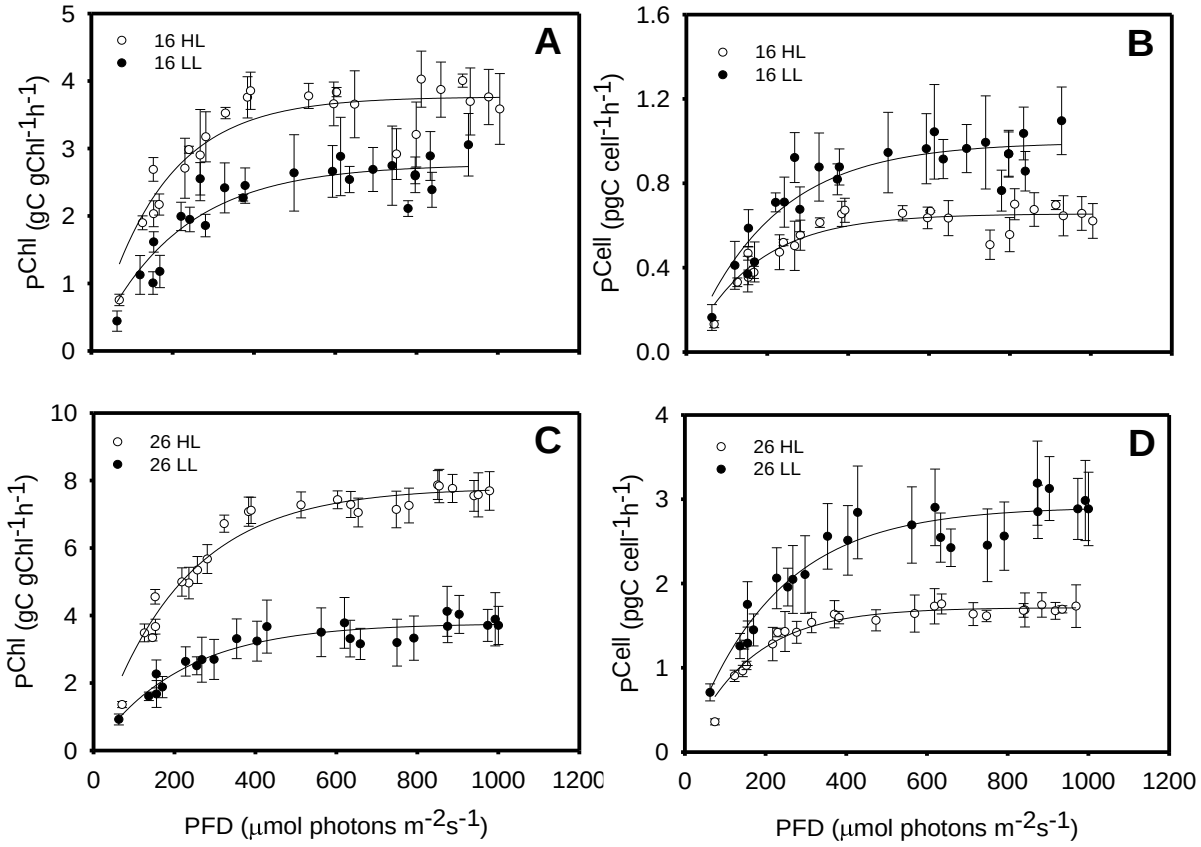

Figure 6-14. Temperature and irradiance dependencies of the chlorophyll *a*-specific rate of photosynthesis (P^{Chl} in unit g C· g Chl^{-1} h^{-1}) (A and C) and the cell-specific rate of photosynthesis (P^{Cell} in unit pg C· $cell^{-1}$ h^{-1}) (B and D) of *T. weissflogii* under different treatments: 16 HL, 16 LL, 26 HL, and 26 LL. Values are mean and standard errors (SE) for three replicate vessels, n = 3.

Table 6-7. Photosynthetic rate parameters of *T. weissflogii* at different treatments. Values are mean and standard errors (SE) for three replicate vessels, n = 3. Means followed by the same letter were not significantly different (one way ANOVA Tukey's test; $p < 0.05$).

Parameter*	Treatment	Photosynthetic rate derived from Chlorophyll		Cell	
		Mean	SE	Mean	SE
P_{max}	16 HL	3.52^{b}	0.06	0.67^{A}	0.06
	16 LL	2.49^{a}	0.13	0.94^{B}	0.07
	26 HL	6.65^{c}	0.42	1.55^{C}	0.06
	26 LL	3.64^{b}	0.32	2.50^{D}	0.42
α	16 HL	0.024^{a}	0.001	0.0044^{A}	0.0001
	16 LL	0.021^{a}	0.001	0.0081^{B}	0.0003
	26 HL	0.016^{b}	0.001	0.0040^{A}	0.0001
	26 LL	0.012^{b}	0.001	0.0083^{B}	0.0003
E_k	16 HL	149^{b}	6	154^{A}	2
	16 LL	119^{a}	5	124^{B}	4
	26 HL	416^{d}	6	421^{C}	4
	26 LL	295^{c}	17	312^{D}	18

* Unit: P^{Chl}_{max} : gC gChl^{-1} h^{-1}; P^{Cell}_{max} : pg C cell^{-1} h^{-1}; α (P^{Chl}) : gC gChl^{-1} h^{-1} (µmol photons m^{-2}s^{-1})$^{-1}$; α (P^{Cell}) : pg C cell^{-1} h^{-1} (µmol photons m^{-2}s^{-1})$^{-1}$; E_k : µmol photons m^{-2} s^{-1}.

6.4.9 Light absorption

The magnitude and shape of the abosprtion spectra (a^{Chl}) for *T. weissflogii* varied in response to varying temperatures and irradiances (Fig. 6-15). Chlorophyll *a* specific absorption at the blue peak, a^{Chl} (440 nm), and at the red peak, a^{Chl} (675 nm), increased with increasing temperature and irradiance. The ratio of a^{Chl} (440) to a^{Chl} (675) also increased with increasing temperature and irradiance (Table 6-8).

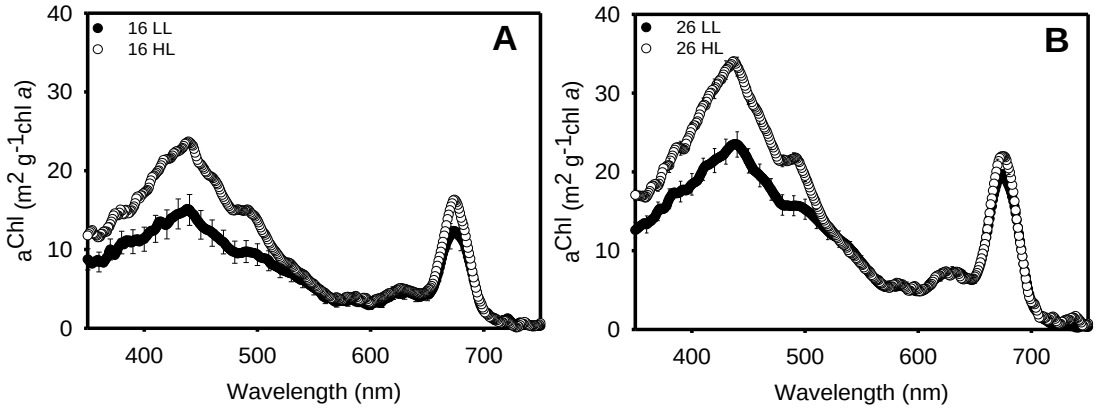

Figure 6-15. *In vivo* chlorophyll *a* specific absorption spectra (a^{Chl}) for *Thalassiosira weissflogii*. Shown are the mean values and standard errors (every 10 nm) for three replicate vessels (n=3) at temperature and irradiance of 16 LL and 16 HL (A) and 26 LL and 26 HL (B). Closed dots are low light and open dots are high light.

Table 6-8. Values of a^{Chl} (440 nm), a^{Chl} (675 nm) and of the ratio a^{Chl} (440 nm): a^{Chl} (675 nm) in *Thalassiosira weissflogii* grown at different temperatures and irradiances.

Treatments	a^{Chl} (m^{-2} g^{-1}chl a) at wavelengths		Ratio of a^{Chl} (440 nm) to a^{Chl} (675 nm)
	440 (nm)	675 (nm)	
16 HL	23.59	16.19	1.46
16 LL	15.01	12.27	1.22
26 HL	33.36	21.93	1.52
26 LL	23.48	19.66	1.19

6.4.10 Pigments

Five accessory pigments (beta carotene, chlorophyll *c*, diatoxanthin, diadinoxanthin, and fucoxanthin), in addition to chlorophyll *a*, were found (Table 6-9). There were significant changes in total accessory pigments with temperature and irradiance. The 16 HL treatment had the highest ratio of the total pigments to chl *a*, whereas the 26 LL treatment had the lowest. The ratio of chl *c* to chl *a* ratio was not affected by temperature, but this ratio increased with increased irradiance at a constant 16°C. The ratio of photoprotective pigment (beta carotene) to

chl *a* varied with temperature and irradiance. The ratio of xanthophyll cycle pigments (diatoxanthin and diadinoxanthin) to chl *a* increased with increased irradiance. That ratio was 3.5 times higher in the cells grown under 16 HL compared to the cells grown under 16 LL.

Table 6-9. Pigment composition [mol accessory pigment (mol chl *a*)$^{-1}$] of *Thalasiosira weissflogii* grown under different temperatures and irradiances. Values are mean and standard errors (SE) for three replicate vessels, n = 3. Means with a row followed by the same letter were not significantly different (one way ANOVA Tukey's test; $p < 0.05$).

Pigment	Temperature (ºC) and irradiance							
	16 HL		16 LL		26 HL		26 LL	
	Mean	SE	Mean	SE	Mean	SE	Mean	SE
Beta C	0.0049^{A}	0.0005	0.0187^{B}	0.0006	0.0056^{A}	0.0002	0.0090^{C}	0.0010
DT	0.14^{A}	0.01	0.03^{B}	0.00	$0.07^{C,D}$	0.01	$0.05^{B,D}$	0.01
Chl *c*	0.25^{A}	0.00	0.13^{B}	0.01	0.12^{B}	0.01	0.12^{B}	0.01
DD	0.94^{A}	0.04	$0.12^{B,D}$	0.00	0.56^{C}	0.03	0.15^{D}	0.01
Fuco	0.59^{A}	0.01	1.18^{B}	0.03	$0.90^{C,D}$	0.04	0.85^{D}	0.04
DD+DT	0.92^{A}	0.02	0.26^{B}	0.00	0.73^{C}	0.06	0.21^{B}	0.01
Total pigment	1.92^{A}	0.08	1.50^{B}	0.01	1.66^{B}	0.09	1.17^{C}	0.07
(DD+DT)/Fuco	1.82^{A}	0.02	0.13^{B}	0.00	0.73^{C}	0.07	0.21^{D}	0.01
DT/(DD+DT)	0.13^{A}	0.02	0.21^{B}	0.01	0.11^{A}	0.00	0.26^{B}	0.04
Chl *c*/Fuco	0.21^{A}	0.00	0.21^{A}	0.00	0.14^{B}	0.01	0.14^{B}	0.00

Beta C: Beta carotene, DT: Diatoxanthin, Chl *c*: Chlorophyll *c*, DD: Diadinoxanthin, Fuco: Fucoxanthin; Total pigment = Σ(Beta C+ DT + Chl *c* + DD + Fuco)

6.4.11 Fatty acid profile

There were significant differences in total cellular fatty acid content of *T. weissflogii* under different growth phases, temperatures, and irradiances (Fig 6-16). The total cellular fatty acid content increased significantly from exponential to stationary growth phase (two way ANOVA; $p < 0.05$). The cellular fatty acid content at 26 LL under stationary growth phase (138.4 ± 6.4 pg cell^{-1}) was about 8 times higher than under exponential growth phase (17.4 ± 1.8 pg cell^{-1}).

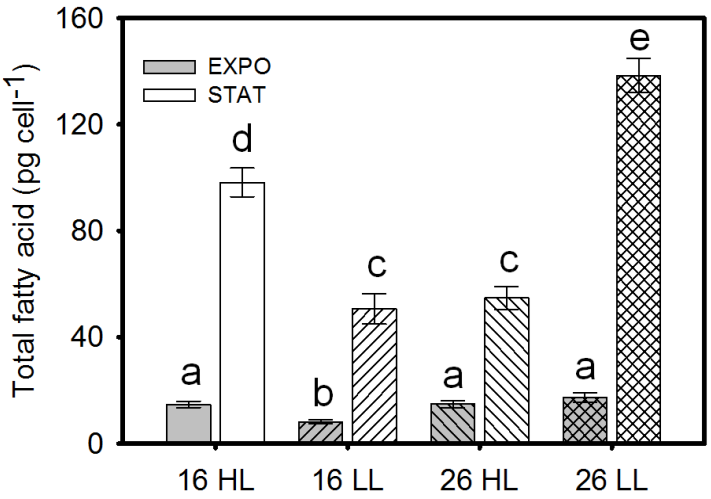

Figure 6-16. Cellular fatty acid content of *T. weissflogii* in semi-continuous culture phase (EXPO: grey bars) and stationary phase (STAT: white bars). Mean values ± standard errors are shown for three replicate vessels (n=6) at 16 HL, 16 LL, 26 HL, and 26 LL. Bars labelled with the same letter were not significantly different (two way ANOVA Turkey's test; $p < 0.05$).

Table 6-10. Mean of cellular fatty acid content (pg cell^{-1}) for *T. weissflogii* grown at different growth phases, temperatures and irradiances. Values are mean and standard errors (SE) for three replicate vessels, n = 3. Means with a row followed by the same letter were not significantly different (two way ANOVA Tukey's test; p< 0.05). Shown in bold face are the most abundant fatty acids.

Fatty acid	Treatments															
	16 HL				16 LL				26 HL				26 LL			
	EXPO	SE	STAT	SE	EXPO	SE	STAT	SE	EXPO	SE	STAT	SE	EXPO	SE	STAT	SE
Lauric acid	0.02	0.00	0.02	0.01	0.07	0.01	0.06	0.01	0.02	0.00	0.03	0.00	0.04	0.00	0.05	0.01
Myristoleic acid	0.02	0.00	0.04	0.01	0.07	0.01	0.05	0.00	0.02	0.00	0.07	0.01	0.06	0.00	0.08	0.02
Myristic acid	**1.22^{A}**	**0.11**	**4.76^{B}**	**0.45**	**0.65^{A}**	**0.04**	**2.43^{A}**	**0.19**	**1.09^{A}**	**0.14**	**4.68^{B}**	**0.44**	**2.20^{A}**	**0.21**	**6.73^{B}**	**0.63**
Pentadecanoic acid	0.23	0.01	1.48	0.21	0.13	0.03	0.64	0.18	0.15	0.01	1.20	0.08	0.19	0.02	2.08	0.24
Palmitoleic acid	**4.28^{A}**	**0.27**	**29.55^{B}**	**1.62**	**2.14^{A}**	**0.17**	**17.36^{C}**	**1.75**	**3.77^{A}**	**0.30**	**14.77^{C}**	**1.19**	**4.76^{A}**	**0.58**	**44.80^{D}**	**1.80**
Palmitic acid	**3.60^{A}**	**0.26**	**40.36^{B}**	**1.36**	**1.52^{A}**	**0.09**	**18.30^{C}**	**1.65**	**3.49^{A}**	**0.26**	**14.46^{C}**	**0.94**	**3.20^{A}**	**0.38**	**51.19^{D}**	**1.51**
γ-Linolenic acid	0.07	0.01	0.37	0.06	0.13	0.02	0.11	0.02	0.07	0.01	0.20	0.02	0.08	0.00	0.75	0.13
Linoleic acid	0.08	0.01	0.56	0.09	0.11	0.01	0.33	0.02	0.08	0.02	0.28	0.02	0.15	0.01	1.11	0.12
Oleic acid	0.09	0.01	0.71	0.10	0.17	0.02	0.34	0.09	0.07	0.00	0.18	0.01	0.12	0.01	0.76	0.02
Elaidic acid	0.01	0.00	0.75	0.06	0.26	0.03	1.74	0.35	0.16	0.03	0.70	0.06	0.08	0.02	1.22	0.16
Stearic acid	0.06	0.00	0.44	0.07	0.11	0.01	0.39	0.08	0.07	0.01	0.34	0.00	0.10	0.01	1.16	0.30
Arachidonic	0.05	0.00	0.10	0.01	0.20	0.03	0.58	0.47	0.07	0.00	0.27	0.02	0.13	0.01	0.42	0.11
cis-5,8,11,14,17-Eicosapentaenoic acid	**3.85^{A}**	**0.41**	**15.62^{B}**	**1.08**	**1.50^{A}**	**0.13**	**7.02^{C}**	**0.68**	**4.43^{A}**	**0.35**	**14.83^{B}**	**1.27**	**4.14^{A}**	**0.29**	**22.98^{D}**	**0.79**
cis-8,11,14-Eicosatrienoic acid	0.04	0.00	0.27	0.05	0.18	0.02	0.22	0.04	0.05	0.00	0.19	0.02	0.11	0.01	0.51	0.06
Arachidic acid	0.02	0.00	0.04	0.00	0.10	0.01	0.06	0.01	0.02	0.00	0.02	0.00	0.06	0.00	0.07	0.02
cis-4,7,10,13,16,19-Docosahexaenoic acid	**0.96^{A}**	**0.08**	**3.00^{B}**	**0.23**	**0.43^{A}**	**0.07**	**0.79^{A}**	**0.18**	**1.23^{A}**	**0.19**	**2.39^{B}**	**0.22**	**1.74^{A}**	**0.21**	**3.68^{B}**	**0.34**
Behenic acid	0.02	0.00	0.05	0.01	0.10	0.01	0.09	0.00	0.03	0.00	0.04	0.00	0.06	0.00	0.56	0.05
Lignoceric acid	0.05	0.00	0.11	0.01	0.22	0.03	0.17	0.01	0.05	0.00	0.13	0.01	0.13	0.00	0.25	0.05
Total fatty acid (pg cell^{-1})	14.68	1.18	98.21	5.42	8.10	0.73	50.67	5.73	14.87	1.33	54.78	4.30	17.36	1.78	138.38	6.36

EXPO: semi-continuous culture phase; STAT: stationary phase; HL: high light (500 µmol photons m^{-2}s^{-1}); LL: low light (50 µmol photons m^{-2} s^{-1}); 16: 16°C; 26: 26°C. Statistical analyses were not conducted on fatty acids less than 1 pg cell^{-1}.

Table 6-11. Fatty acid composition (as % of total fatty acids ± standard error) of *T. weissflogii* grown at different growth phases, temperatures and irradiances. Values are mean and standard errors (SE) for three replicate vessels, n = 3. Means with a row followed by the same letter were not significantly different (two way ANOVA Tukey's test; $p < 0.05$). Shown in bold face are the most abundant fatty acids.

Fatty acid	Treatments															
	16 HL				16 LL				26 HL				26 LL			
	EXPO	SE	STAT	SE	EXPO	SE	STAT	SE	EXPO	SE	STAT	SE	EXPO	SE	STAT	SE
Lauric acid	0.12	0.01	0.03	0.01	0.89	0.08	0.13	0.02	0.11	0.01	0.05	0.00	0.25	0.03	0.03	0.00
Myristoleic acid	0.13	0.01	0.04	0.00	0.90	0.07	0.10	0.00	0.15	0.01	0.12	0.00	0.33	0.02	0.05	0.01
Myristic acid	**8.34^{A}**	**0.56**	**4.85^{B}**	**0.46**	**8.12^{A}**	**0.62**	**4.83^{B}**	**0.23**	**7.47^{A}**	**0.87**	**8.52^{A}**	**0.16**	**12.72^{C}**	**0.31**	**4.85^{A}**	**0.36**
Pentadecanoic acid	1.54	0.03	1.49	0.15	1.70	0.39	1.34	0.43	0.98	0.05	2.19	0.02	1.12	0.04	1.50	0.15
Palmitoleic acid	**29.29^{A}**	**0.79**	**30.07^{A}**	**0.64**	**26.34^{B}**	**1.09**	**34.26^{C}**	**0.19**	**25.37^{B}**	**0.55**	**26.94^{B}**	**0.16**	**27.13^{B}**	**0.89**	**32.36^{C}**	**0.88**
Palmitic acid	**24.56^{A}**	**0.53**	**41.11^{B}**	**0.36**	**18.84^{C}**	**0.75**	**36.19^{D}**	**0.87**	**23.50^{A}**	**0.50**	**26.45^{A}**	**0.33**	**18.25^{C}**	**0.70**	**37.04^{D}**	**1.49**
γ-Linolenic acid	0.49	0.06	0.38	0.05	1.63	0.13	0.22	0.02	0.44	0.03	0.37	0.01	0.49	0.04	0.54	0.09
Linoleic acid	0.53	0.09	0.57	0.07	1.29	0.10	0.66	0.03	0.51	0.10	0.51	0.01	0.87	0.07	0.80	0.10
Oleic acid	0.62	0.01	0.72	0.08	2.02	0.14	0.64	0.11	0.49	0.01	0.33	0.01	0.68	0.05	0.55	0.02
Elaidic acid	0.10	0.01	0.76	0.03	3.25	0.33	3.38	0.41	1.10	0.17	1.31	0.22	0.45	0.11	0.88	0.13
Stearic acid	0.43	0.02	0.44	0.05	1.38	0.10	0.81	0.20	0.48	0.01	0.62	0.06	0.58	0.05	0.85	0.24
Arachidonic acid	0.32	0.02	0.10	0.01	2.45	0.19	0.99	0.77	0.44	0.02	0.48	0.01	0.78	0.09	0.30	0.08
cis-5,8,11,14,17-Eicosapentaenoic acid	**26.03^{A}**	**1.64**	**15.94^{B}**	**1.19**	**18.60^{B}**	**1.27**	**13.88^{C}**	**0.48**	**29.88^{D}**	**1.17**	**27.03^{A}**	**0.28**	**24.17^{A}**	**1.10**	**16.60^{B}**	**0.24**
cis-8,11,14-Eicosatrienoic acid	0.30	0.01	0.27	0.04	2.26	0.18	0.43	0.03	0.35	0.02	0.35	0.01	0.68	0.07	0.37	0.04
Arachidic acid	0.15	0.01	0.04	0.00	1.24	0.10	0.12	0.01	0.16	0.02	0.04	0.00	0.35	0.04	0.05	0.01
cis-4,7,10,13,16,19-Docosahexaenoic acid	**6.57^{A}**	**0.37**	**3.05^{B}**	**0.12**	**5.25^{A}**	**0.68**	**1.51^{C}**	**0.21**	**8.04^{D}**	**0.86**	**4.35^{B}**	**0.15**	**9.97^{D}**	**0.62**	**2.65^{C}**	**0.19**
Behenic acid	0.16	0.01	0.05	0.01	1.20	0.11	0.18	0.02	0.18	0.02	0.08	0.01	0.38	0.04	0.40	0.03
Lignoceric	0.32	0.02	0.11	0.01	2.63	0.19	0.34	0.00	0.37	0.03	0.24	0.01	0.78	0.07	0.18	0.04
% SFA	35.62	1.19	48.12	1.05	36.01	2.34	43.93	1.78	33.23	1.51	38.19	0.58	34.44	1.27	44.89	2.32
% MUFA	30.15	0.82	31.58	0.76	32.52	1.64	38.39	0.71	27.11	0.74	28.71	0.40	28.60	1.07	33.85	1.04
% PUFA	34.23	2.20	20.30	1.47	31.48	2.55	17.69	1.53	39.66	2.19	33.10	0.46	36.96	1.99	21.26	0.74

% SFA: % of total saturated fatty acid; % MUFA: % of total monounsaturated fatty acid; % PUFA: % of total polyunsaturated fatty acid. Statistical analyses were not conducted on fatty acids less than 2 % of total fatty acids.

18 types of fatty acids from C12-C24 were detected. Most of these contributed < 1 pg cell^{-1} and < 1 % of total fatty acids (Tables 6-10 and 6-11). The five most abundant fatty acids were myristic acid (C14:0; 5-13% of total), palmitic acid (C16:0; 25-34% of the total), palmitoleic acid (16:1; 18-41% of the total), eicosapentanoic acid (C20:5; 14-27% of the total) and docosahexaenoic acid (22:6; 2-10% of the total) in both exponential and stationary phases.

The saturated fatty acid (SFA) and monounsaturated fatty acids (MUFA) increased with time in stationary phase cultures, whereas polyunsaturated fatty acids (PUFA) dropped. The percentages of both SFA and MUFA declined with increased temperature (from 16 to 26°C) in the semi-continuous cultures, whereas the percentage of PUFA increased. SFA at 16 HL was the highest at approximately 48 % of the total fatty acids in the stationary phase. PUFA at 26 HL was the greatest at around 40 % of the total fatty acids.

Eicosapentaenoic acid (EPA or C20:5n) was the main PUFA (30% total fatty acids, at 26 HL) and was followed by docosahexaenoic acid (DHA or C22:6n) (10%, at 26 LL). The content of myristic (C14:0) and the palmitic (C16:0) acid as SFA and the palmitoleic (C16:1) as MUFA varied with temperature and irradiance. The palmitoleic and palmitic acid increased with age of culture, whereas the myristic acid, EPA, and DHA declined.

6.5 Discussion

6.5.1 Temperature and irradiance versus cell abundance and growth rate

The increase of cell abundance with dilution rate was observed in *T. weissflogii* grown in nutrient-limited semi-continuous cultures when the cultures reached steady-state biomass (Fig. 6-1). Similarly, Chauton *et al.* (2013) reported that cell biomass production increased with increasing dilution rates and cell density was maximum at dilution rate 0.65 day^{-1} (from 0.33 to 1.1 day^{-1}) in the diatom *Phaeodactylum tricornutum* grown at 20ºC and illuminated with 100 µmol photons m^{-2} s^{-1} in 16:8 (light:dark) cycles. This suggests that dilution rates affected cell abundance of *T. weissflogii*. The growth rates (GR) of *T. weissflogii* grown under different dilution rates were close to theoretically calculated values, indicating that the supply rates of the culture medium. At higher dilution rate, cells might be able to grow faster due to high nutrient replacement of medium (Takeya *et al*. 2004). The results presented here are in agreement with the studies by Reichert *et al*. (2006) on nutrient-sufficient semicontinuous culture of the cyanobacterium *Spirulina platensis*, where a daily dilution rate at 25 or 50% (v/v) resulted in an increase growth rate.

6.5.2 Temperature and irradiance versus chl *a* and elemental composition

Intracellular chl *a* content increased with increased temperature under low light in *T. weissflogii*. This is associated with an increased in either the size or number of photosynthetic units (Sakshaug *et al*. 1997). In the same way, photosynthesis rate per chlorophyll *a* and cell (P^{chl} and P^{cell}) also increased. This effect of temperature on the cellular content of chl *a* is in accordance with the results of diatom *Thalassiosira weissflogii* in nutrient-deplete growth condition under either 100 µM nitrate or 100 µM ammonium (Strzepek & Price 2000) and of green algal *Dunaliella tertiolecta* grown under nutrient-replete growth conditions (Sosik & Mitchell 1994).

An increase of the C:N and C:chl *a* ratios with increased temperature was observed in this study. The C:N ratios were greater than the Redfield C:N ratio of 6.6 which allows optimal growth of non-limiting culture (Geider & La Roche 2002). This indicats that *T. weissflogii was* maintained under nitrogen-limited conditions. Similarly, Stramski *et al*. (2002) mentioned that there was a reduction of cellular nitrogen and chl *a* in *T. pseudonana* grown under nitrogen-limited chemostat culture (60 µM nitrate) when compared with replete nutrient culture.

The cellular chl *a* content decreased with increasing irradiance in microalgae grown under nitrogen-limited condition which was previously observed in *Phaeodactylum tricornutum* (Ramos *et al*. 2012), in *T. pseudonana* (Stramski *et al*. 2002), in *Dunaliella tertiolecta* (chlorophyta), *T. pseudonana*, and *Skeletonema costatum* (Kolber *et al.* 1988). In this investigation, the C:N ratio showed no consistent trend with increasing irradiance at 16^{o}C, whereas the C:N ratio decreased with increasing irradiance at 26^{o}C. Because the amount of organic carbon at low light was higher than at high light and nitrogen content varied under nitrogen limitation. Therefore, the variation of C:N ratios reflected changes in cell carbon. Stramski *et al*. (2002) reported that the increase of C:chl *a* ratio with increasing irradiance has been observed in *T. pseudonana* and the reduction of intracellular chl *a* content was accompanied by an increase of C:chl *a* ratio of diatom grown under nitrogen limitation.

The results showed that the C:chl *a* ratio in *T. weissflogii* progressively increased with elevated irradiance. Similarly, the C:chl *a* ratio of diatom *Thalassiosira allenii* was positively correlated with temperature (>25^{o}C) under both saturating and non-saturating light (Redalje & Laws 1983). The C:chl *a* ratio also was correlated with growth rate positively under the increased irradiance; however, this correlaion was not response with the increased temperature. Moreover, the light saturation index (E_k) as an indicator of plankton photoacclimation also showed a positive relationship with increased irradiance. These results agree with the bio-optical moldel. Therefore, the correlation of C:chl *a* with growth rate supports the bio-optical model.

6.5.3 Temperature and irradiance versus cell size

Eukaryotic cell size is an important characteristic for survival and adaptation (Davie & Petersen 2012). Cell size depends on growth rate which associates with metabolic rate and cell division rate. There was no significant temperature-specific difference in the mean cell volume of *T. weissflogii* grown under nitrogen limitation, indicating that cell size did not influence growth rate. That result could be consistent with findings of past studies by Sosik & Mitchell (1991) which suggested that cell size of *Dunaliella tertiolecta* did not vary systematically with growth rate at nitrogen-insufficient condition. Therefore, in this study, *T. weissflogii* grown under different temperature with high irradiance is likely to be at the constant division rate and cell abundance. Since the effect of temperature on cell size in diatoms grown under nitrogen limitation has been rarely studied. Therefore, cell size of microalgae grown under nutrient replete condition will be considered next. Different investigators have found different relationships between cell size and temperature under nutrient sufficient condition. For examples, cell size was found to increase with temperature in the diatoms *T. pseudonana* and *Phaeodactylum tricornutum* (Thompson *et al.* 1992), and in the green chlorococcal alga *Scenedesmus obliquus* (Cepák *et al*. 2007).

In this study, cell size of *T. weissflogii* decreased with increased irradiance under nitrogen insufficient condition. This is supported by Sosik *et al.* (1989) which revealed that increasing cell size with decreasing irradiance was observed in *T. weissflogii* grown under nitrogen sufficient condition. Additionally, cell size of 6 microalgae grown in nutrient-replete medium varied with irradiance from 25 to 750 μmol photons m^{-2} s^{-1}; however, *T. weissflogii, Chaetoceros gracilis* and *Coscinodiscus* sp. decreased with increasing irradiance at a range of from 25 to 90 μmol photons $m^{-2}s^{-1}$ (Fujiki & Taguchi 2002). These phenomenon could be consistent with findings of past studies by Zachleder & Cepák (1987), which suggested that a decrease in light intensity caused a decrease of the mother cell size as well as the decrease of daughter cell number per

mother cell of alga *Scenedesmus quadricauda* grown under different light conditions. Cell size of daughter did not change under low light intensity due to the growth rate decreased markedly. Therefore, in this study, the division rate and cell abundance of *T. weissflogii* is likely to decrease under low irradiance. This implies that the sink rates of microalgae as well as their susceptibilities to zooplankton grazing are functions of cell size. Consequently, microalgal size is a major determinant of the food web and material transfer rates in the rivers, lakes and oceans.

6.5.4 Temperature and irradiance versus nucleotide

There were no significant differences observed in DNA content in *T. weissflogii* grown under different temperatures and irradiances. This is confirmed by DNA volume when stained with DAPI (Fig. 6-13B). Temperature and irradiance affected RNA content. This indicates that RNA plays important role in growth and cell cycle (Olsen *et al.* 1986).

The ratio of RNA:protein correlated well with the growth rates of *T. weissflogii* grown under different irradiances; however, it was not significantly correlated to the RNA:protein ratio under different temperatures. This suggests that increasing RNA:protein ratio under irradiances reflects the control of the rate protein synthesis by the number of ribosomes. When the growth rate increased, the rate of ribosome function approached a maximum value, corresponding to amino acid polymerization. This is parallel with total amino acid results responded with irradiance but did not react with temperature. This situation is referred to as the growth-rate hypothesis. Therefore, RNA:protein ratio supported growth rate hypothesis under variable irradiance. While temperature did not influence RNA:protein ratio, this is against growth rate hypothesis.

6.5.5 Temperature and irradiance versus biochemical composition

Protein

In this study, the protein content of *T. weissflogii* grown under N limitation decreased with increased temperature with low light, reflecting increased metabolic activity. This results was consistent with previous observations of *Phaeodactylum tricornutum* grown under nitrogen limitation (40 µM ammonium) (Terry *et al.* 1985). Moreover, this finding is in accordance with the results of Harrison *et al*. (1990) who observed that protein content decreased in diatoms *Isochrysis galbana*, *Chaetoceros calcitrans*, and *Thalassiosira pseudonana* grown under nitrogen-limited medium (ratio of N: Si: P = 14: 26: 1). These phenomenon could decrease the growth rate and the efficiency of carbon utilisation at the non-optimal temperature condition (Raven & Geider 1988). Additionally, an increase in free amino acid concentration is an indicator of the lower protein content in *T. weissflogii*.

The results showed protein contents decreased with the increasd irradiance. Similarly, Liu *et al*. (2012) found that protein contents were lower at high light (250 and 400 µmol photons m^{-2} s^{-1}) in green alga *Scenedesmus* sp. 11-1 grown under nitrogen deficient condition. This suggests that the light supply could influence the metabolic activity. Post *et al.* (1985) demonstrated that the thylakoid stacking in chloroplast of *T. weissflogii* exposed with HL was fewer than with LL, reflecting high light intensity could damage the chloroplastidial activity. Therefore, intracellular chl *a* content reduced at high irradiance which led to low efficiency of metabolic activity. The protein pathway is especially blocked by a lack of sufficient nitrogen under the high light.

Carbohydrate

The inconsistent variations of carbohydrate content with temperature were observed in *T. weissflogii.* The finding is consistent with the results of Carvalho *et al*. (2009) who reported the inconsistent variation of the internal amounts of carbohydrate with temperature (10-26^{o}C) for hapophyte *Pavlova lutheri* at the late exponential phase under five irradiance levels from 60 to

240 µmol photons m^{-2} s^{-1}. Additionally, Srirangan *et al.* (2015) reported that there was no significant change of the starch contents with increasing temperature when *Dunaliella viridis* grown under high light. Those reports suggest that there are a correlation between the effects of temperature and light. This may lead to inverse variations in a biochemical parameter with one effect, depending on the stated value of the other effect (Carvalho *et al*. 2009).

Carbohydrate contents also decreased with increased light intensity. There are variations of carbohydrate content in microalgae grown under different conditions. For example, Sun *et al.* (2014) found that carbohydrate content from *Neochloris oleoabundans* grown under nitrogen depleted condition increased with increasing light intensity from 50 to 100 µmol photons m^{-2} s^{-1}, but decreased when the light intensity was increased from 100 to 300 µmol photons m^{-2} s^{-1}. Ho *et al*. (2012) also mentioned that an increase in light intensity from 60 to 420 µmol photons m^{-2} s^{-1} could lead to an increase in carbohydrate content in *Scenedesmus obliquus*, but a further increase in light intensity did not improve accumulation of carbohydrates. Therefore, this suggests that the optimal light lead to high carbohydrate content while carbohydrate contents observed in *T. weissflogii* decreased at the below and above optimal light intensity.

Neutral lipid

In this study, intracellular neutral lipid contents did not change in response to different temperature and irradiance under exponential phase. Similarly, Harrison *et al*. (1990) reported that the lipid as % ash-free dry weight remained relatively constant under nitrogen-limitation for all three microalgae and the amount of lipid per cell did not show a consistent trend with irradiances for three microalgae harvested mid-logarithmic growth phase. Neutral lipid per biovolume of *T. weissflogii* increased with irradiance. This result was similar to the results of Nile red-stained neutral lipid droplets seen under microscope (Fig. 6-13C), reflecting the relation between neutral lipid and cell size.

There are variations in neutral lipid content in the different treatments at stationary phase. Some investigators have reported that neutral lipid increased with increased temperature. For example, *Scenedesmus obtusus* XJ-15 grown under different temperatures (17, 25, and 33 °C) and light intensity 100 µmol photons m^{-2} s^{-1} at nitrogen-deplete condition had neutral lipids increased with increasing temperature and that there was more lipid contents than nitrogen sufficient condition (Xia *et al*. 2015). Moreover, *Chlamydomonas reinhardtii* and *Chlorella vulgaris* mutants had more neutral lipid after temperature was increased when compared with the wild type under PFD 150 µmol photons m^{-2} s^{-1} (Yao *et al.* 2012).

In this work, the highest lipid productivity achieved in cultures of *T. weissfloii* was recorded at 2.85 mg L^{-1} d^{-1} under 16 HL and nitrogen limitation at stationary phase. Compared to the other studies on *Thalassiosira* species, this value was lesser because of characteristic of algal species (Griffiths & Harrison 2009). For example, d'Ippolito et al. (2015) reported lipid productivity of 0.43-0.54 mg L^{-1} d^{-1} in 2 species of *T. rotula*, of 3.48-7.27 mg L^{-1} d^{-1} in 3 species of *T. weissfloii*, and of 1.72 mg L^{-1} d^{-1} in *T. pseudonana* when cells grew in nutrient sufficient medium of 2-L polycarbonate flasks at 20°C, PFD 200 µmol m^{-2} s^{-1} on a 14:10 h light dark cycle and harvested under stationary phase (d'Ippolito et al. 2015). Although the lipid productivity of *T. weissflogii* was lower than other *Thalassiosira* stains, the high PUFAs concentration (EPA and DHA) is suitable for the calanoid copepod and fish diet (Kiatmetha *et al*. 2011).

6.5.6 Temperature and irradiance versus amino acids

Free and combined amino acids were observed in *T. weissflogii* grown under nitrogen limitation. Most studies reported the amino acid contents of microalgae grown under nitrogen replete conditions (da Silva Gorgônio *et al.* 2013; Becker 2007; Barbarino & Lourenço 2005; Kaiser & Benner 2005). To our knowledge, this is the first report showing 16 amino acids profile under nitrogen deplete conditions in T. *weissflogii*.

Free amino acids

In the data presented here, free amino acids accounted for around 16-22 percent of total amino acid content in *T. weissflogii*. Arginine, serine, glutamic acid, and valine had the highest free amino acid content. There are variations of amino acid profile in microalgae that depends on species and environment. For example, Derrien *et al.* (1998) reported that free amino acid in 5 microalgae (*Tetraselmis suecica*, *Skeletonema costatum*, *Chaetoceros calcitrans*, *Thalassiosira* sp., and *Isochrysis galbana*) varied remarkably among different species.

Temperature did not affect free amino acid content; however, the concentration of most free amino acid increased with decreased irradiance. The mechanism(s) responsible for the changes of free amino acid with combined temperature and irradiance are not clearly understood. However, Hernández-Sebastià *et al.* (2005) suggested that free amino acid asparagine probably has a role in the control of storage-product accumulation in developing seeds of low- and high-protein soybean lines.

Combined amino acids

Glutamic acid was the most abundant amino acid (11-14 % total amino acid). In contrast, cysteine as a sulphur containing amino group had the lowest (1.0-1.4 % total amino acid) in all treatment. A small amount of cysteine is often found in plants and microalgae. These results are similar to da Silva Gorgônio *et al*. (2013) who found that glutamic acid and aspartic acid were the most abundant amino acids in all microalgae *Dunaliella tertiolecta*, *Isochrysis galbana*, and *Tetraselmis gracilis* grown under nutrient-replete condition.

In this investigation, both temperature and irradiance influenced the amount of combined amino acid. The combined amino acid content increased with increased temperature. Methionine, valine, phenylalanine and isoleucine as essential amino acid in animal and humans change significantly with temperatures while histidine was not affected. The combined non-essential amino acid profiles showed major variations among treatments. The combined amino acid

content increased with decreased light intensity. The increase in the synthesis of some amino acids under low light stress and nitrogen limited condition may be related to loss of photosynthetic activity under low light intensities (Salomon *et al*. 2013). However, the role of the amino acids accumulated during light stress and nitrogen limited-condition is presently not known for any microalgae (Chia *et al.* 2015).

6.5.7 Temperature and irradiance versus accessory pigments

Chl *a* specific absorption coefficient (a^{Chl}) is used widely as the fundamental index of light absorption by phytoplankton pigments. a^{Chl} varied in response to varying temperatures and irradiances due to changes in package effect and the relative proportion of chl *a* and accessory pigments (Bricaud *et al*. 1988). The package effect is used to describe the decrease of the absorption coefficient of pigments in a cell compared to the absorption potential for the same amount of pigment in solution (Geider & Osborne 1987; Kirk 1976).

a^{Chl} was higher at low irradiance than at high irradiance regardless temperature or a^{Chl} was the highest at low growth rate. This observation was consistent with a previous study of *T. pseudonana* (Stramski *et al*. 2002) and marine chlorophyte *Dunaliella teriolecta* (Sosik & Mitchell 1994) under nitrogen limitation. Changes in pigment composition are associated with specific absorption at the blue chl *a* peak because absorption spectra of chl *a* and accessory pigments are overlapped in this region (Sosik & Mitchell 1994). The response of the various accessory pigments to temperature and irradiance of cell grown under N-limitation leads to increase of a^{Chl} at low growth rate.

Fucoxanthin (as light harvesting pigment) increased but DD+DT (as photoprotective pigment) to chl *a* ratio decreased with increasing temperature under high light. Additionally, the ratio of total accessory pigments to chl *a* was higher at low temperature (14^{o}C) than at high temperature (22^{o}C), indicating the capacity of cell balance between energy trapped by temperature-insensitive photochemical reactions (called energy source) and the energy utilized through

temperature-dependent metabolism, development, and growth (called energy sinks) (Ensminger *et al.* 2006; Hüner *et al*. 2013). This result, together with previous chl *a* analyses showing that changes of light harvesting pigment and photoprotective pigment reflects the ability of this diatom to tolerate with low or high temperature and irradiance. Similarly, Anning *et al.* (2001) mentioned that temperature affected changes in excitation pressure of photosynthesis in diatom *Chaetoceros calcitrans.* The increase of photoprotective pigments are associated with light-harvesting pigment at lower temperature that may protect an excess of excitation energy from reaction centre. In another study, Maxwell *et al.* (1994) examined effect of two different temperatures on pigment of green alga *Chlorella vulgaris*. The photoprotective pigments at low temperature (5^{o}C) were higher than at high temperature (27^{o}C).

6.5.8 Temperature and irradiance versus photosynthesis rate

The Chl *a*-specific light saturated rate of photosynthesis rate (P_m^{Chl}) increased with increased temperature. The positive correlation between P_m^{Chl} and temperature is consistent with observations in diatom *Leptocylindrus danicus* grown under nitrogen-replete medium *(*Verity 1981) and in *Amphora* cf. *coffeaeformis* grown in nitrogen-sufficient condition (Salleh & McMinn 2011). The cell-specific light saturated rate of photosynthesis (P_m^{Cell}) also increased with increased temperature. This finding is consistent with the results in *Chaetoceros calcitrans* grown under nitrogen-replete medium (Anning *et al*. 2001). Increases of P_m^{Chl} and E_k values at high temperature are likely to have resulted from increased Rubisco activity when cells were shifted to a higher temperature as the rates of light-saturated photosynthesis are often controlled by the activity of Calvin cycle enzyes (Kuebler *et al.* 1991). These phenomena probably may be regulated by temperature (Oquist, 1983; Raven & Geider, 1988).

The decrease of slope (α) when cells were placed at high temperatures may result from damage of photosynthetic apparatus as indicated by the declines in the effective quantum yield that was observed in *C. sublittoralis* (Salleh & McMinn 2011).

The P_m^{Chl} increased when cells were grown at high irradiance. This change could result from the reduction of intracellular chl *a* at high temperature and light intensity. This finding is the same result as was found in *Skeletonema costatum* grown under nitrogen-sufficient condition and different irradiance (Anning *et al.* 2000). Conversely, the low P_m^{Cell} observed at high irradiance. This observation is paralleled with nitrogen, suggesting that cell may lose the potential to carry out high rate of photosynthesis at nitrogen limitation condition (Osborne & Geider 1986). Cells at lower irradiance have higher rate photosynthesis than at higher irradiance. This may be associated with the increase of intracellular carbon at low irradiance and Rubisco activity may shift in control of light-saturated photosynthesis and mimic the marine diatom *Skeletonema costatum* grown under nitrogen-replete medium that was observed by Anning *et al.* (2000).

6.5.9 Temperature and irradiance versus fatty acid profile

Five predominant fatty acids (C14:0, C16:0, C16:1, C20:5n, and C22:6n) were found in *T. weissflogii*. Similarly, Siegenthaler & Murata (2006) reported that the main fatty acids are often found in glycerolipids of chloroplast of marine algae, namely, α-linolenic acid (C18:3), palmitic (C16:0), eicosapentaenoic acid (EPA, C20:5) and docosahexaenoic acid (DHA, C22:6). Moreover, the C14:0, C16:0, C16:1, and C20:5 were major components of the marine oleaginous diatom *Fistulifera* sp. strain JPCC DA0580 grown under both nutrient-deficient and nutrient-sufficient conditions (Liang *et al*. 2013), and of marine diatom *Phaeodactylum tricornutum* and *Chaetoceros* sp. grown under nitrogen-limited condition (Reitan *et al.* 1994). However, the distribution of fatty acid contents in diatoms depends on specific species and growth environmental conditions.

Total fatty acid increased with increased temperature in N-limited *T. weissflogii*. Similarly, *Dunaliella salina* grown in N-depleted medium gave lipid content that was 78% more than the N-replete samples at 26^{o}C, while the differential for 16^{o}C was 28% (Liu *et al.* 2013). This may be indicated that a temperature-dependent enzymatic reactions (eg. RUBISCO) at low temperature are lower than those at high temperatures.

The increase in percentage SFA and MUFA levels and the decrease of PUFA levels with decreased temperature observed in *T. weissflogii* is in accordance with the results of Hoffmann *et al*. (2010) who examined SFA and MUFA of chlorophyte *Nannochloropsis salina* grown in the different nitrate concentrations (75-1800 µmol L^{-1} NO_3^-) and temperatures (17-26^{o}C). Nitrogen limitation might be lead to excess accumulation of electrons in the electron transport chain (ETC) generated by the light driven photosystems (Hoffmann *et al.* 2010). This accumulation stimulates an overproduction of reaction oxygen species (ROS) (Alscher *et al*. 1997) which negatively influence both membrane lipids and photosynthesis (Huner *et al.* 1996). The synthesis of long-chain (C18) fatty acid requires nicotinamide adenine dinucleotide phosphate (NADPH) as a reducing agent approximately 24 molecules which are higher than protein and carbohydrate synthesis (Hu *et al.* 2008). This is indicated that fatty acid synthesis results in a relaxation of an overreduced ETC (Rabbani *et al*. 1998; Mendoza *et al.* 1999; Hofmann *et al.* 2010) which may occur under nitrate limitation.

In this investigation, total fatty acid content increased with increased irradiance, consistent with results from Gonçalves *et al*. (2013) who observed the effect of light intensities (36, 72, 96, and 126 µmol photons m^{-2} s^{-1}) on the cultures of the chlorophytes *Chlorella vulgaris* and *Pseudokirchneriella subcapitata* grown under N-limitation, and from Solovchenko *et al*. (2008) who found the influence of light intensities (35, 200 and 400 µmol photons m^{-2} s^{-1}) on the unicellular freshwater chlorophyte *Parietochloris incisa* under nitrogen limitation. The higher lipid content under high irradiance may result from the storage of excessive light energy into

chemical energy as fatty acid to avoid photooxidative cell damage (Niyogi 1999; Solovchenko *et al*. 2008).

The results showed that EPA (C20:5) and DHA (C22:6) increased with increased irradiance. The increase of PUFAs at high light under nitrogen limitation probably related to reaction centre protein like D1/D2 (in PSII) into the thylakoid membrane and light harvesting protein complexes. Nitrogen-insufficient conditions may disrupt the assimilation of the chloroplast membrane and photosynthesis because cells were not capable to counteract the decreased chl *a* and protein inside the thylakoid membrane (Mock & Kroon 2002). Therefore, PUFAs play important role for the maintenance of photosynthetic membrane function (Klyachko-Gurvich *et al*. 1999). These regulating mechanisms are probably used to establish membrane integrity and consequently active photosynthesis in algae or higher plants or sea ice diatoms (Mock & Kroon 2002).

Apart from effect of temperature and irradiance, the total cellular fatty acid content increased significantly from exponential to stationary stages. These results are in accordance with Schwenk *et al.* (2013) reported total fatty acids increased significantly from exponential to stationary growth phase in 19 brackish and marine microalgae. Thus, *T. weissflogii* is known to produce the nutritionally important PUFAs: EPA and DHA for aquaculture or fish diet. The increased production of PUFAs in presence of stationary phase might add to the economic utility of this algal strain.

6.6 Conclusions

- By growing the marine diatom *Thalassiosira weissflogii* in nitrogen-limited condition under different temperatures and irradiances, it was possible to generate cells which were different in their elemental and biochemical composition.
- Cellular elemental composition varied with growth condition. Carbon content and C:N ratio were higher in cells with a reduced growth rate at low irradiance regardless of temperature.
- The change of environmental conditons led to small cell size and high cell density of *T. weissflogii* grown at high radiance. This is implications on its ability to absorb nutrients quickly enough to feed itself for survival.
- *T. weissflogii* acclimated to irradiance successfully through changes in the intracellular chlorophyll *a* content and provided the high photoprotective pigments content at high irradiance.
- Amino acid concentration is maintained at different levels during the different environmental conditions. This would be of importance to know the right condition of culturing the algae. Moreover, algal amino acid containing essential and non-essential amino acid for humans and animals could be useful in pharmaceutical industry.
- High neutral lipid, PUFAs, and lipid productivity (mg L^{-1} day^{-1}) were observed when cells were grown at high light and low temperature. This indicates that cells need to produce substances (or secondary metabolites) to increase its chance of survival under these conditions and suggests that *T. weissflogii* was able to adapt to temperature and irradiance tested.
- The temperature and irradiance affected the RNA content, whereas irradiance only affected the RNA:protein. Therefore, the relationship between growth rate and the RNA:protein supported the growth rate hypothesis under variable irradiance; however, that was not the case under variable temperature. In the same way, irradiance only affected the C:chl. The relationship between growth rate and the C:chl supported the

bio-optical hypothesis under variable irradiance; however, not under variable temperature.

Chapter 7: The effect of dilution rate on growth rate of diatom *Thalassiosira weissflogii* CCMP 1056

7.1 Introduction

Diatoms are unicellular or colonial eukaryotes mainly surrounded by an amorphous silica cell wall called a frustule. They are capable of converting solar energy to chemical energy via photosynthesis. Diatoms, like other microalgae, produce numerous metabolites including natural pigments (Pennington *et al*., 1988; Bertrand 2010; Xia *et al*. 2013), polyunsaturated fatty acids (Tonon *et al*. 2002; Wen & Chen 2003; Jiang & Gao 2004; Chautona *et al*. 2015), biopolymers (Hoagland *et al*. 1993; Wolfstein & Stal 2002; Underwood & Paterson 2003), and bioactive compounds (Mimouni *et al*. 2012; Raposo *et al*. 2013a,b). Those and other high-value chemicals are important sources that can be used in commercial and industrial applications such as pharmaceutical, food, fuel, and aquaculture products (Pulz & Gross 2004).

The technique of algal culture plays a key role in determining the yield and composition of biomass. The semi-continuous technique involves supplying fresh medium to a culture at intervals to compensate for the withdrawal of culture from the bioreactor during the operational period (Yamanè & Shimizu 1984). The aim of semi-continuous culture is to maintain maximum growth rate during the exponential phase for maximum production. The semi-continuous system was used to grow the marine diatom *Skeletonema costatum* for amino acid and glucan production at different pH values from 6.5 to 9.0 (Taraldsvik & Myklestad 2000). Additionally, diatom *Thalassiosila pseudonana* grown in semi-continuous culture allowed a high nutritional production value, at lower operating costs (Vásquez-Suárez *et al*. 2013). In marine diatom, *Phaeodactylum tricornutum* grown at nutrient-sufficient condition also gave a stable chlorophyll *a* to carbon ratio under semi-continuous culture (Otero *et al*. 1998). Moreover, cyanobacteria *Spirulina platensis* maintained under a semi-continuous cultivation gave a high growth rate and high productivity that was two to four times higher than those obtained in batch cultivation (Reichert *et al*. 2006).

Dilution rate is one of the key variables in the operation of continuous and fed-batch cultures. Dilution rate is defined as the volumetric flow rate of replaced medium divided by the volume of the culture (Eq.1)

$$D\ \%\ = \left(\frac{F}{V}\right) X\ 100 \qquad (1)$$

Where: D is dilution rate (day^{-1}), F is the volumetric flow rate of nutrient (litre day^{-1}), and V is volume of the culture (litre).

Dilution rate is one of the key variables in the operation of microalgal cultures. Microalgae grown under the high load of nutrient lead to fast growth rate. In contrast, microalgae have slow growth rate when cells grown under low nutrient. *T. weissflogii* can typically flow with the currents which might contain low or high nutrients. To understanding the elemental and biochemical composition of *T. weissflogii* under different nutrient concentration, the examination of effect of dilution rate in the cultures was set in a laboratory. Most studies have showed the accumulation of various chemicals in diatoms changes when the environment is modified. Therefore, the aim of this study was to examine the effect of the dilution rate on the growth rate and high-value chemicals of diatom *T. weissflogii* in a semi-continuous culture.

7.2 Operating conditions and sampling

Thalassiosira weissflogii CCMP 1051 was grown in 2 litre pyrex vessels with 1.8 litre working volume in artificial seawater (Berges *et al*. 2001) enriched to f/2 plus silicate (Guillard & Ryther 1962) medium, with 3 mM $NaHCO_3$ and 1 nM Na_2SeO_3. Cells in exponential phase were used to inoculate semi-continuous cultures that were grown into nutrient limitation in medium containing 20 µM NaH_2PO_4, 200 µM $NaNO_3$, f/8 metals, and f/4 vitamins. Triplicate cultures were incubated at temperatures of 26°C and photosynthetic photon flux densities of 500 ± 10 µmol photons m^{-2} s^{-1} on a 14:10 h light:dark cycle. The semi-continuous process was started after cultures reached late exponential phase of growth. At this time, 540 mL medium was removed and the same volume of fresh sterile medium was fed into the culture every day to maintain at a dilution rate of 30% day^{-1}. Similarly, to achieve a dilution rate of 60% day^{-1}, 1,080 mL sterile medium was replaced every day. The cultures were gently stirred with a magnetic stir bar and continuously aerated with filtered air through a 0.22 µm membrane filter.

Samples were collected from each of the three replicate cultures on three occasions during the exponential phase and then the culture was allowed to grow without feeding into stationary phase (day 7). Cell abundance was determined daily using a haemocytometer. Samples during the exponential phase were collected to measure particulate phosphorus (PP), nitrogen (PN), organic carbon (POC), and protein. While carbohydrate, neutral lipid, pigments, and fatty acid profiles were determined both the exponential and stationary phases. Elemental (PP, PN, POC) and biochemical (carbohydrate, neutral lipid, protein, fatty acid) composition were measured using the methods described in chapter 2.

7.3 Statistical analysis

Statistical analysis was performed using Statistical Package for the Social Sciences (SPSS version 19). A paired sample student t-test was performed for pair-wise comparison, while an analysis of variance (ANOVA) with the post hoc test (Tukey HSD) used for multiple comparisons.

7.3 Results

7.3.1 Cell density and growth rate

The effect of dilution rate on the biomass of *T. weissflogii* grown under the exponential phase culture is shown in Fig. 7-1. In the triplicate cultures at a dilution rate of 30% day^{-1}, cells increased during the first 3 days and became constant, with a density of 21 $x10^4 \pm 6 \times 10^3$ (mean ± SE) cells mL^{-1} during the exponential phase and then gradually increased until on day 7 of the stationary phase. A similar growth pattern was observed in the cultures at a dilution rate of 60% day^{-1}; however, these showed a lower cell density ($14 x10^4 \pm 3 \times 10^3$) than in a dilution rate of 30% day^{-1}.

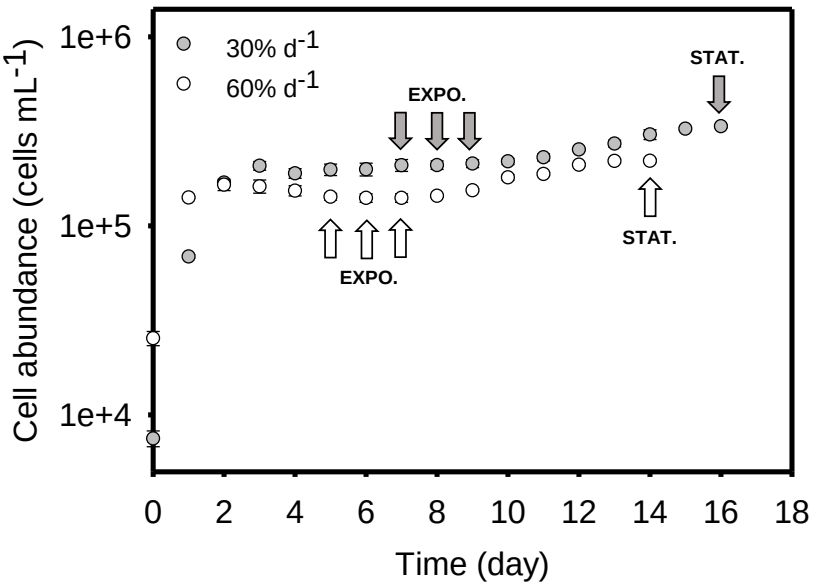

Figure 7-1. Dilution rate dependence of cell abundance of *T. weissflogii* cultures harvested during the exponential (EXPO.; n=9) and stationary (STAT.; n=3) phases. Mean values ± standard errors are shown for triplicate vessels at dilution rate 30% (grey dots) and 60% day^{-1} (white dots).

Among the harvested cells during the exponential phase culture, growth rate at a dilution rate of 60% day^{-1} was approximately 0.89 ± 0.02 (mean ± SE) day^{-1}, whereas at a dilution rate of 30% day^{-1} the growth rate was 0.40 ± 0.1 day^{-1} (Fig. 7-2A). Intracellular chlorophyll *a* (chl *a*) content increased as dilution rate increased, following the same pattern as growth rate (Fig. 7-2B). Intracellular chl *a* at a dilution rate of 60% day^{-1} was significantly higher than at a dilution rate of 30% day^{-1} ($p<0.01$).

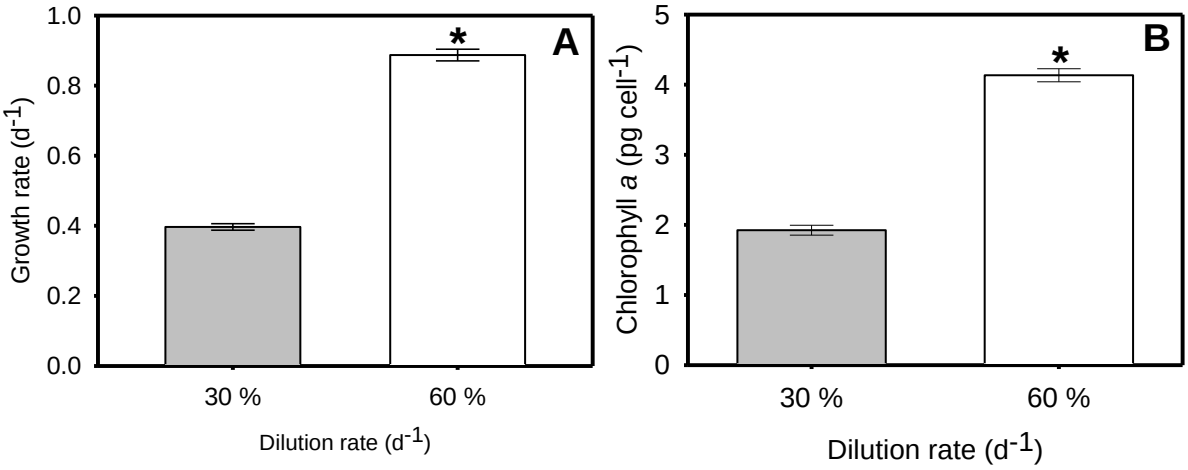

Figure 7-2. Dilution rate dependence of growth rate (A) and intracellular chlorophyll *a* content (B) in *T. weissflogii* harvested under the exponential phase. Mean values ± standard errors (n = 9) are shown for triplicate vessels at dilution rate 30% (grey bar) and 60% day^{-1} (white bar). The asterisks indicate statistical significance (Student's t-test; $p<0.01$).

7.3.2 The particulate phosphorus (PP), nitrogen (PN), and organic carbon (POC)

The impact of dilution rate on cellular PP, PN, and POC contents was significant. Cells grown at a dilution rate of 60% day^{-1} had the highest POP content roughly 2.80 ± 0.04 pg $cell^{-1}$. Cellular PP content was approximately two-fold lower at a dilution rate of 30% day^{-1} (Fig. 7-3A).

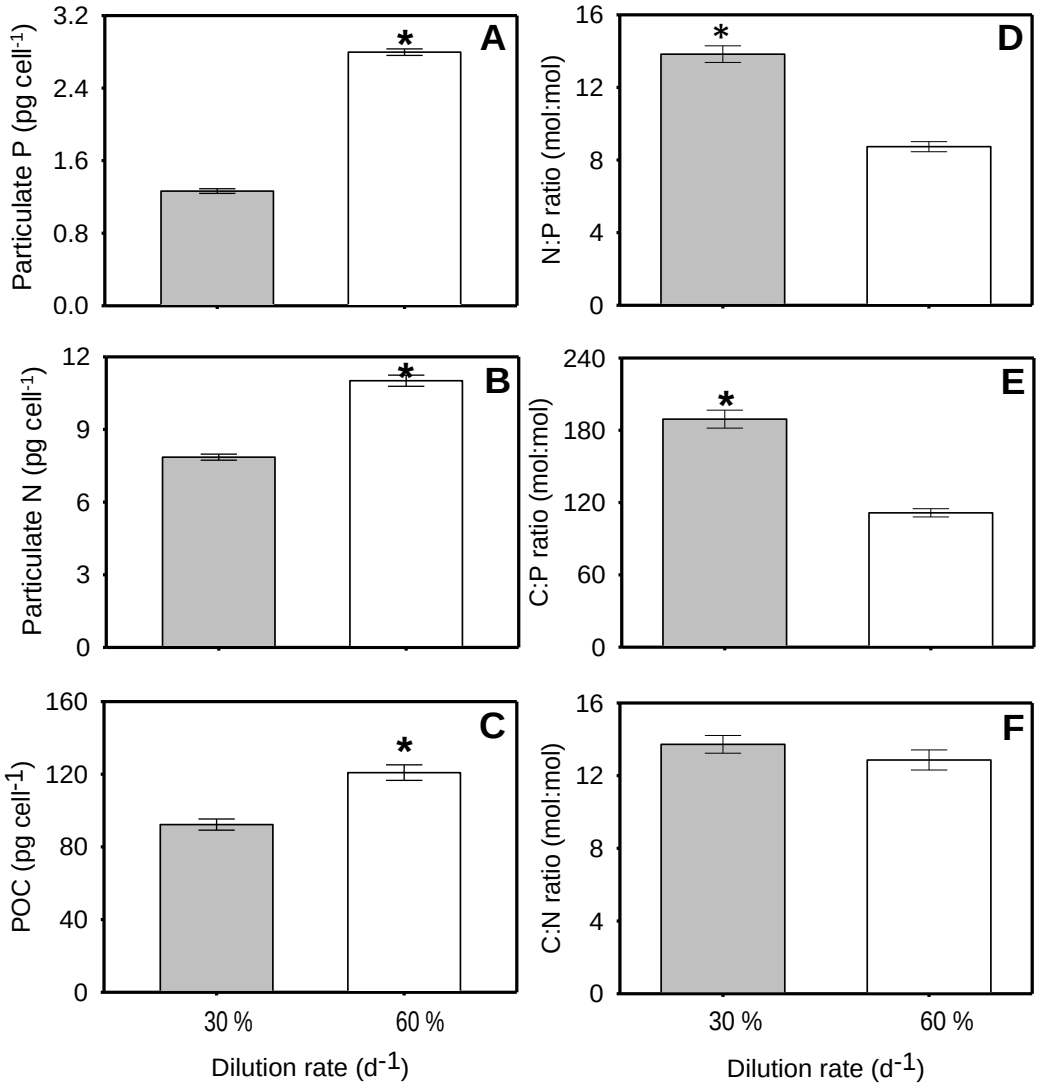

Figure 7-3. Dilution rate dependence of particulate P (A), N (B), and organic carbon (C) in *T. weissflogii.* Mean values ± standard errors are shown for triplicate vessels at dilution rate 30% (grey bar) and 60% day^{-1} (white bar). The asterisks indicate statistical significance (Student's t-test; $p<0.01$).

Similarly, cellular PN and POC contents at a dilution rate of 60% day^{-1} were significantly higher than at a dilution rate of 30% day^{-1} at $p<0.01$ (Fig. 7-3B,C). The N:P ratios were 14 and 9 at a dilution rate of 30% and 60% day^{-1} respectively (Fig. 7-4D). The C:N:P ratios were different,

respectively 189:14:1 and 111:9:1, at a dilution rate of 30% and 60% day^{-1} (Fig. 7-4E) but the C:N were not significantly different (Fig. 7-4F).

The C:chl *a* ratio decreased with elevated dilution rate while the C:chl *a* was negatively correlated with the growth rate (Figs. 7-4A,B). The C:chl *a* ratio at a dilution rate of 30% day^{-1} was approximately 48 g C (g Chl *a*)$^{-1}$, whereas at a dilution rate of 60% day^{-1} the C:chl *a* ratio was 29.

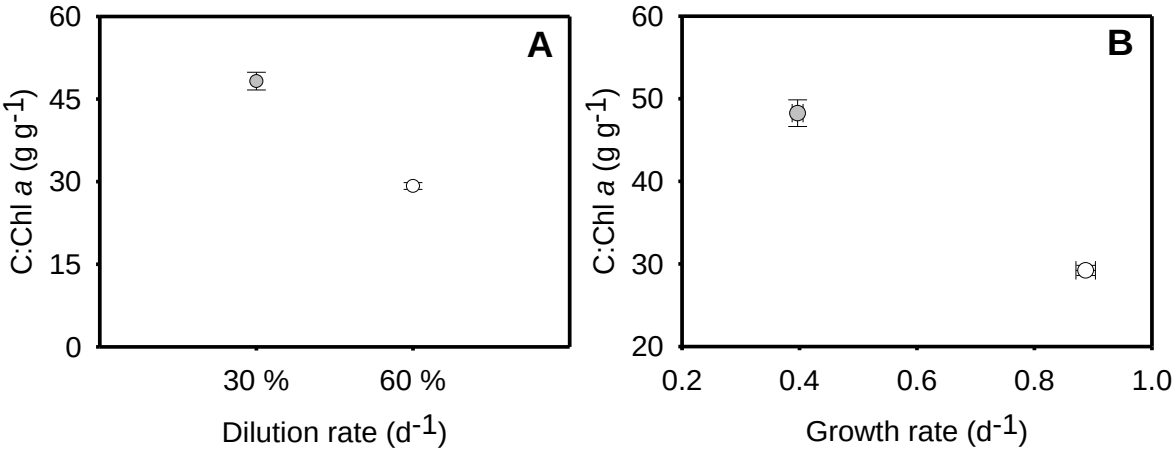

Figure 7-4. Dilution rate dependence of the C:chl *a* ratio (A) and relationship of growth rate and C:chl *a* ratio (B) in *T. weissflogii.* Mean values ± standard errors are shown for triplicate vessels at dilution rate 30% (grey bar) and 60% day^{-1} (white bar).

7.3.3 Protein, carbohydrate, and neutral lipid

The cellular protein content, determined during the exponential phase, was significantly higher at a dilution rate of 30% day^{-1} than of 60% day^{-1} (Fig. 7-5A). The cellular carbohydrate content, determined during the exponential and stationary growth phases, was higher at a dilution rate of 30% day^{-1} than of 60% day^{-1} (Fig. 7-5B). The carbohydrate content at a daily dilution rate of 30% day^{-1} was significantly lower in the exponential phase than at the stationary phase, while that the opposite response ($p<0.01$) was observed at a dilution rate of 60% day^{-1}.

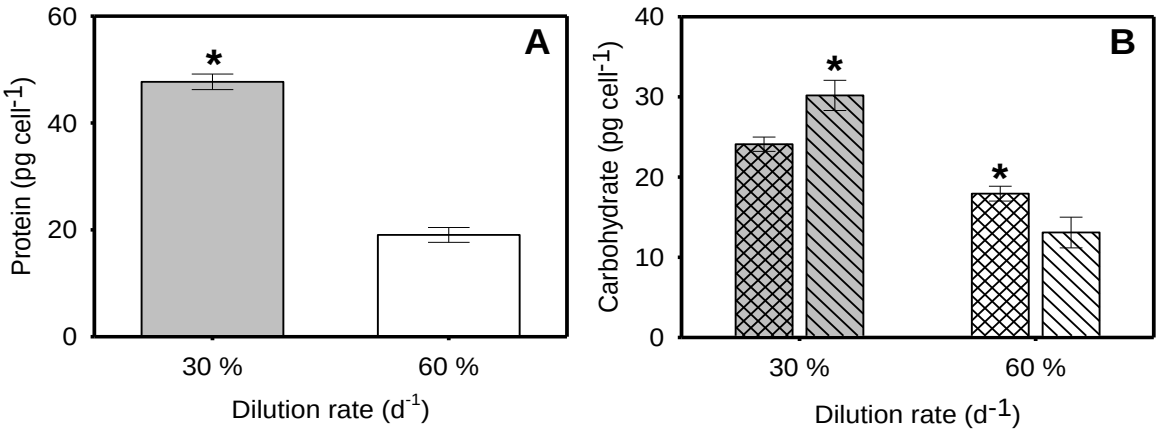

Figure 7-5. Dilution rate dependence of protein and carbohydrate contents in *T. weissflogii* harvested under exponential (▩) and stationary phases (▨). Mean values ± standard errors are shown for triplicate vessels at dilution rate 30% (grey bar) and 60% day^{-1} (white bar). The asterisks indicate statistical significance (Student's t-test; $p<0.01$).

Cellular neutral lipid content assessed using Nile red staining method was not significantly different at dilution rates of 30% and 60% day^{-1} during the exponential phase (Fig. 7-6). Although the neutral lipid content at a dilution rate of 30% day^{-1} (6.59 ± 0.58 pg cell^{-1}) was slightly higher than at that of 60% (5.31 ± 0.55 pg cell^{-1}), the difference was not significant. Neutral lipid content gradually increased from the exponential to the stationary phase. The neutral lipid content during the stationary phase increased at a greater extent in cultures previously maintained at a dilution rate of 30% day^{-1} than in the cultures maintained at a dilution rate of 60% day^{-1}.

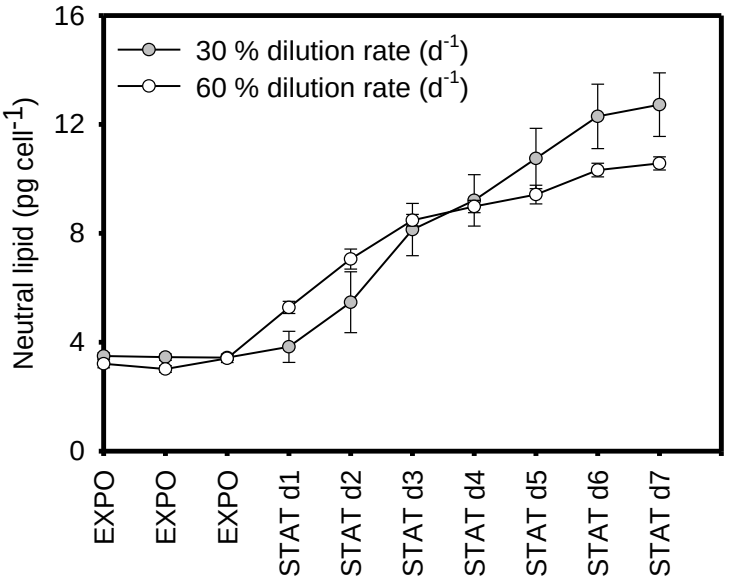

Figure 7-6. Dilution rate dependence of neutral lipid of *T. weissflogii* harvested at exponential (EXPO.; n=9) and stationary (STAT.; n=9) phases. Mean values ± standard errors are shown for of triplicate vessels at dilution rate 30% (grey dots) and 60% day^{-1} (white dots).

7.3.4 DNA and RNA

Cellular DNA and RNA contents increased significantly with a higher dilution rate ($p<0.01$). At dilution rate 60% day^{-1} DNA content was about 2.5 times higher than that found at dilution rate 30% day^{-1} (Fig. 7-7A) , whereas RNA content tripled from at a dilution rate of 60% day^{-1} (Fig. 7-7B). The difference in RNA:DNA ratios between dilution rates of 30% and 60% day^{-1} were also significant at $p< 0.05$ (Fig. 7-7C). The ratio RNA:protein increased with the growth rate (Fig. 7-8).

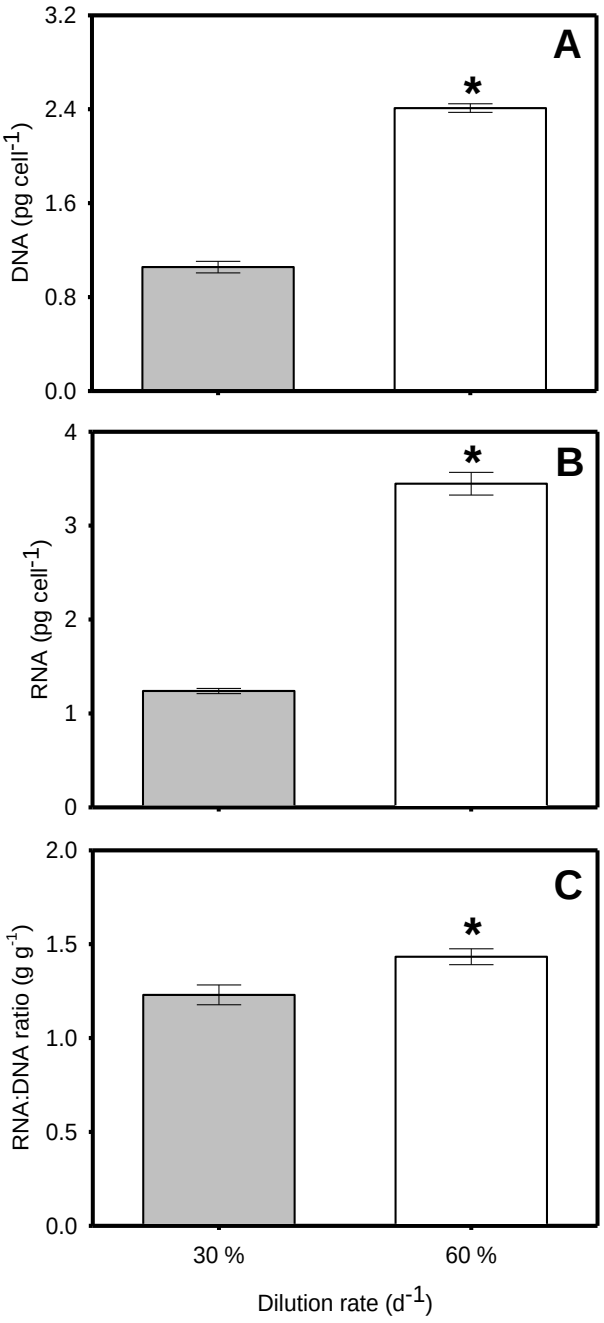

Figure 7-7. Dilution rate dependence of DNA, RNA contents, and the RNA:DNA ratio in *T. weissflogii.* Values are mean ± standard errors for three replicate vessels (n = 6) at dilution rate 30% (grey bar) and 60% day^{-1} (white bar). The asterisks indicate statistical significance (Student's t-test; $p<0.01$).

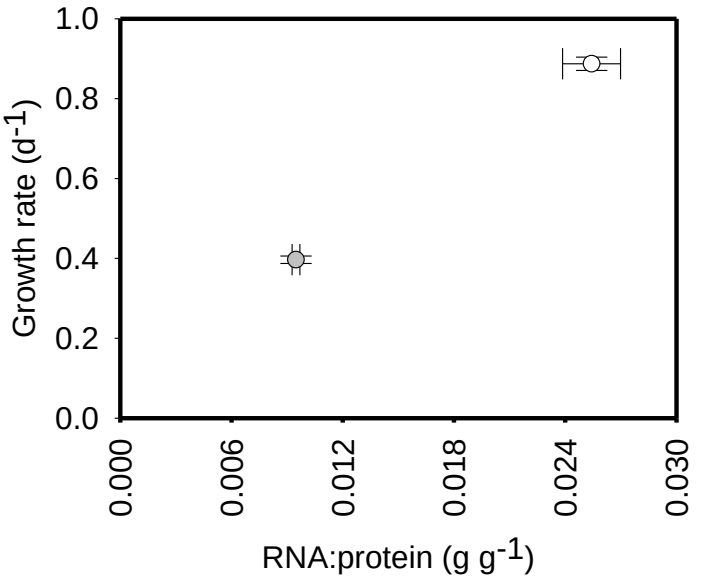

Figure 7-8. Growth rate dependence of the RNA:protein ratio in *T. weissflogii.* Mean values ± standard errors are shown for triplicate vessels (n=6) at dilution rate 30% (grey dot) and 60% day^{-1} (white dot).

7.3.5 Pigments

Five accessory pigments (beta carotene, chlorophyll *c*, diatoxanthin, diadinoxanthin, and fucoxanthin), in addition to chlorophyll *a*, were found in cells incubated at both dilution rates. As expected, the ratios of these accessory pigments to chl *a* were significantly higher during the stationary phase than the exponential phase in both the dilution rates of 30% and 60% day^{-1} (Table 7-1). In addition, the ratios of the main pigment components to chl *a* at dilution rate 60% day^{-1} were lower than at dilution rate 30% day^{-1}. The ratio of xanthophyll cycle pigment (diatoxanthin and diadinoxanthin) to chl *a* and to fucoxanthin increased during the stationary phase. The ratios of diatoxanthin to xanthophyll cycle were similar under the exponential phase of different dilution rates.

Table 7-1. Pigment composition (mol mol chl a^{-1}) of *Thalassiosira weissflogii* grown under different dilution rates. Values are mean and standard errors (SE) for three replicate vessels, n = 6. Means with a row followed by the same letter are not significantly different (two way ANOVA Tukey's test; p< 0.05).

Pigments (mol mol chl a^{-1})	Dilution rate (day^{-1})							
	0.3				0.6			
	EXPO.		STAT.		EXPO.		STAT.	
	Mean	SE	Mean	SE	Mean	SE	Mean	SE
Beta C	0.01^{A}	0.00	0.05^{D}	0.00	0.03^{B}	0.00	0.04^{C}	0.00
DT	0.19^{B}	0.04	0.04^{A}	0.16	0.07^{C}	0.00	0.86^{D}	0.02
DD	0.83^{B}	0.30	3.45^{D}	0.14	0.31^{A}	0.01	1.67^{C}	0.03
Chl *c*	0.30^{B}	0.02	0.70^{D}	0.02	0.11^{A}	0.01	0.43^{C}	0.01
Fuco	0.85^{B}	0.02	4.24^{D}	0.23	0.68^{A}	0.01	2.92^{C}	0.05
Chl *c*/Fuco	0.35^{B}	0.02	0.16^{A}	0.02	0.17^{A}	0.01	0.15^{A}	0.01
(DD+DT)/Chl *a*	1.02^{A}	0.04	6.43^{C}	0.02	0.38^{B}	0.01	2.53^{D}	0.02
(DD+DT)/Fuco	1.21^{C}	0.04	1.52^{D}	0.02	0.56^{A}	0.01	0.87^{B}	0.01
DT/(DD+DT)	0.19^{A}	0.03	0.46^{C}	0.02	0.18^{A}	0.01	0.34^{B}	0.02

Beta C: Beta carotene, DT: Diatoxanthin, DD: Diadinoxanthin, Chl *c*: Chlorophyll *c*, and Fuco: Fucoxanthin.

7.3.6 Fatty acid profile

The fatty acid compositions of *T. weissflogii* under different growth conditions are shown in Table 7-2. Total fatty acid content (pg $cell^{-1}$) were three higher during the stationary growth phase than during the exponential growth phase at dilution rate 30 % day^{-1}. Although 31 fatty acids were detected, most of these contribute to <1 % to the total fatty acid (Table 7-3). The six most abundant fatty acids were myristic acid (C14:0; 6.54-9.21% of total), pentadecanoic acid (C15:0; 1.93-2.97 % of the total), palmitic acid (C16:0; 17.58-21.61 % of the total), palmitoleic acid (C16:1; 26.84-43.79 % of the total), eicosapentanoic acid (C20:5; 12.88-26.82 % of the total) and docosahexaenoic acid (C22:6; 2.95-8.41 % of the total). Of these six fatty acids, there were no significant changes only in pentadecanoic acid during exponential growth phase at

dilution rate 30 % and 60 % day^{-1}. The biggest change was observed for palmitoleic acid which was 20.95 % and 38.70 % higher during the stationary growth phase than during the exponential growth phase stage at dilution rate 30% and 60 % day^{-1} respectively.

Eicosapentanoic acid (EPA) during exponential growth phase gave 24-27 % fatty acid; however, there was no significant change in fatty acid content in exponential growth phase in both dilution rates 30% and 60 % day^{-1}. Meanwhile, docosahexaenoic acid (DHA) during exponential phase gave 7-8 % fatty acid. The long-chain fatty acids EPA and DHA during the stationary phase had lower % fatty acid content than the exponential phase at both dilution rates.

The total monounsaturated fatty acids (MUFA) from exponential phase to stationary phases increased by 20 % (from 35.41 to 44.25 % total MUFA) and 36 % (from 29.79 to 46.86 % total MUFA) at dilution rate 30% and 60% day^{-1} respectively. Total saturated fatty acid (SFA) contents were similar in both growth phases and dilution rates. Polyunsaturated fatty acid (PUFA) dropped from the exponential phase to the stationary phase in both dilution rates of 30% and 60% day^{-1}.

Table 7-2. Fatty acid composition (pg cell^{-1}) for *Thalassiosira weissflogii* grown under different dilution rates. Shown in bold face are the most abundant fatty acids. Values are mean and standard errors (SE) for three replicate vessels. Means with a row followed by the same letter are not significantly different (two way ANOVA Tukey's test; $p < 0.05$). Values shown in bold face are the most abundant fatty acids.

Fatty acid (pg cell^{-1})	Dilution rate (day^{-1})							
	0.3				0.6			
	EXPO.		STAT.		EXPO.		STAT.	
	Mean	SE	Mean	SE	Mean	SE	Mean	SE
Lauric acid	0.01	0.00	0.00	0.00	0.00	0.00	0.01	0.00
Tridecanoic acid	ND	ND	0.05	0.02	ND	ND	0.02	0.01
Myristic acid	**1.16^{A,B}**	**0.09**	**5.07^{C}**	**0.25**	**0.86^{A}**	**0.07**	**1.37^{B}**	**0.28**
Myristoleic acid	0.03	0.00	0.09	0.01	0.02	0.00	0.05	0.00
Pentadecanoic acid	**0.40^{A}**	**0.04**	**1.64^{D}**	**0.25**	**0.22^{A,C}**	**0.02**	**0.55^{B}**	**0.06**
cis-10-Pentadecenoic acid	0.07	0.00	0.23	0.03	0.04	0.00	0.09	0.01
Palmitic acid	**3.23^{B}**	**0.22**	**11.91^{C}**	**0.63**	**2.04^{A}**	**0.34**	**3.96^{B}**	**0.24**
Palmitoleic acid	**5.79^{B}**	**0.28**	**23.21^{D}**	**0.78**	**3.12^{A}**	**0.15**	**9.19^{C}**	**0.32**
cis-10-Heptadecenoic acid	0.04	0.00	0.11	0.01	0.03	0.00	0.05	0.01
Stearic acid	0.09	0.01	0.24	0.02	0.06	0.00	0.14	0.01
Elaidic acid	0.17	0.02	0.40	0.04	0.10	0.01	0.27	0.03
Oleic acid	0.14	0.01	0.35	0.04	0.09	0.01	0.25	0.03
Linolelaidic acid	0.00	0.00	0.11	0.01	0.02	0.01	0.05	0.00
Linoleic Acid	0.18	0.01	0.37	0.04	0.17	0.01	0.25	0.02
gamma-Linolenic acid	0.20	0.01	0.39	0.04	0.15	0.01	0.26	0.02
Arachidic acid	0.03	0.00	0.09	0.01	0.03	0.00	0.04	0.00
Linolenic acid	0.05	0.00	0.11	0.01	0.06	0.01	0.09	0.01
Eicosenoic acid	ND	ND	0.03	0.02	0.01	0.01	ND	ND
Heneicosanoic acid	0.02	0.00	0.06	0.00	0.03	0.00	0.03	0.00
cis-11,14-Eicosadienoic acid	0.08	0.00	0.10	0.02	0.05	0.01	0.08	0.04
cis-8,11,14-Eicosatrienoic acid	0.09	0.00	0.28	0.02	0.08	0.00	0.16	0.01
Behenic acid	0.04	0.00	0.10	0.01	0.04	0.00	0.05	0.00
cis-11,14,17-Eicosatrienoic acid	0.04	0.01	0.11	0.01	0.04	0.01	0.06	0.00
cis-5,8,11,14-Eicosatetraenoic acid	0.10	0.02	0.45	0.03	0.09	0.02	0.26	0.02
Erucic acid	0.02	0.01	0.12	0.01	0.04	0.01	0.03	0.01
Tricosanoic acid	0.01	0.01	0.07	0.01	0.03	0.00	0.04	0.00
cis-13,16-Docosadienoic acid	0.00	0.00	0.06	0.00	0.00	0.00	ND	ND
cis-5,8,11,14,17-Eicosapentaenoic acid	**4.20^{C}**	**0.20**	**7.58^{D}**	**0.62**	**3.12^{B}**	**0.15**	**2.70^{A}**	**0.14**
Lignoceric acid	0.03	0.00	0.05	0.00	0.02	0.00	0.03	0.00
Nervonic acid	ND	ND	0.10	0.02	0.06	0.01	0.04	0.02
4,7,10,13,16,19-Docosahexaenoic acid	**1.18^{A}**	**0.03**	**1.63^{B}**	**0.21**	**0.98A**	**0.06**	**0.84^{A}**	**0.10**
Total fatty acid (pg cell^{-1})	17.39	0.98	55.13	3.19	11.62	0.89	21.00	1.41

SFA= Saturated fatty acid; MUFA= Monounsaturated fatty acid; PUFA= Polyunsaturated fatty acid; EXPO= exponential phase (n=6); STAT= stationary phase (n=3); ND= not detected. Statistical analyses were not conducted using ANOVA on fatty acids less than 1 pg cell^{-1}.

Table 7-3. Fatty acid composition (% of total fatty acid) for *Thalassiosira weissflogii* grown under different dilution rates. Values are mean and standard errors (SE) for three replicate vessels. Means with a row followed by the same letter are not significantly different (two way ANOVA Tukey's test; $p < 0.05$). Shown in bold face are the most abundant fatty acids.

Fatty acid	Dilution rate (day^{-1})							
	0.3				0.6			
	EXPO.		STAT.		EXPO.		STAT.	
	Mean	SE	Mean	SE	Mean	SE	Mean	SE
Lauric acid	0.07	0.01	0.01	0.00	0.03	0.02	0.00	0.00
Tridecanoic acid	ND	ND	0.10	0.04	ND	ND	0.08	0.04
Myristic acid	**6.69^{A}**	**0.36**	**9.20^{B}**	**0.67**	**7.41^{A}**	**0.24**	**6.54^{A}**	**0.64**
Myristoleic acid	0.17	0.02	0.16	0.01	0.19	0.04	0.25	0.01
Pentadecanoic acid	**2.31^{A}**	**0.17**	**2.97^{A}**	**0.17**	**1.93^{A}**	**0.03**	**2.61^{A}**	**0.19**
cis-10-Pentadecenoic acid	0.38	0.01	0.42	0.06	0.39	0.01	0.44	0.03
Palmitic acid	**18.58^{A}**	**1.13**	**21.61^{A}**	**1.28**	**17.58^{A}**	**1.64**	**18.89^{A}**	**0.94**
Palmitoleic acid	**33.28^{B}**	**1.24**	**42.11^{C}**	**3.37**	**26.84^{A}**	**1.58**	**43.79^{C}**	**1.45**
cis-10-Heptadecenoic acid	0.20	0.01	0.19	0.01	0.23	0.03	0.23	0.02
Stearic acid	0.53	0.02	0.44	0.02	0.53	0.01	0.65	0.04
Elaidic acid	0.99	0.07	0.73	0.10	0.86	0.05	1.27	0.11
Oleic acid	0.80	0.04	0.63	0.08	0.75	0.03	1.21	0.14
Linolelaidic acid	0.03	0.02	0.20	0.02	0.18	0.06	0.23	0.01
Linoleic Acid	1.03	0.02	0.68	0.03	1.48	0.05	1.20	0.07
gamma-Linolenic acid	1.14	0.04	0.70	0.07	1.28	0.08	1.26	0.07
Arachidic acid	0.18	0.01	0.16	0.01	0.27	0.01	0.20	0.01
Linolenic acid	0.30	0.01	0.21	0.01	0.52	0.05	0.43	0.03
Eicosenoic acid	ND	ND	0.05	0.03	0.07	0.04	ND	ND
Heneicosanoic acid	0.12	0.02	0.11	0.01	0.24	0.01	0.17	0.00
cis-11,14-Eicosadienoic acid	0.45	0.03	0.19	0.08	0.42	0.06	0.38	0.20
cis-8,11,14-Eicosatrienoic acid	0.51	0.01	0.51	0.01	0.70	0.02	0.77	0.04
Behenic acid	0.21	0.01	0.19	0.01	0.31	0.01	0.26	0.01
cis-11,14,17-Eicosatrienoic acid	0.21	0.04	0.19	0.02	0.38	0.05	0.31	0.01
cis-5,8,11,14-Eicosatetraenoic acid	0.57	0.11	0.82	0.03	0.79	0.16	1.25	0.06
Erucic acid	0.13	0.05	0.22	0.05	0.38	0.05	0.16	0.06
Tricosanoic acid	0.06	0.03	0.13	0.03	0.28	0.01	0.20	0.01
cis-13,16-Docosadienoic acid	ND	ND	0.12	0.02	0.03	0.02	ND	ND
cis-5,8,11,14,17-Eicosapentaenoic acid	**24.14^{B}**	**0.72**	**13.75^{A}**	**3.34**	**26.82^{B}**	**0.94**	**12.88^{A}**	**0.81**
Lignoceric acid	0.15	0.01	0.08	0.01	0.20	0.01	0.16	0.03
Nervonic acid	ND	ND	0.18	0.07	0.49	0.07	0.19	0.07
4,7,10,13,16,19-Docosahexaenoic acid	**6.77^{B}**	**0.34**	**2.95^{A}**	**0.34**	**8.41^{C}**	**0.34**	**4.02^{A}**	**0.40**
Sum SFA	28.72	1.87	34.90	1.88	28.65	2.09	29.53	1.94
Sum MUFA	35.41	1.49	44.25	3.90	29.79	2.03	46.86	1.77
Sum PUFA	35.87	1.36	20.84	4.76	41.56	1.87	23.61	2.52

SFA= Saturated fatty acid; MUFA= Monounsaturated fatty acid; PUFA= Polyunsaturated fatty acid; EXPO= exponential phase (n=6); STAT= stationary phase (n=3); ND= not detected. Statistical analyses were not conducted using ANOVA on fatty acids less than 1% of total.

7.4 Discussion

7.4.1 Dilution rate versus growth rate, chl *a* and elemental composition

The effect of dilution rate on the diatom *Thalassiosira weissflogii* CCMP 1051 growth has been observed in an exponential semi-continuous culture. Cell abundance dropped significantly as the dilution rate increased, in line with the chemostat theory (Rhee 1989). The findings are consistent with the results of Chauton *et al*. (2013) who observed the biomass of diatom *Phaeodactylum tricornutum* CCMP 2561 were grown in exponential fed-batch cultures at five different dilution rates under N or P limitation. The growth rate decreased at the low dilution rate because of the depletion of nutrients in medium. Higher growth rates require a higher flow-through, i.e. more quantities of sterile medium. Moreover, the growth rate increased with the higher renewal rate in cyanobacterium *Spirulina platensis* LEB-52 that was grown during the semi-continuous culture (Reichert *et al*. 2006).

The increased dilution rate resulted in higher cellular phosphorus (P), nitrogen (N), and organic carbon (C) contents. In general, the optimal N:P ratio was suggested to be around 16:1 of the Redfield ratio; however, in this study the N:P ratios <16 that suggested phosphorus is not an inhibiting element of *T. weissflogii* growth. At both dilution rates of 30% and 60% per day^{-1}, the C:N ratios were greater than the Redfield C:N ratio of 6.6 which allows optimal growth of nutrient-replete culture (Geider & La Roche 2002). This indicats that *T. weissflogii* was maintained under a nitrogen-limited condition. The cellular chl *a* content decreased with the low dilution rate in *T. weissflogii*. This has been previously observed in *Phaeodactylum tricornutum* and *Spirulina platensis* (Chauton *et al*. 2013; Reichert *et al*. 2006). Intracellular chl *a* content followed the same pattern as the growth rate due to high-nutrient supply rate. The C:chl *a* is a sensitive indicator of algal physiological condition and the growth rate that is highly variable depending on culture conditions of microalgae (Laws & Bannister 1980; Geider 1987). This study showed a drop in the C:chl *a* ratio could result from limited nutrient and high cell density at a high dilution rate.

Both protein and carbohydrate content were significantly higher at a daily dilution rate of 30% than at a dilution rate 60% day^{-1} under the exponential phase. This indicates that the dilution of medium stimulated production of energy-rich compounds and promoted the formation of protein. It also suggests that the high carbohydrate as an energy source that is required for repair and maintenance of the damage induced by the high light (Chandrasekaran *et al*. 2014). Chen & Thornton (2015) mentioned that the total carbohydrate of *Thalassiosira wessiflogii* (CCMP 1051), which was grown at different dilution rates under N-limited semi-continuous culture, were negatively correlated with growth rate. The data in Morales-Sánchez *et al*. (2014) also showed that there was significant accumulation of lipid and carbohydrate in *Neochloris oleoabundans* (Class Chlorophyceae) grown under N limitation in heterotrophic fed-batch culture. This indicates that carbohydrate could be negatively correlated with growth rate because chl *a* and growth rate had the same pattern at different dilution rates. Those results showed the growth rate was high and the cells consumed carbohydrate as the primary product of photosynthesis to produce structure component (mainly protein).

7.4.2 Dilution rate versus DNA, RNA, and RNA:protein

DNA content of *T. weissfolgii* remained between 1 and 2 % of cellular carbon at dilution rate 30 and 60% day^{-1} respectively. This finding is similar to what Holm-Hansen (1969) said, that the DNA content in unicellular algae is equal to approximately 1% to 3 % of the cellular organic carbon. RNA and protein synthesis are closely related in the process of growth. The ratio RNA:protein may be used to determine *in situ* growth rates; however, that depends on the developmental state of studied organism (Nicklisch & Steinberg 2009). *T. weissflogii* showed a significant correlation between RNA:protein ratio and the growth rate during the exponential phase. Similarly, in the diatoms *Cyclostephanos invisitatus* and *Stephanodiscus minutulus* grown under saturated nutrients both RNA:protein and RNA:DNA were positively correlated with a specific growth rate (Nicklisch & Steinberg 2009).

7.4.3 Dilution rate versus accessory pigment

Cells showed higher amount of photoprotection pigments (diadinoxanthin, fucoxanthin) at a dilution rate of 30% per day^{-1} than of 60% per day^{-1}. This suggests that cells can cope with limited condition by generating more photoinhibition pigments. The high amount of fucoxanthin, widely present in many picoeukaryotes and phytoplankton species, was found during both exponential and stationary phases at the dilution rate 30% day^{-1} because of the captured green light; 490 - 570 nm (Di Valentin *et al*. 2012). Additionally, diadinoxanthin (epoxide-containing xanthophylls) presents at the antenna side of the photosystem I and II (Frank *et al*. 1996), which was mostly found in diatom incubated in high irradiance (Goss & Jakob 2010). Latasa (1995) stated that diadinoxanthin of *T. weissflogii* could be stimulated when the cells become harmful due to the high irradiance. This may indicate that a lower dilution rate would be best for the synthesis of xanthophyll pigments. The ratio of the xanthophyll cycle pigments to chl *a* increased at a lower dilution rate, similar to the case of diatom *Phaeodactylum tricornutum* Bohlin (CCMP 1327) grown under nutrient starvation (Geider *et al*. 1993). It is suggested that the increase of the xanthophyll pool generates strategy for quenching photo-oxidative damage. Moreover, those pigments constitute the increase dissipation of excitation energy in the pigment bed upstream from the reaction centres (Geider *et al*. 1993).

7.4.4 Dilution rate versus fatty acid profile

The main six fatty acid constituents were identified in *T. weissflogii* including palmitoleic acid, palmitic acid, myristic acid, pentadecanoic acid, eicosapentanoic acid (EPA), and docosahexaenoic acid (DHA). This result is similar to fatty acid profile found from frustules of *T. weissflogii* CCMP 1049 (Suroy *et al*. 2014). Moreover, diatom *Chaetoceros muelleri* had the same major fatty acid as in this study except arachidonic acid was replaced pentadecanoic acid (Liang *et al*. 2006). The data in Jeffryes *et al*. (2013) also showed similar results and reported that diatom *Cyclotella* sp. grown under silicon-depleted culture gave the three main fatty acids:

palmitoleic acid, palmitic acid and eicosapentanoic acid. EPA and DHA as regulators of biological functions decreased as the culture aged in this study.

The fatty acid content was higher at low dilution (30%) than high dilution rate (60%) of medium per day. The pattern of fatty acid concentration was similar to the growth rate, suggesting that the concentration of fatty acid increased with increasing growth rate. Another effect of dilution rate on *T. weissflogii* was to prolong exponential phase. This leads to the high PUFAs as nutritional value for aquatic animals. However, the content of pamitic and palmitoleic acid were higher at stationary phase (44 % of total fatty acid) than exponential phase (27 % of total fatty acid). Thus, fatty acid production of *T. weissflogii* could be an alternative source for biofuel production.

7.5 Conclusions

- The marine diatom *Thalassiosira weissflogii* was cultivated with different dilution rates during the autotrophic growth under semi-continuous conditions. Dilution rate in the present study affected the elemental and biochemical composition. A low dilution rates resulted in a higher cell density (cells mL^{-1}) of smaller cells that contained lower particulate organic carbon (POC), particulate nitrogen (PN) and particulate phosphorus (PP) contents.
- Cells grown at a low daily dilution rate of 30% per day had more high-value chemicals (pigments, lipid, and carbohydrate) than cells grown at the higher daily dilution rate of 60% per day. Fucoxanthin, an antioxidative agent, was at the highest pigment content under exponential and stationary phases. The palmitoleic acid (C16:1) was at the greatest content following palmitic acid (C16:0) and meristic (14:0) which are used in biofuels and cosmetics preparation. EPA and DHA, long-chain polysaturated fatty acids (PUFAs), are found in cells grown under both dilution rates. The advantages of exponential phase culture for PUFAs production are short duration and simple operation. This results imply that *T. weissflogii* can be a commercial source for the spontaneous production under the exponential phase with a low dilution rate.

Chapter 8: General discussion

In this chapter, the main findings with regard to the research goals are summarised and the general conclusion based on the findings of the studies presented in this thesis are described. Moreover, the experimental outcomes of the impact of biotechnological implication are considered and the suggestions for the further research into higher education are presented.

Many issues need to be considered when developing link between protocol and research. These issues can be divided into the protocol development and the method implementation for research in chapters 5, 6 and 7. One of the aims of this research is to develop and implement the protocol to obtain accurate and reliable measurement. The studies presented in this thesis were focused on the development of fluorescence-based neutral lipid content using Nile red (NR) and the development of method for determining the combined amino acid composition of microalgae using ultra performance liquid chromatography (UPLC), which were presented in chapters 3 and 4 respectively. The central aim of the studies was to studies on the effects of environmental conditions on elemental and biochemical composition of two marine microalgae. Furthermore, the effect of dilution rate, the availability of substrates, in the culture media was also considered in this thesis. The haptophyte *Emiliania huxleyi* grown under different temperatures was presented in chapter 5, whereas the diatom *Thalassiosira weissflogii* grown under the combined temperature and light was presented in chapter 6. The overarching aim of the studies was to focus on the physiological and metabolic responses of two marine microalgae. The findings of the studies reported in chapter 3 provided the optimal method for quantifying the neutral lipid in the diatom *T. weissflogii*; which was applied in chapters 6 and 7. While the studies reported in chapter 4 provided the efficient method for quantifying the combined amino acid in marine microalgae; which was used in chapters 5 and 6.

8.1 The method development for research

8.1.1 Development and application of Nile red (NR) fluorescence based method for quantification of neutral lipid content in a marine diatom

Challenges of development in staining the lipid droplets in microalgae have obstructed owing to the rigid cell wall. Accurate characterisation of neutral lipid is a crucial aspect of research in the biotechnological application such as biofuels. The efficient, fast, convenient, and reproducible method for the quantification of neutral lipid using NR in the diatom *T. weissflogii* was presented in chapter 3. In this study, the optimum of excitation wavelengths for the neutral lipid determination was 529 nm and excitation wavelengths was 589 nm. The optimal concentration of NR is 1.0 µg mL^{-1} with the dimethyl sulfoxide (DMSO) concentration of 5 % (v/v) for 5 min incubation at range of cells concentration 200,000-400,000 cells mL^{-1} in darkness at room temperature. By using DMSO as a stain carrier to assist NR penetration across the cell membrane and decrease hydrophobicity, it enhances lipid staining efficiency and increases the fluorescence intensity of stained cells (Chen *et al* 2009; Doan & Obbard 2011). To date, there are no other reports on development and improvement of neutral lipid content using NR in the diatom *T. weissflogii.* The success of the improved NR staining procedure in the diatom *T. weissflogii* suggests that this study opens a path to an intensive study on the diatom *T. weissflogii* for enhancing biomass and lipid productivity for biodiesel production and could decrease cost to achieve in commercial scale of biofuel production.

8.1.2 Development of method for determining the combined amino acid composition in microalgae

Flynn *et al.* 2010 reported that the uncertainty of the RNA:protein ratio results in the misinterpretation of data for testing the growth rate hypothesis, which predicts a correlation between growth rate and phosphorus content in microalgae. Furthermore, the measurement of protein and nucleic acids are part of problems. The determined RNA:protein ratio depends on the selected method assay and protein standard. Consequently, the RNA:protein ratio has a

tendency to be overestimated. To overcome this problem, the development of method for determining amino acids in protein of microalgae was focused. The efficient and reproducible method for the quantification of the combined amino acid composition using UPLC was presented in chapter 4. This method used 6-aminoquinolyl-N-hydroxysuccinimidyl carbamate (AQC) [AccQ·Tag method] with pre-column derivatization to provide a shorter analysis time (10 min) than conventional methods. This analysis provided better separation and sensitivity than previously existing methods. Moreover, the derivertised samples were stable up to one week in room temperature. Bovine serum albumin (BSA) was used as a representative protein standard for hydrolysis of a hydrophobic peptide bond to obtain amino acid composition. 76 % of recovery was estimated from mass detected-amino acid by hydrolysed BSA compared with mass expected-amino acid from universal protein resource (http://www.uniprot.org/uniprot/P02769). This suggests that amino acids from hydrolysed BSA and subsequent derivatisation with AccQ Tag ultra reagent provided an efficient protocol to quantify amino acids in marine microalgae samples. The sensitivity and detection limits of amino acids by using mass spectrometry detector were achieved strictly. However, 24 % losing of recovery amino acids might result in the hydrolysed sample solution was oxidised during transferring from hydrolysis to dry process. To increase more percentage of amino acid recovery, a Water Pico·Tag Workstation® which can hydrolyse and dry sample under vacuum is recommended to ensure complete deaeration.

8.2 The method implementation for research

The Nile red fluorescence based method which was developed in chapter 3 allowed better quantification of cellular neutral lipid content for *T. weissflogii* grown under different temperature and irradiance during the exponential growth and stationary growth phase in chapter 6 and for *T. weissflogii* grown under dilution rates in chapter 7. In these chapters, Nile red fluorescence intensity from stained cellular neutral lipids increased with culturing time. However, lipid content accumulation is different between each microalgal species, which depend on environment

conditions. For example, the maximum neutral lipid accumulation was acquired at day 18 in green algal *Chlorella saccharophila* under heterotrophic growth conditions (Isleten-Hosoglu *et al*. 2012), and at day 7 in dinoflagellate *Prorocentrum micans* and diatom *Phaeodactylum tricornutum* under nitrogen deprivation (Wu *et al*. 2014) which measured by Nile red fluorescence based method. Therefore, this developed method would allow researchers to know the maximum neutral lipid content with time and to determinate cultivation. Although neutral lipid accumulation of *T. weissflogii* was determined until day 7 in both chapters 6 and 7, neutral lipid content should be measured continuously for conducting future research to know the highest lipid accumulation and harvest cells for lipid extraction. This suggests that the developed method is also a faster way for future researchers searching for potential lipid producing microalgal species and can be applied for up scaling in a cost-effective way.

The method for determining the combined amino acid composition which was developed in chapter 4 allowed better quantification of *E. huxleyi* grown under different temperatures in chapter 5 and of *T. weissflogii* grown under different temperatures and irradiances in chapter 6. Seventeen amino acids were found in *E. huxleyi* and *T. weissflogii.* The combined amino acid contents of two microalgae were lesser than their protein contents which were determined using bicinchoninic acid assay (BCA) and BSA was used as a protein standard. This suggests that high protein contents from BCA assay might result from some interfering compounds which generate more BCA-Cu^{+} complex and lead to obtain more strongly chromogenic. This was found to result in an *overestimation* of the protein content. Those interfering compounds are 1) disulfide and sulfhydryl groups in protein, 2) aliphatic amines and ammonia or ammonium ion as well as 3) glucose as reducing agent from breaking cells (Smith *et al*. 1985; Lovrien & Matulis 1995 see support protocol 2). This indicates that the developed method of the combined amino acid provides accurate protein content and can solve the problems the uncertainty of the RNA:protein ratio in microalgae.

8.3 The effect of environmental conditions to the physiological and metabolic responses of marine microalgae

These developed methods were used an implementation to measure the elemental and biochemical composition of microalgae grown under different environmental conditions in chapters 5, 6 and 7. The results showed new information on a variety of adaptive response of marine microalgae. The physiological and metabolic responses are measured by elemental and biochemical processes. The main physical factors regulating microalgal cell growth and metabolic activity are temperature and irradiance. Low temperatures have an effect by decreasing enzyme activity, membrane fluidity and electron transfer in electron transport chains therefore leading to a decrease of photosynthesis and consequently in reduction of growth in microalgae. High temperatures lead to a decrease in enzyme activity as well by denaturation and degradation of some proteins which disturb function of cell membranes because of changes in their composition and physical state. High temperature may reduce the efficiency of photosynthesis especially photosystem II and decrease of ribulose-1,5-bisphosphate (Rubisco) activity.

Cells living under low light condition lead to increase light harvesting capacity and photosynthetic efficiency as well as reduce dark respiration. While cells are exposed to high light, light can stimulate the generation of excited states that can form deleterious singlet oxygen. To reduce the excitation pressure, cell will reduce the photosynthetic pigment in the cell. The interaction between temperature and light intensity can play an important role in algal growth and metabolic regulation.

Stressful conditions such as high or low temperature often in combination with high light can lead to unbalance of the energy equilibrium within a microalgal cell and an increase of excess free radicals. Apparently, at high light cellular chlorophyll *a* content of *T. weissflogii* (chapter 6) was lower than at low light. However, cells probably enhance survival by producing pigments such as beta carotene and fucoxanthin as antioxidant properties to interact with and detoxify these harmful compounds. Beta carotene and fucoxanthin content were found to increase at high temperature in *E. huxleyi* (chapter 5) while these pigments were found to increase under the combination of low temperature with low light in *T. weissflogii* (chapter 6).

Microalgae can be grown under extreme environmental conditions or unfavourable conditions. The combined temperatures and light intensity are unfavourable conditions such as high temperature with high irradiance or low temperature with high irradiance etc. resulting in changes in elemental and biochemical composition of *T. weissflogii* (chapter 6). However, in this research nutrient limitation may influence factor coexistence resulting in growth limitation. The reverse can take place; light can have secondary effects on primary product (Wynne & Rhee 1986).

To survive in non-optimal conditions, microalgae trigger stimulation and/or reduction which generate different mechanisms. For example, beta carotene as antioxidant pigment in *T. weissflogii* (chapter 6) at high light had more content than at low light. While decreasing the proportion of saturated and unsaturated fatty acids by increasing cis-double bond or shortening fatty acid chains was found in *T. weissflogii* grown at high light. The unsaturated fatty acid particularly eicosapentaenoic acid (EPA) and docosahexaenoic acid (DHA) was produced to protect or compensate substance in the cell resulting in research applications and leading to the benefits to humans in pharmaceutical industry.

8.4 The biotechnological implications

Microalgae are capable of increasing the nutrient value of the human food and animal feed, as well as pharmaceutical and cosmetic industries. The high value-compounds were obtained from this research such as amino acid, pigments, and fatty acid.

Amino acids

Seventeen amino acid components were identified from *E. huxleyi* (chapter 5) and *T. weissflogii* (chapter 6). Six essential amino acids such as histidine, lysine, methionine, valine, phenylalanine, and isoleucine found in both microalgae are important role in building block hormones, proteins for humans and animals. Lysine and methionine found in both studied microalgae were used in animal feed. Those amino acids constitute the largest share (56%) of the total amino acid market (Leuchtenberger *et al*. 2005). While three of eleven non-essential amino acids such as glutamic acid, aspartic and phenylalanine were used in food industry. Glutamic acid is a flavour enhancer of monosodium glutamate. Aspartic and phenylalanine are starting materials for the peptide sweetener (Leuchtenberger *et al*. 2005). This suggests that amino acids were found in this research could be an alternative source for serving biotechnological industry.

Pigments

Carotenoid contents were found in *E. huxleyi* and *T. weissflogii*, (in chapters 5, 6 and 7) and fucoxanthin was found in *T. weissflogii* (in chapters 6 and 7). Although both microalgae had low carotenoid content, many studies have mentioned that beta carotene and fucoxanthin are high value products because they possess properties that protect against cell damage and cancer by scavenging free radicals. Beta carotene also is a precursor that can be converted into vitamin A (Chidambara-Murthy *et al*. 2005; El Baz *et al.* 2002; Plaza *et al*. 2009). The antioxidant properties from carotenoid were claimed in nutraceutical applications resulting in the market value of carotenoids reached over US$ 1,000 million or approximately £ 630 million (Del Campo

et al. 2007). In addition, carotenoids are used in cosmetics and food products as feed additives for poultry, livestock, fish/ ornamental fish and crustaceans (Del Campo *et al*. 2007). Recently, the growing market of carotenoid has increased due to the interest of bio-produced resources instead of synthesis. Thus, it is good opportunities for microalgae to be one of the possible candidates for carotene production to reserve in many applications.

Fatty acids

T. weissflogii (in chapters 6 and 7) is rich sources of EPA (19-30 % total fatty acids) and DHA (5-10 % total fatty acids), while *E. huxleyi* (in chapter 5) gave lower EPA (3-4% total fatty acids) and DHA (6-8 % total fatty acids). Among the marine strains, the prymnesophytes as *Isochrysis galbana* and *Pavlova lutheri* gave DHA approximately 6-14% total fatty acids and EPA around 5-26% of the total fatty acids (Carvalho & Malcata 2000), whereas diatoms as *Phaeodactylum tricornutum* is rich source of EPA (26% of the total fatty acids) (Hu *et al.* 2008). This is suggested that PUFAs microalgae were species-specific. Therefore, *T. weissflogii* could have possibility to use in nutraceutical and pharmacological applications.

Nevertheless, since microalgae production is regarded high benefits, it is necessary to develop culture techniques to reach massive biomass production and high value-compounds for making biofuel feed stock, nutraceutical and pharmaceutical industries. There are some suggestions:

- Mixotrophic/heterotrophic culture

Since microalgae in this work were grown under phototrophic condition. The growth characteristics and high-value composition of microalgae are known to significantly depend on the cultivation treatments (Chen *et al*. 2011). Using organic carbon as both the energy and carbon source called heterotrophic cultivation in some microalgae which can not only grow under phototrophic conditions. While the situation when microalgae undergo photosynthesis use both organic compounds and inorganic carbon (CO_2) as a carbon source for growth called mixotrophic cultivation. Mixotrophic/heterotrophic culture can reach high biomass and could

potentially reduce the cost of biodiesel production because using industrial effluent, municipal wastewater or food-processing wastes etc. as organic substrates. For example, *Phaeodactylum tricornutum* grown in bubble columns using glycerol gave significantly higher biomass productivity than those using fructose in the fed-batch cultures Ceron-Garcia *et al.* 2013).

While mixed microalgae (Diatoms, *Scenedesmus* sp., and *Chlorella* sp.) from natural field grown under heterotrophic culture using domestic wastewater showed increase of lipid productivity.

In addition, it promoted wastewater treatment efficiency as substrate degradation and nutrient removal (Devi *et al.* 2012).

• Carbon dioxide (CO_2)

Microalgae can fix carbon dioxide from atmosphere and industrial exhaust gases e.g. flue gas; however, CO_2 in this work comes from air containing 400 parts per million (ppm) that is little concentration. CO_2 concentration is varied to depend on species. For example, *Cheatoceros muelleri* cultivated under different CO_2 aeration conditions (0.03–30%). *C. muelleri* presented the highest growth rate, the maximum biomass productivity, the highest total and neutral lipid accumulation when cell grew under 10% CO_2 aeration levels. While *Nannochloropsis oculata* grown under 2% CO_2 aeration treatment showed the maximal biomass and lipid productivity (Chiu *et al*. 2009).

• Salinity

There are variations of salinity concentrations for lipid production in microalgae. *T. weissflogii* grown under different salinities (25, 30, 35, 40, 45 and 50 psu) showed the lipid production was higher at salinities < 35 psu (García *et al*. 2012). The diatom *Nitzschia laevis* grown under high salt concentrations 10 to 20 g/L gave the degree of fatty acid unsaturation of both neutral and polar lipid fractions increased sharply. This changes is suggested that a decrease in membrane permeability and fluidity under high salt concentration. In addition, under NaCl concentration of 20 g/L this diatom obtained 71.3% of total EPA existed in polar lipid (Chen *et al*. 2008).

• Metabolic engineering

The development of homologous recombination-based gene transformation has been reported in literatures. This may potential to understanding fundamental metabolic and cellular processes and conduct to improve lipid and PUFA content. The modified genes were widely done in microalgae such as *Nannochloropsis oceanica* (Kaye *et al.* 2015), *Phaeodactylum tricornutum* (Bowler *et al.* 2008), *Chlamydomonas reinhardtii* (Merchant *et al.* 2007; Nguyen *et al.* 2013), *Thalassiosira pseudonana* (Tonon *et al.* 2005; Armbrust *et al.* 2004), *Cyanidioschyzon merolae* (Matsuzaki *et al.* 2004), *Ostreococcus tauri* (Derelle *et al.* 2006), *Ostreococcus lucimarinus* (Palenik *et al.* 2007), and *Micromonas pusilla* (Worden *et al.* 2009).

8.5 The ecological implications

E. huxleyi is one of 5,000 species of phytoplankton and is extremely ubiquitous except the polar oceans (http://www.soes.soton.ac.uk/staff/tt/). Phytoplankton are the primary producers in ocean food webs, providing both the energy and the essential biochemical components (e.g., essential amino and fatty acids) required by zooplankton, fishes and other marine animals. For example, marine microalgae are important organisms in the production of polyunsaturated fatty acids (PUFAs) in marine food chains (Guschina & Harwood 2006). Both eicosapentaenoic acid (EPA) and docosahexaenoic acid (DHA) are generally found in diatoms and dinoflagellates (Volkman *et al.* 1989; Mansour *et al*. 2005; Boelen *et al.* 2013). However, the haptophyte *E. huxleyi* cells contain more fatty acids at low temperature (chapter 5).

Stress environmental conditions have a major impact on their food nutritional value of microalgae which could have implications for food web productivity (Huertas *et al*. 2011). Temperature changes due to global warming may affect food webs by affecting nutrient supply or due to preferential grazing (Huertas *et al*. 2011). It is probable that the influence of temperature on growth of *E. huxleyi* leads to the changed in physical and chemical properties,

with the result being cells that a smaller at high temperature. While *T. weissflogii* (chapter 6) had a smaller size at high temperature and high light (26 HL). This is indicated that small cells are capable to adapt their cells to tolerate with increased temperature and it has been assumed that the climate change and global warming will benefit small-sized phytoplankton (Daufresne *et al*. 2009; Morán *et al*. 2010).

References

Emiliania huxleyi taxonomy URL
http://www.algaebase.org/search/species/detail/?species_id=51619 07.06.15

Scanning electron micrograph of *Emiliania huxleyi*
http://www.noc.soton.ac.uk/soes/staff/tt/eh/ accessed 6/04/2015

Thalassiosira weissflogii taxonomy URL
http://www.algaebase.org/search/species/detail/?species_id=32240 accessed 18/09/2015

The chemical derivitisation in analysis of amino acids
http://www.waters.com/waters/en_GB/AccQ%E2%80%A2Tag-and-Pico%E2%80%A2Tag-Methods/nav.htm?cid=1000897&locale=en_GB accessed 8/05/2015

Abdo, S. M., Ahmed, E., El-Enin, S. A., Din, R. S. E., Diwani, G. E.and Ali, G. 2014 Qualitative and quantitative determination of lipid content in microalgae for biofuel. *Journal of Algal Biomass Utilization,* **5**(3): 23-28.

Aidar, E., Gianesella-Galvão, S. M. F., Sigaud, T. C. S., Asano, C. S., Liang, T. H., Rezende, K. R. V., ... & Sandes, M. A. L. (1994). Effects of light quality on growth, biochemical composition and photo synthetic production in *Cyclotella caspia* Grunow and *Tetraselmis gracilis* (Kylin) Butcher. *Journal of Experimental Marine Biology and Ecology*, **180**(2), 175-187.

Aktar, W., Sengupta, D., & Chowdhury, A. (2009). Impact of pesticides use in agriculture: their benefits and hazards. *Interdisciplinary Toxicology*, **2**(1), 1-12.

Amaro, H. M., Guedes, A. C., & Malcata, F. X. (2011). Advances and perspectives in using microalgae to produce biodiesel. *Applied Energy*, **88**(10), 3402-3410.

Anand, J., & Arumugam, M. (2015). Enhanced lipid accumulation and biomass yield of *Scenedesmus quadricauda* under nitrogen starved condition. *Bioresource Technology*, **188**, 190-194.

Anning, T., Harris, G. & Geider, R. J. (2001). Thermal acclimation in the marine diatom *Chaetoceros calcitrans* (Bacillariophyceae). *European Journal of Phycology*, **36**, 233-241.

Anning, T., MacIntyre, H. L., Pratt, S. M., Sammes, P. J., Gibb, S., & Geider, R. J. (2000). Photoacclimation in the marine diatom *Skeletonema costatum*. *Limnology and Oceanography*, **45**(8), 1807-1817.

Araújo, S. C. & Garcia, V. M. T. (2005). Growth and biochemical composition of the diatom *Chaetoceros* cf*. wighamii* brightwell under different temperature, salinity and carbon dioxide levels. I. Protein, carbohydrates and lipids. *Aquaculture,* **246**, 405-412.

Arendt, K. E., Jónasdóttir, S. H., Hansen, P. J., & Gärtner, S. (2005). Effects of dietary fatty acids on the reproductive success of the calanoid copepod *Temora longicornis*. *Marine Biology*, **146**(3), 513-530.

Armbrust, E. V., Berges, J. A., Bowler, C., Green, B. R., Martinez, D., Putnam, N. H., ... & Rokhsar, D. S. (2004). The genome of the diatom *Thalassiosira pseudonana*: ecology, evolution, and metabolism. *Science*, **306**(5693), 79-86.

Armstrong, R. A. (2006). Optimality-based modeling of nitrogen allocation and photoacclimation in photosynthesis. *Deep-Sea Research Part II*, **53***,* 513-531.

Armstrong, R. A., Lee C., Hedges J. I., Honjo S. & Wakeham S.G. (2002). A new mechanistic model for organic carbon fluxes in the ocean: based on the quantitative association of POC with ballast minerals. *Deep-Sea Research*, **49**, 219–236.

Arsalane, W., Rousseau, B. & Duval, J.C. (1994) Influence of the pool size of the xanthophyll cycle on the effects of light stress in a diatom: competition between photoprotection and photoinhibition. *Photochemistry and Photobiology*, **60**(3), 237-243.

Ashraf, M. & Harris, P.J.C. (2004). Potential biochemical indicators of salinity tolerance in plants. *Plant Science*, **166,** 3–16.

Aslam, S.N., Cresswell-Maynard, T., Thomas, D.N. & Underwood, G.J.C. (2012). Production and characterisation of the intra- and extracellular carbohydrates and polymeric substances (EPS) of three sea ice diatom species, and evidence for a cryoprotective role for EPS. *Journal of Phycology,* **48**, 1494-1509.

Aspinall, D. & Paleg L.G. (1981). Proline accumulation: physiological aspects. In: Paleg L.G., Aspinall D. eds. *The physiology and biochemistry of drought resistance in plants.* Australia: Academic Press, 205-240.

Bank, R. A., Jansen, E. J., Beekman, B., & te Koppele, J. M. (1996). Amino acid analysis by reverse-phase high-performance liquid chromatography: improved derivatization and detection conditions with 9-fluorenylmethyl chloroformate. *Analytical Biochemistry*, **240**(2), 167-176.

Banse, K. (1976). Rates of growth, respiration and photosynthesis of unicellular algae as related to cell size-A review. *Journal of Phycology*, **12**, 135-140.

Barbarino, E., & Lourenço, S. O. (2005). An evaluation of methods for extraction and quantification of protein from marine macro-and microalgae. *Journal of Applied Phycology*, **17**(5), 447-460.

Barclay, W. & Zeller, S. (1996). Nutritional Enhancement of n-3 and n-6 Fatty Acids in Rotifers and *Artemia nauplii* by Feeding Spray-dried *Schizochytrium* sp. *Journal of the World Aquaculture Society,* **27**(3), 314-322.

Bates, T. S., Charlson, R. J. & Gammon, R. H. (1987). Evidence for the climatic role of marine biogenic sulphur. *Nature,* **329**, 319-321.

Bayraktaroğlu, E., Legović, T., Velasquez, Z. R., & Cruzado, A. (2003). Diatom *Thalassiosira weissflogii* in oligotrophic versus eutrophic culture: models and ultrastructure. *Ecological Modelling*, **170**(2), 237-243.

Becker, E. W. (2007). Micro-algae as a source of protein. *Biotechnology Advances*, **25**(2), 207-210.

Becker, W. (2004). 18 Microalgae in Human and Animal Nutrition. *Handbook of Microalgal Culture: Biotechnology and Applied Phycology*, 312pp.

Behrenfeld, M. J., Boss E., Siegel D. A. & Shea D. M. (2005). Carbon-based ocean productivity and phytoplankton physiology from space. *Global Biogeochemistry Cycles*, **19**, 1-114.

Behrenfeld, M. J., Maranon, E., Siegel, D. A. & Hooker S. B. (2002). Photoacclimation and nutrient based model of light-saturated photosynthesis for quantifying oceanic primary production. *Marine Ecology Progress Series,* **228***,* 103-117.

Berelson, W. M., Balch, W. M., Najjar, R., Feely, R. A., Sabine, C., & Lee, K. (2007). Relating estimates of $CaCO_3$ production, export, and dissolution in the water column to measurements of $CaCO_3$ rain into sediment traps and dissolution on the sea floor: A revised global carbonate budget. *Global Biogeochemical Cycles*, **21**(1).

Berges, J. A., Varela, D. E. & Harrison, P. J. (2002). Effects of temperature on growth rate, cell composition and nitrogen metabolism in the marine diatom *Thalassiosira pseudonana (Bacillariophyceae). Marine Ecology Progress Series,* **225***,* 139-146.

Berges, J.A., Franklin, D.J. & Harrison, P.J. 2001. Evolution of an artificial seawater medium: improvements in enriched seawater, artificial water over the last two decades. *Journal of Phycology,* **37**, 1138-1145.

Bernard, O., & Rémond, B. (2012). Validation of a simple model accounting for light and temperature effect on microalgal growth. *Bioresource technology*, **123**, 520-527.

Berner, T., Dubinsky, Z., Wyman, K., & Falkowski, P. G. (1989). Photoadaptation and the "package" effect in *Dunaliella tertiolecta* (chlorophyceae). *Journal of Phycology*, **25**(1), 70-78.

Bertozzini, E., Galluzzi, L., Penna, A., & Magnani, M. (2011). Application of the standard addition method for the absolute quantification of neutral lipids in microalgae using Nile red. *Journal of Microbiological Methods*, **87**(1), 17-23.

Bertrand, M. (2010). Carotenoid biosynthesis in diatoms. *Photosynthesis Research*, **106**(12), 89-102.

Betancort Rodríguez, J. R., García Reina, G., & Santana Rodríguez, J. J. (1997). Determination of free amino acids in microalgae by high-performance liquid chromatography using pre-column fluorescence derivatization. *Biomedical Chromatography*, **11**(6), 335-336.

Binder, B. J., & Liu, Y. C. (1998). Growth rate regulation of rRNA content of a marine *Synechococcus* (Cyanobacterium) strain. *Applied and Environmental Microbiology*, **64**(9), 3346-3351.

Bidigare, R. R., Smith, R. C. Baker, K. S. & Marra, J. (1987). Oceanic primary production estimates from measurements of spectral irradiance and pigment concentrations. *Global Biogeochemical Cycles,* **1***,* 171-186.

Blanchard, G. F., Guarini, J. M., Gros, P. & Richard, P. (1997). Seasonal effect on the relationship between the photosynthetic capacity of intertidal microphytobenthos and temperature. *Journal of Phycology,* **33***,* 723-728.

Blankenship, D. T., Krivanek, M. A., Ackermann, B. L., & Cardin, A. D. (1989). High-sensitivity amino acid analysis by derivatization with O-phthalaldehyde and 9-fluorenylmethyl chloroformate using fluorescence detection: applications in protein structure determination. *Analytical Biochemistry*, **178**(2), 227-232.

Blasco, D., Packard, T. T. & Garfield, P. C. (1982). Size dependence of growth rate, respiratory electron transport system activity and chemical composition in marine diatoms in the laboratory. *Journal of Phycology*, **18**, 58-63.

Boelen, P., van Dijk, R., Damsté, J.S.S., Rijpstra, W.I.C. & Buma, A.G.J. 2013. On the potential application of polar and temperate marine microalgae for EPA and DHA production. *AMB Express*, **3**, 26

Boogers, I., Plugge, W., Stokkermans, Y. Q., & Duchateau, A. L. (2008). Ultra-performance liquid chromatographic analysis of amino acids in protein hydrolysates using an automated pre-column derivatisation method. *Journal of Chromatography A*, **1189**(1), 406-409.

Borowitzka, L. J., Moulton, T. P., & Borowitzka, M. A. (1984). The mass culture of *Dunaliella salina* for fine chemicals: from laboratory to pilot plant. *Hydrobiologia*, **116/117**:115-121.

Borowitzka, M. A., Huisman, J. M., & Osborn, A. (1991). Culture of the astaxanthin-producing green alga *Haematococcus pluvialis*. Effects of nutrients on growth and cell type. *Journal of Applied Phycology*, **3**(4), 295-304.

Borowitzka, L. J., & Borowitzka, M. A. (1990). Commercial production of β-carotene by Dunaliella salina in open ponds. *Bulletin of marine science*, **47**(1), 244-252.

Bowler, C., Allen, A. E., Badger, J. H., Grimwood, J., Jabbari, K., Kuo, A., ... & Montsant, A. (2008). The *Phaeodactylum* genome reveals the evolutionary history of diatom genomes. *Nature*, **456**(7219), 239-244.

Bowen, H.J.M. (1979). Environmental chemistry of the elements. London (UK): Academic Press.

Boyce, D. G., Lewis, M. R., & Worm, B. (2010). Global phytoplankton decline over the past century. *Nature*, **466**(7306), 591-596.

Brand, L. E. (1994). Physiological ecology of marine coccolithophores. *In*: *Coccolithophores* (Ed. By Winter A and Siesser W.G.) Cambridge University Press. pp. 39-49.

Bremer, H. & Dennis, P. P. (1996). Modulation of chemical composition and other parameters of the cell growth rate. *In* Escherichia coli and Salmonella: Cellular and Molecular Biology, 2nd edn, pp. 1553–1568. Editor by F. C. Neidhardt and others. Washington, DC: American Society for Microbiology.

Breuer, G., Lamers, P. P., Martens, D. E., Draaisma, R. B., & Wijffels, R. H. (2013). Effect of light intensity, pH, and temperature on triacylglycerol (TAG) accumulation induced by nitrogen starvation in *Scenedesmus obliquus*. *Bioresource Technology*, **143**, 1-9.

Bricaud, A., Bédhomme, A. L., & Morel, A. (1988). Optical properties of diverse phytoplanktonic species: experimental results and theoretical interpretation. *Journal of Plankton Research*, **10**(5), 851-873.

Brody, M., & Vatter, A. E. (1959). Observations on cellular structures of *Porphyridium cruentum*. *The Journal of Biophysical and Biochemical Cytology*, **5**(2), 289-294.

Bronk, D. A., Lomas, M. W., Glibert, P. M., Schukert, K. J. & Sanderson, M. P. (2000). Total dissolved nitrogen analysis: comparisons between the persulfate, UV and high temperature oxidation methods. *Marine Chemistry,* **69**, 163-178.

Bronk, D. A. & Ward, B. B. (2000). Magnitude of dissolved organic nitrogen release relative to gross nitrogen uptake in marine systems. *Limnology and Oceanography*, **45**(8), 1879-1883.

Bronk, D. A., Lomas, M. W., Glibert, P. M., Schukert, K. J. & Sanderson, M. P. (2000). Total dissolved nitrogen analysis: comparisons between the persulfate, UV and high temperature oxidation methods. *Marine Chemistry*, **69**(1), 163-178.

Brown, C. W. & Yoder, J. A. (1994). Coccolithophorid blooms in the global ocean. *Journal of Geophysical Research,* **99***,* 7467-7482.

Brown, M. R. (1991). The amino-acid and sugar composition of 16 species of microalgae used in mariculture. *Journal of Experimental Marine Biology and Ecology*, **145**(1), 79-99.

Brown, M. R., Jeffrey, S. W., Volkman, J. K., & Dunstan, G. A. (1997). Nutritional properties of microalgae for mariculture. *Aquaculture*, **151**(1), 315-331.

Brown, S. L., Landry, M. R., Neveux, J. & Dupouy, C. (2003). Microbial community abundance and biomass along a 180 degrees transect in the equatorial Pacific during an El Niño-Southern Oscillation cold phase. *Journal of Geophysical Research,* **108***,* 8139.

Brown, T. E., & Richardson, F. L. (1968). The effect of growth environment on the physiology of algae: light intensity. *Journal of Phycology*, **4**(1), 38-54.

Brunet, C., Chandrasekaran, R., Barra, L., Giovagnetti, V., Corato, F., & Ruban, A. V. (2014). Spectral radiation dependent photoprotective mechanism in the diatom *Pseudo-nitzschia multistriata*. *PloS ONE*, **9**(1), e87015.

Buitenhuis, E.T., de Baar, H. J. W. & Veldhuis, M. J. W. (1999). Photosynthesis and calcification by *Emiliania huxleyi* (Prymnesiophyceae) as a function of inorganic carbon speicies. *Journal of Phycology,* **35,** 949-959.

Burdge, G. C., Jones, A. E., & Wootton, S. A. (2002). Eicosapentaenoic and docosapentaenoic acids are the principal products of α-linolenic acid metabolism in young men. *British Journal of Nutrition*, **88**(04), 355-363.

Cahu, C., Guillaume, J. C., Stephan, G., & Chim, L. (1994). Influence of phospholipid and highly unsaturated fatty acids on spawning rate and egg and tissue composition in *Penaeus vannamei* fed semi-purified diets. *Aquaculture*, **126**(1), 159-170.

Calder, P.C. (2010). Omega-3 fatty acids and inflammatory processes. *Nutrients*, **2**, 355-374.

Carvalho, A. P., & Malcata, F. X. (2000). Effect of culture media on production of polyunsaturated fatty acids by *Pavlova lutheri*. *Cryptogamie Algologie*, **21**(1), 59-71.

Carvalho, A. P., Monteiro, C. M., & Malcata, F. X. (2009). Simultaneous effect of irradiance and temperature on biochemical composition of the microalga *Pavlova lutheri*. *Journal of Applied Phycology*, **21**(5), 543-552.

Cepák, V., Přibyl, P., Vítová, M., & Zachleder, V. (2007). The nucleocytosolic and chloroplast cycle in the green chlorococcal alga *Scenedesmus obliquus* (Chlorophyceae, Chlorococcales) grown under various temperatures. *Phycologia*, **46**(3), 263-269.

Cermeño, P., Dutkiewicz, S., Harris, R. P., Follows, M., Schofield, O., & Falkowski, P. G. (2008). The role of nutricline depth in regulating the ocean carbon cycle. *Proceedings of the National Academy of Sciences*, **105**(51), 20344-20349.

Ceron-Garcia, M. C., Fernandez-Sevilla, J. M., Sanchez-Miron, A., Garcia-Camacho, F., Contreras-Gomez, A., & Molina-Grima, E. (2013). Mixotrophic growth of Phaeodactylum tricornutum on fructose and glycerol in fed-batch and semi-continuous modes. *Bioresource Technology*, **147**, 569-576.

Chandrasekaran, R., Barra, L., Carillo, S., Caruso, T., Corsaro, M. M., Dal Piaz, F., ... & Brunet, C. (2014). Light modulation of biomass and macromolecular composition of the diatom *Skeletonema marinoi*. *Journal of Biotechnology*, **192**, 114-122.

Charlson, R. J., Lovelock, J. E., Andreae, M. O. & Warren, S. G. (1987). Oceanic phytoplankton, atmospheric sulphur, cloud albedo and climate. *Nature.* **326**, 655-661.

Chauton, M. S., Olsen, Y. & Vadstein, O. (2013). Biomass production from the microalga *Phaeodactylum tricornutum*: Nutrient stress and chemical composition in exponential fed-batch cultures. *Biomass and Bioenergy*, **58**, 87-94.

Chautona, M.S., Reitan Reitan, K.I., Norskerc, N.H., Tveteråsd, R., & Kleivdale HT. (2015). A techno-economic analysis of industrial production of marine microalgae as a source of EPA and DHA-rich raw material for aquafeed: Research challenges and possibilities. *Aquaculture*, **436**, 95-103.

Chen J. & Thornton D.C.O. (2015). Transparent exopolymer particle production and aggregation by a marine planktonic diatom (*Thalassiosira weissflogii*) at different growth rates. *Journal of Phycology*, **51**(2), 381-393.

Chen, G. Q., Jiang, Y., & Chen, F. (2008). Salt-induced alterations in lipid composition of diatom *Nitzschia laevis* (Bacillariophyceae) under heterotrophic culture condition. *Journal of Phycology*, **44**(5), 1309-1314.

Chen, G. Q., Jiang, Y., & Chen, F. (2008). Variation of lipid class composition in *Nitzschia laevis* as a response to growth temperature change. *Food Chemistry*, **109**(1), 88-94.

Chen, M., Li, J., Dai, X., Sun, Y. & Chen, F. (2011). Effect of phosphorus and temperature on chlorophyll *a* contents and cell sizes of *Scenedesmus obliquus* and *Microcystis aeruginosa*. *Limnology*, **12**(2), 187-192.

Chen, W., Sommerfeld, M., & Hu, Q. (2011). Microwave-assisted Nile red method for in vivo quantification of neutral lipids in microalgae. *Bioresource Technology*, **102**(1), 135-141.

Chen, W., Zhang, C., Song, L., Sommerfeld, M., & Hu, Q. (2009). A high throughput Nile red method for quantitative measurement of neutral lipids in microalgae. *Journal of Microbiological Methods*, **77**(1), 41-47.

Chia, M. A., Lombardi, A. T., Melão, M. D. G. G., & Parrish, C. C. (2015). Combined nitrogen limitation and cadmium stress stimulate total carbohydrates, lipids, protein and amino acid accumulation in *Chlorella vulgaris* (Trebouxiophyceae). *Aquatic Toxicology*, **160**, 87-95.

Chinnasamy, S., Bhatnagar, A., Hunt, R. W., & Das, K. C. (2010). Microalgae cultivation in a wastewater dominated by carpet mill effluents for biofuel applications. *Bioresource Technology*, **101**(9), 3097-3105.

Chiu, S. Y., Kao, C. Y., Tsai, M. T., Ong, S. C., Chen, C. H., & Lin, C. S. (2009). Lipid accumulation and CO_2 utilization of *Nannochloropsis oculata* in response to CO_2 aeration. *Bioresource Technology*, **100**(2), 833-838.

Christaki, E., Bonos, E., Giannenas, I., & Florou-Paneri, P. (2013). Functional properties of carotenoids originating from algae. *Journal of the Science of Food and Agriculture*, **93**(1), 5-11.

Cirulis, J. T., Strasser, B. C., Scott, J. A., & Ross, G. M. (2012). Optimization of staining conditions for microalgae with three lipophilic dyes to reduce precipitation and fluorescence variability. *Cytometry Part A*, **81**(7), 618-626.

Claquin, P., Probert, I., Lefebvre, S. & Veron, B. (2008). Effects of temperature on photosynthetic parameters and TEP production in eight species of marine microalgae. *Aquatic Microbial Ecology,* **51***,* 1–11.

Cohen, S. A. (2003). Amino Acid Analysis Using Pre-Column Derivatization with 6-Aminoquinolyl-N-Hydroxysuccinimidyl Carbamate. In *Protein Sequencing Protocols* (pp. 143-154). Humana Press, USA.

Cohen, Z. (1999) Chemicals from Microalgae. Taylor & Francis, London, p. 419.

Colla, L. M., Reinehr, C. O., Reichert, C., & Costa, J. A. V. (2007). Production of biomass and nutraceutical compounds by *Spirulina platensis* under different temperature and nitrogen regimes. *Bioresource Technology*, **98**(7), 1489-1493.

Collos, Y., Mornet, F., Sciandra, A., Waser, N., Larson, A., & Harrison, P. J. (1999). An optical method for the rapid measurement of micromolar concentrations of nitrate in marine phytoplankton cultures. *Journal of Applied Phycology*, **11**(2), 179-184.

Converti, A., Casazza, A. A., Ortiz, E. Y., Perego, P., & Del Borghi, M. (2009). Effect of temperature and nitrogen concentration on the growth and lipid content of *Nannochloropsis oculata* and *Chlorella vulgaris* for biodiesel production. *Chemical Engineering and Processing: Process Intensification*, **48**(6), 1146-1151.

Cook, J. R. (1963). Adaptations in growth and division in *Euglena* effected by energy supply. *The Journal of protozoology*, **10**(4), 436-444.

Cooper, M. S., Hardin, W. R., Petersen, T. W., & Cattolico, R. A. (2010). Visualizing" green oil" in live algal cells. *Journal of Bioscience and Bioengineering*, **109**(2), 198-201.
Cullen, J.J. (1990). On models of growth and photosynthesis in phytoplankton. *Deep-Sea Research,* **37***,* 667-683.

d'Ippolito, G., Sardo, A., Paris, D., Vella, F. M., Adelfi, M. G., Botte, P., ... & Fontana, A. (2015). Potential of lipid metabolism in marine diatoms for biofuel production. *Biotechnology for Biofuels*, **8**(1), 28.

da Silva Gorgônio, C. M., Aranda, D. A. G., & Couri, S. (2013). Morphological and chemical aspects of *Chlorella pyrenoidosa, Dunaliella tertiolecta, Isochrysis galbana* and *Tetraselmis gracilis* microalgae. *Nature Science,* **7**(5), 783-791.

Dadáková, E., Křížek, M., & Pelikánová, T. (2009). Determination of biogenic amines in foods using ultra-performance liquid chromatography (UPLC). *Food Chemistry*, **116**(1), 365-370.

Daume, S., Long, B.M. & Crouch, P. (2003). Changes in amino acid content of an algal feed species (*Navicula* sp.) and their effect on growth and survival of juvenile abalone (*Haliotis rubra*). *Journal of Applied Phycology,* **15***,* 201–207.
Davie, E., & Petersen, J. (2012). Environmental control of cell size at division. *Current opinion in cell biology*, **24**(6), 838-844.

Davison, I. R. (1991). Environmental effects on algal photosynthesis: temperature. *Journal of Phycology*, **27**(1), 2-8.

de Castro Araújo, S., & Garcia, V. M. T. (2005). Growth and biochemical composition of the diatom *Chaetoceros* cf. *wighamii* brightwell under different temperature, salinity and carbon dioxide levels. I. Protein, carbohydrates and lipids. *Aquaculture*, **246**(1), 405-412.

de Jesus Raposo, M. F., de Morais, R. M. S. C. & de Morais, A. M. M. B. (2013). Bioactivity and applications of sulphated polysaccharides from marine microalgae. *Marine drugs*, **11**(1), 233-252.

de Jesus Raposo, M. F., de Morais, R. M. S. C. & de Morais, A. M. M. B. (2013). Health applications of bioactive compounds from marine microalgae. *Life Sciences*, **93**(15), 479-486.

de Jonge V. N. (1980) Fuctuations in the organic carbon to chlorophyll *a* ratios for estuarine benthic diatom populations. *Marine Ecology Progress Series,* **2**, 345-353.

De la Noüe, J., & Ni Eidhin, D. (1988). Improved performance of intensive semicontinuous cultures of *Scenedesmus* by biomass recirculation. *Biotechnology and Bioengineering*, **31**(5), 397-406.

De Martino, A., Amato, A., & Bowler, C. (2009). Mitosis in diatoms: rediscovering an old model for cell division. *Bio Essays*, **31**(8), 874-884.

Defew, E. C., Perkins, R. G. & Paterson, D. M. (2004). The influence of light and temperature interactions on a natural estuarine microphytobenthic assemblage. *Biofilms,* **1***,* 21–30.

Del Campo, J. A., García-González, M., & Guerrero, M. G. (2007). Outdoor cultivation of microalgae for carotenoid production: current state and perspectives. *Applied Microbiology and Biotechnology*, **74**(6), 1163-1174.

D'Elia, C.F., Ryther, J.H. & Losordo, T.M. (1977). Productivity and nitrogen balance in large scale phytoplankton cultures. *Water Resources,* **11**, 1031-1040.

Derelle, E., Ferraz, C., Rombauts, S., Rouzé, P., Worden, A. Z., Robbens, S., ... & Moreau, H. (2006). Genome analysis of the smallest free-living eukaryote *Ostreococcus tauri* unveils many unique features. *Proceedings of the National Academy of Sciences*, **103**(31), 11647-11652.

Derrien, A., Coiffard, J. M. L., Coiffard, C. & De Roeck-Holtzhauer, Y. (1998). Free amino acid analysis of five microalgae. *Journal of Applied Phycology,* **10***,* 131–134.

Derrien, A., Coiffard, L. J., Coiffard, C., & De Roeck-Holtzhauer, Y. (1998). Free amino acid analysis of five microalgae. *Journal of Applied Phycology*, **10**(2), 131-134.

Devi, M. P., Subhash, G. V., & Mohan, S. V. (2012). Heterotrophic cultivation of mixed microalgae for lipid accumulation and wastewater treatment during sequential growth and starvation phases: effect of nutrient supplementation. *Renewable Energy*, **43**, 276-283.

Di Valentin,M., Büchel, C., Giacometti, G.M. & Carbonera D. (2012). Chlorophyll triplet quenching by fucoxanthin in the fucoxanthin-chlorophyll protein from the diatom *Cyclotella meneghiniana*. *Biochemical and Biophysical Research Communications,* **427***,* 637–641.

Diaz, J., Lliberia, J. L., Comellas, L., & Broto-Puig, F. (1996). Amino acid and amino sugar determination by derivatization with 6-aminoquinolyl-N-hydroxysuccinimidyl carbamate followed by high-performance liquid chromatography and fluorescence detection. *Journal of Chromatography A*, **719**(1), 171-179.

Dimier, C., Corato, F., Tramontano, F. & Brunet, C. (2007). Photoprotection and xanthophyll-cycle activity in three marine diatoms. *Journal of Phycology*, **43**(5), 937-947.

Dipak, P., & Lele, S. (2005). Carotenoid production from microalga, *Dunaliella salina*. *Indian Journal of Biotechnology*, **4**(8), 476-483.

Doan, T. T. Y., & Obbard, J. P. (2011). Improved Nile red staining of *Nannochloropsis* sp. *Journal of Applied Phycology*, **23**(5), 895-901.

Dortch, Q. (1982). Effect of growth conditions on accumulation of internal nitrate, ammonium, amino acids, and protein in three marine diatoms. *Journal of Experimental Marine Biology and Ecology*, **61**(3), 243-264.

Dortch, Q., Roberts, T. L., Clayton Jr, J. R., & Ahmed, S. I. (1983). RNA/DNA ratios and DNA concentrations as indicators of growth rate and biomass in planktonic marine organisms. *Marine ecology progress series,* **13**(1), 61-71.

Doshi, M., Watanabe, S., Niimoto, T., Kawashima, H., Ishikura, Y., Kiso, Y., & Hamazaki, T. (2004). Effect of dietary enrichment with n-3 polyunsaturated fatty acids (PUFA) or n-9 PUFA on arachidonate metabolism in vivo and experimentally induced inflammation in mice. *Biological and Pharmaceutical Bulletin*, **27**(3), 319-323.

Drillet, G., Jørgensen, O. G. N., Sørensen, F. T., Ramløv, H. & Hansen, W. B. (2006). Biochemical and technical observations supporting the use of copepods as live feed organisms in marine larviculture. *Aquaculture Research,* **37***,* 756-772.

Dubois, M., Gilles, K. A., Hamilton, J. K., Rebers, P., & Smith, F. (1956). Colorimetric method for determination of sugars and related substances. *Analytical Chemistry*, **28**(3), 350-356.

Dutta, A. K., Kamada, K., & Ohta, K. (1996). Spectroscopic studies of nile red in organic solvents and polymers. *Journal of Photochemistry and Photobiology A: Chemistry*, **93**(1), 57-64.

Edwards, M., & Richardson, A. J. (2004). Impact of climate change on marine pelagic phenology and trophic mismatch. *Nature*, **430**(7002), 881-884.

Elsey, D., Jameson, D., Raleigh, B., & Cooney, M. J. (2007). Fluorescent measurement of microalgal neutral lipids. *Journal of Microbiological Methods*, **68**(3), 639-642.

Emmerson, W. D. (1980). Ingestion, growth and development of *Penaeus indicus* larvae as a function of *Thalassiosira weissflogii* cell concentration. *Marine Biology*, **58**(1), 65-73.

Enright, C. T., Newkirk, G. F., Craigie, J. S. & Castell, J. D. (1986). Evaluation of phytoplankton as diets for juvenile *Ostrea edulis* L. *Journal of Experimental Marine Biology and Ecology*, **96**(1), 1-13.

Eppley, R. W. (1972). Temperature and phytoplankton growth in the sea. Fishery Bulletin, **70**(4), 1063-1085.

Escoubas, J. M., Lomas, M., La Roche, J. & Falkowski, P. G. (1995). Light intensity regulation of *cab* gene transcription is signaled by the redox state of the plastoquinone pool. *Proceedings of the National Academy of Sciences*, **92**(22), 10237-10241.

European Standard EN 14214 (2004). Automotive Fuels – Fatty Acid Methyl Esters (FAME) for Diesel Engines – Requirements and Test Methods.

Fábregas, J., Maseda, A., Domínguez, A., & Otero, A. (2004). The cell composition of *Nannochloropsis* sp. changes under different irradiances in semicontinuous culture. *World Journal of Microbiology and Biotechnology*, **20**(1), 31-35.

Fakhry, E. M., & El Maghraby, D. M. (2015). Lipid accumulation in response to nitrogen limitation and variation of temperature in *Nannochloropsis salina*. *Botanical Studies*, **56**(1), 1-8.

Falkowski, P.G & La Roche J (1991). Acclimation to spectral irradiance in algae. *Journal of Phycology,* **27**, 8-14.

Falkowski P. G. & Raven J. A. (2007). Aquatic photosynthesis. Princeton university press. pp 484.

Falkowski, P. G., Dubinsky, Z., & Wyman, K. (1985). Growth-irradiance relationships in phytoplankton. *Limnology and Oceanography*, **30**(2), 311-321.

Falkowski, P. G., Katz, M. E., Knoll, A. H., Quigg, A., Raven, J. A., Schofield, O., & Taylor, F. J. R. (2004). The evolution of modern eukaryotic phytoplankton. *Science*, **305**(5682), 354-360.

Ferńandes, E., Fritz, J. J. & Balch, W. M. (1996). Chemical composition of the coccolithophorid *Emiliania huxleyi* under light-limited steady state growth. *Journal of Experimental Marine Biology and Ecology,* **207***,* 149-16.

Ferrer-Álvarez, Y. I., Ortega-Clemente, L. A., Pérez-Legaspi, I. A., Hernández-Vergara, M. P., Robledo-Narváez, P. N., Ríos-Leal, E., & Poggi-Varaldo, H. M. (2015). Growth of *Chlorella vulgaris* and *Nannochloris oculata* in effluents of Tilapia farming for the production of fatty acids with potential in biofuels. *African Journal of Biotechnology*, **14**(20), 1710-1717.

Field B. C., Behrenfeld M. J., Randerson J. T. & Falkowski P. (1998). Primary production of the biosphere: Integrating terrestrial and oceanic components. *Science*, **281**, 237-240.

Field, C. J., & Schley, P. D. (2004). Evidence for potential mechanisms for the effect of conjugated linoleic acid on tumor metabolism and immune function: lessons from n− 3 fatty acids. *The American Journal of Clinical Nutrition*, **79**(6), 1190S-1198S.

Finkel Z. V., Beardall J.,Flynn K. J., Quigg A., Rees T. A. & Raven J. A. (2010). Phytoplankton in a changing world: cell size and elemental stoichiometry. *Journal of Plankton Research*, **31**, 119-137.

Finkel, Z. V., Beardall, J., Flynn, K. J., Quigg, A., Rees, T. A. V., & Raven, J. A. (2009). Phytoplankton in a changing world: cell size and elemental stoichiometry. *Journal of Plankton Research*, fbp098, 1-19.

Finkel, Z. V., Beardall, J., Flynn, K. J., Quigg, A., Rees, T. A. V., & Raven, J. A. (2010). Phytoplankton in a changing world: cell size and elemental stoichiometry. *Journal of Plankton Research*, **32**, 119-132.

Finkel, Z. V., Quigg, A., Raven, J. A., Reinfelder, J. R., Schofield, O. E., & Falkowski, P. G. (2006). Irradiance and the elemental stoichiometry of marine phytoplankton. *Limnology and Oceanography*, **51**(6), 2690-2701.

Fischer, R., Andersen, T., Hillebrand, H. & Ptacnik, R. (2014). The exponentially exponential phase culture as a reliable alternative to conventional chemostats. *Limnology and Oceanography: Methods*, **12**, 432-440.

Fogg, G.E. & Thake, B. (1987) Algal Cultures and Phytoplankton Ecology. The University of Wisconsin Press, Madison, WI, USA, 269pp.

Fowler, S. D., & Greenspan, P. H. I. L. L. I. P. (1985). Application of Nile red, a fluorescent hydrophobic probe, for the detection of neutral lipid deposits in tissue sections: comparison with oil red O. *Journal of Histochemistry & Cytochemistry*, **33**(8), 833-836.

Francois, R., Honjo, S., Krishfield, R., Manganini, S. (2002). Factors controlling the flux of organic carbon to the bathypelagic zone of the ocean. *Global Biogeochemical Cycles*, **16**, 1-20.

Frank, H.A., Cua, A., Chynwat, V., Young, A., Gosztola, D. & Wasielewski, M.R. (1996). The lifetimes and energies of the first excited singlet states of diadinoxanthin and diatoxanthin: the role of these molecules in excess energy dissipation in algae. *Biochimica et Biophysica Acta,* **1277**(3), 243-52.

Frankignoulle, M., Canon, C., & Gattuso, J. P. (1994). Marine calcification as a source of carbon dioxide: Positive feedback of increasing atmospheric CO_2. *Limnology and Oceanography*, **39**(2), 458-462.

Fu, F. X., Warner, M. E., Zhang, Y., Feng, Y. & Hutchins, D. A. (2007). Effects of increased temperature and CO_2 on photosynthesis, growth, and elemental ratio in marine *Synechococcus* and *Prochlorococcus* (Cyanobateria). *Journal of Phycology,* **43**, 485-496.

Fuentes-Grünewald, C., Bayliss, C., Zanain, M., Pooley, C., Scolamacchia, M., & Silkina, A. (2015). Evaluation of batch and semi-continuous culture of *Porphyridium purpureum* in a photobioreactor in high latitudes using Fourier Transform Infrared spectroscopy for monitoring biomass composition and metabolites production. *Bioresource Technology*, **189**, 357-363.

Fujiki, T., & Taguchi, S. (2002). Variability in chlorophyll a specific absorption coefficient in marine phytoplankton as a function of cell size and irradiance. *Journal of Plankton Research*, **24**(9), 859-874.

Fujiki, T., Toda, T., Kikuchi, T., & Taguchi, S. (2003). Photoprotective response of xanthophyll pigments during phytoplankton blooms in Sagami Bay, Japan. *Journal of Plankton Research*, **25**(3), 317-322.

Funk, C.D. (2001). Prostaglandins and leukotrienes: advances in eicosanoids biology. *Science*, **294**, 1871-1875.

Furnas, M. (1978). Influence of temperature and cell size on the division rate and chemical content of the diatom *Chaetoceros curvisetum* Cleve. *Journal of Experimental Marine Biology and Ecology*, **34**(2), 97-109.

García, N., López-Elías, J. A., Miranda, A., Huerta, P. N., & García, A. (2012). Effect of salinity on growth and chemical composition of the diatom *Thalassiosira weissflogii* at three culture phases. *Latin American Journal of Aquatic Research*, **40**(2), 435-440.

García-González, M., Moreno, J., Manzano, J. C., Florencio, F. J., & Guerrero, M. G. (2005). Production of *Dunaliella salina* biomass rich in 9-cis-β-carotene and lutein in a closed tubular photobioreactor. *Journal of biotechnology*, **115**(1), 81-90.

Gardner, W. S., & Miller, W. H. (1980). Reverse-phase liquid chromatographic analysis of amino acids after reaction with o-phthalaldehyde. *Analytical Biochemistry*, **101**(1), 61-65.

Geider, R. J. (1987). Light and temperature dependence of the carbon to chlorophyll ratio in microalgae and cyanobacteria: implications for physiology and growth of phytoplankton. *New Phytologist,* **106***,* 1-34.

Geider, R. J. & La Roche, J. L. (2002). Redfield revisited: variability of C: N : P in marine microalgae and its biochemical basis. *European Journal of Phycology*, **37**, 1-17.

Geider, R. J. (1993). Quantitative phytoplankton ecophysiology: implications for primary production and phytoplankton growth. *ICES Marine Science Symposia,* **197**, 52-62.

Geider, R. J., & Osborne, B. A. (1987). Light absorption by a marine diatom: experimental observations and theoretical calculations of the package effect in a small *Thalassiosira* species. *Marine Biology*, **96**(2), 299-308.

Geider, R. J., MacIntyre, H. L. & Kana, T. M. (1996). A dynamic model of photoadaptation in phytoplankton. *Limnology Oceanography,* **41***,* 1-15.

Geider, R. J., MacIntyre, H. L. & Kana, T. M. (1997). Dynamic model of phytoplankton growth and acclimation: responses of the balanced growth rate and the chlorophyll *a*:carbon ratio to light, nutrient-limitation and temperature. *Marine Ecology Progress Series,* **148***,* 187-200.

Geider, R. J., Maclntyre, H. L., & Kana, T. M. (1998). A dynamic regulatory model of phytoplanktonic acclimation to light, nutrients, and temperature. *Limnology and Oceanography*, **43**(4), 679-694.

Geider, R. J., Platt, T., & Raven, J. A. (1986). Size dependence of growth and photosynthesis in diatoms: a synthesis. *Marine Ecology Progress Series*, **30***:*93-104.

Geider, R.J. & La Roche, J. (2002). Redfield revisited: variability of C: N: P in marine microalgae and its biochemical basis. *European Journal of Phycology*, **37**, 1-17.

Geider, R.J. (1987). Light and temperature dependence of the carbon to chlorophyll *a* ratio in microalgae and cyanobacteria: implications for physiology and growth of phytoplankton. *New Phytologist,* **106**, 1-34.

Geider, R.J., La Roche, J., Olaizola, M. & Greene, R.M. (1993). Response of the photosynthetic apparatus of *Phaeodactylum tricornutum* (Bacillariophyceae) to nitrate, phosphate or iron starvation. *Journal of Phycology,* **29**, 755-766.

Ghoneim, N. (2000). Photophysics of Nile red in solution: steady state spectroscopy. *Spectrochimica Acta Part A: Molecular and Biomolecular Spectroscopy*, **56**(5), 1003-1010.

Ghozzi, K., Omrane, H., Challouf, R. & Ben Dhiab, R. (2014). Modelling biochemical composition of thermo tolerant *Cosmarium* strain isolated from Tunisian Geothermal water, as function of temperature and light intensity. *Journal of Algal Biomass Utilization,* **5**(4): 1-8.

Goericke, R., & Welschmeyer, N. A. (1992). Pigment turnover in the marine diatom *Thalassiosira weissflogii*. I. the $14CO_2$-labeling kinetics of chlorophyll a. *Journal of Phycology,* **28**(4), 498-507.

Goiris, K., Van Colen, W., Wilches, I., León-Tamariz, F., De Cooman, L., & Muylaert, K. (2015). Impact of nutrient stress on antioxidant production in three species of microalgae. *Algal Research*, **7**, 51-57.

Goldman, J. C. & Ryther, J. H. (1975). Nutrient transformations in mass cultures of marine algae. *Journal of Environmental Engineering,* **101**, 351-364.

Goldman, J. C. & Ryther, J. H. (1976). Temperature-influenced species competition in mass cultures of marine phytoplankton. *Biotechnology Bioengineering,* **18***,* 1125-1144.

Goldman, J. C. (1977). Biomass production in mass cultures of marine phytoplankton at varying temperatures. *Journal of Experimental Marine Biology and* Ecology, **27**, 161-169.

Goldman, J. C. (1979). Bioengineering aspects of inorganic carbon supply to mass algal cultures. In: Proceedings third annual biomass energy systems conference. Rep. SERI/TP-33-285. Solar Energy Research Institute. Golden, Colorado, p. 25-32.

Goldman, J. C., & Mann, R. (1980). Temperature-influenced variations in speciation and chemical composition of marine phytoplankton in outdoor mass cultures. *Journal of Experimental Marine Biology and Ecology*, **46**(1), 29-39.

Gonçalves, A. L., Pires, J. C., & Simões, M. (2013). Lipid production of *Chlorella vulgaris* and *Pseudokirchneriella subcapitata*. *International Journal of Energy and Environmental Engineering*, **4**(1), 1-6.

Gordillo, F. J., Goutx, M., Figueroa, F. L., & Niell, F. X. (1998). Effects of light intensity, CO2 and nitrogen supply on lipid class composition of *Dunaliella viridis*. *Journal of Applied Phycology*, **10**(2), 135-144.

Gordon, N., Neori, A., Shpigel, M., Lee, J., & Harpaz, S. (2006). Effect of diatom diets on growth and survival of the abalone *Haliotis discus hannai* postlarvae. *Aquaculture*, **252**(2), 225-233.

Gosch, B. J., Lawton, R. J., Paul, N. A., de Nys, R. & Magnusson, M. (2015). Environmental effects on growth and fatty acids in three isolates of *Derbesia tenuissima* (Bryopsidales, Chlorophyta). *Algal Research,* **9***,* 82-93.

Goss, R. & Jakob, T. (2010). Regulation and function of xanthophyll cycle-dependent photoprotection in algae. *Photosynthesis Research*, **106**(1-2), 103-22.

Goulden, C.E. & Place, A.R. 1990. Fatty acid synthesis and accumulation rates in daphniids *Journal of Experimental Zoology,* **256**, 168-178.

Greenspan, P., & Fowler, S. D. (1985). Spectrofluorometric studies of the lipid probe, Nile red. *Journal of Lipid Research*, **26**(7), 781-789.

Griffiths, M. J., & Harrison, S. T. (2009). Lipid productivity as a key characteristic for choosing algal species for biodiesel production. *Journal of Applied Phycology*, **21**(5), 493-507.

Gromiha M.M. (2010). Protein Bioinformatics: From Sequence to Function. 339 pp. Academic Press.

Guihéneuf, F., Mimouni, V., Ulmann, L., & Tremblin, G. (2008). Environmental factors affecting growth and omega 3 fatty acid composition in *Skeletonema costatum*: The influences of irradiance and carbon source. *Diatom Research*, **23**(1), 93-103.

Guillard, R.R.L. & Ryther, R.H. (1962) Studies of marine plankton diatoms. I *Cyclotella nana* Hustedt and *Denotula confervaceae* (Cleve) Gran. *Canadian Journal of Microbiology*, **8**, 229-239.

Guiry, M. D. (2012). How many species of algae are there? *Journal of Phycology*, **48**(5), 1057-1063.

Guschina, I.A. & Harwood, J.L. (2006). Lipids and lipid metabolism in eukaryotic algae. *Progress Lipid Research*. **45**,160-186.

Halac, S. R., Villafañe, V. E., & Helbling, E. W. (2010). Temperature benefits the photosynthetic performance of the diatoms *Chaetoceros gracilis* and *Thalassiosira weissflogii* when exposed to UVR. *Journal of Photochemistry and Photobiology B: Biology*, **101**(3), 196-205.

Hamm, C. E., Merkel, R., Springer, O., Jurkojc, P., Maier, C., Prechtel, K., & Smetacek, V. (2003). Architecture and material properties of diatom shells provide effective mechanical protection. *Nature*, **421**(6925), 841-843.

Hardie, D. G. (1991). Biochemical messengers: hormones, neurotransmitters and growth factors. 311pp. Springer Science & Business Media.

Harrison, P. J., Thompson, P. A., & Calderwood, G. S. (1990). Effects of nutrient and light limitation on the biochemical composition of phytoplankton. *Journal of Applied Phycology*, **2**(1), 45-56.

Hecky, R. E., Mopper, K., Kilham, P. & Degens, E. T. (1973). The amino acid and sugar composition of diatom cell-walls. *Marine Biology*, **19**(4), 323-331.

Hemalatha, A., Karthikeyan, P., Manimaran, K., Anantharaman, P. & Sampathkumar P. (2012). Effect of Temperature on the Growth of Marine Diatom, *Chaetoceros simplex* (Ostenfeld, 1901) with Different Nitrate: Silicate Concentrations. *Asian Pacific Journal of Tropical Biomedicine,* S1817-S1821.

Hernández-Sebastià, C., Marsolais, F., Saravitz, C., Israel, D., Dewey, R. E., & Huber, S. C. (2005). Free amino acid profiles suggest a possible role for asparagine in the control of storage-product accumulation in developing seeds of low-and high-protein soybean lines. *Journal of Experimental Botany*, **56**(417), 1951-1963.
Hillebrand, H., Dürselen, C. D., Kirschtel, D., Pollingher, U., & Zohary, T. (1999). Biovolume calculation for pelagic and benthic microalgae. *Journal of Phycology*, **35**(2), 403-424.

Ho, S. H., Chen, C. Y., & Chang, J. S. (2012). Effect of light intensity and nitrogen starvation on CO_2 fixation and lipid/carbohydrate production of an indigenous microalga *Scenedesmus obliquus* CNW-N. *Bioresource Technology*, **113**, 244-252.

Hoagland, K. D., Rosowski, J. R., Gretz, M. R., & Roemer, S. C. (1993). Diatom extracellular polymeric substances: function, fine structure, chemistry, and physiology. *Journal of Phycology*, **29**(5), 537-566.

Hoffmann, M., Marxen, K., Schulz, R., & Vanselow, K. H. (2010). TFA and EPA productivities of *Nannochloropsis salina* influenced by temperature and nitrate stimuli in turbidostatic controlled experiments. *Marine Drugs*, **8**(9), 2526-2545.

Holligan, P. M., Fernandez, E., Aiken, J., Balch, W. M., Burkill, P. H., Finch, M., Groom, S. B., Malin, G., Muller, K., Purdie, D. A., Robinson, C., Trees, C. C., Turner, S. M. & Van der Wal, P. (1993). A biogeochemical study of the coccolithophore *Emiliania huxleyi* in the north Atlantic. *Global Biogeochemical Cycles,* **7***,* 879-900.

Holm-Hansen, O. (1969). Algae: amounts of DNA and organic carbon in single cells. *Science,* **163**, 87-8.

Hong, J. L. (1994). Determination of amino acids by precolumn derivatization with 6-aminoquinolyl-N-hydroxysuccinimidyl carbamate and high performance liquid chromatography with ultraviolet detection. *Journal of Chromatography A*, **670**(1), 59-66.

Horwitz, W. (2002). Official Methods of Analysis of AOAC International, vol. I, 17th ed., AOAC, Gaithersburg, MD, USA

Hou, S., He, H., Zhang, W., Xie, H., & Zhang, X. (2009). Determination of soil amino acids by high performance liquid chromatography-electro spray ionization-mass spectrometry derivatized with 6-aminoquinolyl-N-hydroxysuccinimidyl carbamate. *Talanta*, **80**(2), 440-447.

Houghton, J. T., Ding, Y., Griggs, D. J., Noguer, M., Van der Linden, P. J., Dai, X., Maskell, K. & Johnson, C. A. (2001). Climate Change 2001: The Scientific Basis. Cambridge University Press, Cambridge, UK, 881 pp.

Hu, Q. (2004). Environmental Effects on Cell Composition. In Handbook of Microalgal Culture: Biotechnology and Applied Phycology; Richmond, A., Ed.; Blackwell: Oxford, UK, pp 83–93.

Hu, Q., Sommerfeld, M., Jarvis, E., Ghirardi, M., Posewitz, M., Seibert, M., & Darzins, A. (2008). Microalgal triacylglycerols as feedstocks for biofuel production: Perspectives and advances. *The Plant Journal*, **54**(4), 621-639.

Huang, G. H., Chen, G., & Chen, F. (2009). Rapid screening method for lipid production in alga based on Nile red fluorescence. *Biomass and Bioenergy*, **33**(10), 1386-1392.

Huertas, I. E., Rouco, M., López-Rodas, V., & Costas, E. (2011). Warming will affect phytoplankton differently: Evidence through a mechanistic approach. *Proceedings of the Royal Society of London B: Biological Sciences*, **278**(1724), 3534-3543.

Hüner, N. P., Bode, R., Dahal, K., Hollis, L., Rosso, D., Krol, M., & Ivanov, A. G. (2012). Chloroplast redox imbalance governs phenotypic plasticity: the "grand design of photosynthesis" revisited. *Frontiers in plant science*, **3**.

Hüner, N. P. A., Maxwell, D. P., Gray, G. R., Savitch, L. V., Krol, M., Ivanov, A. G., & Falk, S. (1996). Sensing environmental temperature change through imbalances between energy supply and energy consumption: redox state of photosystem II. *Physiologia Plantarum*, **98**(2), 358-364.

Impellizzeri, G., Mangiafico, S., Piattelli, M., Sciuto, S., Fattorusso, E., Santacroce, C., & Sica, D. (1977). Amino-acid profiles in red algae. *Biochemical Systematics and Ecology*, **5**(2), 77-80.

Iqbal, M., & Zafar, S. I. (1993). Effects of photon flux density, CO_2, aeration rate, and inoculum density on growth and extracellular polysaccharide production by *Porphyridium cruentum*. *Folia Microbiologica*, **38**(6), 509-514.

Islam, M.A., Magnusson, M., Brown, R.J., Ayoko, A.G., Nabi, N.M. & Heimann, K. (2013). Microalgal species selection for biodiesel production based on fuel properties derived from fatty acid profiles. *Energies*, **6**, 5676-5702.

Ismar, S. M., Hansen, T., & Sommer, U. (2008). Effect of food concentration and type of diet on *Acartia* survival and naupliar development. *Marine Biology*, **154**(2), 335-343.

Jaswir, I., Noviendri, D., Hasrini, R. F., & Octavianti, F. (2011). Carotenoids: Sources, medicinal properties and their application in food and nutraceutical industry. *Journal of Medicinal Plants Research*, **5**(33), 7119-7131.

Jeener, R. (1953). Ribonucleic acid and protein synthesis in continuous cultures of *Polytomella caeca*. *Archives of biochemistry and biophysics*, **43**(2), 381-388.

Jeffrey, S.W., Mantoura, R.F.C. & Wright S.W. 2005. Phytoplankton pigments in oceanography: Guidelines to modern methods. UNESCO. 667p.

Jeffryes, C., Rosenberger, J. & Rorrer, G.L. (2013). Fed-batch cultivation and bioprocess modeling of *Cyclotella* sp. for enhanced fatty acid production by controlled silicon limitation. *Algal Research*, **2**, 16-27.

Jiang, H. & Gao, K. (2004). Effects of lowering temperature during culture on the production of polyunsaturated fatty acids in the marine diatom *Phaeodactylum tricornutum* (Bacillariophyceae). *Journal of Phycology*, **40**(4), 651-654.

Jose, J., & Burgess, K. (2006). Benzophenoxazine-based fluorescent dyes for labeling biomolecules. *Tetrahedron*, **62**(48), 11021-11037.

Kaiser, K., & Benner, R. (2005). Hydrolysis-induced racemization of amino acids. *Limnology and Oceanography: Methods*, **3**(8), 318-325.

Kakinuma, M., Coury, D. A., Kuno, Y., Itoh, S., Kozawa, Y., Inagaki, E., ... & Amano, H. (2006). Physiological and biochemical responses to thermal and salinity stresses in a sterile mutant of *Ulva pertusa* (Ulvales, Chlorophyta). *Marine Biology*, **149**(1), 97-106.

Kalacheva, G. S., Zhila, N. O., Volova, T. G., & Gladyshev, M. I. (2002). The effect of temperature on the lipid composition of the green alga *Botryococcus*. *Microbiology*, **71**(3), 286-293.

Kana, T. M., Geider, R. J., & Critchley, C. (1997). Regulation of photosynthetic pigments in micro-algae by multiple environmental factors: a dynamic balance hypothesis. *New Phytologist*, **137**(4), 629-638.

Karpagam, R., Raj, K. J., Ashokkumar, B., & Varalakshmi, P. (2015). Characterization and fatty acid profiling in two fresh water microalgae for biodiesel production: Lipid enhancement methods and media optimization using response surface methodology. *Bioresource technology*, **188**, 177-184.

Karsten, U., Schumann, R., Rothe, S., Jung, I., & Medlin, L. (2006). Temperature and light requirements for growth of two diatom species (Bacillariophyceae) isolated from an Arctic macroalga. *Polar Biology*, **29**(6), 476-486.

Karwath, B., Janofske, D., Tietjen, F. & Willems, H. (2000). Temperature effects on growth and cell size in the marine calcareaous dinoflagellate *Thoracospaera heimii*. *Marine Micropaleontology,* **39***,* 43-51.

Kaye, Y., Grundman, O., Leu, S., Zarka, A., Zorin, B., Didi-Cohen, S., ... & Boussiba, S. (2015). Metabolic engineering toward enhanced LC-PUFA biosynthesis in *Nannochloropsis oceanica*: Overexpression of endogenous Δ12 desaturase driven by stress-inducible promoter leads to enhanced deposition of polyunsaturated fatty acids in TAG. *Algal Research*, **11**, 387-398.

Kiatmetha, P., Siangdang, W., Bunnag, B., Senapin, S., & Withyachumnarnkul, B. (2011). Enhancement of survival and metamorphosis rates of *Penaeus monodon* larvae by feeding with the diatom *Thalassiosira weissflogii*. *Aquaculture International*, *19*(4), 599-609.

Kiefer, D. A. & Mitchell, B. G. (1983). A simple, steady state description of phytoplankton growth based on absorption cross section and quantum efficiency. *Limnology and Oceanography*, **28**(4), 770-776.

Kilham, S., Kreeger, D., Goulden, C., & Lynn, S. (1997). Effects of nutrient limitation on biochemical constituents of *Ankistrodesmus falcatus*. *Freshwater Biology*, **38**(3), 591-596.

Kirk, J. T. O. (1994). Light and Photosynthesis in Aquatic Ecosystems. Cambridge University Press, Cambridge, 509 pp.

Kirk, J. T. O. (1976). A theoretical analysis of the contribution of algal cells to the attenuation of light within natural waters. *New Phytologist*, **77**(2), 341-358.

Klaas, C., & Archer, D. E. (2002). Association of sinking organic matter with various types of mineral ballast in the deep sea: Implications for the rain ratio. *Global Biogeochemical Cycles*, **16**(4), 63-71.

Klausmeier, C. A., Litchman, E., Daufresne, T. & Levin, S. A. (2004). Optimal nitrogen-to-phosphorus stoichiometry of phytoplankton. *Nature,* **429***,* 171-174.

Klein Breteler, W.C.M., Schogt, N. & Rampen, S.W. (2005). Effect of diatom nutrient limitation on copepod development: the role of essential lipids. *Marine Ecology Progress Series,* 291, 125-133.

Klyachko-Gurvich, G. L., Tsoglin, L. N., Doucha, J., Kopetskii, J., & Semenenko, V. E. (1999). Desaturation of fatty acids as an adaptive response to shifts in light intensity. *Physiologia Plantarum*, **107**(2), 240-249.

Knothe, G. (2012). Fuel properties of highly polyunsaturated fatty acid methyl esters. Prediction of fuel properties of algal biodiesel. *Energy Fuels*, **26**, 5265–5273.

Koester, J. A., Brawley, S. H., Karp-Boss, L., & Mann, D. G. (2007). Sexual reproduction in the marine centric diatom *Ditylum brightwellii* (Bacillariophyta).*European Journal of Phycology*, **42**(4), 351-366.

Kolber, Z., Zehr, J., & Falkowski, P. (1988). Effects of growth irradiance and nitrogen limitation on photosynthetic energy conversion in photosystem II. *Plant Physiology*, **88**(3), 923-929.

Kováčik, J., Klejdus, B., Hedbavny, J., & Bačkor, M. (2010). Effect of copper and salicylic acid on phenolic metabolites and free amino acids in *Scenedesmus quadricauda* (Chlorophyceae). *Plant Science*, **178**(3), 307-311.

Kramer, J. G. & Morris, I. (1990). Growth regulation in irradiance limited marine *Synechococcus* sp. WH 7803. *Archives of microbiology,* **154**, 286-293.

Krawiec, R. W. (1982). Autecology and clonal variability of the marine centric diatom *Thalassiosira rotula* (Bacillariophyceae) in response to light, temperature and salinity. *Marine Biology*, **69**(1), 79-89.

Krishnamoorthy, G. & Ira (2001). Fluorescence lifetime distribution in characterizing membrane microheterogeneity. *Journal of Fluorescence*, **11**(4), 247-253.

Kuebler, J. E., Davison, I. R. & Yarish, C. (1991). Photosynthetic adaptation to temperature in the red algae *Lomentaria baileyana* and *Lomentaria orcadensis*. *Europe Journal of Phycology.* **26**, 9–19.

Kuebler, J. E., Davison, I. R., & Yarish, C. (1991). Photosynthetic adaptation to temperature in the red algae *Lomentaria baileyana* and *Lomentaria orcadensis*. *British Phycological Journal*, **26**(1), 9-19.

Lacour, T., Sciandra, A., Talec, A., Mayzaud, P., & Bernard, O. (2012). Neutral lipid and carbohydrate productivities as a response to nitrogen status in *Isochrysis* sp. (T-iso; haptophyceae): starvation versus limitation. *Journal of phycology*, **48**(3), 647-656.

Lassen, M. K., Nielsen, K. D.,Richardson, K., Garde, K. & Schlüter, L. (2010). The effects of temperature increases on a temperate phytoplankton community-A mesocosm climate change scenario. *Journal of Experimental Marine Biology and Ecology*, **383**, 79-88.

Latasa, M. (1995). Pigment composition of *Heterocapsa* sp. and *Thalassiosira weissflogii* growing in batch cultures under different irradiances. *Scientia Marina*, **59**(1), 25-37.

Laws, E. A., & Bannister, T. T. (1980). Nutrient- and light limited growth of *Thalassiosira fluviatilis* in continuous culture, with implications for phytoplankton growth in the ocean. *Limnology Oceanography*, **25**, 457-473.

Le Bouteiller, A., Leynaert, A., Landry, M. R., Le Borgne, R., Neveux, J., Rodier, M., ... & Brown, S. L. (2003). Primary production, new production, and growth rate in the equatorial Pacific: Changes from mesotrophic to oligotrophic regime. *Journal of Geophysical Research: Oceans (1978–2012)*, **108**(C12).

Lee, Y. K., & Shen, H. (2004). Basic Culturing Techniques. *Handbook of microalgal culture: biotechnology and applied phycology*, Edited by Amos Richmond, Blackwell Publishing Ltd 40-56p.

Lee, S. J., Yoon, B. D., & Oh, H. M. (1998). Rapid method for the determination of lipid from the green alga *Botryococcus braunii*. *Biotechnology Techniques*, **12**(7), 553-556.

Lefebvre, S. C., Benner, I., Stillman, J. H., Parker, A. E., Drake, M. K., Rossignol, P. E., Okimura, K. M., Komada, T. & Carpenter, E. J. (2012). Nitrogen source and pCO_2 synergistically affect carbon allocation, growth and morphology of the coccolithophore *Emiliania huxleyi*: potential implications of ocean acidification for the carbon cycle. *Global Change Biology,* **18***,* 493-503.

Leonados, N. & Harris, G. N. (2006). Comparative effects of light on pigment of two strains of *Emiliania Huxleyi* (Haptophyta). *Journal of phycology,* **42***,* 1217-1224.

Lepetit, B., Volke, D., Gilbert, M., Wilhelm, C., & Goss, R. (2010). Evidence for the existence of one antenna-associated, lipid-dissolved and two protein-bound pools of diadinoxanthin cycle pigments in diatoms. *Plant Physiology*, **154**(4), 1905-1920.

Lepp, P. W., & Schmidt, T. M. (1998). Nucleic acid content of *Synechococcus* spp. during growth in continuous light and light/dark cycles. *Archives of microbiology*, **170**(3), 201-207.

Leuchtenberger, W., Huthmacher, K., & Drauz, K. (2005). Biotechnological production of amino acids and derivatives: current status and prospects. *Applied Microbiology and Biotechnology*, **69**(1), 1-8.

Li, W. K. W. (1980). Temperature adaptation in phytoplankton: Cellular and photosynthetic characteristics. In Falkowski, P.G. (ed.) *Primary productivity in the sea*. Plenum Press, New York, pp. 259-279.

Li, Y., Han, D., Sommerfeld, M., & Hu, Q. (2011). Photosynthetic carbon partitioning and lipid production in the oleaginous microalga *Pseudochlorococcum* sp. (Chlorophyceae) under nitrogen-limited conditions. *Bioresource Technology*, **102**(1), 123-129.

Liang, Y., Beardall, J. & Heraud, P. (2006). Effects of nitrogen source and UV radiation on the growth, chlorophyll fluorescence and fatty acid composition of *Phaeodactylum tricornutum*and *Chaetoceros muelleri* (Bacillariophyceae). *Journal of Photochemistry and Photobiology B: Biology,* **82**(3), 161-172.

Liang, Y., Beardall, J., & Heraud, P. (2006). Changes in growth, chlorophyll fluorescence and fatty acid composition with culture age in batch cultures of *Phaeodactylum tricornutum* and *Chaetoceros muelleri* (Bacillariophyceae). *Botanica Marina*, **49**(2), 165-173.

Lin, Y. H., Chang, F. L., Tsao, C. Y., & Leu, J. Y. (2007). Influence of growth phase and nutrient source on fatty acid composition of *Isochrysis galbana* CCMP 1324 in a batch photoreactor. *Biochemical Engineering Journal*, **37**(2), 166-176.

Liu, B. H., & Lee, Y. K. (2000). Secondary carotenoids formation by the green alga *Chlorococcum* sp. *Journal of Applied Phycology*, **12**(3-5), 301-307.

Liu, J., Mukherjee, J., Hawkes, J. J., & Wilkinson, S. J. (2013). Optimization of lipid production for algal biodiesel in nitrogen stressed cells of *Dunaliella salina* using FTIR analysis. *Journal of Chemical Technology and Biotechnology*, **88**(10), 1807-1814.

Liu, J., Sun, Z., Zhong, Y., Huang, J., Hu, Q. & Chen, F. (2012). Stearoyl-acyl carrier protein desaturase gene from the oleaginous microalga *Chlorella zofingiensis*: cloning, characterization and transcriptional analysis*. Planta,* **236** *(*6), 1665**–**1676.

Liu, J., Yuan, C., Hu, G., & Li, F. (2012). Effects of light intensity on the growth and lipid accumulation of microalga Scenedesmus sp. 11-1 under nitrogen limitation. *Applied Biochemistry and Biotechnology*, **166**(8), 2127-2137.

Lomas, M. W. & Glibert, P. M. (1999). Temperature regulation of nitrate uptake: a novel hypothesis about nitrate uptake and reduction in cool-water diatoms. *Limnology Oceanography,* **44**, 556-572.

Lomas, M. W., & Glibert, P. M. (1999). Interactions between NH_4^+ and NO_3^- uptake and assimilation: comparison of diatoms and dinoflagellates at several growth temperatures. *Marine Biology*, **133**(3), 541-551.

Los, D. A., Mironov, K. S. & Allakhverdiev, S. I. (2013). Regulatory role of membrane fluidity in gene expression and physiological functions. *Photosynthesis Research*, **116**(2-3), 489-509.

Lovrien, R., & Matulis, D. (1995). Assays for total protein. *Current Protocols in Protein Science*.

Lynn, S. G., Kilham, S. S., Kreeger, D. A., & Interlandi, S. J. (2000). Effect of nutrient availability on the biochemical and elemental stoichiometry in the freshwater diatom *Stephanodiscus minutulus* (bacillariophyceae). *Journal of Phycology*, **36**(3), 510-522.

Man, N., & Carr, N. G. (1974). Control of macromolecular composition and cell division in the blue-green alga *Anacystis nidulans*. *Journal of general microbiology*, **83**(2), 399-405.

Mansour, M.P., Frampton, D.M.F., Nichols, P.D., Volkman, J.K. & Blackburn, S.I. 2005. Lipid and fatty acid yield of nine stationary-phase microalgae: applications and unusual C24-C28 polyunsaturated fatty acids. *Journal of Applied Phycology*, **17**, 287-300.

Masojídek, J., Torzillo, G., Kopecký, J., Koblížek, M., Nidiaci, L., Komenda, J., ... & Sacchi, A. (2000). Changes in chlorophyll fluorescence quenching and pigment composition in the green alga *Chlorococcum* sp. grown under nitrogen deficiency and salinity stress. *Journal of Applied Phycology*, **12**, 417-426.

Matsuzaki, M., Misumi, O., Shini, T., Maruyama, S., Takahara, M., Miyagishima, S. Y., ... & Kuroiwa, T. (2004). Genome sequence of the ultrasmall unicellular red alga *Cyanidioschyzon merolae* 10D. *Nature*, **428**(6983), 653-657.

McKew, B. A., Davey, P., Finch, S. J., Hopkins, J., Lefebvre, S. C., Metodiev, M. V., ... & Geider, R. J. (2013). The trade-off between the light-harvesting and photoprotective functions of fucoxanthin-chlorophyll proteins dominates light acclimation in *Emiliania huxleyi* (clone CCMP 1516). *New Phytologist*, **200**(1), 74-85.

McKew, B. A., Lefebvre, S. C., Achterberg, E. P., Metodieva, G., Raines, C. A., Metodiev, M. V. & Geider, R. J. (2013). Plasticity in the proteome of *Emiliania huxleyi* CCMP 1516 to extremes of light is highly targeted. *New Phytologist*, **200**(1), 61-73.

Melis, A. (1991). Dynamics of photosynthetic membrane composition and function. *Biochimica et Biophysica Acta (BBA)-Bioenergetics*, **1058**(2), 87-106.

Mendoza, H., Martel, A., Del Río, M. J., & Reina, G. G. (1999). Oleic acid is the main fatty acid related with carotenogenesis in *Dunaliella salina*. *Journal of Applied Phycology*, **11**(1), 15-19.

Merchant, S. S., Prochnik, S. E., Vallon, O., Harris, E. H., Karpowicz, S. J., Witman, G. B., ... & Mittag, M. (2007). The *Chlamydomonas* genome reveals the evolution of key animal and plant functions. *Science*, **318**(5848), 245-250.

Mezcua, M., Agüera, A., Lliberia, J. L., Cortés, M. A., Bagó, B., & Fernández-Alba, A. R. (2006). Application of ultra performance liquid chromatography–tandem mass spectrometry to the analysis of priority pesticides in groundwater.*Journal of Chromatography A*, **1109**(2), 222-227.

Miller, C. B. & Wheeler, P. A. (2012). Biological oceanography. John Wiley & Sons, Ltd. pp 464.

Mimouni, V., Ulmann, L., Pasquet, V., Mathieu, M., Picot, L., Bougaran, G., Cadoret, J.P., Manceau, A.M. & Schoefs, B. (2012). The potential of microalgae for the production of bioactive molecules of pharmaceutical interest. *Current Pharmaceutical Biotechnology*, **13**(15), 2733-2750.

Miyachi, S., Miyachi, S., & Kamiya, A. (1978). Wavelength effects on photosynthetic carbon metabolism in *Chlorella*. *Plant and Cell Physiology*, **19**(2), 277-288.

Moal, J., Martin-Jezequel, V., Harris, R. P., Samain, J. F., & Poulet, S. A. (1987). Interspecific and intraspecific variability of the chemical-composition of marine-phytoplankton. *Oceanologica acta*, **10**(3), 339-346.

Mock, T., & Kroon, B. M. (2002). Photosynthetic energy conversion under extreme conditions-I: Important role of lipids as structural modulators and energy sink under N-limited growth in Antarctic sea ice diatoms. *Phytochemistry*, **61**(1), 41-51.

Mohan, S. V., & Devi, M. P. (2012). Fatty acid rich effluent from acidogenic biohydrogen reactor as substrate for lipid accumulation in heterotrophic microalgae with simultaneous treatment. *Bioresource technology*, **123**, 627-635.

Mojaat, M., Pruvost, J., Foucault, A., & Legrand, J. (2008). Effect of organic carbon sources and Fe^{2+} ions on growth and β-carotene accumulation by *Dunaliella salina*. *Biochemical Engineering Journal*, **39**(1), 177-184.

Montagnes, D. J. S. & Franklin, D. J. (2001). Effect of temperature on diatom volume, growth rate, and carbon and nitrogen content: reconsidering some paradigms. *Limnology and Oceanography*, **46**, 2008-2018.

Morán, X. A., Lopez-Urrutia, A., Calvo-Diaz, A. & Li, W. K. W. (2010). Increasing importance of small phytoplankton in a warmer ocean. *Global Change Biology*, **16**(3), 1137-1144.

Morgan-Kiss, R. M., Priscu, J. C., Pocock, T., Gudynaite-Savitch, L., & Huner, N. P. (2006). Adaptation and acclimation of photosynthetic microorganisms to permanently cold environments. *Microbiology and Molecular Biology Reviews*, **70**(1), 222-252.

Morris, I. & Glover, H. E. (1974). Questions on the mechanism of temperature adaptation in marine phytoplankton. *Marine Biology*, **24**,147-154.

Morris, I., Glover, H. E., & Yentsch, C. S. (1974). Products of photosynthesis by marine phytoplankton: the effect of environmental factors on the relative rates of protein synthesis. *Marine Biology*, **27**(1), 1-9.

Mouget, J. L., Tremblin, G., Morant-Manceau, A., Morançais, M., & Robert, J. M. (1999). Long-term photoacclimation of *Haslea ostrearia* (Bacillariophyta): effect of irradiance on growth rates, pigment content and photosynthesis. *European Journal of Phycology*, **34**(2), 109-115.

Mousing, E. A., Ellegaard, M. & Richardson, K. (2014). Global patterns in phytoplankton community size structure-evidence for a direct temperature effect. *Marine Ecology Progress Series*, **497**, 25-38.

Mozaffarian, D., & Wu, J. H. (2011). Omega-3 fatty acids and cardiovascular disease: Effects on risk factors, molecular pathways, and clinical events.*Journal of the American College of Cardiology*, **58**(20), 2047-2067.

Msanne, J., Xu, D., Konda, A.R., Casas-Mollano, J.A., Awada, T., Cahoon, E.B. & Cerutti, H. (2012). Metabolic and gene expression changes triggered by nitrogen deprivation in the photoautotrophically grown microalgae *Chlamydornonas reinhardtii* and *Coccomyxa* sp. C-169. *Phytochemistry,* **75***,* 50–59.

Mulbry, W., Kondrad, S., & Buyer, J. (2008). Treatment of dairy and swine manure effluents using freshwater algae: fatty acid content and composition of algal biomass at different manure loading rates. *Journal of Applied Phycology*, **20**(6), 1079-1085.

Murata N. & Sato N. (1978). Studies on the absorption spectra of chlorophyll *a* in aqueous dispersions of lipids from the photosynthetic membranes. *Plant and Cell Physiology,* **19**(3): 401-410.

Murata, N., & Fork, D. C. (1975). Temperature dependence of chlorophyll *a* fluorescence in relation to the physical phase of membrane lipids algae and higher plants. *Plant Physiology*, **56**(6), 791-796.

Naidu, B.P., Paleg, L.G, Aspinall, D., Jennings, A.C., Jones, G.P. (1991). Amino acid and glycine-betaine accumulation in cold stressed seedlings. *Phytochemistry*, **30,** 407-409.

Nakahara, T., Yokochi, T., Higashihara, T., Tanaka, S., Yaguchi, T. & Honda, D. (1996). Production of docosahexaenoic and docosapentaenoic acids by *Schizochytrium* sp. isolated from Yap Islands. *Journal of the American Oil Chemists' Society*, **73**(11), 1421-1426.

Nakamura, Y., & Imamura, M. (1983). Change in properties of starch when photosynthesized at different temperatures in *Chlorella vulgaris*. *Plant science letters*, **31**(2), 123-131.

Nakamura, Y., & Miyachi, S. (1982). Effect of temperature on starch degradation in *Chlorella vulgaris* 11h cells. *Plant and Cell Physiology*, **23**(2), 333-341.

Natunen, K., Seppälä, J., Schwenk, D., Rischer, H., Spilling, K., & Tamminen, T. (2014). Nile red staining of phytoplankton neutral lipids: species-specific fluorescence kinetics in various solvents. *Journal of Applied Phycology*, **27**(3), 1161-1168.

Nicklisch, A. & Steinberg, C. E. W. (2009). RNA/protein and RNA/DNA ratios determined by flow cytometry and their relationship to growth limitation of selected planktonic algae in culture *European Journal of Phycology,* **44**(3), 297-308.

Nimer, N. A., Guan, Q. & Merrett, M. J. (1994). Extra- and Intra-celular carbonic anhydrase in relation to culture age in a high-calcificying strain of *Emiliania huxleyi* Lohmann. *New Phytologist*, **126**, 601-607.

Nishida, I., & Murata, N. (1996). Chilling sensitivity in plants and cyanobacteria: The crucial contribution of membrane lipids. *Annual review of plant biology*, **47**(1), 541-568.

Nishikawa, T., & Yamaguchi, M. (2006). Effect of temperature on light-limited growth of the harmful diatom *Eucampia zodiacus* Ehrenberg, a causative organism in the discoloration of *Porphyra* thalli. *Harmful Algae*, **5**(2), 141-147.

Niyogi, K. K. (1999). Photoprotection revisited: genetic and molecular approaches. *Annual Review of Plant Biology*, **50**(1), 333-359.

Olson, R. J., Vaulot, D., & Chisholm, S. W. (1986). Effects of environmental stresses on the cell cycle of two marine phytoplankton species. *Plant Physiology*, **80**(4), 918-925.

Öquist, G. (1983). Effects of low temperature on photosynthesis. *Plant, Cell & Environment*, **6**(4), 281-300.

Ördög, V., Stirk, W. A., Bálint, P., van Staden, J., & Lovász, C. (2012). Changes in lipid, protein and pigment concentrations in nitrogen-stressed *Chlorella minutissima* cultures. *Journal of Applied Phycology*, **24**(4), 907-914.

Osborne, B. A., & Geider, R. J. (1986). Effect of nitrate-nitrogen limitation on photosynthesis of the diatom *Phaeodactylum tricornutum* Bohlin (Bacillariophyceae). *Plant, Cell & Environment*, **9**(8), 617-625.

Otero, A., Domínguez, A., Lamela, T., García, D., & Fábregas, J. (1998). Steady-states of semicontinuous cultures of a marine diatom: Effect of saturating nutrient concentrations. *Journal of Experimental Marine Biology and Ecology*, **227**(1), 23-33.

Ou, K., Wilkins, M. R., Yan, J. X., Gooley, A. A., Fung, Y., Sheumack, D., & Williams, K. L. (1996). Improved high-performance liquid chromatography of amino acids derivatised with 9-fluorenylmethyl chloroformate. *Journal of Chromatography A*, **723**(2), 219-225.

Paasche, E. (2002). A review of the coccolithophorid *Emiliania huxleyi* (Prymnesiophyceae), with particular reference to growth, coccolith formation, and calcification−photosynthesis interactions. *Phycologia*, **40**, 503-529.

Palenik, B., Grimwood, J., Aerts, A., Rouzé, P., Salamov, A., Putnam, N., ... & Grigoriev, I. V. (2007). The tiny eukaryote *Ostreococcus* provides genomic insights into the paradox of plankton speciation. *Proceedings of the National Academy of Sciences*, **104**(18), 7705-7710.

Parrott, L. M., & Slater, J. H. (1980). The DNA, RNA and protein composition of the cyanobacterium *Anacystis nidulans* grown in light-and carbon dioxide-limited chemostats. *Archives of microbiology*, **127**(1), 53-58.

Patil, V., Källqvist, T., Olsen, E., Vogt, G. & Gislerød, H. R. (2007). Fatty acid composition of 12 microalgae for possible use in aquaculture feed. *Aquaculture International*, **15**(1), 1-9.

Pennington, F., Guillard, R. R., & Liaaen-Jensen, S. (1988). Carotenoid distribution patterns in Bacillariophyceae (diatoms). *Biochemical Systematics and Ecology*, **16**(7), 589-592.

Phatarpekar, P. V., Sreepada, R. A., Pednekar, C. & Achuthankutty, C. T. (2000). A comparative study on growth performance and biochemical composition of mixed culture of *Isochrysis galbana* and *Chaetoceros calcitrans* with monocultures*. Aquaculture*, **181**, 141-155.

Pick, U., & Rachutin-Zalogin, T. (2012). Kinetic anomalies in the interactions of Nile red with microalgae. *Journal of Microbiological Methods*, **88**(2), 189-196.

Pisal, D.S. & Lele, S.S. (2005) Carotenoid production from microalgae, *Dunaliella salina*. *Indian Journal of Biotechnology*, **4**, 476-483.

Platt, T. G. C. L., Gallegos, C. L., & Harrison, W. G. (1980). Photoinhibition of photosynthesis in natural assemblages of marine phytoplankton. *Journal of Marine Research,* **38***,* 687-701.

Poyton, R. O. (1973). Effect of growth rate on the macromolecular composition of *Prototheca zopfii*, a colorless alga which divides by multiple fission. *Journal of bacteriology*, **113**(1), 203-211.

Price, L. L., Yin, K. & Harrison, P. J. (1998). Influence of continuous light and L:D cycles on the growth and chemical composition of Prymnesiophyceae including coccolithophores. *Journal of Experimental Marine Biology and Ecology*, **223**, 223–234.

Priscu, J.C., Priscu, L.R., Palmisano, A.C. & Sullivan, C.W., 1990. Estimation of neutral lipid-levels in Antarctic Sea ice microalgae by Nile red fluorescence. *Antarctic Science,* **2***,* 149-155.

Pulz, O., & Gross, W. (2004). Valuable products from biotechnology of microalgae. *Applied Microbiology and Biotechnology*, **65**(6), 635-648.

Rabbani, S., Beyer, P., Lintig, J. V., Hugueney, P., & Kleinig, H. (1998). Induced β-carotene synthesis driven by triacylglycerol deposition in the unicellular alga *Dunaliella bardawil*. *Plant Physiology*, **116**(4), 1239-1248.

Quinlan, A. V. (1986). A semicontinuous culture model that links cell growth to extracellular nutrient concentration. *Biotechnology and Bioengineering*, **28**(10), 1455-1461.

Radwan, S. S. (1991). Sources of C20-polyunsaturated fatty acids for biotechnological use. *Applied Microbiology and Biotechnology*, **35**(4), 421-430.

Raghavan, G., Haridevi, C. K. & Gopinathan, C. P. (2008). Growth and proximate composition of the *Chaetoceros calcitrans* f. *pumilus* under different temperature, salinity and carbon dioxide levels. *Aquaculture Research*, **39**, 1053-1058.

Rajadurai, M., Poornima, E. H., Narasimhan, S. V., Rao, V. N. R., & Venugopalan, V. P. (2005). Phytoplankton growth under temperature stress: laboratory studies using two diatoms from a tropical coastal power station site.*Journal of Thermal Biology*, **30**(4), 299-305.

Ras, M., Steyer, J. P., & Bernard, O. (2013). Temperature effect on microalgae: a crucial factor for outdoor production. *Reviews in Environmental Science and Bio/Technology*, **12**(2), 153-164.

Rausch, T. (1981). The estimation of micro-algal protein content and its meaning to the evaluation of algal biomass I. Comparison of methods for extracting protein. *Hydrobiologia*, **78**(3), 237-251.

Raven, J. A. (2013). RNA function and phosphorus use by photosynthetic organisms. *Frontiers in plant science*, **4**, 1-13.

Raven, J.A.V. & Geider, R.J. (1988). Temperature and algal growth. *New Phytology*, **110**, 441-461.

Redalje, D. G., & Laws, E. A. (1983). The effects of environmental factors on growth and the chemical and biochemical composition of marine diatoms. I. Light and temperature effects. *Journal of Experimental Marine Biology and Ecology*, **68**(1), 59-79.

Reef, R., Pandolfi, J. M., & Lovelock, C. E. (2012). The effect of nutrient enrichment on the growth, nucleic acid concentrations, and elemental stoichiometry of coral reef macroalgae. *Ecology and evolution*, **2**(8), 1985-1995.

Reichert, C. D. C., Reinehr, C. O. & Costa, J. A. V. (2006). Semicontinuous cultivation of the cyanobacterium *Spirulina platensis* in a closed photobioreactor. *Brazilian Journal of Chemical Engineering*, **23**(1), 23-28.

Reitan, K. I., Rainuzzo, J. R., & Olsen, Y. (1994). Effect of nutrient limitation on fatty acid and lipid content of marine Microalgae. *Journal of Phycology*, **30**(6), 972-979.

Renaud, S. M., Thinh, L. V., Lambrinidis, G. & Parry, D. L. (2002). Effect of temperature on growth, chemical composition and fatty acid composition of tropical Australian microalgae grown in batch cultures. *Aquaculture*, **211**(1), 195-214.

Renaud, S. M., Zhou, H. C., Parry, D. L., Thinh, L. V. & Woo, K. C. (1995). Effect of temperature on the growth, total lipid content and fatty acid composition of recently isolated tropical microalgae *Isochrysis* sp., *Nitzschia closterium*, *Nitzschia paleacea*, and commercial species *Isochrysis* sp. (clone T. ISO). *Journal of Applied phycology*, **7**(6), 595-602.

Rhee, G. Y. (1989). Continuous culture algal bioassays for organic pollutants in aquatic ecosystems. *Hydrobiologia*, **188**(1), 247-258.

Rhee, G., & Gotham, I. J. (1981). The effect of environmental factors on phytoplankton growth: Temperature and the interactions of temperature with nutrient limitation. *Limnology and Oceanography*, **26**(4), 635-648.

Rhee, G.Y. (1982). Effects of environmental factors and their interactions on phytoplankton growth. *Advances in Microbial Ecology*, **6**, 33-74.

Ritchie, R. J. (2006). Consistent sets of spectrophotometric chlorophyll equations for acetone, methanol and ethanol solvents. *Photosynthesis Research*, **89**(1), 27-41.

Robertson, K. J., Williams, P. M. & Bada, J. L. (1987). Acid hydrolysis of dissolved combined amino acids in seawater: A precautionary note. *Limnology and oceanography*, **32**(4), 996-997.

Roleda M. Y., Slocombe S. P., Leakey R. J. G., Day J. G., Bell E. M. & Stanley M. S. (2013). Effects of temperature and nutrient regimes on biomass and lipid production by six oleaginous microalgae in batch culture employing a two-phase cultivation strategy. *Bioresource Technology*, **129**, 439-449.

Rontani, J. F., Marty, J. C., Miquel, J. C., & Volkman, J. K. (2006). Free radical oxidation (autoxidation) of alkenones and other microalgal lipids in seawater. *Organic Geochemistry*, **37**(3), 354-368.

Roopnarain, A., Gray, V. M., & Sym, S. (2014). Influence of nitrogen stress on *Isochrysis galbana* strain U4, a candidate for biodiesel production. *Phycological Research*, **62**(4), 237-249.

Rost, B. & Riebesell, U. (2004). Coccolithophores and the biological pump: responses to environmental changes. In: Coccolithophores: form molecular processes to global impact. Hans R. Thlerstein; Jeremy R. Young (Eds.) Berlin, Springer, 99-125.

Rousch J. M., Bingham S. E. & Sommerfeld M. R. (2003). Changes in fatty acid profiles of thermo-intolerant and thermo-tolerant marine diatoms during temperature stress. *Journal of Experimental Marine Biology and Ecology*, **295**, 145-156.

Saavedra, M. D. P. S., & Voltolina, D. (1994). The chemical composition of *Chaetoceros* sp. (Bacillariophyceae) under different light conditions. *Comparative Biochemistry and Physiology Part B: Comparative Biochemistry*, **107**(1), 39-44.

Sakamoto, T., & Bryant, D. A. (1997). Growth at low temperature causes nitrogen limitation in the cyanobacterium *Synechococcus* sp. PCC 7002. *Archives of Microbiology*, **169**(1), 10-19.

Salazar, C., Armenta, J. M., & Shulaev, V. (2012). An UPLC-ESI-MS/MS assay using 6-Aminoquinolyl-N-Hydroxysuccinimidyl Carbamate derivatization for targeted amino acid analysis: application to screening of *Arabidopsis thaliana* mutants. *Metabolites*, **2**(3), 398-428.

Salazar, C., Armenta, J. M., Cortes, D.F. & Shulaev, V. (2012). Combination of AccQ·Taq-Ultra Performance Liquid Chromatographic method with tandem Mass Spectrometry for the analylsis of amino acids. In Alterman, Michail A.; Hunziker, Peter (Eds.) Amino Acid Analysis: Methods and Protocols: *Methods in Molecular Biology*. Vol. 828, 363 pp.

Salleh, S., & McMinn, A. (2011). The effects of temperature on the photosynthetic parameters and recovery of two temperate benthic microalgae, *Amphora* cf. *coffeaeformis* and *Cocconeis* cf. *sublittoralis* (Bacillariophyceae). *Journal of Phycology*, **47**(6), 1413-1424.

Salomon, E., Bar-Eyal, L., Sharon, S., & Keren, N. (2013). Balancing photosynthetic electron flow is critical for cyanobacterial acclimation to nitrogen limitation. *Biochimica et Biophysica Acta (BBA)-Bioenergetics*, **1827**(3), 340-347.

Sandnes, J. M., Källqvist, T., Wenner, D., & Gislerød, H. R. (2005). Combined influence of light and temperature on growth rates of *Nannochloropsis oceanica*: linking cellular responses to large-scale biomass production. *Journal of Applied Phycology*, **17**(6), 515-525.

Sarwar, G., & Botting, H. M. (1989). Rapid analysis of nutritionally important free amino acids in serum and organs (liver, brain, and heart) by liquid chromatography of precolumn phenylisothiocyanate derivatives. *Journal Association of Official Analytical Chemists*, **73**(3), 470-475.

Saurina, J., & Hernandez-Cassou, S. (1994). Determination of amino acids by ion-pair liquid chromatography with post-column derivatization using 1, 2-naphthoquinone-4-sulfonate. *Journal of Chromatography A*, **676**(2), 311-319.

Schlesinger, D. A. & Shuter, B. J. (1981). Patterns of growth and cell composition of freshwater algae in light-limited continuous cultures. *Journal of Phycology*, **17**, 250–6.

Seoane, S., Zapata, M. & Orive, E. (2009). Growth rates and pigment patterns of haptophytes isolated from estuarine waters. *Journal of Sea Research*, **62**(4), 286-294.

Shang, S. F., & Wang, H. (1996). Sensitive determination of amino acids in kelp by reversed phase high performance liquid chromatography with precolumn derivatization using phenylisothiocyanate. *Chromatographia*, **43**(5-6), 309-312.

Sharma, S. S., & Dietz, K. J. (2006). The significance of amino acids and amino acid-derived molecules in plant responses and adaptation to heavy metal stress. *Journal of Experimental Botany*, **57**(4), 711-726.

Shelp, B. J., Bown, A. W., & McLean, M. D. (1999). Metabolism and functions of gamma-aminobutyric acid. *Trends in plant science*, **4**(11), 446-452.

Shimura, S., & Fujita, Y. (1975). Changes in the activity of fucoxanthin-excited photosynthesis in the marine diatom *Phaeodactylum tricornutum* grown under different culture conditions. *Marine Biology*, **33**(3), 185-194.

Shrager, J., Hauser, C., Chang, C. W., Harris, E. H., Davies, J., McDermott, J., ... & Grossman, A. R. (2003). *Chlamydomonas reinhardtii* genome project. A guide to the generation and use of the cDNA information. *Plant Physiology*, **131**(2), 401-408.

Siegenthaler, P. A., & Murata, N. (Eds.). (2006). *Lipids in photosynthesis: structure, function and genetics* (Vol. 6). Advances in photosynthesis and respiration. Kluwer academic publishers, Dordrecht, USA, 324 pp.

Simopoulos, A. P. (2002). The importance of the ratio of omega-6/omega-3 essential fatty acids. *Biomedicine & pharmacotherapy*, **56**(8), 365-379.

Singh, J., & Gu, S. (2010). Commercialization potential of microalgae for biofuels production. *Renewable and Sustainable Energy Reviews*, **14**(9), 2596-2610.
Smetacek, V. (1999). Diatoms and the ocean carbon cycle. *Protist*, **150**(1), 25-32.

Stevenson R.J. & Pan Y. (1999) Assessing environmental conditons in rivers and Streams with diatoms. In The diatoms: applications for the environmental and earth sciences, Stoermer E.F. & Smol J.P. Edt. Cambridge university press, UK. 469 p.

Smith, P. K., Krohn, R. I., Hermanson, G. T., Mallia, A. K., Gartner, F. H., Provenzano, M., ... & Klenk, D. C. (1985). Measurement of protein using bicinchoninic acid. *Analytical biochemistry*, **150**(1), 76-85.

Smith, G. J., Zimmerman, R. C., & Alberte, R. S. (1992). Molecular and physiological responses of diatoms to variable levels of irradiance and nitrogen availability: growth of *Skeletonema costatum* in simulated upwelling conditions. *Limnology and Oceanography*, **37**(5), 989-1007.

Smith, R., Stapleford, L. & Ridings, R. (1994). The acclimated response of growth, photosynthesis, composition, and carbon balance to temperature in the psychrophilic ice diatom *Nitzschia seriata*. *Journal of Phycology,* **30**, 8-16.

Snoeijs, P., Busse, S., & Potapova, M. (2002). The importance of diatom cell size in community analysis. *Journal of Phycology*, **38**(2), 265-281.

Solovchenko, A. E., Khozin-Goldberg, I., Didi-Cohen, S., Cohen, Z., & Merzlyak, M. N. (2008). Effects of light intensity and nitrogen starvation on growth, total fatty acids and arachidonic acid in the green microalga *Parietochloris incisa*. *Journal of Applied Phycology*, **20**(3), 245-251.

Solórzano, L. & Sharp, J. H. (1980). Determination of total dissolved phosphorus and particulate phosphorus in natural waters. *Limnology and Oceanography*, **25**(4), 754-758.

Sorokin, C., & Krauss, R. W. (1958). The Effects of light intensity on the growth rates of green algae. *Plant physiology*, **33**(2), 109.

Sosik, H. M., & Mitchell, B. G. (1991). Absorption, fluorescence, and quantum yield for growth in nitrogen-limited *Dunaliella tertiolecta*. *Limnology and Oceanography*, **36**(5), 910-921.

Sosik, H. M., & Mitchell, B. G. (1994). Effects of temperature on growth, light absorption, and quantum yield in *Dunaliella tertiolecta* (chlorophyceae). *Journal of Phycology*, **30**(5), 833-840.

Sosik, H. M., Chisholm, S. W., & Olson, R. J. (1989). Chlorophyll fluorescence from single cells: Interpretation of flow cytometric signals. *Limnology and Oceanography*, **34**(8), 1749-1761.

Srirangan, S., Sauer, M. L., Howard, B., Dvora, M., Dums, J., Backman, P., & Sederoff, H. (2015). Interaction of temperature and photoperiod increases growth and oil content in the marine microalgae *Dunaliella viridis. PLoS ONE*, **10**(5): e0127562.

Stoermer, E. F. & Julius, M. L. (2003). Centric Diatoms. In: Freshwater Algae of North America (J.D. Wehr & R.G. Sheath, eds), 559-594. Academic Press, Amsterdam.

Stolte, W., Kraay, G. W., Noordeloos, A. A. & Riegman, R. (2000). Genetic and physiological variation in pigment composition of *Emiliania huxleyi* (Prymnesiophyceae) and the potential use of its pigment ratios as a quantitative physiological marker. *Journal of Phycology*, **36**(3), 529-539.

Stramski, D., Sciandra, A., & Claustre, H. (2002). Effects of temperature, nitrogen, and light limitation on the optical properties of the marine diatom *Thalassiosira pseudonana. Limnology and Oceanography*, **47**(2), 392-403.

Strickland, J. D. H. (1968). Continuous measurement of in vivo chlorophyll *a* precautionary note. *Deep-Sea Research*. **15**, 225-227.

Strickland, J.D.H. & Parsons, T.R. (1972). A practical handbook of seawater analysis. Fisheries Research Board of Canada, Ottawa, Canada, 310 pp.

Strzepek, R. F., & Price, N. M. (2000). Influence of irradiance and temperature on the iron content of the marine diatom *Thalassiosira weissflogii* (Bacillariophyceae). *Marine Ecology Progress Series*, **206**, 107-117.

Stuart, M. C., van de Pas, J. C., & Engberts, J. B. (2005). The use of Nile Red to monitor the aggregation behavior in ternary surfactant-water-organic solvent systems. *Journal of Physical Organic Chemistry*, **18**(9), 929-934.

Su, C.H., Chien, L.J., Gomes, J., Lin, Y.S., Yu, Y.K., Liou, J.S. & Syu, R.J. (2011). Factors affecting lipid accumulation by *Nannochloropsis oculata* in a two-stage cultivation process. *Journal of Applied Phycology,* **23** (5), 903-908.

Sukenik, A., Carmeli, Y., & Berner, T. (1989). Regulation of fatty acid composition by irradiance level in the eustigmatophyte *Nannochloropsis* sp. *Journal of Phycology*, **25**(4), 686-692.

Sukhanova, I. N. & Flint, M. V. (1998). Anomalous blooming of coccolithophorids over the eastern Bering Sea shelf. *Oceanology*, **38**, 502-505.

Sun, X., Cao, Y., Xu, H., Liu, Y., Sun, J., Qiao, D., & Cao, Y. (2014). Effect of nitrogen-starvation, light intensity and iron on triacylglyceride/carbohydrate production and fatty acid profile of *Neochloris oleoabundans* HK-129 by a two-stage process. *Bioresource Technology*, **155**, 204-212.

Suroy, M. Moriceau, B., Boutorh, J. & Goutx, M. (2014). Fatty acids associated with the frustules of diatoms and their fate during degradation - A case study in *Thalassiosira weissflogii. Deep Sea Research Part I: Oceanographic Research Papers,* **86**, 21-31.

Sutton, D. C., & Hoegh-Guldberg, O. (1990). Host-zooxanthella interactions in four temperate marine invertebrate symbioses: assessment of effect of host extracts on symbionts. *The Biological Bulletin*, **178**(2), 175-186.

Suzuki, Y. & Takahashi, M. (1995). Growth responses of several diatom species isolated from various environments to temperature. *Journal of Phycology*, 31, 880-888.

Swartz, M. E. (2005). Ultra performance liquid chromatography (UPLC): An introduction. Separation Science Re-Defined. *LCGC Supplement*, **8**, 8-14.

Szabados, L., & Savouré, A. (2010). Proline: a multifunctional amino acid. *Trends in plant science*, **15**(2), 89-97.

Taguchi, S. (1976). Relationship between photosynthesis and cell size of marine diatoms. *Journal of Phycology*, **12**, 185-189.

Taguchi, S., Hirata, J. A. & Laws, E. A. (1987). Silicate deficiency and lipid synthesis of marine diatoms. *Journal of Phycology*, **23**(2), 260-267.

Takeya, K., Kuwata, A., Yoshida, M., & Miyazaki, T. (2004). Effect of dilution rate on competitive interactions between the cyanobacterium *Microcystis novacekii* and the green alga *Scenedesmus quadricauda* in mixed chemostat cultures. *Journal of Plankton Research*, **26**(1), 29-35.

Tang, K. W., & Taal, M. (2005). Trophic modification of food quality by heterotrophic protists: species-specific effects on copepod egg production and egg hatching. *Journal of Experimental Marine Biology and Ecology*, **318**(1), 85-98.

Taraldsvik, M. & Myklestad, S. M. (2000). The effect of pH on growth rate, biochemical composition and extracellular carbohydrate production of the marine diatom *Skeletonema costatum*. *European Journal of Phycology,* **35***,* 189-194.

Taucher, J., Jones, J., James, A., Brzezinski, M. A., Carlson, C. A., Riebesell, U., & Passow, U. (2015). Combined effects of CO_2 and temperature on carbon uptake and partitioning by the marine diatoms *Thalassiosira weissflogii* and *Dactyliosolen fragilissimus*. *Limnology and Oceanography*, **60**(3), 901-919.

Terry, K. L., Hirata, J., & Laws, E. A. (1983). Light-limited growth of two strains of the marine diatom *Phaeodactylum tricornutum* Bohlin: chemical composition, carbon partitioning and the diel periodicity of physiological processes. *Journal of Experimental Marine Biology and Ecology*, **68**(3), 209-227.

Terry, K. L., Hirata, J., & Laws, E. A. (1985). Light-, nitrogen-, and phosphorus-limited growth of *Phaeodactylum tricornutum* Bohlin strain TFX-1: Chemical composition, carbon partitioning, and the diel periodicity of physiological processes. *Journal of Experimental Marine Biology and Ecology*, **86**(1), 85-100.

Tesson, B. & Hildebrand, M. (2013). Characterization and localization of insoluble organic matrices associated with diatom cell walls: insight into their roles during cell wall formation. *PLoS ONE,* **8**.

Thomas, M. K., Kremer, C. T., Klausmeier, C. A., & Litchman, E. (2012). A global pattern of thermal adaptation in marine phytoplankton. *Science*, **338**(6110), 1085-1088.

Thomas, P. H., & Carr, N. G. (1985). The invariance of macromolecular composition with altered light limited growth rate of *Amphidinium carteri* (Dinophyceae). *Archives of microbiology*, **142**(1), 81-86.

Thomas, W. H. (1966). Effects of temperature and illuminance on cell division rates of three species of tropical oceanic phytoplankton, *Journal of Phycology*, **2**, 17-22.

Thompson, P. A., Guo, M. & Harrison, P. J. (1992). Effects of temperature. I. On the biochemical composition of eight species of marine phytoplankton. *Journal of Phycology*, **28**, 481-488.

Thompson, P. A., Guo, M. X., & Harrison, P. J. (1992). Effects of variation in temperature. I. On the biochemical composition of eight species of marine phytoplankton. *Journal of Phycology*, **28**(4), 481-488.

Thompson, P. A., Harrison, P. J. & Whyte, J. N. C. (1990), Influence of irradiance on the fatty acid composition of phytoplankton. *Journal of Phycology*, **26**, 278-288.

Thompson, P. A., Harrison, P. J., & Parslow, J. S. (1991). Influence of irradiance on cell volume and carbon quota for ten species of marine phytoplankton. *Journal of Phycology*, **27**(3), 351-360.

Thorel, M., Fauchot, J., Morelle, J., Raimbault, V., Le Roy, B., Miossec, C., ... & Claquin, P. (2014). Interactive effects of irradiance and temperature on growth and domoic acid production of the toxic diatom *Pseudo-nitzschia* australis (Bacillariophyceae). *Harmful Algae*, **39**, 232-241.

Tibbetts, S. M., Bjornsson, W. J., & McGinn, P. J. (2015). Biochemical composition and amino acid profiles of *Nannochloropsis granulata* algal biomass before and after supercritical fluid CO_2 extraction at two processing temperatures. *Animal Feed Science and Technology*, **204**, 62-71.

Tjahjono, A. E., Hayama, Y., Kakizono, T., Terada, Y., Nishio, N., & Nagai, S. (1994). Hyper-accumulation of astaxanthin in a green alga *Haematococcus pluvialis* at elevated temperatures. *Biotechnology Letters*, **16**(2), 133-138.

Tonon, T., Harvey, D., Larson, T. R. & Graham, I. A. (2002). Long chain polyunsaturated fatty acid production and partitioning to triacylglycerols in four microalgae. *Phytochemistry*, **61**(1), 15-24.

Trabelsi, L., Ouada, H. B., Bacha, H., & Ghoul, M. (2009). Combined effect of temperature and light intensity on growth and extracellular polymeric substance production by the cyanobacterium *Arthrospira platensis*. *Journal of Applied Phycology*, **21**(4), 405-412.

Trench, R. K. (1971). The physiology and biochemistry of zooxanthellae symbiotic with marine coelenterates. III. The effect of homogenates of host tissues on the excretion of photosynthetic products in vitro by zooxanthellae from two marine coelenterates. *Proceedings of the Royal Society of London B: Biological Sciences*, **177**(1047), 251-264.

Tzovenis, I., Fountoulaki, E., Dolapsakis, N., Kotzamanis, I., Nengas, I., Bitis, I., Cladas, Y. & Economou-Amilli, A. (2009). Screening for marine nanoplanktic microalgae from Greek coastal lagoons (Ionian Sea) for use in mariculture. *Journal of Applied Phycology*, **21**,457-469.

Underwood, G. J. & Paterson, D. M. (2003). The importance of extracellular carbohydrate productionby marine epipelic diatoms. *Advances in Botanical Research*, **40**, 183-240.

Utkilen, H. C. (1982). Magnesium-limited growth of the cyanobacterium *Anacystis nidulans*. *Journal of General Microbiology*, **128**(8), 1849-1862.

van de Poll, W. H., Alderkamp, A. C., Janknegt, P. J., Roggeveld, J., & Buma, A. G. (2006). Photoacclimation modulates excessive photosynthetically active and ultraviolet radiation effects in a temperate and an Antarctic marine diatom. *Limnology and Oceanography*, **51**(3), 1239-1248.

van Rijssel, M., & Gieskes, W. W. (2002). Temperature, light, and the dimethylsulfoniopropionate (DMSP) content of *Emiliania huxleyi* (Prymnesiophyceae). *Journal of Sea Research*, **48**(1), 17-27.

Vásquez-Suárez, A., Guevara, M, González, M., Cortez, R. & Arredondo-Vego, B. (2013). Growth and biochemical composition of *Thalassiosira pseudonana* (Thalassiosirales: Thalassiosiraceae) cultivated in semicontinuous system at different culture media and irradiances. *Revista de Biologia Tropical,* **61**(3):1003-13.

Verity, P. G. (1981). Effects of temperature, irradiance, and day length on the marine diatom Leptocylindrus danicus Cleve. I. Photosynthesis and cellular composition. *Journal of Experimental Marine Biology and Ecology*, **55**(1), 79-91.

Volkman, J.K., Jeffrey, S.W., Nichols, P.D., Rogers, G.I. & Garland, C.D. (1989). Fatty acid and lipid composition of 10 species of microalgae used in mariculture. *Journal of Experimental Marine Biology and Ecology,* **128**, 219-240.

Von Bertalanffy, L. (1960). Principles and theory of growth, p. 137-259. In W. N. Nowinski [ed.], Fundamental aspects of normal and malignant growth. Elsevier.

Wada, H., Gombos, Z., & Murata, N. (1994). Contribution of membrane lipids to the ability of the photosynthetic machinery to tolerate temperature stress. *Proceedings of the National Academy of Sciences*, **91**(10), 4273-4277.

Waite, A. & Harrison, P.J. (1992). Role of sinking and ascent during sexual reproduction in the marine diatom *Ditylum brightwell*i. *Marine Ecology Progress Series,* **87**: 113-122.

Walker, J.M. (1996). The bicinchoninic acid (BCA) assay for protein quantitation. In The protein protocols handbook edited by Walker J.M., Humana Press, New Jersey, USA, 809 pp.

Walter, B., Peters, J., van Beusekom, J. E. E., & John, M. S. (2014). Interactive effects of temperature and light during deep convection: a case study on growth and condition of the diatom *Thalassiosira weissflogii. ICES Journal of Marine Science, fsu218.*

Wang, H. T., Meng, Y. Y., Cao, X. P., Ai, J. N., Zhou, J. N., Xue, S. & Wang, W. L. (2015). Coordinated response of photosynthesis, carbon assimilation, and triacylglycerol accumulation to nitrogen starvation in the marine microalgae *Isochrysis zhangjiangensis* (Haptophyta). *Bioresource Technology*, **177**, 282-288.

Wang, X. J., Behrenfeld, M., Le Borgne, R., Murtugudde, R., & Boss, E. (2009). Regulation of phytoplankton carbon to chlorophyll ratio by light, nutrients and temperature in the Equatorial Pacific Ocean: a basin-scale model. *Biogeosciences*, **6**(3), 391.

Watanabe, T. (1993). Importance of docosahexaenoic acid in marine larval fish. *Journal of the World Aquaculture Society*, **24**(2), 152-161.

Wen, Z. Y. & Chen, F. (2003). Heterotrophic production of eicosapentaenoic acid by microalgae. *Biotechnology Advances*, **21**(4), 273-294.

Wen, Z.Y., Jiang, Y. & Chen, F. (2002). High cell density culture of the diatom *Nitzschialaevis* for eicosapentaenoic acid production: fed-batch development. *Process Biochemistry*, **37**(12), 1447-1453.

Westbroek, P., Young, J. R. & Linschooten, K. (1989). Coccolith production (biomineralization) in the marine alga *Emiliania huxleyi*. *Journal of Protozoology*, **36**, 368-73.

White, P. L., Wynn-Williams, D. D., & Russell, N. J. (2000). Diversity of thermal responses of lipid composition in the membranes of the dominant culturable members of an Antarctic fellfield soil bacterial community. *Antarctic Science*, **12**(03), 386-393.

Winter, A., Jordan, R. W. & Roth, P. H. (1994). Biogeography of living coccolithophores in ocean water. In *Coccolithophores* (Ed. By A Winter and W.G. Siesser) Cambridge University Press. pp. 161-177.

Withers, K. J., Grant, A. J., & Hinde, R. (1998). Effects of free amino acids on the isolated symbiotic algae of the coral *Plesiastrea versipora* (Lamarck): absence of a host release factor response. *Comparative Biochemistry and Physiology Part A: Molecular & Integrative Physiology*, **120**(4), 599-607.

Wolfstein, K. & Stal L.J. (2002). Production of extracellular polymeric substances (EPS) by benthic diatoms: the effect of irradiance and temperature. *Marine Ecology Progress Series*, **23**, 613-622.

Worden, A. Z., & Binder, B. J. (2003). Growth regulation of rRNA content in *Prochlorococcus* and *Synechococcus* (marine cyanobacteria) measured by whole-cell hybridization of rRNA - targeted peptide nucleic acids. *Journal of phycology*, **39**(3), 527-534.

Worden, A. Z., Lee, J. H., Mock, T., Rouzé, P., Simmons, M. P., Aerts, A. L., ... & Van de Peer, Y. (2009). Green evolution and dynamic adaptations revealed by genomes of the marine picoeukaryotes *Micromonas*. *Science*, **324**(5924), 268-272.

Wren, S. A., & Tchelitcheff, P. (2006). Use of ultra-performance liquid chromatography in pharmaceutical development. *Journal of Chromatography A*, **1119**(1), 140-146.

Wu, S., Zhang, B., Huang, A., Huan, L., He, L., Lin, A., ... & Wang, G. (2014). Detection of intracellular neutral lipid content in the marine microalgae *Prorocentrum micans* and *Phaeodactylum tricornutum* using Nile red and BODIPY 505/515. *Journal of Applied Phycology*, **26**(4), 1659-1668.

Wynne, D., & Rhee, G. Y. (1986). Effects of light intensity and quality on the relative N and P requirement (the optimum N: P ratio) of marine planktonic algae. *Journal of Plankton Research*, **8**(1), 91-103.

Xia, L., Song, S., & Hu, C. (2015). High temperature enhances lipid accumulation in nitrogen-deprived *Scenedesmus obtusus* XJ-15. *Journal of Applied Phycology*, 1-7.

Xia, S., Wang, K., Wan, L., Li, A., Hu, Q. & Zhang, C. (2013). Production, characterization, and antioxidant activity of fucoxanthin from the marine diatom *Odontella aurita*. *Marine Drugs*, **11**(7), 2667-2681.

Xu, X. L., Ji, W. J., Castell, J. D., & O'dor, R. K. (1994). Influence of dietary lipid sources on fecundity, egg hatchability and fatty acid composition of Chinese prawn (*Penaeus chinensis*) brood stock. *Aquaculture*, **119**(4), 359-370.

Xue, J., Niu, Y. F., Huang, T., Yang, W. D., Liu, J. S., & Li, H. Y. (2015). Genetic improvement of the microalga *Phaeodactylum tricornutum* for boosting neutral lipid accumulation. *Metabolic Engineering*, **27**, 1-9.

Yamanè, T. & Shimazu, S. (1984). Fed-batch techniques in microbial processes, p. 147-194. *In* A. Fiechter [ed.], *Advances in Biochemical Engineering/Biotechnology*.

Yao, S., Brandt, A., Egsgaard, H., & Gjermansen, C. (2012). Neutral lipid accumulation at elevated temperature in conditional mutants of two microalgae species. *Plant Physiology and Biochemistry*, **61**, 71-79.

Yoder, J.A. (1979). Effect of temperature on light-limited growth and chemical composition of *Skeletonema costatum* (Bacillariophyceae). *Journal of Phycology*, **15**, 362-370.

Yokoyama, T., Kan-No, N., Ogata, T., Kotaki, Y., Sato, M., & Nagahisa, E. (2003). Presence of free D-amino acids in microalgae. *Bioscience, Biotechnology, and Biochemistry*, **67**(2), 388-392.

Young, A. & Britton, G. (1990). Photobleaching in the unicellular green alga *Dunaliella parva* 19/9. *Photosynthesis Research*, **25**(2), 129-136.

Yu, E.T., Zendejas, F. J., Lane, P. D., Gaucher, S., Simmons, B. A., & Lane, T. W. (2009). Triacylglycerol accumulation and profiling in the model diatoms *Thalassiosira pseudonana* and *Phaeodactylum tricornutum* (Baccilariophyceae) during starvation. *Journal of Applied Phycology*, **21**(6), 669-681.

Zapata, M., Jeffrey, S. W., Wright, S. W., Rodríguez, F., Garrido, J. L., & Clementson, L. (2004). Photosynthetic pigments in 37 species (65 strains) of Haptophyta: implications for oceanography and chemotaxonomy. *Marine Ecology Progress Series*, **270**, 83-102.

Zapata, M., Rodriguez, F., & Garrido, J. L. (2000). Separation of chlorophylls and carotenoids from marine phytoplankton: a new HPLC method using a reversed phase C8 column and pyridine-containing mobile phases. *Marine Ecology Progress Series*, **195**, 29-45.

Zhu, C. J., Lee, Y. K. & Chao, T. M. (1997). Effects of temperature and growth phase on lipid and biochemical composition of *Isochrysis galbana* TK1. *Journal of Applied Phycology*, **9**, 451-457.

Zondervan, I., Zeebe, R. E., Rost, B. & Riebesell, U. (2001). Decreasing marine biogenic calcification: a negative feedback on rising atmospheric pCO_2. *Global Biogeochemical Cycles,* **15***, 507-516.*

Appendices

Appendix 1. Calculation of free and combined amino acid content

An example of how free and combined amino acid content calculation of *Thalassiosila weissflogii* (chapter 6) were performed follows:

1.1 Free amino acid

The calculation of free amino acid content was determined using the following equations and table 1.

The concentration (pmol μL^{-1}) of the amino acid in the derivatized sample was calculated from the peak area using a standard curve such as glutamic curve (Fig. 1).

Y= aX + b from linear curve of amino acid, where Y is the amino acid concentration (pmol μL^{-1}) and X is the peak area (Area Units = AU).

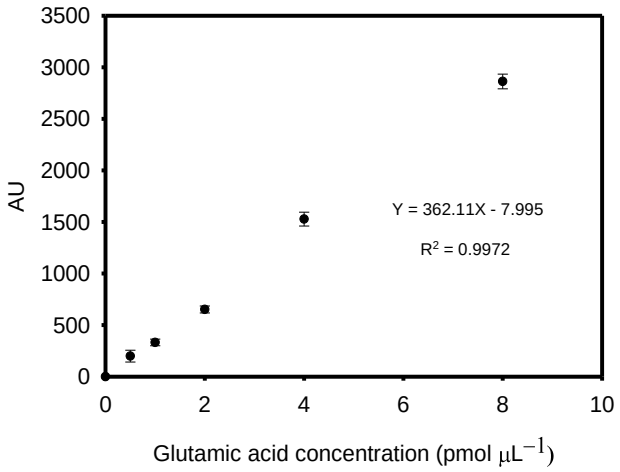

Figure 1. The relationship between concentration of glutamic at concentrations of 0-8 pmol μL^{-1} and AU detected by UPLC.

$$\text{Amino acid (AA) concentration in unit pmol } \mu L^{-1} \text{ from standard curve (column 2)} = \frac{\text{Area unit (AU.) - b}}{\text{Slope (a)}}$$

$$\text{AA concentration on column in unit pmol } \mu L^{-1} \text{ (column 4)} = \text{AA concentration from equation (column 2)} \times \frac{\text{Total derivative solvent (100 µL)}}{\text{Injected sample (2 µL)}}$$

$$\text{AA concentration of culture in unit pmol } \mu L^{-1} \text{ (column 6)} = \text{AA concentration on column in unit pmol } \mu L^{-1} \text{ (column 4)} \times \frac{\text{Total extraction volume (150 µL + 150 µL)}}{\text{Used sample (10 µL)}}$$

$$\text{AA concentration in unit pg cell}^{-1} \text{ (column 8)} = \frac{\text{AA concentration of culture in unit pmol } \mu L^{-1} \text{ (column 6)}}{\text{Cell abundance (cells mL}^{-1})} \times \frac{\text{Molecular weight (column 1)}}{\text{Harvested sample (50 µL)}}$$

Table 1. Data for calculation of fee amino acid content of *Thalassiosila weissflogii* grown at 16 HL.

	Free amino acid								
Amino acid	1	2	3	4	5	6	7	8	9
	MW.	Mean AA (pmol μL^{-1} from equation)	SE	Mean AA (pmol on column)	SE	Mean AA (pmol in culture)	SE	Mean AA (pg $cell^{-1}$)	SE
Arginine	156.19	7.29	0.01	364.59	0.70	9114.65	17.41	0.14	0.00
Serine	87.08	21.05	0.63	1052.72	31.25	26318.03	781.30	0.22	0.01
Glutamic acid	128.6	6.29	2.07	314.64	103.37	7866.08	2584.28	0.10	0.03
Cysteine	103.15	0.39	0.29	19.58	14.65	489.38	366.20	0.01	0.00
Lysine	128.19	4.59	0.73	229.45	36.53	5736.29	913.15	0.07	0.01
Phenylalanine	147.18	4.59	1.63	229.52	81.65	5738.01	2041.36	0.08	0.03
Histidine	137.14	15.27	0.24	763.43	254.62	19085.82	304.66	0.25	0.00
Glycine	57.05	17.34	12.12	866.81	605.84	21670.36	15145.97	0.20	0.04
Threonine	101.11	19.96	1.09	998.00	54.60	24950.11	1365.01	0.24	0.01
Proline	97.12	6.66	0.92	333.14	45.91	8328.46	1147.66	0.08	0.01
Alanine	71.09	5.49	0.61	274.59	30.56	6864.73	763.90	0.05	0.00
Tyrosine	163.18	0.11	0.74	5.33	37.00	133.13	925.06	0.02	0.00
Methionine	131.19	15.57	0.09	778.59	4.45	19464.63	111.24	0.25	0.00
Valine	99.14	8.83	1.29	441.70	64.48	11042.39	1612.08	0.11	0.01
Isoleucine	113.16	5.21	0.64	260.36	32.13	6509.04	803.36	0.07	0.01
Asparagine*	114.6	3.78	1.53	111.79	57.91	2794.78	1447.84	0.04	0.06
Sum								1.93	0.24

* Average of aspartic acid and asparagine

1.2 Combined amino acid

The calculation of combined amino acid content was determined using the following equations and table 2. The concentration (pmol μL^{-1}) of the amino acid in the derivatized sample was calculated from the peak area using a standard curve.

$$\text{Amino acid (AA) concentration in unit pmol } \mu L^{-1} \text{ from standard curve (column 2)} = \frac{\text{Area unit (AU.) - b}}{\text{Slope (a)}}$$

$$\text{AA concentration on column in unit pmol } \mu L^{-1} \text{ (column 4)} = \text{AA concentration from equation (column 2)} \times \frac{\text{Total derivative solvent (100 µL)}}{\text{Injected sample (2 µL)}}$$

$$\text{AA concentration of culture in unit pmol } \mu L^{-1} \text{ (column 6)} = \text{AA concentration on column in unit pmol } \mu L^{-1} \text{ (column 4)} \times \frac{\text{Total volume (extraction 510 µL + resuspension 1.500 µL)}}{\text{Used sample (50 µL)}}$$

$$\text{AA concentration in unit pg cell}^{-1} \text{ (column 8)} = \frac{\text{AA concentration of culture in unit pmol } \mu L^{-1} \text{ (column 6)}}{\text{Cell abundance (cells mL}^{-1}\text{)}} \times \frac{\text{Molecular weight (column 1)}}{\text{Harvested sample (50 µL)}}$$

Percentage of amino acid was calculated:

$$\%\ \text{amino acid} = \frac{\text{Total of each free and combined AA in unit pg cell}^{-1}}{\text{Total of free and combined AA content in unit pg cell}^{-1}} \times 100$$

For example, % aginine of total amino acid

$$\%\ \text{aginine} = \frac{\text{Free AA (aginine = 0.14 pg cell}^{-1}\text{) + Combined AA (aginine = 0.76 pg cell}^{-1}\text{)}}{\text{Total of free AA (aginine = 1.93 pg cell}^{-1}\text{) + Total of combined AA (aginine = 8.38 pg cell}^{-1}\text{)}} \times 100$$

$$\%\ \text{aginine} = \frac{0.90}{10.31} \times 100 = 8.73$$

Table 2. Data for calculation of combined amino acid content in *T. weissflogii* grown at 16 HL.

	T. weissflogii								
Amino acid	1	2	3	4	5	6	7	8	9
	MW.	Mean AA (pmol from equation)	SE.	Mean AA (pmol on column)	SE.	Mean AA (pmol of culture)	SE.	Mean AA (pg cell^{-1})	SE.
Arginine	156.19	24.87	0.71	1243.36	35.65	49982.90	1433.09	0.76	0.03
Histidine	137.14	4.96	0.77	247.85	38.25	9963.62	1537.83	0.13	0.02
Serine	87.08	27.83	0.46	1391.73	22.78	55947.74	915.57	0.47	0.01
Glycine	57.05	34.24	1.23	1711.91	61.27	68818.68	2463.15	0.38	0.02
Glutamic	128.6	41.04	5.86	2051.98	293.10	82489.66	11782.61	1.03	0.15
Threonine	101.11	23.39	0.74	1169.34	36.91	47007.48	1483.78	0.46	0.02
Proline	97.12	25.98	0.83	1298.92	41.58	52216.50	1671.68	0.49	0.02
Alanine	71.09	32.82	2.40	1641.06	120.22	65970.81	4832.76	0.46	0.04
Cysteine	103.15	5.27	0.35	263.74	17.51	10602.36	703.76	0.11	0.01
Lysine	128.19	26.56	4.18	1327.76	209.02	53376.14	8402.59	0.67	0.11
Tyrosine	163.18	14.17	0.26	708.74	13.18	28491.24	529.97	0.45	0.01
Methionine	131.19	9.04	0.58	452.09	28.90	18173.88	1161.97	0.23	0.02
Valine	99.14	28.86	0.91	1442.85	45.55	58002.60	1831.15	0.56	0.02
Phenylalanine	147.18	22.27	1.41	1113.54	70.40	44764.49	2830.06	0.64	0.04
Isoleucine	113.16	24.38	1.37	1219.10	68.71	49007.75	2762.28	0.54	0.03
Asparagine*	114.6	44.82	2.61	2241.21	11.47	90096.71	460.96	0.99	0.16
Sum								8.38	0.70

* Average of aspartic acid and asparagine

Appendix 2: Calculation of pigment composition

Pigment composition from *Emiliania huxleyi* (chapter 5) was employed as a calculation example.

The UPLC chromatograms of 98 % buffered methanol, acetone and *E. huxleyi* were shown in Fig. 2.

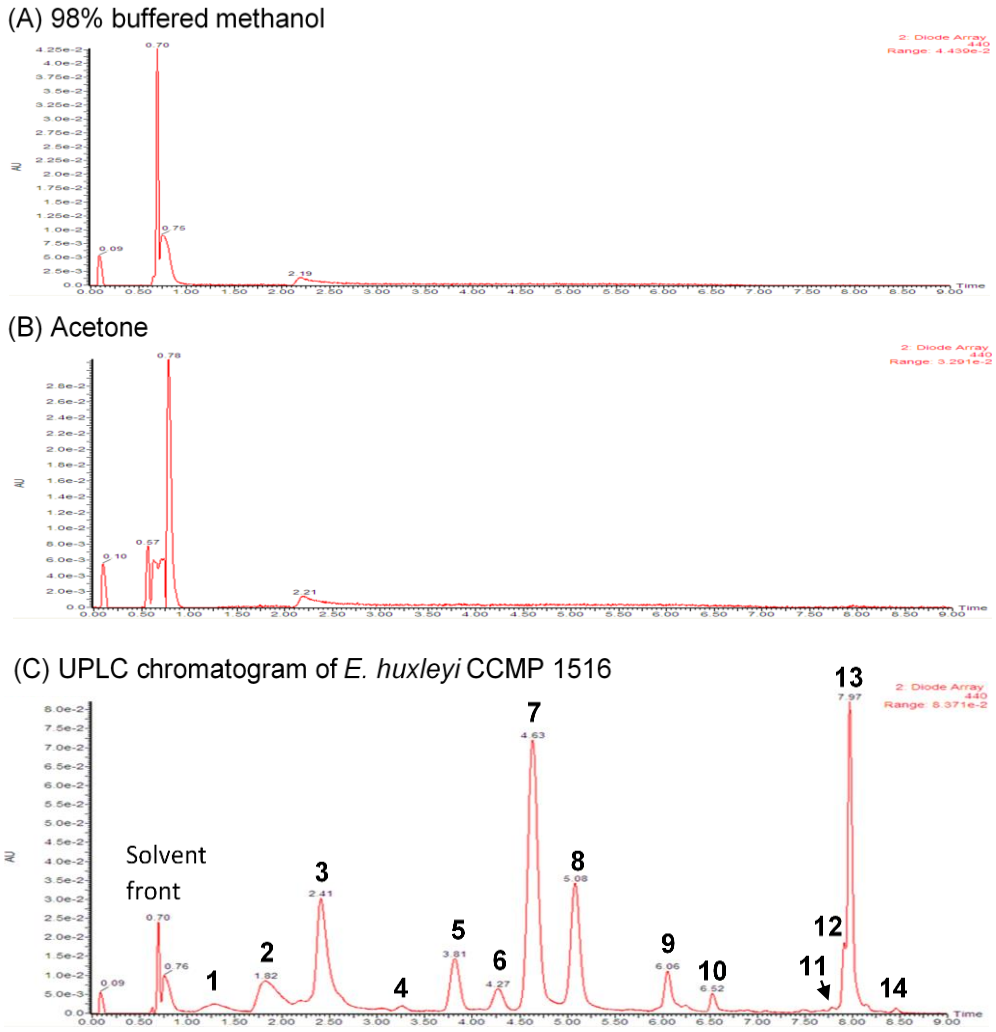

Figure 2. UPLC chromatograms of 98% buffered methanol (A), of acetone (B), and of pigment component of *E. huxleyi* CCMP 1516 (D). Peak identification is as follows: 1=unknown; 2=Chlorophyll C_3 (chl c_3) or Monovinyl chlorophyll c_3 (MV chl c_3); 3= Chllorophyll c_2 (chl c_2); 4= unknown; 5=Fucoxanthin (Fuco); 6= 4-keto-19'-hexanoyloxyfucoxanthin (Hex-kfuco); 7=19'-hexanoyloxyfucoxanthin (Hex-fuco); 8=Diadinoxanthin (DD); 9=Diatoxanthin (DT); 10=unknown; 11=non-polar Chl *a*; 12=unknown; 13= Chlorophyll *a* (chl *a*); 14= β,β-carotene (β,β-car).

An example of how accessory pigment calculation was performed follows:

1). Chlorophyll *a* standard curve preparation

Chlorophyll *a* (chl *a*) powder (C5753-1MG, Sigma Algrich, USA) was dissolved using 2.0 mL 100 % acetone (HPLC glade). Then the chl *a* was scanned from 350- 750 nm using a uv-visible spectrophotometer (GENESIS 10S UV-Vis, Thermo Fisher Scientific Inc.,USA). Chl *a* was determined using the following equation (Jeffrey *et al*. 2005).

$$\text{Chl } a \text{ (g L}^{-1}) = \frac{A_{\lambda\, max}}{\alpha \text{ x } d} \text{x } \frac{Pc}{100}$$

$$= \frac{1.291}{88.15 \text{ x } 1} \text{x } \frac{100}{100}$$

$$= 0.0146454 \text{ g L}^{-1} \text{ or } 14.65 \text{ µg mL}^{-1}$$

Where: $A_{\lambda\, max}$ = the absorbance (absorbance units) at $\lambda\, max$ (662.7 nm)

d = the cuvette path length (cm)

α = the specific extinction coefficient (l g^{-1}cm^{-1}) [α of Chlorophyll a at $\lambda\, max$ (662.7 nm) is 88.15 l g^{-1}cm^{-1} in 100% acetone (Jeffrey *et al*. 2005)]

P_c = chromatographic purity of the primary pigment standard (%) [P_c was assumed 100 % during to a fresh standard and preparation]

The chlorophyll *a* standard curve for pigment assay using UPLC is shown in Fig. 3

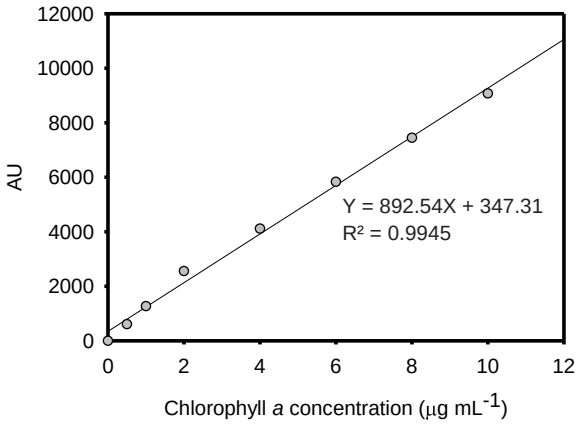

Figure 3. The relationship between chlorophyll *a* concentrations of 1-10 µg mL^{-1} and AU detected by UPLC. Each point in the graph refers to means and standard errors obtained from duplicates.

2) Pigment quantification

Chlorophyll *a* was used as reference pigment. The pigments were quantified as pigment component to chl *a* ratios (mol accessory pigment (mol chl *a*)$^{-1}$). For 4-keto-19'-hexanoyloxyfucoxanthin (Hex-kfuco) whose molar extinction coefficients was not available, the molar extinction coefficient of 19'-hexanoyloxyfucoxanthin (Hex-fuco) was used. The chl c_3 and MV chl c_3 peaks were not separately at 1.82 min (peak no. 2 from fig. 10-2C) called chlorophyll *c* (chl *c*). The molar extinction coefficients (*E*) (Table 3) acquired from Jeffrey *et al.* (2005) were carried out for pigment quantification. The peaks were absorbed at the 440 nm and integrated as area unit (AU).

Table 3. Retention time (min) of pigment component in *E. huxleyii* using UPLC and the molar extinction coefficient (*E*; l $mol^{-1}cm^{-1}$) and wavelength (nm) of pigment component in acetone from Jeffrey *et al*. (2005).

Retention time (min)	Pigment component	Molar extinction coefficient (*E*) (l mol^{-1} cm^{-1})	Wavelength (nm) in acetone
1.82	Chlorophyll c_3	218400	452.9*
	or MV Chlorophyll c_3	218400	452.9**
2.41	Chlorophyll c_2	227000	443.8
3.81	Fucoxanthin	109000	445
4.27	4-keto-19'-hexanoyloxyfucoxanthin	109000	443
4.63	19'-hexanoyloxyfucoxanthin	109000	445
5.08	Diadinoxanthin	130000	447.5
6.05	Diatoxanthin	119000	452
7.97	Chlorophyll *a*	78750	662.7
8.14	β,β-carotene	134000	454

* 100% acetone+1%pyridine

** 90% acetone+1%pyridine

Fucoxanthin, which was employed as a calculation example, was determined using the following equations and table 10-4.

$$E \text{ chl } a \text{ at 440 nm (column 5)} = E \text{ chl } a \text{ at 662.7 nm (see Table 3; 78750)} \times \frac{\text{AU chl } a \text{ at 440 nm (column 1)}}{\text{AU chl } a \text{ at 662.7 nm (column 3)}}$$

$$E \text{ fuco at 443 nm (column 13)} = E \text{ fuco at 443 nm (see Table 3; 109000)} \times \frac{\text{AU fuco at 440 nm (column 7)}}{\text{AU fuco at 443 nm (column 9)}}$$

$$\text{Fuco / chl } a \text{ (mol/mol) (column 13)} = \frac{\text{AU fuco at 440 nm (column 7)}}{\text{AU chl } a \text{ at 440 nm (column 1)}} \times \frac{E \text{ chl } a \text{ at 440 nm (column 5)}}{E \text{ fuco at 440 nm (column 11)}}$$

Fucoxanthin content [mol (mol chl *a*)$^{-1}$] at 18^{o}C (I)

$$\text{Fucoxanthin [mol (mol chl } a)^{-1}] = \frac{1691.83}{4555.07} \times \frac{64751.04}{103659.91} = 0.21$$

Table 4. Data for calculation of fucoxanthin (mol (mol chl *a*) $^{-1}$) of *E. huxleyi*.

Pigment	Chlorophyll *a*						Fucoxanthin							
	1	2	3	4	5	6	7	8	9	10	11	12	13	14
Temp. (°C)	Mean AU at 440 nm	SE	Mean AU at 662.7 nm	SE	Mean *E* at 440 nm	SE	Mean AU at 440 nm	SE	Mean AU at 443 nm	SE	Mean *E* at 440 nm	SE	Fuco/ Chl *a* (mol/mol)	SE
18 (I)	4555.07	198.80	5553.85	251.40	64751.04	371.69	1589.65	109.95	1668.59	106.89	103659.91	2341.70	0.21	0.01
14	3752.64	60.94	4406.02	84.17	67208.16	588.40	762.72	27.83	790.38	28.94	105199.81	206.57	0.13	0.00
18 (II)	5095.88	213.35	6220.47	270.54	64603.67	498.28	1819.10	116.91	1884.01	121.24	105265.63	177.18	0.22	0.01
22	2985.89	104.98	3635.41	108.85	64700.28	1324.55	1043.43	42.03	1188.41	113.77	102204.41	3215.17	0.24	0.02

Appendix 3: Calculation of fatty acid content

Fatty acid content of *Thassasiosira weissflogii* (chapter 6) grown in 16 HL culture was used as a calculation example.

The concentration (µg mL^{-1}) of the fatty acid as fatty acid methyl ester (FAME) in sample was calculated from peak area using a standard curve (eg. palmitic acid curve (Fig. 4)).

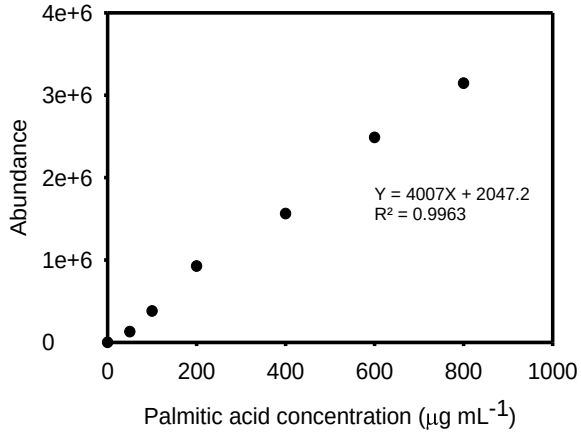

Figure 4. The relationship between total ion chromatogram (TIC) abundance of palmitic acid concentration of 0-800 µg mL^{-1} and AU detected by GC/MS.

The chromatogram of fatty acids standard and retention time (RT) were shown in fig. 5 and table 6. Fatty acid (FA) content (µg mL^{-1}) in sample was then calculated following equation and table 5.

Fatty acid content (µg mL^{-1}) (column 4) = FA content in unit µg mL^{-1} (column 1) X Resuspension with acetone (column 3) X Harvested sample (100 mL)

The conversion from µg $cell^{-1}$ to pg $cell^{-1}$ (1000000 pg $cell^{-1}$ = 1 µg $cell^{-1}$) to obtain FA detected.

$$\text{Fatty acid content (pg cell}^{-1}\text{) (column 5)} = \frac{\text{Fatty acid content (µg mL}^{-1}\text{) (column 4)}}{\text{Cell abundance (cells mL}^{-1}\text{)}} \times 1000000$$

$$\%\text{ total fatty acid content (column 7)} = \frac{\text{Each FA content in unit pg cell}^{-1}\text{ (column 5)}}{\text{Total FA content in unit pg cell}^{-1}\text{ (column 5)}} \times 100$$

For example, lauric acid content (% of total fatty acid)

$$\%\text{ lauric acid content} = \frac{0.02\text{ (pg cell}^{-1}\text{)}}{18.34\text{ (pg cell}^{-1}\text{)}} \times 100 = 0.12$$

Table 5. Data for calculation of fatty acid content and % total fatty acid in *T. weissflogii* grown at 16 HL.

Fatty acid	*T. weissflogii*							
	1	2	3	4	5	6	7	8
	Mean (µg mL^{-1})	SE	Solvent (mL)	FA content (µg)	FA content pg cell^{-1}	SE	% total FA	SE
Lauric acid	0.87	0.05	0.50	0.004	0.02	0.00	0.12	0.01
Myristoleic acid	0.99	0.05	0.50	0.005	0.02	0.00	0.13	0.01
Myristic acid	62.54	5.66	0.50	0.313	1.53	0.11	8.34	0.56
Pentadecanoic acid	11.53	0.75	0.50	0.058	0.28	0.01	1.54	0.03
Palmitoleic acid	219.39	13.91	0.50	1.097	5.35	0.27	29.29	0.79
Palmitic acid	184.54	13.17	0.50	0.923	4.50	0.26	24.56	0.53
γ-Linolenic acid	3.59	0.40	0.50	0.018	0.09	0.01	0.49	0.06
Linoleic acid	3.92	0.64	0.50	0.020	0.10	0.01	0.53	0.09
Oleic acid	4.69	0.35	0.50	0.023	0.11	0.01	0.62	0.01
Elaidic acid	0.74	0.05	0.50	0.004	0.02	0.00	0.10	0.01
Stearic acid	3.18	0.18	0.50	0.016	0.08	0.00	0.43	0.02
Arachidonic	2.33	0.06	0.50	0.012	0.06	0.00	0.32	0.02
cis-5,8,11,14,17-Eicosapentaenoic acid	197.34	21.31	0.50	0.987	4.81	0.41	26.03	1.64
cis-8,11,14-Eicosatrienoic acid	2.26	0.12	0.50	0.011	0.06	0.00	0.30	0.01
Arachidic acid	1.10	0.01	0.50	0.006	0.03	0.00	0.15	0.01
cis-4,7,10,13,16,19-Docosahexaenoic acid	49.21	3.93	0.50	0.246	1.20	0.08	6.57	0.37
Behenic acid	1.21	0.03	0.50	0.006	0.03	0.00	0.16	0.01
Lignoceric acid	2.36	0.03	0.50	0.012	0.06	0.00	0.32	0.02
Total					18.34	1.47	100.00	4.21
% SFA							35.62	2.92
% MUFA							30.15	2.00
% PUFA							34.23	5.39

SFA: saturated fatty acid; MUFA: monounsaturated fatty acid; PUFA: polyunsaturated fatty acid

% SFA = Sum of % lauric acid + myristic acid + pentadecanoic acid + palmitic acid + stearic acid + arachidic acid + behenic acid + lignoceric acid

% MUFA = Sum of % myristoleic acid + palmitoleic acid + oleic acid + elaidic acid

% PUFA = Sum of % γ-linolenic acid + linoleic acid + arachidonic acid + cis-5,8,11,14,17-eicosapentaenoic acid + cis-8,11,14-eicosatrienoic acid + cis-4,7,10,13,16,19-docosahexaenoic acid

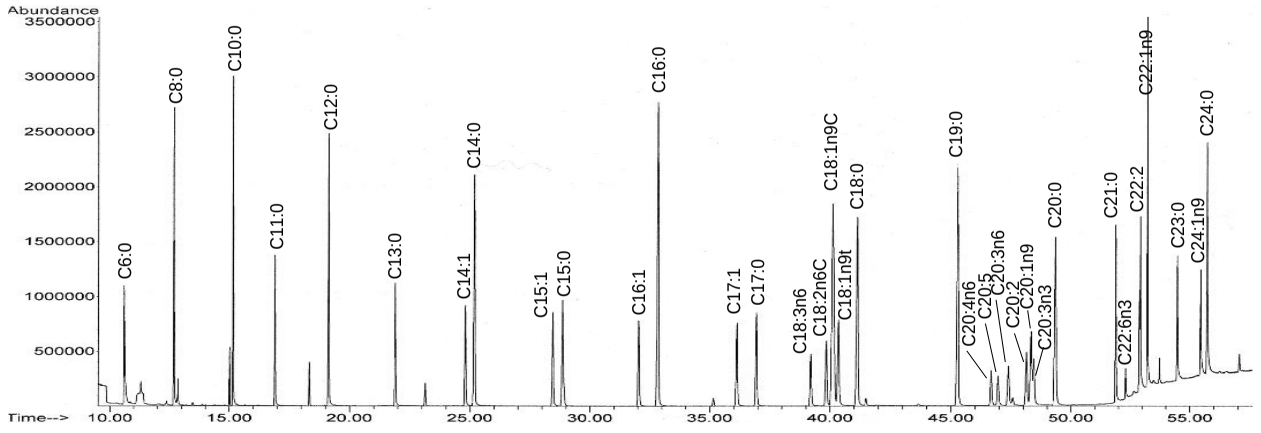

Figure 5. Chromatogram of fatty acid methyl ester (FAME) standard and retention time (min).

Table 6. FAME calibration standards, retention time (RT) and coefficient of determination (R^2).

No.	components	Scientific name	Common name	RT (min)	R^2
1	C6:0	Hexanoic acid methyl ester	Methyl caproate	10.593	0.999
2	C8:0	Octanoic acid methyl ester	Methyl caprylate	12.668	0.992
3	C10:0	Decanoic acid methyl ester	Methyl caprate	15.151	0.993
4	C11:0	Undecanoic acid methyl ester	Methyl undecanoate	16.894	0.994
5	C12:0	Dodecanoic acid methyl ester	Methyl laurate	19.127	0.994
6	C13:0	Tridecanoic acid methyl ester	Methyl tridecanoate	21.889	0.995
7	C14:1	cis-9-Tetradecenoic acid methyl ester	Methyl myristoleate	24.792	0.996
8	C14:0	Tetradecanoate acid methyl ester	Methyl myristate	25.171	0.995
9	C15:0	Pentadecanoic acic methyl ester	Methyl pentadecanoate	28.843	0.991
10	C16:1	cis-9-Hexadecenoic acid methyl ester	Methyl palmitoleate	32.025	0.996
11	C16:0	Hexadecanoic acid methyl ester	Methyl palmitate	32.830	0.996
12	C17:1	cis-10-Heptadecenoic acid methyl ester	Methyl 10-heptadecenoate	36.123	0.996
13	C17:0	Heptadecanoic acid methyl ester	Methyl hepadecanoate	36.933	0.996
14	C18:3n6	6,9,12-Octadecatrienoic acid methyl ester	Methyl gamma linolenate	39.195	0.992
15	C18:2n6c	9,12-Octadecadienoic acid methyl ester	Methyl linoleate	39.836	0.995
16	C18:1n9c	9-Octadecenoic acid methyl ester	Methyl oleate	40.092	0.996
17	C18:1n9t	9-Octadecenoic acid methyl ester	Methyl elaidate	40.337	0.996
18	C18:0	Octadecanoic acid methyl ester	Methyl stearate	41.112	0.995
19	C19:0	Nonadecanoic acid methyl ester	Methyl nonadecanoate	45.268	-
20	C20:4n6	cis-5,8,11,14-Eicosatrienoic acid methyl ester	Methyl arachidonate	46.661	0.991
21	C20:5n3	cis-5,8,11,14,17-Eicosapentaenoic acid methyl ester	Methyl 5,8,11,14,17-Eicosapentaenoate	46.947	0.992
22	C20:3n6	cis-8,11,14-Eicosatrienoic acid methyl ester	Methyl 8,11,14-Eicosatrienoate	47.378	0.992
23	C20:2	cis-11,14-Eicosadienoic acid methyl ester	Methyl 11,14-Eicosadienoate	48.130	0.992
24	C20:1n9	cis-11-Eicosenoic acid methyl ester	Methyl 11-Eicosenoate	48.316	0.995
25	C20:3n3	cis-11,14,17-Eicosatrienoic acid methyl ester	Methyl 11,14,17-Eicosatrienoate	48.433	0.994
26	C20:0	Eicosanoic acid methyl ester	Methyl arachidate	49.342	0.994
27	C21:0	Heneicosanoic acid methyl ester	Methyl heneicosanoate	51.878	0.990
28	C22:6n3	cis-4,7,10,13,16,19-Docosahexaenoic acid methyl ester	Methyl docosahexaenoate	52.292	0.988
29	C22:2	cis-13,16-Docosadienoic acid methyl ester	Methyl docosadienoate	52.863	0.989
30	C22:1n9	13-Docosenoic acid methyl ester	Methyl erucate	52.904	0.995
31	C22:0	Docasanoic acid methyl ester	Methyl behenate	53.212	0.995
32	C23:0	Tricosanoic acid methyl ester	Methyl tricosanoate	54.460	0.991
33	C24:1n9	cis-15-Tetracosenoic acid methyl ester	Methyl nervonate	55.439	0.988
34	C24:0	Tetracosanoic acid methyl ester	Methyl lignocerate	55.707	0.990